Universitat Autònoma de Barcelona

EXPLORING APPROACHES AND BIOTECHNOLOGICAL TOOLS TO BETTER CHARACTERIZE SWEET POTATO VIRUSES

Ornela Chase

UNIVERSIDAD AUTÓNOMA DE BARCELONA

Facultad de Biociencias

Departamento de Biología Animal, Biología Vegetal y Ecología

Programa de Doctorado en Biología y Biotecnología Vegetal

EXPLORING APPROACHES AND BIOTECHNOLOGICAL TOOLS TO BETTER CHARACTERIZE SWEET POTATO VIRUSES

Ornela Chase

Barcelona, 2022

UNIVERSIDAD AUTÓNOMA DE BARCELONA

Facultad De Biociencias

Departamento De Biología Animal, Biología Vegetal y Ecología

Programa De Doctorado En Biología y Biotecnología Vegetal

EXPLORING APPROACHES AND BIOTECHNOLOGICAL TOOLS TO BETTER CHARACTERIZE SWEET POTATO VIRUSES

Dissertation presented by Ornela Chase for the degree of Doctor in Plant Biology and Biotechnology by Universitat Autónoma de Barcelona

Dr. Juan José López-Moya Gómez	**Dr. Montserrat Martín Hernández**	**Ornela Chase**
Thesis director	Thesis tutor	Ph.D. candidate

Barcelona, 2022

This work was carried out at the laboratory of Plant Virology, at the Center for Research in Agricultural Genomics (CSIC-IRTA-UAB-UB) in Barcelona, under the supervision of Dr. Juan José López-Moya. Part of this dissertation was also conducted during short stays at the laboratory of Plant-Pathogen-Insect Interactions at the Institute of Mediterranean and Subtropical Horticulture (IHSM-UMA-CSIC) in Malaga and the laboratory of Prof. George Lomonossoff at the department of Biochemistry and Metabolism, at the John Innes Centre (JIC, Norwich, UK).

It always seems impossible until it is done…

ACKNOWLEDGEMENTS

While completing the writing of my thesis, here comes one of the best and most emotional parts; The part where I can express my gratitude to all the people that supported me throughout these wonderful years, where I learned so much and I will always be thankful for!

In the first place, I want to thank wholeheartedly me thesis director for giving me the opportunity to dive into the Plant Virology world and get so amazed by these tiny and fascinating creatures that can manipulate so genuinely their hosts. Juanjo, I know you dislike when people appraise you but is inevitable for me not to. You have been a great team leader, always willing to help, listen and support the group in any time. I never considered you as a boss but rather like an extraordinary mentor who helped me develop professionally, always staying positive, and motivating me to continue and surpass any difficulty (that clone of FM was a pain and you were always unbelievably supportive-I will never forget it!!). The world needs more people like you, with your positivity and your good heart! Thank you so much for everything!!!

Secondly, I would like to thank George and all Lomonossoff Lab at the JIC, especially Eva and Keith, for making my stay so nice and fruitful. George, I am really grateful you accepted me in your laboratory, and I appreciate so much all the help, advice and feedback. I had a splendid time in Norwich, learned so many new things and although CoVid lockdown made it hard, we managed to have the Newton symposium and I returned with great memories and some wonderful VLPs.

Thirdly, I would also like to express my acknowledgements to Juan Antonio Díaz and all the Lab of Plant-Pathogen-Insect Interaction at ´La Mayora´ in Malaga, for hosting me during the ´cool´ month of July 2021. Working under 38 degrees, 12 hours a day, wasn´t particularly fun, but it was sure lovely working with views on the ´costa de sol´ and of course meet and interact with all the amazing people over there, Irene, Cristina, Lidia, Efren and so many more. Thank you, guys for making me feel at home and enrich my stay with some cool memories. I will definitely revisit for some more espetos!!!

And now it is time for acknowledging my friends and colleagues at CRAG. Uff this is hard as they are so many people that I sincerely want to thank for being part of my life during these incredible years of the thesis. Undoubtedly, I will start with Marisa, the first colleague I met at the Lab and eventually became one of my best and dearest friends in Spain. Thank you so much for showing me everything from zero, for being so patient with me, for transmitting me your motivation and love for science, for helping me with every doubt and troubleshot and of course for your ´motivational´ music (too much reggaeton) at the Lab, making us dance so many times while working (Juanjo you should not read this part haha). ¡¡¡Te quiero mucho Marisita!!! Of course, I want to express my gratitude to Bia as well, for always giving the best advice and transmitting so much tranquility. Thanks to Inma for her help and support and certainly to Tarik who has been a great colleague and friend, always coming up with smart ideas. Undoubtedly, I cannot leave out from this section our newest member, Clara; thanks for being such an amazing colleague and friend, it has been a pleasure sharing experiments and experiences with you! I cannot forget our master students, Giannina, Eric and Pau; thank you guys for being part of the Lab it was lovely to work with you. Moreover, thanks to Adriá, Laia and Ana for our collaboration. A huge thanks to my lovely friends and neighbor colleagues, Bea, Eugenia and Aida; it's so nice to have coincided with you during these years. Last, many thanks to CRAG´s staff from greenhouse services, purchasing, sequencing, bioinformatics, and administrative department for always facilitating our work.

Closing this section, I want to express my gratitude to my family for their constant support, unconditional love and for always believing so much in me. Last but most importantly, I want to thank Bartus, my personal taxi driver for the infinite weekends at CRAG and my greatest supporter who made my years in Barcelona simply beautiful; I am blessed to have crossed paths with you.

SUMMARY

Summary

Viral diseases pose a major challenge to sustainable agriculture. Sweet potato (*Ipomoea batatas*) is one of the most important staple crops worldwide and its production is threatened by many pathogenic viruses which can limit yield and quality, especially when found in mixed infections. The high diversity of viruses that can be present simultaneously in sweet potato plants creates complex pathosystems that require detailed studies for the improvement of control strategies against viral diseases. The present thesis addresses the characterization of important biological aspects of four widespread sweet potato viruses, including the aphid transmitted potyviruses *Sweet potato feathery mottle virus* (SPFMV) and *Sweet potato virus 2* (SPV2) and the whitefly transmitted ipomovirus *Sweet potato mild mottle virus* (SPMMV) and crinivirus *Sweet potato chlorotic stunt virus* (SPCSV). In the first chapter of the dissertation, we compared the natural variability between two isolates of SPMMV, the 130 and the 0900, in two experimental hosts, with special attention to disease symptomatology and viral accumulation in single and mixed infected plants over time. Moreover, we performed sequence comparisons between the two isolates to detect differences that could account for the symptom divergence observed in both *N. tabacum* and *I. nil* plants. Additionally, we explored common hosts between SPMMV and SPCSV for the study of their co-infections and identified novel plants susceptible to SPCSV infection, further expanding its known host range. In the second chapter, we identified and characterized gene products that confer RNA silencing suppressor (RSS) activity in the case of SPV2. Different gene products located at the viral 5´end region of the genome were tested for RSS activity employing co-agroinfiltration assays with a GFP reporter in *N. benthamiana* plants. Visual results under UV revealed that different gene products exhibited RSS activity. Our findings were confirmed by q-RT-PCR and Northern blotting measuring GFP mRNA levels. Additionally, we examined whether these viral proteins were interfering with the systemic movement of the RNA silencing signal. Last, the RSS capacity of SPV2 proteins were also assessed during viral infections using a heterologous expression vector. Finally, and aiming to gain insights on the

molecular mechanisms required for vector specificity and vector-mediated dissemination of sweet potato viruses, in the third chapter, we conducted structural studies based on the production of flexuous virus-like particles (VLPs) in plants, a system with a great potential for nanobiotechnological uses. VLPs of SPFMV, SPV2 and SPMMV were produced through transient expression of their respective CPs in *N. benthamiana* plants, using a self-replicating expression vector. Western blotting with specific antibodies and electron microscopy (EM) imaging of crude extracts of infiltrated leaves confirmed overexpression of CPs and their subsequent assembly into VLPs that resemble the flexuous filaments of the corresponding viruses. The VLPs were purified and used for cryo-EM studies, allowing us to solve their structure at near-atomic resolution. Overall, our results provide further insights about the variability of molecular determinants used by potyvirids to cope with host defenses, revealing a complex evolutionary scenario in the case of sweet potato potyviruses. Moreover, they allowed comparison of the structures of particles corresponding to a potyvirus and an ipomovirus that are able to infect the same host plant but are disseminated by different insect vectors, providing the basis for future studies to better understand their biological properties, and hopefully to design effective and durable control measures.

Resumen

Las enfermedades virales plantean un gran desafío para una producción agrícola sostenible. La batata (*Ipomoea batatas*) es uno de los cultivos más importantes del mundo y su producción está amenazada por muchos virus que pueden limitar su rendimiento y calidad, especialmente cuando aparecen en infecciones mixtas. La gran diversidad de virus que pueden estar presentes simultáneamente en batata crea patosistemas complejos que requieren estudios detallados para mejorar las estrategias de control contra estas enfermedades virales. La presente tesis aborda la caracterización de ciertos aspectos biológicos de cuatro virus de batata, incluidos los potyvirus *Sweet potato feathery mottle virus* (SPFMV) y *Sweet potato virus 2* (SPV2), transmitidos por áfidos, y el ipomovirus *Sweet potato mild mottle virus* (SPMMV) y el crinivirus *Sweet potato chlorotic stunt virus* (SPCSV), transmitidos por mosca blanca. En el primer capítulo del trabajo, comparamos la variabilidad natural entre dos aislados de SPMMV, el 130 y el 0900, en dos huéspedes experimentales, con especial atención en la sintomatología de la enfermedad y la acumulación viral en plantas con infección simple y mixta a lo largo del tiempo. Además, realizamos comparaciones de secuencias entre los dos aislados para detectar diferencias que pudieran explicar la divergencia de síntomas observados en plantas de *N. tabacum* e *I. nil*. También exploramos huéspedes comunes entre SPMMV y SPCSV para el estudio de sus coinfecciones e identificamos nuevas plantas susceptibles a la infección por SPCSV, ampliando aún más su rango de huéspedes conocidos. En el segundo capítulo, identificamos y caracterizamos productos génicos del virus SPV2 que confieren actividad supresora de silenciamiento de ARN (RSS). Se analizó la actividad RSS de diferentes productos génicos ubicados en la región 5’ del genoma viral, empleando ensayos de co-agroinfiltración con una proteína indicadora GFP en

plantas de *N. benthamiana*. Los resultados visuales bajo luz UV revelaron que diferentes productos génicos presentaban actividad supresora. Nuestros hallazgos fueron confirmados por q-RT-PCR y transferencia Northern midiendo los niveles de ARNm de GFP. Además, examinamos si estas proteínas interferían con la señal de silenciamiento de ARN en el movimiento sistémico. Por último, también se evaluó la capacidad RSS de las proteínas de SPV2 durante infecciones virales utilizando un vector de expresión heterólogo. Finalmente, y con el objetivo de obtener información sobre los mecanismos moleculares requeridos para la especificidad de vector en la transmisión mediada por insectos de virus de batata, en el tercer capítulo realizamos estudios estructurales basados en la producción de partículas similares a virus (VLPs) en plantas. Las VLPs de SPFMV, SPV2 y SPMMV se produjeron a través de expresión transitoria de sus respectivas proteínas de cápside (CP) en *N. benthamiana*, utilizando un vector de expresión auto-replicativo. La transferencia Western con anticuerpos específicos y las imágenes de microscopía electrónica (EM) de extractos crudos de hojas infiltradas confirmaron la sobreexpresión de las tres CPs y su posterior ensamblaje en VLPs que se asemejan a los filamentos flexuosos de los virus originales. Las VLPs se purificaron y se usaron para estudios de criomicroscopía electrónica (cryo-EM), lo cual nos permitió resolver su estructura con una resolución casi atómica. En general, nuestros resultados brindan una mayor información sobre la variabilidad de los determinantes moleculares utilizados por los miembros de la familia *Potyviridae* para hacer frente a las defensas del huésped, lo que revela un escenario evolutivo complejo en el caso de los potyvirus de batata. Además, permitieron la comparación de las estructuras de partículas correspondientes a un potyvirus y un ipomovirus que pueden infectar la misma planta huésped pero que son transmitidos por diferentes insectos vectores, proporcionando la base para futuros estudios que ayuden a

comprender mejor sus propiedades biológicas, y que esperamos sirvan para diseñar medidas de control efectivas y duraderas.

Resum

Les malalties virals plantegen un gran repte per a una producció agrícola sostenible. El moniato (*Ipomoea batatas*) és un dels cultius més importants a nivell mundial i la seva producció està amenaçada per molts virus que poden limitar-ne el rendiment i la qualitat, especialment quan es troben en infeccions mixtes. La gran diversitat de virus que poden estar presents simultàniament al moniato crea patosistemes complexos que requereixen d'estudis detallats per tal de millorar les estratègies de control contra aquestes malalties virals. Aquesta tesi aborda la caracterització de certs aspectes biològics de quatre virus de moniato, incloent els potyvirus *Sweet potato feathery mottle virus* (SPFMV) i *Sweet potato virus 2* (SPV2), transmesos per àfids, així com l'ipomovirus *Sweet potato mild mottle virus* (SPMMV) i el crinivirus *Sweet potato chlorotic stunt virus* (SPCSV), transmesos per mosca blanca. Al primer capítol del treball, comparem la variabilitat natural entre dos aïllats de SPMMV, el 130 i el 0900, en dos hostes experimentals, amb especial atenció a la simptomatologia de la malaltia i l'acumulació viral en plantes amb infeccions simples i mixtes. A més, fem comparacions de seqüències entre els dos aïllats per tal de detectar diferències que poguessin explicar la divergència de símptomes observats en plantes de *N. tabacum* i d' *I. nil*. També explorem hostes comuns entre SPMMV i SPCSV per a l'estudi de les coinfeccions, i identifiquem noves plantes susceptibles a la infecció per SPCSV, ampliant encara més el seu rang d'hostes coneguts. Al capítol segon, identifiquem i caracteritzem productes gènics de SPV2 que confereixen activitat supressora del silenciament d'ARN (RSS). Es va analitzar l'activitat RSS de diferents productes gènics ubicats a la regió 5' del genoma viral, emprant assajos de coagroinfiltració en plantes de *N. benthamiana* amb la proteïna GFP com a indicadora. Els resultats visuals sota llum UV van revelar que els diferents productes gènics exhibien activitat supressora. Aquests resultats van ser confirmats mitjançant q-RT-PCR i Northern blot, tècniques que permeten mesurar els nivells d'ARNm corresponents a la GFP. A més, es va examinar si aquestes proteïnes interferien amb el senyal de silenciament d'ARN durant el moviment sistèmic. D'altra banda, també es va avaluar la capacitat RSS

de les proteïnes de SPV2 durant infeccions virals utilitzant un vector d'expressió heteròleg. Finalment, amb l'objectiu d'obtenir més informació sobre els mecanismes moleculars necessaris per a l'especificitat dels insectes vectors, i sobre la disseminació de virus de moniato mediada per aquests, durant el capítol tercer es van dur a terme estudis estructurals basats en la producció de partícules similars a virus (VLPs) en plantes. Les VLPs de SPFMV, SPV2 i SPMMV es van produir a través de l'expressió transitòria de les seves proteïnes CP corresponents a *N. benthamiana*, utilitzant un vector d'expressió autoreplicatiu. Assajos de Western Blot i imatges de microscòpia electrònica (EM) d'extractes crus de fulles infiltrades, van confirmar la sobreexpressió de les CP i el seu acoblament posterior en VLPs que s'assemblaven als filaments flexuosos dels virus originals. Les VLPs es van purificar i es van fer servir per a estudis de crio-microscòpia electrònica cryo-EM, permetent-nos resoldre la seva estructura amb una resolució gairebé atòmica. En general, els nostres resultats ofereixen més informació sobre la variabilitat dels determinants moleculars utilitzats pels membres de la família *Potyviridae* per fer front a les defenses de l'hoste. A més, els resultats van permetre la comparació de les estructures de partícules corresponents a un potyvirus i un ipomovirus que poden infectar la mateixa planta hoste però que són transmesos per diferents insectes vectors, proporcionant la base per a futurs estudis per comprendre millor les seves propietats biològiques i que esperem que serveixen per a dissenyar mesures de control efectives i duradores.

ABBREVIATIONS

Viruses cited in the present thesis

AltMV	*Alternanthera mosaic virus*
ANRSV	*Areca palm necrotic ringspot virus*
BaMV	*Bamboo mosaic virus*
BaYMV	*Barley yellow mosaic virus*
BVMoV	*Bellflower veinal mottle virus*
BVY	*Blackberry virus Y*
BYDV-PAV	*Barley yellow dwarf virus-PAV*
CaMV	*Cauliflower mosaic virus*
CBSV	*Cassava brown streak virus*
CCYV	*Cucurbit chlorotic yellows virus*
CeLV	*Celery latent virus*
CMV	*Cucumber mosaic virus*
CocMoV	*Coccinia mottle virus*
CTV	*Citrus tristeza virus*
CVYV	*Cucumber vein yellowing virus*
CYSDV	*Curcubit yellow stunting disorder virus*
GLRaV	*Grapevine leafroll associated viruses*
IYVV	*Ipomoea yellow vein virus*
LIYV	*Lettuce infectious yellows virus*
MacMV	*Maclura mosaic virus*
PapMV	*Papaya mosaic virus*
PepMV	*Pepino mosaic virus*
PeWBVYV	*Pepper whitefly-born vein yellows virus*
PPV	*Plum pox virus*
PRSV	*Papaya ringspot virus*
PVA	*Potato virus A*
PVX	*Potato virus X*
PVY	*Potato virus Y*
PYVV	*Potato yellow vein virus*
RMV	*Ryegrass mosaic virus*
RoYMV	*Rose yellow mosaic virus*
RRSV	*Rice ragged stunt virus*
SMV	*Soybean mosaic virus*
SPC6V	*Sweet potato C-6 virus*
SPCFV	*Sweet potato chlorotic fleck virus*
SPCSV	*Sweet potato chlorotic stunt virus*

SPCV	*Sweet potato collusive virus*
SPFMV	*Sweet potato feathery mottle virus*
SPLCCaV	*Sweet potato leaf curl Canary virus*
SPLCESV	*Sweet potato leaf curl Spain virus*
SPLCGV	*Sweet potato leaf curl Georgia virus*
SPLCSCV	*Sweet potato leaf curl South Carolina virus*
SPLCUV	*Sweet potato leaf curl Uganda virus*
SPLCV	*Sweet potato leaf curl virus*
SPLCV-CN	*Sweet potato leaf curl China virus*
SPMaV	*Sweet potato mosaic associated virus*
SPMMV	*Sweet potato mild mottle virus*
SPMSV	*Sweet potato mild speckling virus*
SPPV	*Sweet potato pakakuy virus*
SPRSV	*Sweet potato ringspot virus*
SPV2	*Sweet potato virus 2*
SPVC	*Sweet potato virus C*
SPVCV	*Sweet potato vein clearing virus*
SPVG	*Sweet potato virus G*
SPVMV	*Sweet potato vein mosaic virus*
SPYDV	*Sweet potato yellow dwarf virus*
SqVYV	*Squash vein yellowing virus*
SRBSDV	*Southern rice black-streaked dwarf virus*
TBSV	*Tomato bushy stunt virus*
TEV	*Tobacco etch virus*
TICV	*Tomato infectious chlorosis virus*
TMMoV	*Tomato mild mottle virus*
TMV	*Tobacco mosaic virus*
ToCV	*Tomato chlorosis virus*
TriMV	*Triticum mosaic virus*
TSWV	*Tomato spotted wilt virus*
TuMV	*Turnip mosaic virus*
TVMV	*Tobacco vein mottling virus*
TYLCCNV	*Tomato yellow leaf curl China virus*
UCBSV	*Ugandan cassava brown streak virus*
WMV	*Watermelon mosaic virus*
WSMV	*Wheat streak mosaic virus*
ZYMV	*Zucchini yellow mosaic virus*

Other abbreviations

aa	Amino acids
AGO	Argonaute proteins
Avr	Avirulence proteins
bp	Base pair
CI	Cylindrical Inclusion
CP	Coat protein
CPm	Minor coat protein
Cryo-EM	Cryo-electron microscopy
DCLs	Dicer-like proteins
DNA	Deoxyribonucleic acid
DNase	Deoxyribonuclease
dpa	Days post agroinfiltration
dpi	Days post inoculation
dsRNA	Double-stranded RNA
EM	Electron microscopy
EtBr	Ethidium bromide
ETI	Effector-triggered immunity
g	gram
GFP	Green fluorescent protein
HCPro	Helper component proteinase
HR	Hypersensitive response
HTS	High-throughput sequencing
ICTV	International Committee on Taxonomy of Viruses
IgG	Immunoglobulin G
kb	Kilobase
kDa	Kilodalton
l	Liter
LB	Luria-Bertani media
M	Molar
MEAM-1	Middle East-Minor Asia 1 biotype of *B. tabaci*
MED	Mediterranean biotype of *B. tabaci*
min	Minute
mM	Millimolar
mRNA	Messenger RNA
ng	Nanogram

NGS	Next generation sequencing
NIa	Nuclear inclusion protein (a)
NIb	Nuclear inclusion protein (b)
NLRs	Nucleotide-binding site / leucine-rich repeat receptors
ORF	Open reading frame
P1	Protein P1
P3	Protein P3
PAMP	Pathogen associated molecular patterns
PCR	Polymerase chain reaction
PIPO	Pretty interesting potyviral ORF
PISPO	Pretty interesting sweet potato potyviral ORF
poly-A	Polyadenylated
PTGS	Post-transcriptional gene silencing
PTI	PAMP-triggered immunity
qRT-PCR	Quantitative real-time reverse transcription-PCR
RdRP	RNA-dependent RNA polymerase
RISC	RNA-induced silencing complex
RNA	Ribonucleic acid
RNAi	RNA interference
RNase	Ribonuclease
RNA-seq	RNA sequencing
RSS	RNA silencing suppressor
SDS-PAGE	Polyacrylamide gel electrophoresis in presence of SDS
SNR	Signal to noise ratio
ssRNA	Single stranded RNA
UTR	Untranslated region
UV	Ultraviolet
vasiRNAs	Virus-activated siRNAs
VLPs	Virus-like particles
VOCs	Volatile organic compounds
VPg	Genome-linked viral protein
YEB	Yeast extract beef media for *Agrobacterium*
µl	Microliter
2D	Two dimensions
3D	Three dimensions

CONTENTS

Contents

INTRODUCTION

1. Introduction

1.1 Sweet potato

Sweet potato (*Ipomoea batatas*) is a dicotyledonous root crop of high agronomical importance within the family *Convolvulaceae*. It is an hexaploid species, with a genome having 90 chromosomes that presumably resulted from a cross event between a diploid and a tetraploid ancestor (Hu et al. 2003). The plant consists of different edible parts, including the roots, leaves and vines, being one of the most nutritious vegetables in terms of vitamins, macro- and microelements composition (Mukhopadhyay et al. 2011). It contains a variety of different pigments, resulting in distinct flesh colors ranging between white, yellow, orange, red or purple (Mohanraj and Sivasankar 2014). Apart from human consumption, it is also used for animal feeding and traditional medicinal purposes thanks to its high content in beta-carotene (precursor of vitamin A) and other nutrients with pharmacological potential (Laurie et al. 2015; Amoanimaa-Dede et al. 2020). Paradoxically, it is considered along with other wild relative *Ipomoea* species, a naturally transgenic plant since it bears homologous sequences to *Agrobacterium* spp. T-DNA (Kyndt et al. 2015; Quispe-Huamanquispe et al. 2019). Its first domestication is traced approximately over 5.000 years ago, in two different regions, including the Central and South America and then it was distributed to Polynesia and Melanesia during the pre-Colombian period (Roullier et al. 2013). Around the 1500s it was introduced to Europe by the Spaniards and later it was spread to places with warmer climates such as regions of sub-Saharan Africa and Asia (Loebenstein 2009). To date, sweet potato is cultivated in over 110 countries around the world (Figure I1), mainly in tropical and sub-tropical regions, with most of the production concentrated in Asia (approximately 80%). Over 89 million tons of sweet potato were cultivated during 2020, with China representing the first producer, followed by Malawi and Tanzania, in east Africa (FAOSTAT, 2022). It is ranked the 11th most important staple crop worldwide, and 5th in developing countries, particularly for regions around Lake Victoria, where it is considered a food security product, since millions of low-income farmers rely on its

production for their nutrition and subsistence (Scott 2021). Agronomically, sweet potato is a highly versatile crop because it requires only minor inputs, has a relatively short growing cycle (90-120 days) and can tolerate a wide range of adverse environmental conditions, including drought or infertile soils (Jones 2021). Despite being a perennial crop, it is mainly cultivated as annual and is mostly reproduced by vegetative vine cuttings (Loebenstein 2012). This multiplication practice implies a higher susceptibility to different pathogens, in particular viruses, further described in the following section.

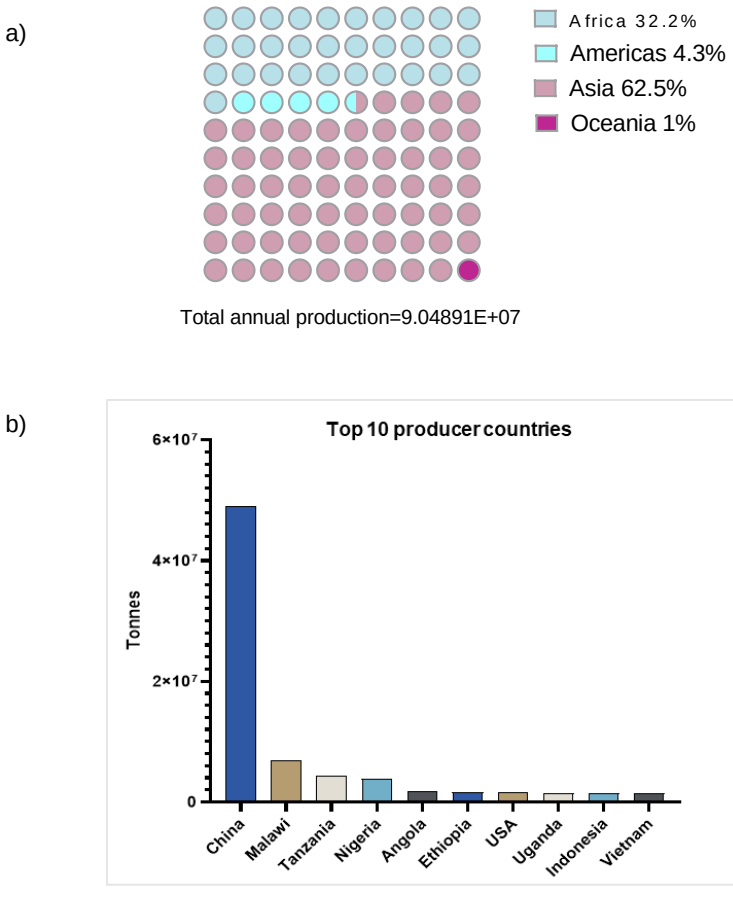

Figure I1. Worldwide sweet potato production. Graphical representation of a) sweet potato annual yield percentage in different continents and b) top 10 countries with the highest production during 2020. Data exported from FAOSTAT, 2022 (https://www.fao.org/faostat/en/?#data/QCL/visualize)

1.1.1 Sweet potato viral diseases

Several biotic agents can affect or limit sweet potato production, including pests, like the sweet potato weevil and the whitefly *Bemisia tabaci*, fungi or most predominantly virus diseases occurring mainly due to clonal propagation of the crop and thus favoring virus accumulation over generations (Loebenstein et al. 2009). Viral diseases have been reported for over 50 years in Africa, and more recently in Asia, America and Australia, practically having a worldwide distribution (Schaefers 1976; Clark and Hoy 2006; Tairo et al. 2006; Loebenstein et al. 2009). Up to date, over 30 different viruses (listed in Table I1) have been reported to infect sweet potato, mostly transmitted by the aphid *Myzus persicae* or the whitefly *Bemisia tabaci* (Clark et al. 2012). As novel technologies for high-throughput sequencing are steadily improving, this list is expected to be further extended with newly identified members, thanks to constant optimization of detection techniques (Edgar et al. 2022). Apart from CMV, a virus with one of the broadest host range of all known plant viruses, the rest of species affecting sweet potato are highly specific to the genus *Ipomoea*, suggesting that sweet potato might be a host with a cellular environment allowing only certain viruses to propagate and establish a successful infection (Kreuze et al. 2021).

Among different phytoviruses affecting sweet potato, the members of the family *Geminiviridae* are the most abundant ones, causing predominantly only mild or no symptoms, although in some cases measuring their effect on total yield remains elusive (Lozano et al. 2009; Fiallo-Olivé et al. 2020). Different studies performed in United States, South Africa or Kenya reported significant yield losses only in certain varieties infected with begomovirus members or co-infected by begomoviruses and potyviruses (Ling et al. 2010; Mulabisana et al. 2019; Wanjala et al. 2020).

Table I1. Reported viruses infecting sweet potato (Adapted by Clark *et al.* 2012).

Family	**Genus**	**Virus**
Betaflexiviridae	*Carlavirus*	SPCFV, SPC6V
Bromoviridae	*Cucumovirus*	CMV
Caulimoviridae	*Badnavirus*	SPPV
	Cavemovirus	SPCV
	Solendovirus	SPVCV
Closteroviridae	*Crinivirus*	SPCSV
Geminiviridae	*Begomovirus*	IYVV, SPLCV, SPLCCaV, SPLCLaV, SPLCV-CN, SPLCGV, SPLCESV, SPLCSCV, SPLCUV, SPMaV
	Mastrevirus	SPSV-1
Luteoviridae	*Polerovirus*	SPLSV
Potyviridae	*Potyvirus*	SPFMV, SPVC, SPVG, SPV2, SPLV, SPMSV, SPVMV, SPYDV
	Ipomovirus	SPMMV, SPYDV
Secoviridae	*Nepovirus*	SPRSV

The most prevalent and widespread viruses affecting sweet potato are the aphid-borne *Sweet potato feathery mottle virus* (SPFMV, genus *Potyvirus*, family *Potyviridae*) and the whitefly-borne *Sweet potato chlorotic stunt virus* (SPCSV, genus *Crinivirus*, family *Closteroviridae*), leading to detrimental yield losses of up to 80% due to strong synergistic interactions when co-infecting the same plant, denominated as sweet potato virus

disease (SPVD) (Karyeija et al. 2000; Gibson and Kreuze 2015). Cultivars affected by SPVD show a pronounced disease phenotype characterized by general chlorosis, leaf distortion and stunting, accompanied by enhanced reductions in tuber quality and production (Gibson et al. 1998). When potyviruses interact and synergize with unrelated viruses, usually the viral load of the partner virus increase significantly, an effect presumably attributed to the potent RNA silencing suppressor capacity of the potyviral HCPro protease (Pruss et al. 1997). However, in the case of SPVD this effect is reversed: the potyvirus RNA titers are greatly boosted while the titers of the crinivirus remain stable or slightly decrease, a phenomenon potentially linked to the RNA silencing activity of SPCSV RNase III (Karyeija et al. 2000; Cuellar et al. 2009; Cuellar 2014). Other members of the family *Potyviridae,* including the ipomovirus SPMMV or the potyviruses SPV2, SPVC or SPVG are rather relevant as well, since their presence has been experimentally confirmed in different regions of Africa, Israel or United States and they can also synergize with SPCSV, significantly affecting sweet potato quality and production. (Mukasa et al. 2006; Untiveros et al. 2007; Tugume et al. 2016; Kreuze et al. 2021).

Despite the devastating consequences of sweet potato viral diseases, favored by constant germplasm exchange due to global trade, there are still no effective control strategies for complete eradication of viral pathogens affecting the crop. Given the importance of SPVD in developing countries, an extensive number of studies have been conducted to shed light on the mechanisms related to virus susceptibility over the last 20 years, leading to development and adoption of efficient detection protocols, necessary for virus surveillance and for the protection of virus-free growing regions (Kokkinos and Clark 2006; Opiyo et al. 2010; Huang et al. 2019; Kreuze et al. 2021). However, very little is known regarding the crop resistance mechanisms, considering the genomic complexity of this heterozygous hexaploid species. Whereas different approaches have been adopted to alleviate the negative impact of viral diseases, mainly based on sanitation and trading of virus-free reproductive material, the high cost and lack of solid and well-established preventive programs compose an important impediment in developing countries (Alconero 1975; Walkey and Cooper 1975; Wang et al. 2009).

Another front to fight against viral diseases is by leveraging natural genetic resistance in breeding programs, however only few cultivars are adequate for this purpose due to scarcity of resistant genotypes in sweet potato and crossing constrains between sweet potato cultivars and wild *Ipomoea* species bearing described resistance genes (Karyeija et al. 1998). Nonetheless, newly developed genetic and genomic tools, including a reference genome for sweet potato, have enabled substantial progress and modernization of the current breeding efforts (Yang et al. 2017; Wu et al. 2018; Mwanga et al. 2021). Despite the achieved progress, the obtainment of viable resistant cultivars still poses a challenging task which is further troubled by the diversity sweet potato viruses and their complex interactions, often resulting in perplexing outcomes. Therefore, further studies elucidating these aspects are crucial for the generation of effective means to contain viral diseases and provide either resistant cultivars, or effective strategies that can sustain or enhance livelihood and prevent malnutrition in developing countries.

1.2 The intriguing world of plant viruses

Viruses constitute the most ample group of microorganisms on our planet and virtually all living organisms, including *Archaea*, *Bacteria* and *Eukaryotes* are prone to viral infections (Abrescia et al. 2012). Their discovery is traced over a century ago when two independent scientists, Dimitri Ivanovsky and Martinus Willem Beijerinck, observed that the causal agent of tobacco mosaic disease was filterable and retained its infectious properties, characterizing it as "contagium vivum fluidum" (Mayer 1886; Lustig and Levine 1992) . That discovery laid the foundation of virology hallmark as a new scientific discipline, where *Tobacco mosaic virus* (TMV, genus *Tobamovirus*, family *Virgaviridae*) had a pivotal contribution in the origins of virology field. During decades, research efforts were concentrated on the discovery and control approaches aiming to the elimination of viruses threatening human, animal or plant health, however recent discoveries showed that viruses are not only ‘bad news’ but they are also essential part for the global ecosystem, especially plant viruses, considering that 80% of our planet’s biomass is covered by plants (Lefeuvre et al. 2019). Indeed, viruses have played a substantial role to

the advancement of our knowledge in fundamental aspects of molecular and cellular biology and related processes, including the nature of genetic material, its replication, transcription and translation (Watson and Crick 1953; Kogoma 1993; Scholthof 2004; Abrescia et al. 2012). Being composed by a nucleic acid molecule (ribonucleic or deoxyribonucleic acid) tightly protected by a proteinaceous capsid shell, viruses have an immense genetic diversity, contributing to the actual genetic diversification among different organisms through horizontal gene transfer (Dolja and Koonin 2011; Koonin 2016).

Classification of viruses is not a straightforward task considering their complexity, and the advent of novel genomic tools such as high-throughput sequencing, has expanded greatly the discovery of new viral species awaiting to be accommodated to specific taxonomic groups. Currently, the most frequently used classification includes the categories proposed by the International Committee on Taxonomy of Viruses (ICTV, https://talk.ictvonline.org/information/) based on the Baltimore clustering that grouped viruses depending on their type of genome (Baltimore, 1971). According to ICTV, viruses are organized into distinct groups following specific taxonomic criteria by order, family, genus and species (Fauquet 2008; Walker et al. 2021). On the other hand, the Baltimore classification (Figure I2), originally conceived by the Nobel-Prize winning biologist David Baltimore, groups viruses into 7 specific classes, based on the nature of their genetic material, including double-stranded DNA (dsDNA), positive sense single-stranded DNA (+ssDNA), double-stranded RNA (dsRNA), positive-sense single-stranded RNA (+ssRNA), negative-sense single-stranded RNA (-ssRNA), ssRNA-RT viruses (with a DNA intermediate in their life cycle) and dsDNA-RT (with an RNA intermediate in their life) (Baltimore 1971; Dolja et al. 2020). Since the first report of TMV over 130 years ago, more than 1.744 new viral species have been described to infect plants, currently distributed in 90 genera, accounting for 25 different families (Singh et al. 2020; Walker et al. 2021). The genetic material of plant viruses consists of DNA or RNA molecules, organized in a variety of different forms, including single or double stranded chains, presenting multipartite or segmented forms (Hull 2021). RNA viruses are predominant among the virome of land plants, followed by their +ssDNA

peers (Zaitlin and Palukaitis 2000; Koonin et al. 2020). The current number of identified plant viruses represents only a small fraction of the extant viral species and a plethora of new variants are to be discovered (Claverie et al. 2018).

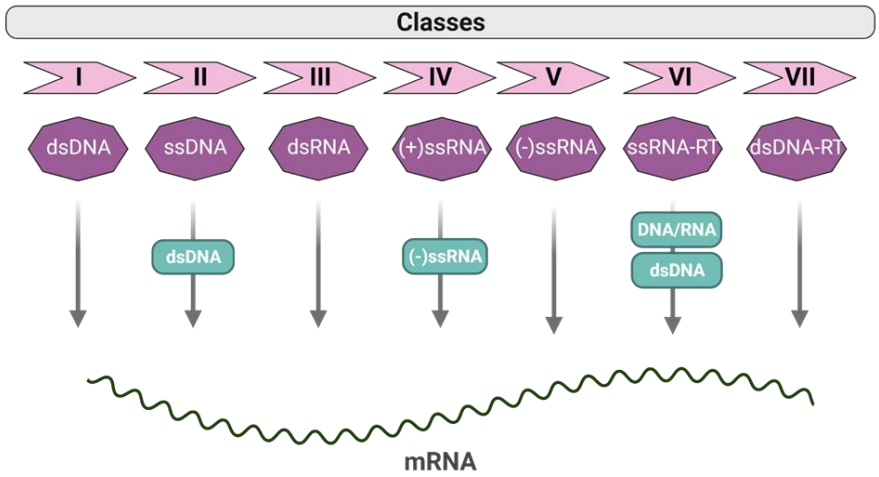

Figure I2. Baltimore classification system. Seven different groups are depicted based on the nature of genetic composition of their genomes and strategy to generate mRNA.

The structural organization of plant viruses is highly ordered as their genetic material is most frequently protected by a proteinaceous shell formed by multiple subunits of a protein designated as capsid or coat protein (CP), whereas some species can be encapsidated by two or more different CPs. In contrast to several animal viruses, phytoviruses are usually non-enveloped and can be divided into two major groups in terms of structural conformation, including icosahedral or helical capsid symmetry (Rossmann 2013; Louten 2016). The space limitations imposed by an icosahedral architecture entails size restrictions for the virus genome while in the case of helical viruses their coat protein can be extended along the entire length of their nucleic acid, thereby viruses with the latter structural organization tend to have larger genomes.

In terms of agricultural relevance, plant viruses comprise one of the most important groups of plant pathogens, being responsible for considerable

yield and quality losses in many important crops and thus leading to severe economic consequences in a global scale (Jones 2021). They are responsible for nearly half of the emerging and re-emerging plant disease epidemics at a worldwide scale, and their adverse economic impact is constantly augmented due to climate change and agricultural intensification practices aiming to fulfill the feeding needs of the exponentially growing population (Anderson et al. 2004). Despite that plant viruses do not impose a direct threat to humans or animals as they are generally unable to infect them, there is a substantial amount of studies and ongoing research dedicated to the development of effective control strategies to prevent the deteriorating impact of viral agents affecting major crops globally (Scholthof et al. 2011).

1.2.1 The family *Potyviridae*

The *Potyviridae* (order *Patatavirales*, class *Stelpaviricetes*, phylum *Pisuviricota*, kingdom *Orthornavirae*) composes the largest family of plant-infecting RNA viruses, counting circa 237 species currently grouped into twelve different genera (Table I2) including *Arepavirus, Bevemovirus, Brambyvirus, Bymovirus, Celavirus, Ipomovirus, Macluravirus, Poacevirus, Roymovirus, Rymovirus, Tritimovirus* and *Potyvirus* while three species remain still unassigned (Inoue-Nagata et al. 2022). All potyvirids share the same structural composition, forming flexible rod-shaped filaments of varying sizes (650 nm to 950 nm long and 11-20nm in diameter), composed by multiple copies of a single CP helically arranged around the RNA genome and protecting it from the hostile environment (Hull 2014).

Their genome consists of a monopartite positive-sense single-stranded RNA molecule (+ssRNA) of 8-11 kb, flanked by two small untranslated regions on the 5´and 3´prime, and translated into a large polyprotein (circa 350kDa) that is subsequently processed by three viral-encoded proteinases into mature gene products with multifunctional roles (Valli et al. 2021). Members of the genus *Bymovirus* divide their genome into two +ssRNA molecules (bipartite), deviating from the common potyvirids genomic organization and each molecule is encapsidated in different

virions. The phylogenetic origins of potyvirids genomes can be connected to many unrelated viruses, either within or outside their phylum and evolutionary studies suggest that their emergence may have coincided with the dawn of agriculture, a notion that it is further supported by their broad host range and worldwide distribution (Gibbs et al. 2008; Dolja et al. 2020).

Table I2. List of *Potyviridae* genera, indicating their genome organization and their corresponding natural vector.

Genus	Type member species	Genome	Vector
Arepavirus	*Areca palm necrotic ringspot virus*	Monopartite (+)ssRNA	Unknown
Bevemovirus	*Bellflower veinal mottle virus*	Monopartite (+)ssRNA	Unknown
Brambyvirus	*Blackberry virus Y*	Monopartite (+)ssRNA	Unknown
Bymovirus	*Barley yellow mosaic virus*	Bipartite (+)ssRNA	Plasmodiophorids
Celavirus	*Celery latent virus*	Monopartite (+)ssRNA	Unkown
Ipomovirus	*Sweet potato mild mottle virus*	Monopartite (+)ssRNA	Whiteflies
Macluravirus	*Maclura mosaic virus*	Monopartite (+)ssRNA	Aphids
Poacevirus	*Triticum mosaic virus*	Monopartite (+)ssRNA	Mites
Potyvirus	*Potato virus Y*	Monopartite (+)ssRNA	Aphids
Roymovirus	*Rose yellow mosaic virus*	Monopartite (+)ssRNA	Unkown
Rymovirus	*Ryegrass mosaic virus*	Monopartite (+)ssRNA	Mites
Tritimovirus	*Wheat streak mosaic virus*	Monopartite (+)ssRNA	Mites

A common core spanning the genomic region from P3 up to CP seems to be conserved in roughly all genera, including 8 mature gene products (P3, 6K1, CI, 6K2, VPg, NIa-Pro, NIb and CP) located in the middle and C-terminus of the viral polyprotein (Revers and García 2015). Additionally, two more proteins, the P3N-PIPO and P3N-ALT, produced.

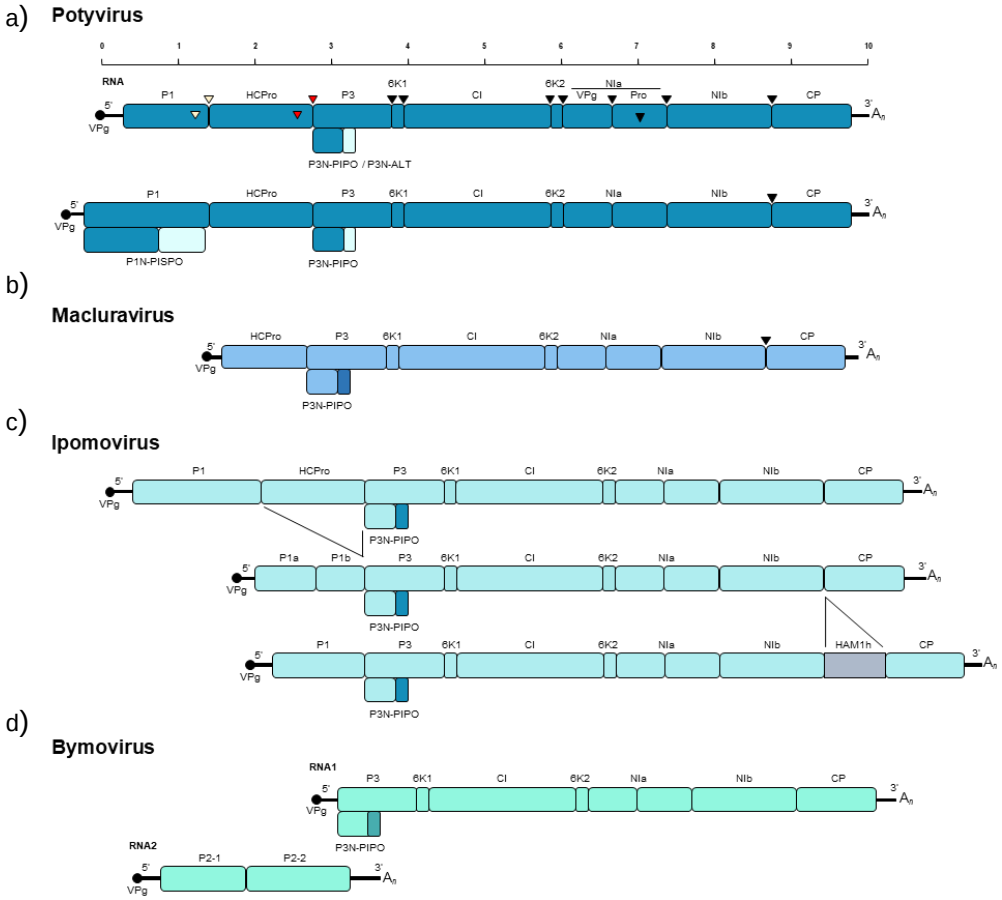

Figure I3. Scheme of the genomic organization of different members of the *Potyviridae* family. Viral RNA is illustrated as a solid black line, covalently linked to the VPg protein at the 5´end (black circle) and the polyA tail located at the 3´end. Viral gene products derived by proteolytic cleavage are depicted as boxes with their corresponding names. Black and colored arrows on the top of the first map indicate the specific cleavage sites recognized by the viral-encoded proteases (color matching proteases). Below each map are shown the products produced by polymerase slippage at conserved G2A6 motifs. (a) Genome maps of PVY (top), the type member of the genus *Potyvirus* and SPFMV (bottom), a representative member of the sweet potato infecting subgroup that encodes a second out-of-frame protein, the denominated P1N-PISPO, present only in sweet potato potyviruses. (b) Macluravirus genomic organization, lacking P1 cistron. (c) Representative maps of three ipomoviruses; SPMMV, CVYV and CBSV showing peculiarities at the 5´end, where HCPro is only present in the first virus while the rest of the members encode two different P1 proteases, denominated P1a and P1b. An additional HAM1-like gene, located between NIb and CP coding sequences, is present in the last virus. (d) Genome map of the bipartite bymovirus BYMV, showing the two +ssRNAs, encoding for two polyproteins.

The most divergent modules are found in the polyprotein N-terminal part, which bears cistrons that can be distinct among the different genera or even within the species of the same genus, resulting in functional heterogeneity among different species (Cui and Wang 2019; Pasin et al. 2022). For instance, sweet potato-infecting potyviruses present a pretty interesting sweet potato potyviral ORF (PISPO) within the P1 cistron (Figure I3, a), giving rise to a frameshift protein, the P1N-PISPO, again through transcriptional slippage (Rodamilans et al. 2015; Mingot et al. 2016; Untiveros et al. 2016). Another peculiarity is found in *Sweet potato mild mottle virus* (SPMMV), the type member of genus *Ipomovirus*, encoding for a helper component protein and resembling species of genus *Potyvirus*, whereas other ipomoviruses are devoid of that cistron and instead produce two different types of P1 proteases (Figure I3, c), belonging to distinct phylogenetic lineages (Valli et al. 2007; Pasin et al. 2014). Some members contain an additional protein denominated Maf1/ham1-like pyrophosphatase (HAM1) implicated in host-specific infection processes (Mbanzibwa et al. 2009; Valli et al. 2022). Also, an Alkylation B domain (AlkB) is present in P1 cistron of *Endive necrotic mosaic virus* (ENMV, genus *Potyvirus*) and *Blackberry virus Y* (BVY, genus *Brambyvirus*), proposed to maintain genomic integrity and promoting long-term viral infection (Susaimuthu et al. 2008; van den Born et al. 2008; Martínez-Pérez et al. 2017).

1.2.1.1 The genus *Potyvirus*

The genus Potyvirus represents the most abundant group within the family *Potyviridae*, currently encompassing 195 described species with a wide geographical distribution (Inoue-Nagata et al. 2022). In terms of economical relevance, potyviruses compose the most important group of plant RNA viruses since they can infect a broad range of hosts, including species of high agronomical importance, leading to detrimental yield and quality losses. Representing almost 15% of all known plant viruses, several potyviruses pose a major challenge to food security, especially in tropical and subtropical regions of developing countries, being responsible for devastating disease outcomes (Jones and Naidu 2019). Their presence has been confirmed in a worldwide scale, with most species

being reported in the United States, China, Australia, Brazil, India, France, Italy and United Kingdom (Gadhave et al. 2020). Owning to their economic impact, they are one of the most well-studied plant virus groups and several aspects related to their molecular biology have been elucidated and thoroughly reviewed (Revers and García 2015; Pasin et al. 2022), although there is still a substantial amount of knowledge and insights yet to be discovered. Their genome consists of a +ssRNA molecule, what is encapsidated by several hundreds of CP units, forming flexuous left-handed helices (Figure I4) of around 680-950 nm in length and 11-13 nm in diameter (Valli et al. 2021).

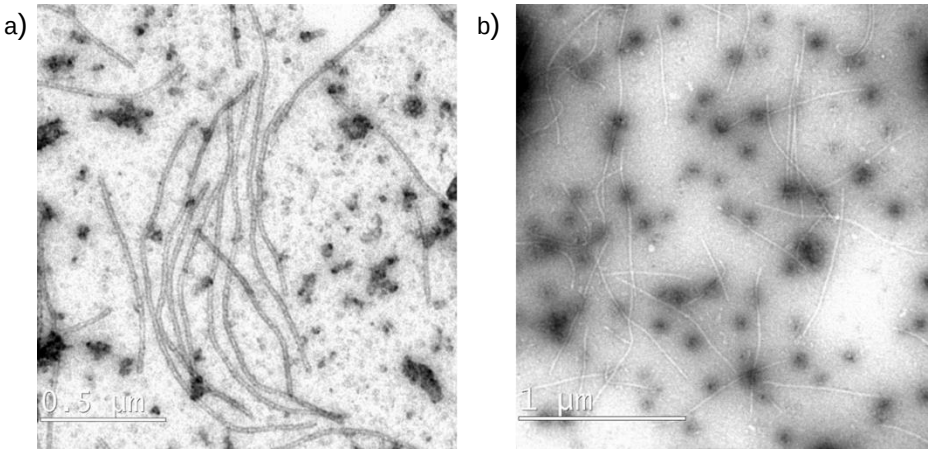

Figure I4. Electron micrographs of two *Potyviridae* members. Negative-stained, purified virions of (a) the potyvirus *Sweet potato virus 2* (SPV2) and (b) the ipomovirus *Sweet potato mild mottle virus* (SPMMV). Images were captured using JEM-1400, fitted with a Gatan camera. Size bars included at bottom left.

Virions are mainly composed by the coat protein (95%) and a minor part of RNA (5%) with each particle containing a single RNA copy, coated by approximately 2000 CP blocks. Some potyvirus particles may also contain a small proportion of other minor viral components, such as the CI, HCPro and VPg (Torrance et al. 2006; Gabrenaite-Verkhovskaya et al. 2008). The RNA genome translates for a single large polyprotein further cleaved

into up to 10 mature proteins by proteolytic activity of three viral-encoded endopeptidases (Adams et al. 2005). According to their position on the viral polyprotein, the resulting functional peptides include the P1, HCPro, P3, 6K1, CI, 6K2, NIa-VPg, NIa-Pro, NIb and the CP. An additional protein designated as P3N-PIPO is produced as well by a +1 frameshift of the viral polymerase in conserved G_2A_6 nucleotide motifs located inside the P3 genomic region (Chung et al. 2008). Interestingly, during the proteolytic processing, partially processed subproducts may also arise and their functional role at some stage of the virus cycle cannot be discarded (Merits et al. 2002). As already mentioned in the section 1.2.1, merely potyviruses infecting sweet potato encode for an additional gene product, the P1N-PISPO, embedded in P1 genomic region and produced by the same mechanism as the transframe P3N-PIPO (Rodamilans et al. 2015). Basically, all potyviral proteins are characterized by a multifunctional nature since they display several roles during the viral cycle and can participate in different processes to promote virulence. From N to C, the functionalities of the different proteins are described next:

The P1 protein is a chymotrypsin-like serine protease that self-cleaves its carboxyl-terminus to be released from the remainder polyprotein (Verchot et al. 1991), ensuring proper functionality of HCPro (see below), a process which results crucial for virus viability (Verchot and Carrington 1995a; Shan et al. 2015). Moreover, it has been regarded as host range determinant and linked with virus adaptation in specific environments by modulation of the RNA replication (Shan et al. 2018; Cui and Wang 2019). Another activity attributed to P1 is the enhancement of the RNA silencing activity of HCPro when preceding it in *cis* (Anandalakshmi et al. 1998; Pruss et al. 2004; Valli et al. 2007), although recent data relate this phenomenon to translational reinforcement of HCPro assisted by P1, independently of the RNA silencing (Tena Fernández et al. 2013; Pasin et al. 2014).

HCPro, the cysteine protease following P1, is one of the most if not the most studied potyviral protein (Syller 2005; Revers and García 2015). Its first characterized role as a helper component in aphid-mediated transmission of potyviruses resulted in its current name (HC stands for

"helper component") and similar to P1, it self-cleaves to unbind from the viral polyprotein and exert its functions (Kassanis and Govier 1971; Carrington et al. 1989). As one of the most multitasking viral peptides, HCPro participates in a plethora of interactions to promote viral infection, actively interfering and suppressing the plant RNA silencing machinery (Kasschau and Carrington 1998; Anandalakshmi et al. 1998; Valli et al. 2018). Apart from interacting with the viral CP facilitating the virus aphid dispersion (Blanc et al. 1997), it also plays a role in CP stabilization and proper viral encapsidation, increasing virus progeny yields and promoting their systemic spread (Valli et al. 2014; De et al. 2020).

The P3 comprises one of the least studied potyviral proteins and its precise functions remain ambiguous, although it contributes to viral replication, pathogenesis and symptomatology (Klein et al. 1994; Luan et al. 2016). P3N-PIPO, the transframe peptide embedded within P3, has been shown to assist the viral cell-to-cell movement through plasmodesmata, in association with the viral CI and the host factor pCaP1 (Wen and Hajimorad 2010; Vijayapalani et al. 2012; Chai et al. 2020).

The 6K1 protein has been demonstrated to be an active component of the potyviral replication complex and thus contributing to the regulation of viral multiplication (Kekarainen et al. 2002; Cui and Wang 2016).

The cylindrical inclusion protein (CI) constitutes a multifunctional product exhibiting ATP binding and RNA helicase properties (Lain et al. 1990; Eagles et al. 1994; Sorel et al. 2014). Potyvirus infected cells often exhibit typical pinwheel-shaped structures formed by CI subunits and the protein is implicated in viral replication and intercellular movement, serving as a docking point for transferring potyvirus replication vesicles to neighboring cells through plasmodesmata (PD), probably in collaboration with P3N-PIPO (Movahed et al. 2017).

The 6K2 protein plays a major role in potyviral RNA amplification by promoting the formation of endoplasmic reticulum (ER)-mediated replication vesicles, where amplifications occurs (Wei and Wang 2008; Movahed et al. 2017).

The NIa protein is partially auto-cleaved, resulting in two functional elements, the VPg and the peptidase domain NIa-Pro (Dougherty and Dawn Parks 1991). It can form pseudocrystalline inclusions, detected in the nucleus and cytoplasm of infected cells (Kassanis 1939; Knuhtsen et al. 1974; Marťin et al. 1992). The functional implications of VPg have been widely studied (Jiang and Laliberté 2011), including its role in viral RNA translation mediated by its interaction with the elf4E host factor or its contribution to RNA silencing suppression (Mäkinen and Hafrén 2014; Cheng and Wang 2017; Saha and Mäkinen 2020). NIa-Pro comprises the major potyviral protease, proteolytically cleaving the processing sites in the central and C-terminal regions of the potyviral polyprotein (reviewed by Adams et al. 2005; Revers and García 2015). It also exhibits DNase activity, presumably contributing to the regulation oh host gene expression during the viral infection (Anindya and Savithri 2004).

The NIb is one of the most conserved proteins among potyvirids since it displays RNA replicase functions in an RNA-dependent manner (Hong and Hunt 1996; Ivanov et al. 2014).

Last, the potyviral CP is primarily responsible for virion assembly and genome protection, however its intrinsically disordered nature in certain domains enables multiple interactions with other viral, host or vector factors, further expanding its functional contributions. Apart from genome encapsidation, the CP is implicated in aphid-mediated transmission and viral cell-to-cell and long distance movement (Atreya et al. 1995; Martínez-Turiño and García 2020).

Sweet potato feathery mottle virus (SPFMV)

SPFMV (genus *Potyvirus*, family *Potyviridae*) is the most prevalent pathogen infecting sweet potato (*Ipomoea batatas*) globally (Clark et al. 2012). The first detection of SPFMV is traced around 1950s, in regions of East Africa and ever since its presence have been reported in almost every tropical and subtropical zone where the crop is cultivated (Sheffield 1957). Its host range is rather narrow, including *Ipomoea spp.* species within family *Convolvulaceae* and some additional wild plants grown

around sweet potato fields, which can presumably serve as virus reservoirs (Tugume et al. 2008). In nature it is transmitted non-persistently by several aphid species, including *A. gossypii, M. persicae, A. craccivora, and L. erysimi* (Kennedy and Moyer 1982; Wosula et al. 2012) while it can be mechanically inoculated to different experimental hosts such as *N. benthamiana* and *C. amaranticolor.* Virus diagnosis can be readily achieved by grafting on *I. setosa* or *I. nil*, eliciting characteristic vein clearing, banding and ringspots. Sweet potato plants infected by merely SPFMV present low viral titers and only mild or no symptomatology, primarily manifested on older leaves as faint circular spots or light green veinal patterns, although some specific strains can also affect the roots (Clark et al. 2013). The symptoms of SPFMV are greatly pronounced when the virus is found in co-infections with SPCSV, causing the designated SPVD (thoroughly explained in section 1.1.1), highly frequent in all sweet potato growing areas (Karyeija et al. 2000). The high susceptibility towards SPVD has been fundamentally associated with the RNA silencing suppression mechanisms of the partner viruses and more recent transcriptomic data indicate that a downregulation of the plant salicylic-acid defense response may be also affecting the strong disease outcome (Gibson and Kreuze 2015; Bednarek et al. 2021).

SPFMV reference genome was determined by direct RNA sequencing and its genome length was estimated at 10.820 bp, excluding the poly-A tail at the 3' prime (Sakai et al. 1997). Its genome organization present the typical potyviral architecture, encoding for a single polyprotein which is subsequently cleaved into mature functional peptides by the proteolytic activity of viral endopeptidases (Figure I5, a). As already described in the section 1.2.1.1, SPFMV and most of the rest of sweet potato infecting potyviruses, encode for an additional protein denominated P1N-PISPO that is produced through polymerase slippage in G_2A_{6-7} motifs of P1, with *Sweet potato latent virus* (SPLV, genus *Potyvirus*, family *Potyviridae*) being the only exception (Wang et al. 2013). The presence of P1N-PISPO was initially predicted by bioinformatic tools (Clark et al. 2012; Li et al. 2012) and subsequently confirmed by RNA sequencing data (Rodamilans et al. 2015). The functional implications of this protein were explored by previous members in our group and showed that P1N-PISPO was able to

block the plant RNA silencing pathway, overtaking the role from HCPro, the universal potyviral RSS protein (Mingot et al. 2016; Untiveros et al. 2016). Another peculiarity of SPFMV is the size of its P1 genomic region, encoding for the largest P1 protease among all potyviruses. The C-terminus of this protein is highly conserved among potyvirus members, however its N-terminus domain seems to be highly divergent and only shares homology with P1 of viruses within SPFMV lineage or the ipomovirus SPMMV (Untiveros et al. 2010; Li et al. 2012). Although SPFMV was initially divided into four different groups, including the east African (EA), the russet crack (RC), the ordinary (O) and the common (C) strains, posterior studies categorized the C strain members as a separate virus species, designated as *Sweet potato virus C* (SPVC) (Kreuze et al. 2000; Untiveros et al. 2010). SPFMV along with SPV2, SPVC and SPVG form a separate phylogenetic lineage and contain highly homologous sequences, likely indicative of the possible occurrence of different recombination events between them (Untiveros et al. 2008; Li et al. 2012).

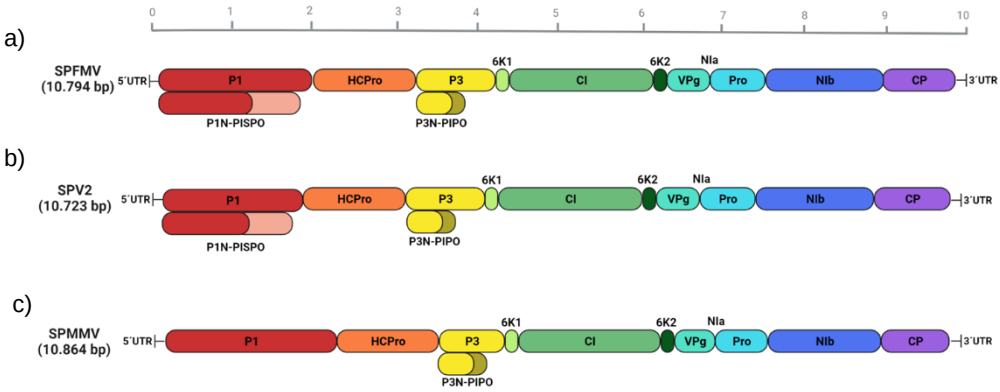

Figure I5. **Figure I5**. Genomic structure of (a) SPFMV, (b) SPV2 and (c) SPMMV. The viruses are composed by a +ssRNA molecule, encoding for up to ten mature gene products derived by proteolytic processing of a large polyprotein in the same ORF. Generated proteins are depicted in boxes with their corresponding names inside or above. An additional gene product denominated P3N-PIPO is produced through polymerase slippage, while a second transframe product derived from a similar mechanism, the P1N-PISPO, is only present in the potyviruses SPFMV and SPV2. VPgs at 5' and polyA tails at 3' ends are not shown.

Sweet potato virus 2 (SPV2)

Sweet potato virus 2 (SPV2, genus *Potyvirus*, family *Potyviridae*) is a common pathogen infecting sweet potato and was the second viral agent after SPFMV to be described from diseased sweet potatoes in Taiwan during the 80s (Rossel and Thottappilly 1988). Sequence analysis of its 3´ genomic region classified it as a separate species from SPFMV and SPVG, a notion that was also supported by distinct biological and serological properties between them (Tairo et al. 2006). Its presence has been confirmed in practically all sweet potato growing regions and several identified isolates seem to present distinctive molecular and biological features correlating with their geographical distribution (Souto et al. 2003; Tairo et al. 2006; Ateka et al. 2007; Trenado et al. 2007; Perez-Egusquiza et al. 2009; Jo et al. 2020). Since its first detection in 1987, the biological and molecular properties of SPV2 remained largely unknown until Ateka and colleagues thoroughly characterized the virus in 2004 (Ateka et al. 2004). They showed that indeed SPV2 is a typical potyvirus member, sharing the same morphological (Figure I4, a) and genomic (Figure I5, b) features with other species within its genus. Experimental data derived by RNA sequencing of SPV2 infected plants have confirmed the production of the transframe P1N-PISPO protein (Mingot et al. 2016) a fact previously predicted by bioinformatic analysis (Clark et al. 2012; Li et al. 2012). Similar to SPFMV, SPV2 is transmitted non-persistently by several aphid species and its host range includes several *Ipomoea* and *Nicotiana* species, inducing mild symptomatology such as vein clearing and leaf malformation (Figure I6).

Its relevance in single infections of sweet potato is rather low since it does not provoke visual symptoms, however in mixed infections with SPCSV the outcomes are more exacerbated, leading to substantial yield losses (Souto et al. 2003; Tairo et al. 2006). The importance of SPV2 in contributing to the SPVD has been often masked by the almost universal presence of SPFMV in infected plants. Phylogenetic studies have placed SPV2 within SPFMV lineage as they share high sequence similarity (with identities around 65%), frequently causing cross-reaction between their antisera (Li et al. 2012). The CP C-terminal domain is the most conserved

region between them, and early studies might have erroneously detected SPV2 as SPFMV in mixed infection, leading to misinterpretations of the actual importance of SPV2 in sweet potato viral disease.

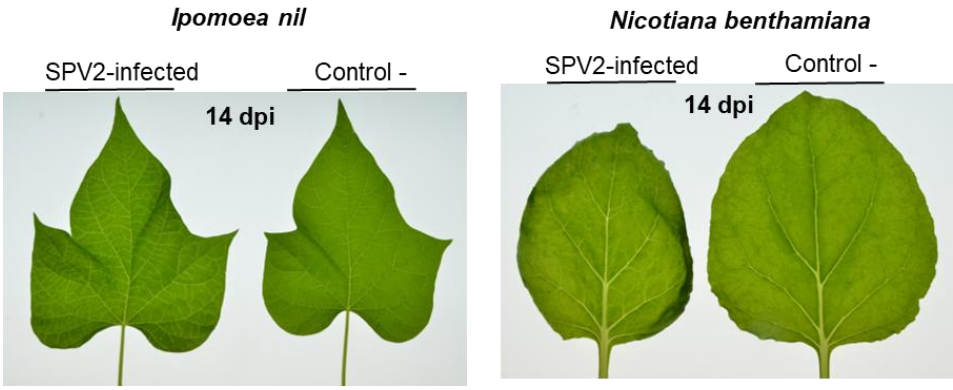

Figure I6. Symptoms of SPV2 infection on infected leaves of *I. nil* (left panel) and *N. benthamiana* (right panel) at 14 dpi. Leaves of non-infected control plants are shown for comparison.

1.2.1.2 The genus *Ipomovirus*

At present, the genus *Ipomovirus* counts with seven identified members primarily infecting sweet potato, cassava, cucurbits, tomato and eggplant (Inoue-Nagata et al. 2022). The officially recognized members composing this genus include in alphabetical order: *Cassava brown streak virus* (CBSV), *Coccinia mottle virus* (CocMoV), *Cucumber yellowing vein virus* (CVYV), *Squash vein yellowing virus* (SqVYV), *Sweet potato mild mottle virus* (SPMMV), *Tomato mild mottle virus* (TMMoV) and *Ugandan cassava brown streak virus* (UCBSV). They collectively differ with the members of other genera by their transmission mode, primarily carried out semi-persistently by the whitefly *B. tabaci*. As typical *Potyviridae* members, they comprise a +ssRNA of circa 10 kb which is translated into a large polyprotein spanning approximately 3000 residues (from 2902 to 3011 aa in the different species) and proteolytically cleaved into several mature gene products. The derived proteins are similar to those of the viruses in the genus *Potyvirus*, with some exceptions mainly located on the 5´ region of their genomic sequence where some members lack the HCPro cistron

and encode a duplicated form of P1 in tandem (P1a and P1b) instead (Valli et al. 2021). Intriguingly, CBSV and UCBSV produce an additional Maf/ham1 pyrophosphatase of non-canonical nucleotides, present in the junction between NIb and CP and presumably implicated in viral fitness, being host specific and acting coordinately with the viral RdRP (Valli et al. 2022). Although the function of different *Ipomovirus* proteins is comparatively less studied to that of their *Potyvirus* homologs, specific conserved motifs and domains can facilitate functional interpretations (Dombrovsky et al. 2014). Structurally, ipomoviruses are assembled into flexuous rod-shaped filaments of 800-950 nm in length and apart from their whitefly-mediated dispersal, they are also readily transmitted by grafting or sap inoculation to experimental hosts.

Sweet potato mild mottle virus (SPMMV)

Sweet potato mild mottle virus (SPMMV, genus *Ipomovirus*, family *Potyviridae*) constitutes the type member of genus *Ipomovirus* and presumably originated in eastern Africa (Tairo et al. 2005). Its first detection is estimated around the 1950s, firstly termed as *Sweet potato virus B* and posteriorly as SPMMV by Hollings and coworkers, that isolated it and fully characterized its biological properties (Sheffield 1957; Hollings et al. 1976). Its presence has been confirmed in several geographical areas around the world, especially in African countries where it is the third most prevalent sweet-potato infecting virus (Loebenstein 2015). Considering the relatively narrow host range of sweet potato potyvirids, SPMMV has been detected in 21 wild species of the family *Convolvulaceae* and has also been transmitted to species of 14 botanical families (Hollings et al. 1976; McGregor et al. 2009). Different sweet potato cultivars vary greatly in symptom expression upon SPMMV infection and some of them result mostly symptomless. In widely used experimental hosts like *N. tabacum*, SPMMV induces more conspicuous symptomatology including leaf mottling, puckering and distortion (Figure I7). Although SPMMV pathogenic importance is presumably rather low in single infections, its titers increase significantly in mixed infection with the crinivirus SPCSV, as a result of viral synergism between the two partners, leading to substantial yield losses (Mukasa et al. 2006; Untiveros et al.

2007). Morphologically, SPMMV virions are slightly longer compared to those of *Potyvirus* members, reaching lengths of up to 1.2 μm whilst maintaining the overall architecture of flexuous filaments (Figure I4, b). Its genetic composition resembles highly a typical *Potyvirus*, having a +ssRNA that encodes for 11 mature gene products, cleaved by viral encoded proteases (Figure I5, c). Along with TMMoV are the only ipomoviruses encoding for HCPro, although SPMMV-HCPro lacks certain conserved domains presumably accounting for the divergence in vector organism (Colinet et al. 1998). Regarding this point, and despite the fact that SPMMV was first described as a whitefly-borne virus, any attempt to reproduce its transmission using *B. tabaci* or other whitefly species have repeatedly failed under laboratory conditions and its transmission mode still remains elusive (Hollings et al. 1976; Dombrovsky et al. 2014). Nonetheless, considering that the vector specificity is indeed a hallmark for the rest of ipomoviruses and that SPMMV was originally characterized as whitefly-transmitted, the repeated failure to reproduce the transmission results seems to be caused by unknown issues of the isolates tested or the laboratory experimental conditions.

Figure I7. Characteristic symptoms of SPMMV infection in *N. tabacum* plants. A non-inoculated plant is shown on the left panel, and a SPMMV-infected plant of the same age is shown on the right panel.

1.2.2 The family *Closteroviridae*

The family *Closteroviridae* (order *Martellivirales*, class *Alsuviricetes*, phylum *Kitrinoviricota*, kingdom *Orthornavirae*) encompasses circa 57 species of plant RNA viruses, bearing the longest RNA genomes among all known plant viral pathogens, with lengths from 15.5 up to 19.5 kb (Dolja et al. 2006). The last ICTV report for *Closteroviridae* members (2020) classified them into four different genera, however this number has been recently expanded by three more taxonomic groups after a ratification during March of 2022 (Fuchs et al. 2020). Currently the family is divided into *Ampleovirus, Bluvavirus, Closterovirus, Crinivirus, Menthavirus, Olivavirus and Velarivirus* genera, primarily distinguished by phylogenetic relationships of their amino acids sequences, the number of genomic RNAs and ORFs, the vector specificity or the virion length (https://talk.ictvonline.org/ictv-reports/ictv_online_report/positive-sense-rna-viruses/w/closterovirida). Being +ssRNA viruses, closterovirids present a diverse set of genetic organization, presumably derived by recombination events and strong selective pressure, with members containing mono-, bi- or tripartite genomes that are expressed into mature gene products by employing distinct strategies (Rubio 2013). These expression strategies are based on the proteolytic cleavage of ORF or the +1 ribosomal frameshifting for the gene products located on the 5´proximal genomic region, whereas genes located on the 3´ terminal zone are expressed through subgenomic mRNAs (Agranovsky 2016). Their most distinctive feature compared to other plant RNA viruses is the presence of a protein homologous to the cellular heat-shock proteins HSP70 (termed as HSP70h) or the production of duplicated and diverged gene products such as the major and minor coat protein, termed as CP and CPm, respectively (Ruiz et al. 2018). Morphologically, they form flexuous and exceptionally long filamentous particles of 950-2200 nm in length and 10-13 nm in diameter, that are assembled into a structurally uniform main body (composed by CP units), followed by a segmented tail (composed by CPm units). At least 5 different proteins are incorporated into the particles and their overall morphology resembles a ´rattlesnake´ (Agranovsky et al. 1995). Based on their genus, they rely on different arthropods for plant-to-plant spread, including aphids (*Closterovirus*),

mealybugs (*Ampelovirus*) and whiteflies (*Crinivirus*), whereas the vectors of members in other genera such as *Velarivirus* are still unknown (Agranovsky 2016). Being restricted to the phloem and only occasionally to mesophyll and epidermis, they are transmitted in a semi-persistent mode regardless their vector type, while only few members within the genus *Closterovirus* can be transmitted by sap inoculation as well (Fuchs et al. 2020). Closterovirids can infect a broad range of hosts including herbaceous and woody plants, causing acute or chronic infections to agriculturally important crops like citrus trees, sugar beets, cucurbits and tomato (Martelli 2019). Nonetheless, the host range of individual members is rather narrow with only few exceptions for species belonging to the genus *Crinivirus*. Certain members of the family cause detrimental losses in agriculturally relevant crops, estimated to millions of dollars annually. For instance, *Citrus tristeza virus* (CTV) is the most important virus disease of citrus plantations worldwide whereas Grapevine leafroll associated viruses can severely affect the vine health or wine quality (Martelli et al. 2012; Tzanetakis et al. 2013). Notably, they can lead to substantial disease outcomes when they co-infect the same host with other unrelated viruses as a result of produced synergistic effects.

1.2.2.1 The genus *Crinivirus*

Presently the genus *Crinivirus* counts with 14 identified species, exclusively transmitted by whiteflies in the genera *Bemisia* and *Trialeurodes,* being responsible for globally emerging diseases, especially in tropical and subtropical regions where vector populations are more abundant (Tzanetakis et al. 2013). Their geographical distribution is highly dependent on that of their vector's spread, as their interactions are highly specific; some members are transmitted only by a single whitefly species, while others by diverse species in different genera (Wisler et al. 1998). They are phloem-restricted pathogens, and they require long acquisition periods (24-48h) for effective transmission, following a semipersistent mode. Most criniviruses have bipartite +ssRNA genomes of 15.3-17.7 kb in total, capped at their 5´end and encapsidated separately into flexuous filaments averaging 650-900 nm in length (Kiss et al. 2013). Contrarily to potyviruses, their genome does not present a polyadenylated (poly-A) tail

at the 3´end. RNA 1 encodes for proteins primarily implicated in viral replication and host RNA silencing while RNA 2 encodes for several gene products with diverse functions in the virus cycle, such as genome encapsidation. The only exception to this genomic arrangement is the *Potato yellow vein virus* (PYVV) which comprises three RNA segments (Livieratos et al. 2004). Research studies with *Lettuce infectious yellows virus* (LIYV), the type member of the genus, have revealed important insights related to replication processes which seem to follow a different pattern in some species (Salem et al. 2009). Their host range is broad, including plants of several botanical families and some members are considered important disease agents affecting vegetables and greenhouse crops, with certain species also identified in small fruit or horticultural hosts (Maliogka et al. 2019). In terms of symptomatology, they usually cause interveinal leaf chlorosis, yellowing or thickening, which primarily affects the older leaves and gradually expands to the younger parts, reducing the plant´s photosynthetic capacity and causing substantial yield losses. Nonetheless, some members do not induce strong symptomatology and remain latent in single infections, whilst in co-infections with other unrelated viruses the symptoms can be exacerbated; a typical example is SPCSV, that in combination with SPFMV causes detrimental disease outcomes as a result of viral synergism (Tzanetakis et al. 2013). Over the last three decades, several important discoveries have been made regarding the molecular biology and epidemiology of criniviruses and their control has been primarily addressed through the management of their whitefly vectors using different insecticides, or more recently by integrated pest management, which seems to be the most effective approach (Wintermantel 2016).

Sweet potato chlorotic stunt virus (SPCSV)

Sweet potato chlorotic stunt virus (SPCSV, genus *Crinivirus*, family *Closteroviridae*) is a widespread pathogen of sweet potato and can occur symptomless or inducing mild symptomatology, including slight leaf yellowing, upward rolling or vein swelling (Cohen et al. 1992). Symptom expression varies geographically and is highly dependent on the host variety. Its host range accommodates species mainly restricted to the

family *Convolvulaceae* (Cohen et al. 2001; Tugume et al. 2016). It causes minimal yield losses in single infections whereas in complex infection with other viruses, like the potyvirus SPFMV it can prove devastating (details in section 1.1.1). Early studies have determined its full genome sequence composed by a bipartite +ssRNA (Figure I8), the RNA 1 and the RNA 2 with 8,6 and 8,1 Kb, rendering it the largest genome for a crinivirus identified to date, following the monopartite genome of CTV in the family *Closteroviridae* (Kreuze et al. 2002). Each RNA is encapsidated into separate particles of circa 900-1000 nm in length, forming characteristic ´rattlesnake´ flexuous filaments. RNA 1 is composed by two overlapping ORF, translated into proteins that are mainly implicated in the replication process or RNA silencing suppression, while RNA 2 contains up to seven ORFs and encodes for gene products associated with a broad range of functions such as virion assembly, cell-to-cell movement and vector-mediated dispersal (Cuellar et al. 2008; Kiss et al. 2013; Tugume et al. 2013). In nature it is transmitted semi-persistently by several whitefly species like *B. tabaci*, *B. afer* sensu lato and *T. vaporiorum* and has been identified in most sweet potato grown areas (Loebenstein 2012). Studies related to SPCSV population composition revealed divergent viral isolates that can differ up to 25% in nucleotide sequence and exhibit high variability among the different genes, suggesting a polyphyletic evolutionary pattern (Tairo et al. 2005; Tugume et al. 2016).

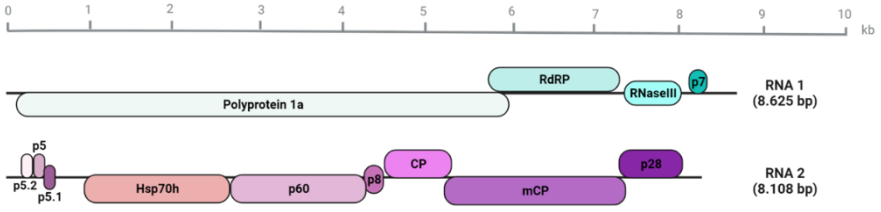

Figure I8. Representative illustration of SPCSV genome. The viral genome is composed by two segments of +ssRNA molecules, RNA 1 and RNA 2, probably capped at the 5' end and without polyA tail, depicted as black lines with the corresponding gene products shown in boxes, with their names inside. The different gene products are located at the top, middle or bottom of the RNA line, indicating that different open reading frames are responsible for the production of each protein. Untranslated and intergenic regions are not indicated to simplify the scheme. Translation of certain gene products involves ribosomal frameshift (+1) and production of sub-genomic RNAs (not shown). The complex ORF1a-ORF1b in RNA1 contains replication-related domains like methyltransferase and helicase (not shown) in addition to RdRP.

1.3 Transmission of plant viruses

Given the sessile nature of their host organisms that constrain their movement, the vast majority of phytoviruses rely on biological vectors for their plant-to-plant transmission. These vectors belong in several taxa but in most cases, they are arthropods, primarily sap-sucking insects feeding on the aerial part of the host plant, like aphids or whiteflies (Figure I9). The compatibility between the viral agent and the cell type where it is first injected is a critical component for the initiation of infection. Certain root-infecting viruses are transmitted by soil-inhabiting organisms like nematodes, plasmodiophorids, or chytrids (Roossinck 2015).

a) b)

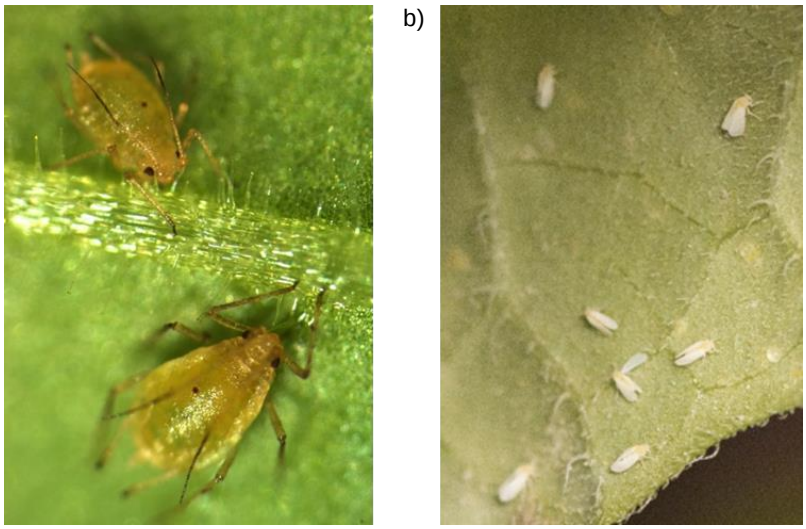

Figure I9. Natural vectors of plant viruses used in the present thesis. (a) Green peach aphid *Myzus persicae.* (b) Whitefly *Bemisia tabaci.*

An important portion of viruses (circa 25%) are spread vertically through seeds or by vegetative propagules like rhizomes, tubers or bulbs (Sastry 2013). Epidemiologically, seed-mediated transmission is important due to long survival periods of the virus inside the viable seed, especially when the host or vector availability is scarce. This way, they also secure their long distance movement, facilitated by bird dispersion or the increased human trade, and generate a primary infection inoculum that posteriorly

can be disseminated by insect vectors (Simmons and Munkvold 2014). Relevant alimentary crops such as cassava, potato, sweet potato, banana, apple, and citrus suffer different viral disease because of their vegetative propagation since the propagative material from an infected plant will give rise to a new cycle of infection on the newly developed plant tissue. Moreover, several species can be also transmitted by mechanical inoculation, penetrating the host cells through open wounds in the epidermis produced by human cultural activities like pruning, or by harsh environmental conditions like strong wind and hail. Mechanical transmitted viruses usually accumulate at high titers on infected tissues and present particularly stable virions capable to survive in the environment for long periods of time, and thus favoring their spread.

1.3.1 Vector-mediated transmission

The immobile nature of plants in combination with the cellulose barrier of their cells have pushed most phytoviruses to utilize plant-feeding insects to ensure their transmission and subsequent survival. This process is highly complex and requires the fine tuning of multiple molecular determinants from part of the virus, the host and the vector (Gutiérrez et al. 2013). Insect transmission can be classified into four main categories, depending on the time of interaction between the virus and its respective vector (Bragard et al. 2013).

First, we can differentiate the non-persistent transmission, where the virus is acquired and inoculated in short periods of time (seconds to minutes) while probing in the plant cells, for instance when selecting and choosing if a new plant is or not an adequate host. In this case, the virus does not require to pass along the vector´s inner body as it is probably retained in the surface of the anterior alimentary tract (Wang and Pirone 1999). To date, all identified viruses following this transmission mode are exclusively vectored by aphids (Whitfield et al. 2015). Interestingly, in some instances, additional viral encoded proteins are necessary for the completion of the process; an emblematic example is the HCPro of potyviruses that acts as a molecular bridge or accessory factor for the reversible retention of the virions to the vector´s mouthparts (Pirone and Blanc 1996).

A second mode, the semi-persistent transmission requires slightly longer acquisition and inoculation periods, that may range from minutes to some hours for the acquisition, and the vector can remain viruliferous for several days, requiring again from minutes to hours in order to inoculate the virus. Again, in this case the virus does not need to penetrate inside the cellular components of the vector since it is most probably attached and retained on the digestive apparatus, without a proper circulation through the body. A considerable amount of phloem-restricted viruses are transmitted in this mode since they require higher periods of feeding for their attachment to the vector´s mouthparts; a typical example are the criniviruses vectored by whiteflies (Singh et al. 2020). Historically both non-persistent and semi-persistent viruses were grouped together as non-circulative viruses, and they were also denominated as stylet- or cuticle-borne viruses since they are presumed to bind on the vectors cuticle and do not penetrate its cellular barriers. However, these names might not be directly applicable to other vectors, while the duration of acquisition, retention and inoculation phases appears as a better alternative criterion for classifying viruses as non-persistent and semi-persistent.

The third major category includes viruses transmitted in a circulative but non-propagative mode, requiring extensive acquisition and inoculation periods that may vary from hours up to several days, while the vector can maintain its viruliferous status throughout its lifespan. Although viruses of this category do not replicate inside the vector, they are able to move through the insect gut to the hemolymph until reaching the salivary glands for their subsequent transmission. Once acquired, they often require a latency time preceding their effective inoculation, a period needed for completing the circulation inside the body of the vector. Most viruses of this group are phloem-limited and belong to different families like the *Luteoviridae*, the *Geminiviridae* and the *Nanoviridae*, being disseminated by different vector species like aphids, whiteflies, leafhoppers, beetles and mirids (Gray et al. 2014).

The fourth and last category, includes the circulative and propagative transmission where the implicated viruses need long acquisition and inoculation periods (from hours up to days) and are capable to replicate

within their vector prior to their transmission, therefore using both the plant and the insect as hosts (Whitfield et al. 2015). Viruses within this category belong to taxonomical families encompassing members that in many cases can infect either animals or plants, like the *Bunyaviridae*, the *Rhaboviridae* and the *Reoviridae,* and in certain cases they can also be transmitted from the insect to its progeny. Evolutionary studies suggest that these viruses may have derived from insect-infecting ancestors that subsequently acquired the capacity to replicate and effectively infect plant cells as well (Hogenhout et al. 2008). One of the most devastating viral disease affecting crops worldwide, the disease caused by *Tomato spotted wilt virus* (TSWV, genus *Tospovirus*, family *Bunyaviridae*), is a well-studied case of a propagative and circulative virus that is acquired by larvae thrips (*Frankliniella occidentalis*) and transmitted by adult individuals that can retain the virus during their entire lifespan (Moritz et al. 2004).

Although the described modes of transmission are highly efficient and extraordinarily specific, many restrictive factors can interfere with these processes and viruses should constantly evolve sophisticated mechanisms to ensure their vector-mediated spread in nature (Gallet et al. 2018). Transmission is indeed a crucial step in virus ecology.

1.3.1.1 Aphids

Arguably aphids constitute one of the most successful insect vector organisms, given their ability to transmit multiple viral species belonging to several taxonomical families (Ng and Perry 2004). They are hemipteran insects, classified into the family *Aphididae* and comprise one of the most abundant groups of arthropods with worldwide distribution, especially in temperate regions. Out of 5000 identified species to date, about 100 of them are considered as a threat to agriculture, primarily because of their virus spread potential. A typical characteristic of aphids is the production of a carbohydrate-rich excretion called honeydew, that mediates a mutualistic relationship with ants. In exchange, aphids gain benefits from the ants, like protection to reduce the numbers of natural predators and

parasites, and also have lower risk of suffering fungal infections (Völkl et al. 1999).

Morphologically, aphids are composed by a tiny egg-shaped body ranging from 1-4 mm in length and divided into three anatomical regions, including the head, the thorax (prothorax, mesothorax and metathorax) and the abdomen (separated into 8 different segments). Both apterae and alate forms can be produced, often in response to environmental conditions when long-distance dispersal is required. Their development is ametabolous, following incomplete metamorphosis from egg to several nymphal stages and finally winged or wingless adults that can reproduce parthenogenetically for many generations, giving birth directly to nymphs. They present a pair of antennae on their head and their thorax bear three pair of legs (one pair/ per segment). Their color can be variable, but most species are green, yellow, or black. Their sap-sucking mouthparts allow them to ingest fluid through the proboscis (also known as stylet) via a pressure gradient. The stylet is a flexible tube that contains two different ducts, the food canal and salivary canal. The most distal part of the stylet, known as acrostyle, has been identified as the binding site of non-persistent viruses and it contains specific, non-glycosylated proteinaceous receptors that interact with intact virions or virus-encoded proteins that facilitate the virion binding (Jayasinghe et al. 2022). Aphids possess a number of specific biological features, rendering them into excellent vectors; 1) their ability of parthenogenesis that gives rise to abundant populations with brief lifespan (an embryonic mother carries several generations of growing embryos), 2) the evolution of polyphenism, producing both winged (alate) and non-winged (apterous) individuals and thus being able to disseminate in long distances, 3) a set of diverse feeding mechanisms, allowing them to colonize a broad range of plant hosts, 4) precise delivery of intact viruses into the host cell (Gadhave et al. 2020). The most common species vectoring plant viruses belong to the genera *Acyrthosiphon*, *Aphis*, *Macrosiphum* and *Myzus*, with *Aphid gossypii* (Clover) and *Myzus persicae* (Suzuki) being the most agriculturally relevant pests (Byers 2008). They can transmit different viral species persistently or non-persistently, depending on the genus of each specific virus; for instance, members of the genus *Potyvirus* or

Cucumovirus are transmitted in a non-persistent manner while member of the genus *Luteovirus* or *Polerovirus* are vectored persistently.

1.3.1.2 Whiteflies

Most viral diseases emerged during the last two decades are attributed to viruses spread by whiteflies (Navas-Castillo et al. 2011). To date, there are over 1500 identified species of whiteflies and among them the complex of species under the name of *Bemisia tabaci* (Gennadius; order *Hemiptera*, family *Aleyrodidae*) constitutes the most important agricultural pest because of its remarkable fitness and invasiveness in the environment, combined with an extensive host range (Martin and Mound 2007). *B. tabaci* was first detected by Gennadius (Gennadius, 1889) on tobacco plants in Greece and it is widely abundant in tropical and subtropical areas or in greenhouses of temperate regions. It infests over 600 cultivated or wild plant species, primarily belonging to the families *Cucurbitaceae*, *Euphorbiaceae*, *Malvaceae* and *Solanaceae* (Malka et al. 2021). They are commonly known with several denominations, such as the cotton, tobacco, or sweet potato whitefly and was presumably originated in Africa and subsequently spread to Europe and Asia, although some studies suggest that its origin might be traced in India or Pakistan, due to large abundance of natural predators in those regions (Brown et al. 1995). *B. tabaci* is not a single species but it forms a complex of at least 46 cryptic species, morphologically indistinguishable, with differences in biochemical and molecular level or in traits such as the number and type of host species, their ability to attract natural predators, their reaction to insecticides or their capacity to transmit viral species (De Barro 2012). Taxonomically they can be grouped into the distinctive cryptic species based on the analysis of the mitochondrial cytochrome oxidase I gene (3.5% of sequence divergence is the cryptic threshold determinant), with the Middle East-Asia Minor 1 (MEAM1, former B biotype) and the Mediterranean (MED, former Q biotype) isolates having the most widespread expansion and being the most invasive within the complex (Dinsdale et al. 2010). Their invasiveness is affected by several factors, among them the phenotype of their endosymbiotic bacteria while their survival is dependent on the obligatory symbiont *Portiera aleyrodidarum*,

since it synthesizes essential amino acids and carotenoids that the whitefly cannot produce (Baumann 2005). Morphologically, they are approximately 1-3 mm long, with a white-yellowish color and their body and wings are covered by a white powdery wax. Their life cycle is relatively short and may vary from three to five weeks, with adult individuals laying 200 up to 400 eggs during their lifespan. As a phloem-feeding insect, *B. tabaci* can provoke direct damage on its hosts by reducing their vigor or by the production of a honeydew subproduct, enhancing the development of a sooty mold and interfering with photosynthesis. Nonetheless, their major impact on cultivated crops is associated with their ability to transmit agriculturally relevant viruses that can lead to devastating viral diseases accompanied by important yield and financial losses (Navas-Castillo et al. 2014). *B. tabaci* can vector both DNA and RNA viruses, including species from the genera *Begomovirus*, *Crinivirus*, *Carlavirus*, *Ipomovirus* and *Torradovirus,* with begomoviruses posing the most serious threat, especially in terms of financial costs (Fiallo-Olivé et al. 2020). They can transmit both semi-persistent and persistent viruses, although in the second case it is still unclear whether the viruses can propagate inside the vector and this remains a matter of debate, especially in the case of the begomovirus TYLCV (Pakkianathan et al. 2015; Sánchez-Campos et al. 2016). Notably, a newly identified polerovirus, the *Pepper whitefly-born vein yellows virus* (PeWBVYV), was successfully transmitted by whiteflies, being the first member within the family *Luteoviridae* not vectored by aphids (Ghosh et al. 2019). The efficiency of the whitefly transmission of distinct viral species can be affected by several factors related to the vector and the virus; interestingly, experimental data have shown that some begomoviruses sharing the same geographical origin with their vector were transmitted at higher rates, as compared with other begomovirus-vector pairs for what their origins did not coincide (McGrath and Harrison 1995). As already mentioned on previous sections, sweet potato is affected by several viral disease caused by whitefly-transmitted agents, like the crinivirus SPCSV or the ipomovirus SPMMV, although in the latter case the vectoring capacity of whiteflies still remains a controversy not probed under experimental conditions (Valverde et al. 2004).

1.3.2 Viral infection process

Considering the size limitation imposed by their small genomes, viruses are required to fine-tune their genetic information and ensure the production of all the necessary components to surpass host defenses and establish a successful infection for subsequent propagation to new hosts. To do so, most viruses encode for multitasking proteins able to participate in several pathways during the infectious cycle and to interact in sophisticated ways with several host factors, ensuring viral viability (Revers and García 2015). Gene expression and virus replication are crucial steps for the generation of viral progeny to complete the infection cycle. Nonetheless, viruses lack a fully autonomous replication machinery and should leverage host components to precisely regulate their genome multiplication. Moreover, viruses should hijack their host's translational machinery to produce essential proteins for their survival, as they do not encode ribosomal proteins (Walsh and Mohr 2011). To better follow the necessary steps and factors required for the virus infectious process, we will focus on the example of the potyvirus infectious cycle (Ivanov et al. 2014), giving a brief overview of the different relevant processes (Figure I10).

The viral cycle starts when the virus arrives to a susceptible host, coming from a previously infected host. In the case of plant-to-plant spread of potyviruses this is mainly conducted by aphids in a non-persistent manner (Gadhave et al. 2020), therefore the infection process begins with the aphid-mediated inoculation of the filamentous virions inside the host cell, a process that requires both HCPro and CP proteins (Kassanis and Govier 1971; Pirone and Blanc 1996; López-Moya et al. 1999; Valli et al. 2018). Once inside the cytoplasm, the helical virions should be uncoated to reveal the RNA genome, for subsequent translation by the plant translational machinery. Potyvirus particles might carry other viral proteins in a minor proportion, such as the VPg, HCPro or CI, however the mechanisms behind the particles disassembly are only partially understood and a possible role (if any) for these minoritarian proteins are still unknown (Torrance et al. 2006; Gabrenaite-Verkhovskaya et al. 2008; Martínez-Turiño and García 2020).

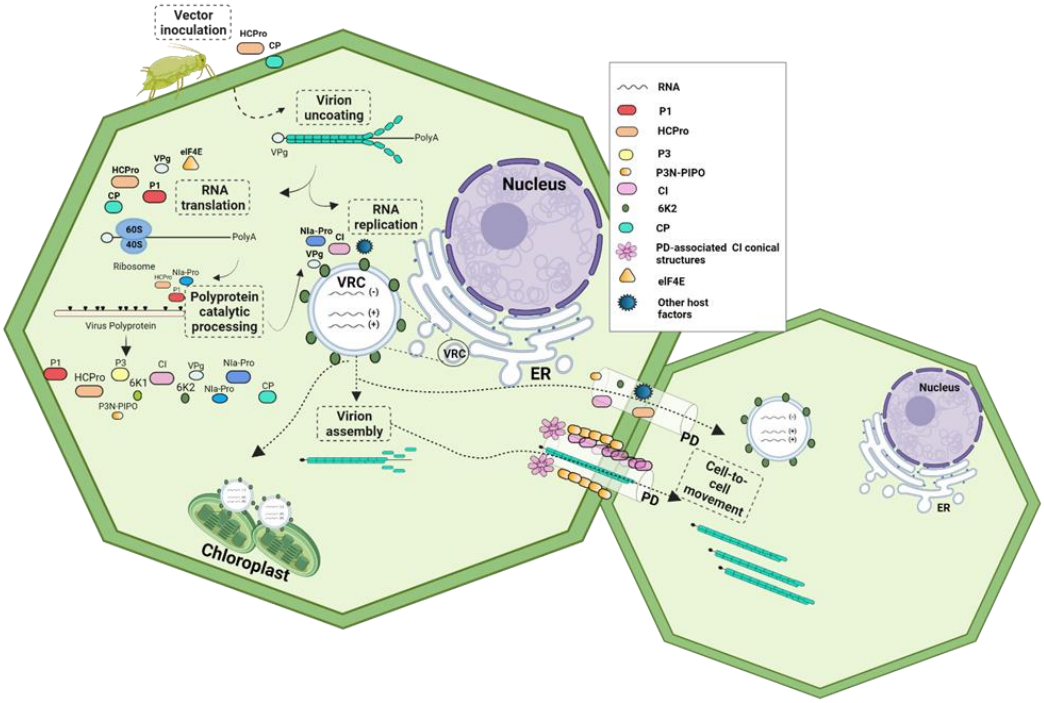

Figure I10. Schematic illustration depicting different steps of the potyviral infectious process. Virions are initially introduced into the host cell by aphid inoculation and undergo virion disassembly to release the viral RNA genome. Translation from the viral RNA occurs hijacking the host translation machinery, generating a large polyprotein that is proteolytically processed into up to ten mature gene products, plus at least one partially trans-frame protein resulting from polymerase slippage. RNA replication takes place within ER-derived membranous structures that hold the viral replication complexes (VRC), induced by 6K2 protein. A sub-population of active VRCs targets and moves towards the chloroplasts, where in some cases part of the RNA replication can occur. Another proportion of 6K2-mediated VRCs might be transported to plasmodesmata (PD) for movement to the adjacent cells, mediated by a set of interactions including the viral 6K2, P3N-PIPO, CI and different host factors. Finally, a proportion of viral progeny is encapsidated by multiple CP subunits and spread to the neighbor cells through PD, assisted by CI-conical structures connected to PD, P3N-PIPO and host factors. The illustrated structures are not represented to scale. (Image created with BioRender.com)

The two most prominent factors likely affecting virion uncoating include the physical perception of the cellular environment and putative interactions with still unknown host factors. Translation seems to occur concurrently with virus disassembly since the exposure of the 5´ genomic region suffices for the recruitment of the host translational machinery (Shaw et al. 1986), often mediated by the viral VPg protein, covalently linked to the viral genome 5´ end. Some potyviruses might be able to initiate translation by a direct interaction between their VPg and the host encoded elF4E translation factor (Beauchemin et al. 2007; Khan et al. 2008; Tavert-Roudet et al. 2017). Nonetheless, other members do not employ the same strategy and seem to follow other VPg-independent alternatives (Riechmann et al. 1989; Gallie 2001; Zeenko and Gallie 2005). Viral translation gives rise to a large polyprotein, proteolytically cleaved by three viral-encoded proteases, namely P1, HCPro and NIa-Pro. The first two proteins auto-process themselves at specific motifs located on their respective C-terminal regions, while NIa-Pro cleaves the rest of the seven virus-encoded products, being able to act in both cis and trans (Goh and Hahn 2021). During viral replication, potyviruses take advantage of their host´s cytoplasmic membranes since they multiply within membranous vesicles formatted by rearrangements of the endoplasmic reticulum (ER), a process primarily induced by the 6K2 protein (Schaad et al. 1997). Moreover, during their propagation they also seem to exploit the chloroplasts´ double-membrane structure, perhaps to evade hosts silencing, since chloroplasts seem to lack this defense mechanism (Bhattacharyya and Chakraborty 2018). Viral RNA amplification should be initiated with the generation of a negative strand template employed for the subsequent amplification of multiple copies of positive sense RNA, a process mediated by NIb, the viral RdRP (Hong and Hunt 1996). Most mature viral gene products are likely involved at some level in the replication machinery (Verchot and Carrington 1995b; Revers and García 2015); the VPg and the CI are essentially relevant during this process, the first acting as primer of amplification and the latter acting as a helicase, unwinding complementary RNA chains.(Lain et al. 1990; Puustinen and Mäkinen 2004; Ivanov et al. 2014). Different viral- and host-encoded proteins participate in replication, forming the viral

replication complexes (VRCs), the core components where replication takes place. These motile replication vesicles can move to plasmodesmata (PD) leveraging the cell secretory pathways and the virus can be transferred to adjacent cells through enlarged PD channels enabled, among other proteins, by CI-pinwheel structures (Patarroyo et al. 2013). Cell-to-cell trafficking of replication vesicles can be facilitated by interactions involving the viral proteins 6K2, P3, P3N-PIPO, CI and the hosts protein pCaP1 (Grangeon et al. 2013; Movahed et al. 2017; Chai et al. 2020). When the RNA progeny gets released from the VRCs it is subjected to three possible scenarios; first it can be targeted by the host RNA silencing machinery for degradation, a process counteracted by viral encoded RNA silencing suppressor proteins (RSS) such as HCPro or VPg (Kasschau and Carrington 1998; Anandalakshmi et al. 1998; Cheng and Wang 2017), second it can be translated through the plant machinery, assisted by VPg and P1 (Eskelin et al. 2011; Martinez and Daros 2014), and third it can be encapsidated by CP units to form fully assembled virions that could further disperse the infection to neighboring cells through PD (Rodríguez-Cerezo et al. 1997; Martínez-Turiño and García 2020). The exact location of replication and virion assembly within an infected cell has not been yet deciphered, however recent studies associated RNA packaging with RNA replication suggest a close link between the two processes (Gallo et al. 2018). Numerous experimental works have stressed the importance of CP in viral movement, as shown by the negative effect on cell-to-cell spread caused by certain CP mutations affecting virion assembly (Dolja et al. 1994; Dolja et al. 1995; Kežar et al. 2019; Hervás et al. 2020; Dai et al. 2020). Notably, CP mutations resulting in aberrant virions did not restrict the ability of potyviruses to spread systemically (Hervás et al. 2020; Dai et al. 2020). Yet, the role of fully assembled virions in potyvirus systemic movement remains largely elusive. Several studies support their active participation in systemic movement due to their presence inside vascular tissues, although authors reported the involvement of replication complexes as well (Otulak and Garbaczewska 2012; Wan et al. 2015). Overall, these studies imply the involvement of assembled particles in viral spread however do not necessarily reflect a strict dependence on them.

1.3.3 Virus-host-vector interactions

As strict intracellular parasites, plant viruses depend on the host cell for the completion of their life cycle and their subsequent propagation to uninfected plants. Therefore, many viral encoded proteins often interact with a multitude of host factors, leveraging different cell pathways in favor of their replication and spread to adjacent cells. These interactions are diverse and evolve continuously since plants, as sessile organisms, display a broad set of constitutive and inducible resistance layers for the recognition and containment of their pathogenic invaders. On the other hand, the attacking pathogens are also constantly evolving to circumvent these sophisticated host defenses, leading to a continuous arm-race between them (Nicaise 2014). When a virus is inoculated into the host cell, either through a natural vector or after mechanical wounding, there are two possible outcomes: 1) the virus will be recognized by the plant sensory machinery and diverse molecular responses will be activated to confront and restrict its propagation (often resulting in an incompatible interaction for the viral invader), or 2) the host will be unable to perceive the invasion signals and the virus will be able to reproduce and establish a successful infection overcoming the host defense machinery (a compatible interaction for the viral invader). Thus, the invaded host can be either resistant or susceptible to infection. In some cases of host-virus parasitic relationships, the infected plant presents only minor symptoms or damages while the virus replicates and moves readily; in those instances the host it is presumed as tolerant (Hammond-Kosack and Jones 1997). During the tripartite relationship among the plant, the virus and its insect vector, substantial physiological changes can occur in the first player, as a result of infection or vector feeding. These changes may be independent, synergistic or antagonistic in terms of attracting or repelling the insect vectors and favoring or impeding the viral transmission (Lefèvre et al. 2009; Blanc and Michalakis 2016). These interactions are extremely complex considering that each player can affect the others directly or indirectly and specific pathosystems may behave differently, lacking a generalized pattern. For instance, in the pathosystem established by CCYV-cucumber-*B. tabaci*, the vector fecundity is positively affected by feeding on infected plants (He et al. 2021). On the

other hand, in in the pathosystem composed by SRBSDV-rice-*Sogatella furcifera* it was shown that although virus transmission was enhanced, the fecundity and egg hatchability of the viruliferous vector were significantly reduced, compromising the viral spread in the long term (Xu et al. 2014). Moreover, pathosystems including hosts that are infected by multiple viruses can alter the insect behavior differentially compared to single infections, like the case of BYDV-cereals-*R. padi* (Minato et al. 2022). A large proportion of viruses are insect-borne; thus, transmission is an essential component of virus fitness. Viruses can modify the host traits to attract their potential vector, facilitating further their plant-to-plant dissemination. It has been long known that visual stimuli such as color (light green and yellow) and shape can affect the selection of a specific host by insect pests and virus-induced symptomatology is usually manifested with alterations of the foliage color, apparently attractive for hemipteran vectors (Li et al. 2016). Apart from the visual cues, plant-emitted volatile organic compounds (VOCs) have been also shown as an important factor for vector attraction and several viruses can modulate the production of such components, optimizing the transmission opportunities (Fereres et al. 2016; Chang et al. 2021). Of course, it should be taken into account that the effect of the olfactory cues on the vector´s alimentary behavior is dynamic and depends on the age of the infected plants and the disease progress (Rajabaskar et al. 2013). Notably, phytoviruses not only improve the host quality for increased vector fecundity and longevity (a frequent case for circulative viruses in genera tospo-, luteo- and geminivirus) but can also modulate negatively those traits to avert long feeding periods and consequently enhance the transmission efficiency of non-circulative viruses (Fereres and Moreno 2009). An emblematic example is the case of CMV (KCPG2 isolate)-infected squash plants that disturb the feeding process of *A. gossypii* or *M. persicae*, enhancing the rapid spread of the viruliferous insect to new uncolonized plants and viz increasing the virus transmission potential (Mauck et al. 2016). This approach is a typical example of the so-called ´pull-push´ strategy, where CMV firstly attract aphids by the emission of volatile cues and once the virus is ingested, it renders the plant less desirable or even repellent, forcing the movement of the vector to other plants and therefore

increasing the transmission efficiency (Carmo-Sousa et al. 2014). It has been widely observed that large densities of hemipteran insects concentrated on a host plant augment the generation of winged individuals, and this observation applies also in the case of certain virus-infected plants that increase the proportion of winged aphids due to overpopulations derived by improved fecundity or longevity. This case could be perceived as an indirect manipulation of the virus towards its vector phenotype that promotes higher emigration rates and consequently higher virus dispersal opportunities (Blanc and Michalakis 2016). Another important yet overlooked factor affecting the transmission of phytoviruses is the capacity of the vector to cross long distances and find the next adequate host for viral propagation. As it is conceived, the three-way relationship including the virus, the host and the vector is highly complex and multiple environmental factors can interfere along the way, however a better understanding of these processes is critical for the establishment of durable and effective control strategies.

1.3.4 Occurrence of mixed infections

A growing body of literature in combination with the advent of high-throughput technologies and metagenomics are revealing that the existence of mixed infections under natural conditions is the rule rather than the exception (Moreno and López-Moya 2020). This type of infection emerges by the co-existence and interplay between two or more viral agents affecting the same plant, arriving either simultaneously or at different timepoints. The moment at which the viruses are inoculated on the host is critical for the infection outcome; when two viruses infect the plant at the same time it is termed as co-infection, while when a virus infects a plant already infected with another virus it is termed as superinfection (Saldaña et al. 2003). The common occurrence of mixed infections can be partially explained by the fact that plant viruses are usually generalist, tending to infect multiple host and additionally are vectored by polyphagous insects, able to transmit more than a single virus to the same plant (Elena et al. 2009; Syller 2014). Co-infection between

unrelated viruses can yield different outcomes in terms of viral interactions, including synergism, mutualism, or antagonism that can directly affect the host plant traits (Syller 2012). The complexity that underpins these interactions is considerably high and predictions on each specific case may not be trivial. Indeed, there are certain cases where mixed infections result in severe disease phenotypes, causing significant yield and quality losses compared to single infections. Such an example is the well-studied case of the co-infection between the potyvirus PVY and the potexvirus PVX, generating a synergistic outcome, where the first viral player assists the replication of the second (Vance 1991). Moreover, the same outcome is observed when PVX is combined with different potyviruses like *Tobacco vein mottling virus* (TVMV) or *Tobacco etch virus* (TEV), indicating that this may be a signature for mixed infections including a potyvirus with an unrelated virus, where the potyvirus partner enhances the titers of the latter (Vance et al. 1995). This idea was further supported by subsequent studies that showed similar interactions in co-infections of other potyviruses with unrelated viral players (Zeng et al. 2007; Mascia et al. 2010). Notably, this is not the case for the co-infection between the potyvirus SPFMV and the crinivirus SPCSV, where the crinivirus apparently enhances the viral loads of the potyvirus (section 1.1.1). Another interesting case is the co-infection between the criniviruses *Tomato infectious chlorosis virus* (TICV) and *Tomato chlorosis virus* (ToCV), resulting in distinct viral accumulation patterns, primarily imposed by the host species in which they are inoculated (Wintermantel et al. 2008). Apart from the viral titers or the host traits and phenotype, mixed infections can also influence the vector attraction and feeding behavior and consequently the transmission of the implicated viruses. For instance, a co-infection between the potyvirus *Watermelon mosaic virus* (WMV) and the crinivirus *Curcubit yellow stunting disorder virus* (CYSDV) resulted in higher titers of the latter virus, coinciding with the kinetics of the previously explained examples, and additionally the study suggested that the presence of the potyvirus may positively influence the vector dissemination of the CYSDV (Domingo-Calap et al. 2020). Another example is the synergistic co-infection between the *Southern rice black-streaked dwarf virus* (SRBSDV) and the *Rice ragged*

stunt virus (RRSV) that resulted in higher acquisition rates of both viruses by their respective planthopper vectors (Li et al. 2014). Our current knowledge on the underlying interactions of mixed infections is disproportionate small given their frequency in natural and agricultural habitats (Roossinck 2015). These knowledge gaps underpinning the virus-virus interactions and their influence on the disease ecology and evolution should be gradually filled so that effective control strategies could be designed (Alcaide et al. 2020). For this reason, part of the present thesis has been focused on the exploratory study of the mixed infection between two common pathogens of sweet potato, using two different experimental hosts.

1.4 Plant defense responses

Plants are constantly challenged by the attack of multiple pathogens. Protection against microbial invasion is provided by diverse cellular and molecular pathways, including highly sophisticated mechanisms that perceive and respond against the attack. These responses can be divided in two categories: the passive and the inducible defense pathways. The first category includes physical or chemical barriers such as waxy cuticles or rigid cell walls, that act as a first protection layer, preventing the pathogen entry (Nishad et al. 2020). The second layer of protection is deployed once the pathogen is perceived through conserved molecular elements, known as pathogen-associated molecular patterns (PAMPs), recognized by specific receptors located on the plasma membrane that activate a general defense cascade, denominated as PAMP-triggered immunity (PTI) (Boller and He 2009; Saijo and Loo 2020). These pattern recognition receptors (PRRs) belong to receptor-like kinase (RLK) or receptor-like protein (RLP) families and play a crucial role in plant immunity (Tang et al. 2017). The activation of PTI induces downstream molecular processes, including the production of reactive oxygen species (ROS), the reinforcement of cells walls and the production of antimicrobial compounds to contain the infection (Lee et al. 2020). Nonetheless, many pathogens can escape the PTI by producing effector proteins directly secreted into the host cytoplasm, evading their recognition, or blocking the host defenses. In turn, plants have co-evolved resistance genes that give

rise to resistance (R) proteins that recognize the microbe effectors and elicit a robust defense response, known as Effector-triggered immunity (ETI). Accumulating evidence indicate that PTI and ETI share several signaling components and elicit similar qualitative transcriptomic changes (Lu and Tsuda 2021). Most R proteins have intracellular localization and belong to the nucleotide-binding site / leucine-rich repeat family of receptors (NLRs) while their activity is controlled by conformational changes (Monteiro and Nishimura 2018). After ETI induction, the microbial spread is often contained by a specific type of localized programmed cell death around the area of infection, known as the hypersensitive response (HR). RNA viruses encode for virulence factors (Avr proteins) that trigger HR or non-HR basal defense responses in resistant host plants while diverse viral proteins, including the coat, movement and replication protein can be recognized by the host cell NLRs and induce resistance against divergent viruses (Zvereva and Pooggin 2012). Generally, plants utilize diverse strategies to suppress viral replication and infection, including gene silencing, immune receptor signaling, hormone-mediated defense, protein degradation or metabolism reprogramming (Incarbone and Dunoyer 2013). Among those, the major mechanism implicated in viral immunity is the RNA silencing or RNA interference (RNAi), playing a pivotal role in plant-virus interactions (Guo et al. 2019).

1.4.1 Antiviral RNAi

All eukaryotes, including plants, appear to have evolved RNAi or RNA silencing as a conserved sequence-specific mechanism implicated in many key biological processes, from regulation of gene expression to genome protection against transposons and antiviral defense (Baulcombe 2004; Guo et al. 2016). The elucidation of RNAi was first initiated over 30 years ago, when researchers attempting to change the color of petunia flowers by transformation of a chalcone-synthase gene (pigmentation enzyme), obtained less pigmented or entirely white flowers due to ´co-suppression´ of homologous mRNAs sequences of the plant (Napoli et al. 1990). Moreover, the Nobel Prize-winning discovery of dsRNA-induced RNAi in invertebrates further advanced our understanding on this remarkable and tightly regulated mechanism (Fire et al. 1998).

Antiviral silencing is triggered by double-stranded RNAs (dsRNAs) with diverse origins, including highly structured viral RNAs, viral replicative intermediates, or de *novo* double-stranded molecules synthesized by host RNA-dependent RNA polymerases (RdRPs) (Zamore et al. 2000; Bass 2000; Hannon 2002). These dsRNAs are processed by the activity of Class 3 RNase III-type Dicer-like (DCL) enzymes into 21-24 nt small interfering RNAs (siRNAs), creating the core components of the silencing pathway (Deleris et al. 2006; Moissiard and Voinnet 2006). In the case of RNA viruses, primarily DCL4 cleaves viral dsRNAs into 21-nt siRNAs, whereas DCL2 occasionally generates 22-nt siRNAs (Pumplin and Voinnet 2013). The cleaved siRNAs get methylated in their 3´ terminal nucleotide by the action of the HEN1 protein, and then both strands of the methylated duplex are incorporated into endogenous Argonaute (AGO) proteins, forming the catalytic part of the RNA-induced silencing complex (RISC) which guides either the cleavage or translation inhibition of homologous mRNA sequences (Figure I11) (Vance and Vaucheret 2001; Carbonell and Carrington 2015).

Other important elements for the antiviral RNA silencing include the RNA-dependent RNA polymerases (RdRPs), implicated in the biogenesis of secondary viral siRNAs and promoting the spread of the silencing signal (Schwach et al. 2005; Qi et al. 2009; Donaire et al. 2009). Indeed, once the silencing is induced at single-cell level, it can spread to neighboring cells through plasmodesmatal channels, and systemically by mobile silencing signals, activating the defense cascade in the entire plant for host-resistance against the same or homology-related viruses (Llave 2010; Melnyk et al. 2011). Plants utilize RNA silencing to arrest the viral infection both directly (as illustrated in Figure I11) and indirectly, by leveraging endogenous sRNAs implicated in the regulation of specific genes that can elicit a more generic antiviral response (Carbonell and Carrington 2015). For instance, CMV infection in *A. thaliana* induces the production of abundant virus-activated siRNAs (vasiRNAs) that map on exons of multiple stress-related genes and guide the widespread silencing

of specific mRNAs to ultimately promote a broad-spectrum antiviral defense (Cao et al. 2014).

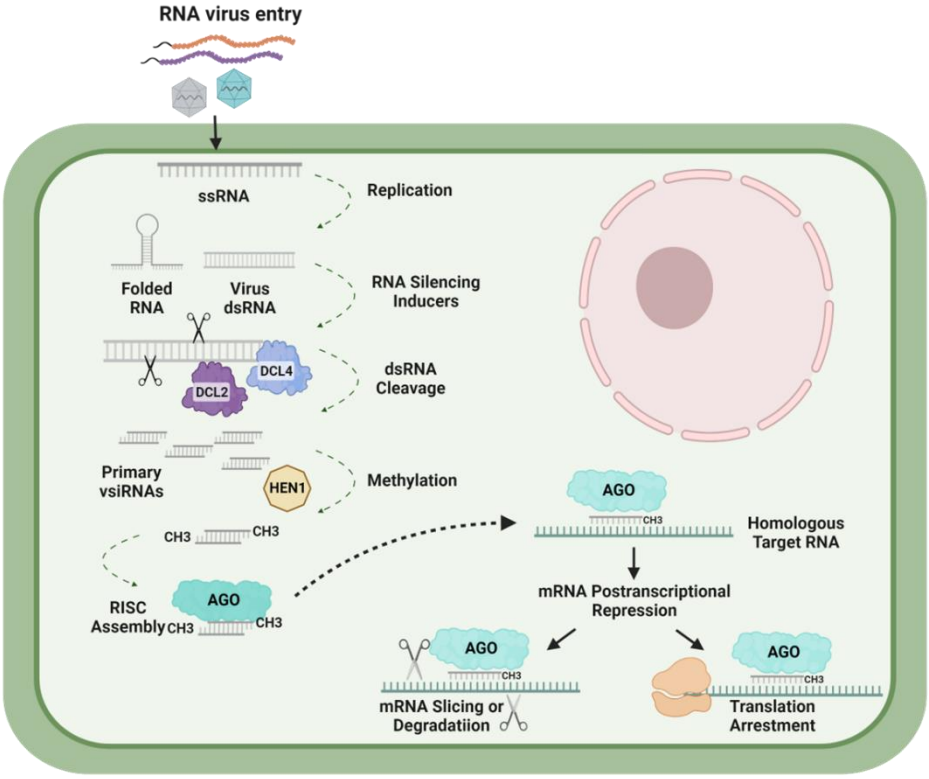

Figure I11. Scheme of the antiviral silencing mechanism induced by RNA viruses in plant cells. The pathway is triggered by virus-derived double-stranded RNAs, either replicative intermediates or secondary structured regions, that are recognized by RNaseIII-like enzymes of the Dicer family (DCLs) and processed into small interfering RNA duplexes of 21-24 nucleotides (siRNAs). Cleaved siRNAs are methylated next, and then recruited by Argonaute proteins (AGOs), forming part of the RNA induced silencing complex (RISC), which can either lead to the degradation of homologous RNAs in a sequence-specific manner, or to repress their translation. (Image created with BioRender)

1.4.2 Virus counter defense mechanisms

To fight and overcome the host defenses, plant viruses have co-evolved diverse strategies and often dedicate a substantial part of their small genomes to encode proteins devoted to suppress the antiviral RNA silencing (Csorba et al. 2015; Li and Wang 2019; Baulcombe 2022). It is noteworthy that virtually all known plant viruses encode at least one RNA silencing suppressor (RSS) protein, which can target the silencing pathway at different levels, acting specifically or at multiple stages of the pathway, being the dsRNA, the siRNA and the AGO proteins the most common targets. The capacity of an individual RSS to act at different stages or through diverse modes may induce a strong suppression of the plant defenses, seriously disturbing the host´s physiological processes, that may in turn compromise the virus replication and dissemination. Therefore, viruses should ensure an equilibrium between the suppression of the host defenses and their further propagation and survival. For this reason, they have developed mechanisms that can modulate the action of their RSS proteins through different subcellular localization or by differences in their suppression strength (Haas et al. 2008; Torres-Barceló et al. 2008). These proteins are highly divergent in terms of sequence, structure or mode of action among unrelated viruses, and therefore a multitude of studies have been dedicated for the identification and elucidation of their molecular functions (Lakatos et al. 2004; Lakatos et al. 2006; Chiu et al. 2010; Giner et al. 2010; Cheng and Wang 2017; Kenesi et al. 2017; Pollari et al. 2020; Kenesi et al. 2021). In mixed infections, the arrestment of the host RNA silencing pathway by one viral partner can benefit the fitness of the second virus and increase its virulence (Baulcombe 2022). Interestingly, the first identified viral RSS was the protease HCPro (Kasschau and Carrington 1998; Anandalakshmi et al. 1998). This is a multifunctional protein involved in many steps during virus infection, notably including silencing suppressor capacity (Lakatos et al. 2006; Lozsa et al. 2008; Valli et al. 2018). Initially, HCPro was thought to be the universal silencing suppressor of all potyvirids, however it was later shown that not all family members contain HCPro, and that not all HCPro are RSSs. Consequently, in some viruses of the family, the RSS function was taken by other gene products, such as the P1 serine protease of

certain ipomoviruses that either encode HCPro or are devoid of it (Janssen et al. 2005; Valli et al. 2006; Giner et al. 2010). The P1 protease was found to act as RSS also in other genera within the family, such as Tritimovirus or Poacevirus (Young et al. 2012; Tatineni et al. 2012; Bagyalakshmi and Viswanathan 2020). The notion of HCPro being the most usual RSS was further questioned, at least in certain members of the genus *Potyvirus*, when two independent studies showed that a transframe gene product named P1N-PISPO, generated by polymerase slippage in SPFMV, but not HCPro, exhibited antisilencing–capacity in standard co-agroinfiltration assays (Mingot et al. 2016; Untiveros et al. 2016). Nonetheless, a subsequent study not only revealed that SPFMV HCPro works as RSS in a PVX-based system, but also questioned the common use of co-agroinfiltration assay as the solely required test to assess whether or not a protein is able to block RNA silencing (Rodamilans et al. 2018). As an additional case, when a newly identified Arepavirus encoding two HCPros in tandem was described, only HCPro2 was shown to exhibit antisilencing activity (Qin et al. 2020). The remarkable variability of genomic arrangements of different gene products in potyvirids have been reviewed recently, illustrating the complexities of non-core elements involved in the arrestment of RNA silencing function (Pasin et al. 2022). Given the huge variability of factors expressed by potyvirids from their 5' end of their genomes, part of this thesis intends to elucidate which proteins of the potyvirus SPV2 contribute to the RSS function. As mentioned, this virus is different to the best studied SPFMV, but it shares many genomic features, including the presence of PISPO.

1.5 Virus-like particles (VLPs)

During the last three decades, the advent of synthetic plant virology has led to some emblematic advancements and breakthroughs towards the application of viruses in medicinal and agricultural nanobiotechnology. The use of biological nanomolecules with certain sizes and specific biophysical properties, like plant viruses or their virus-like particles (VLPs) has increased exponentially due to their great potential and versatility in a broad range of biotechnological applications (Steele et al. 2017). VLPs are highly ordered, proteinaceous structures, that resembles the natural

virion morphology but are devoid of the genetic material necessary for infection and therefore cannot replicate. They can be evoked as ´empty shells´ that share the same three-dimensional properties and immunochemical characteristics with their parent virions (Ding et al. 2018). As for native viruses, we can differ two basic classes of VLP symmetry: the helical and the icosahedral, both composed by repetitive units of the capsid protein/s (Caspar and Klug 1962). Their extensive use in nanobiotechnological platforms is primarily attributed to their highly defined structures accompanied by homogeneity, their considerable degree of flexibility, facilitating their functionalization with diverse types of molecules and their capacity to self-assemble in a variety of heterologous systems (Narayanan and Han 2018). Moreover, plant-virus based VLPs are particularly attractive for applications in nanomedicine since they display a lower risk for human health or the environment as they derive from pathogens not affecting humans or animals, and furthermore they lack infectivity, facilitating their handling and transportation (Balke and Zeltins 2020). Early studies on TMV assembly showed that the isolated coat protein and the viral RNA were able to reconstitute infectious virions *in vitro*, launching for the first time the concept of virus ´self-assembly´ (Fraenkel-Conrat and Williams 1955). Ever since, the coat protein of diverse plant viruses has been shown to self-assemble and form VLPs *in vitro*, including the extensively studied TMV (Butler 1999). Several VLPs types have been produced using heterologous approaches, through transient expression of viral structural protein/s in plants, insects, yeast, or mammalian cells (Kushnir et al. 2012). Among those, the use of plants as a production platform for VLPs and other recombinant proteins has undergone through important advances since they present several advantages in terms of costs, labor and time efficiency (Sainsbury and Lomonossoff 2014). Icosahedral or filamentous VLPs of different plant viruses have been readily produced *in planta* using replicating or non-replicating viral vectors and *Agrobacterium*-mediated delivery (Peyret and Lomonossoff 2013; Mardanova et al. 2017). Interestingly, certain helical rod-shaped VLPs from potexviruses like *Alternanthera mosaic virus* (AltMV), were produced in significantly higher amounts in the presence of a RNA scaffold of vector origin, and the VLPs of other viruses such as the

potyvirus SPFMV and the ipomovirus CVYV were obtained as well (Thuenemann et al. 2021). The extraordinary structural symmetry of helical phytoviruses renders them as excellent candidates in vaccine development since they can be readily engineered to expose immunogenic epitopes on their surface and can easily adapt in diverse conditions. Moreover, they can have an enhanced immunostimulatory effect in humans and animals since their structural components (repetitive units of CP) are phylogenetically and immunologically distant to the mammalian immune system (Denis et al. 2007). An increasing list of plant viruses and VLPs have been explored as potential candidates in the generation of novel vaccine candidates, including AMV, CPMV, CCMV, CMV, BaMV, PaMV, PVX, PVY, TBSV, TMV and ZYMV, while the ongoing research is actively progressing (Balke and Zeltins 2020). As our knowledge on the detailed structure of plant viruses is constantly increasing, their application spectrum is consequently expanding and apart from their utility as vaccine substrates or adjuvants, they have been employed as fluorescent markers, biocatalysts, nanoparticles for bioimaging or biologics purification and nanowires among others (Ibrahim et al. 2019; Evtushenko et al. 2020). Despite their remarkable potential, the atomic structural architecture of plant viruses and their VLPs is comparatively less studied than other virus features, and detailed structural data are necessary for the elucidation of the molecular mechanisms behind essential biological functions like vector-mediated transmission or the improvement of their potential nanobiotechnological applications.

1.6 Electron microscopy (EM) and the new era of cryo-EM

Microscopy has been one of the most groundbreaking techniques in the history of biology. Structural biology, the branch of biology that studies the structural conformation of macromolecules has substantially aided in the elucidation of major biological discoveries, continuously promoting improvements to many medicinal and agricultural challenges (Shi 2014). Given their precise size and high symmetry, plant viruses have been appropriate tools in the advancement of structural biology and the development of rigorous imaging techniques such as electron microscopy

(EM) or cryo-electron microscopy (cryo-EM). The use of the first electron microscope started in the early 1940s and its invention led to the Nobel Prize in Physics in 1986, awarded to Ernst Ruska, who along with Max Knoll built the equipment in 1931. Although the EM shares basic operational principles with the conventional light microscopy, it generates significantly higher resolution images since it uses electron beams with smaller wavelengths than visible light (100.000-fold shorter than photons). This feature facilitates magnifications of up to 2 million times, achieving subnanometer resolutions and rendering it as a remarkably valuable equipment for the analysis of nearly every cellular component or nanoscale pathogen, like plant viruses (Winey et al. 2014). Basically, it is composed by an electron source/gun and different sets of electromagnetic lenses, including condenser, intermediate and projector lenses that control and focus the high-voltage electrons into a fine beam. Briefly, the electrons are fired by the electron gun at a specific voltage and the condenser lenses direct the electron beam into the fixed sample. Then, the accelerated electrons interact and pass through the sample, although most of them simply cross the specimen without interaction (unscattered electrons). Subsequently, the small fraction of the scattered electrons transverse through the objective lens, that will create the initial image which will be then magnified by the projector lenses and will be sent on a fluorescent screen located at the bottom of the microscope or to a detector (direct detection camera) that will eventually generate the final image (Miranda et al. 2015). Despite its potential, one of the main limitations of EM is the specimen fixation preceding the analysis, limiting its use to only ´deceased´ biological samples. Moreover, high ionizing radiation (like electrons) can provoke damage, potentially leading to structural and compositional alterations of the tested sample. Another drawback is the sample dehydration resulting from the microscope column vacuum, potentially causing structural changes as well. These limitations impede the generation of high-resolution structures using micrographs by conventional EM. To overcome these constrains, the advent of cryo-EM revolutionized the field of structural biology. The first conceptualization of this technique was made over 40 years ago, when it was showed that sample freezing preceding EM analysis could preserve the hydrated state

of the sample and therefore hinder the vacuum dehydration (Taylor and Glaeser 1974). Additionally, frozen specimens tolerate better the ionizing radiation, resulting in better image resolutions. Therefore, novel protocols including sample freezing in liquid ethane (previously cooled with liquid nitrogen) were developed, resulting in the formation of vitreous ice (non-crystalline-amorphous state) that encompasses the hydrated sample intact (Dubochet et al. 1982; Dubochet 2012). Cryo-EM generates 3D maps of macromolecules at near-atomic resolution, in combination with image processing and 3D reconstruction techniques, allowing virus structural studies not only in their physiological state but also in biologically relevant environments within a short timeframe (Castón 2013). The cryo-EM imaging uses classical electron microscopes that have been adapted for the preservation and processing of the cryo samples. The 3D reconstruction of the tested macromolecule derives by computational merging of multiple (hundreds to thousands) sample images, taken from different angles while different conditions during the vitrification (pH, ions etc.) can permit precise definition of the viral assembly process (Luque and Castón 2020). Cryo-EM is an optimal imaging technique for highly symmetrical macromolecules like viruses or VLPs, however in the case of small proteins with sizes below 50 kDa it can exhibit some limitations that could be circumvented by the design of a scaffold bearing several copies of small proteins (Liu et al. 2019). In recent years, the quantity of cryo-EM resolved structures has been exponentially growing and the protein with the highest resolution achieved to date is apoferritin, at 1.25 Å (Yip et al. 2020). Although cryo-EM complements other high-resolution imaging techniques like X-ray crystallography or nuclear magnetic resonance (NMR), its advantage in terms of near-atomic resolution analyses, time effectiveness or sample amount, renders it the most adequate choice in structural virology (Jiang and Tang 2017). An example of a high resolution structure obtained by X-ray fiber diffraction is the tobamovirus TMV, which was resolved at 2.9 Å, thanks to its high symmetry and rigid nature (Namba et al. 1989). The structures of other members within the same genus have also been reported (Luque and Castón 2020). However, the structural definition of flexible helical viruses has been considerably more challenging given their intrinsic flexibility that precludes to some extent

high resolution data. Nonetheless, thanks to improvements in cryo-EM and reconstruction algorithms, the precise structure of flexible filamentous viruses was also achieved, with WMV being the first virus of the family *Potyvirida*e with a resolved structure at 4.0 (Zamora et al. 2017). Previously, other flexuous viruses belonging in family *Alphaflexiviridae* had been resolved at near-atomic resolution (DiMaio et al. 2015; Agirrezabala et al. 2015). Since then, two more potyvirus structures, TuMV and PVY, have been also reported (Kežar et al. 2019; Cuesta et al. 2019) providing more structural insights regarding the members of the genus. Moreover, recent cryo-EM studies revealed the near-atomic structures of two additional potexviruses, the AltMV and PVX, further enhancing our knowledge on flexuous filaments (Grinzato et al. 2020; Thuenemann et al. 2021). Overall, the reported viruses or their respective VLPs, present a similar structural organization, forming left-handed helices, composed by 8.8 subunits per turn. The atomic structure of

CPs revealed a main core with helical folding, surrounded by two unstructured terminal parts, the N- and C- termini. Interestingly, CPs of both families contain a conserved region that interacts with the ssRNA and is located within a cavity between the main core and the C-terminus. The ssRNA binding pocket contains several amino acid residues that seem to be conserved in the same position among members of different families of flexuous helical plant viruses (Yang et al. 2012; DiMaio et al. 2015; Agirrezabala et al. 2015; Zamora et al. 2017; Kežar et al. 2019; Cuesta et al. 2019; Grinzato et al. 2020). Despite the considerable amount of structural data regarding several plant viruses, our knowledge is still limited. The third chapter of the present thesis aims to fill this knowledge gap and to provide further structural insights regarding sweet potato viruses using two potyvirids that employ different vector organisms for their transmission.

OBJECTIVES

2. Objectives

The general goal of the present thesis consists in the elucidation of aspects underpinning the infection and transmission mechanisms of different sweet potato viruses, with special attention to their mixed infections. To accomplish this goal, we contemplated the following specific objectives:

1. Comparison of two isolates of the ipomovirus SPMMV in single and mixed infections with one isolate of the crinivirus SPCSV in *N. tabacum* and *I. nil* plants, with special attention to virus accumulation and distribution along the progress of the infection.

2. Exploration of the host range of the crinivirus SPCSV and characterization of possible virus reservoirs.

3. Identification and functional characterization of proteins conferring RNA silencing suppressor activity among those encoded by the potyvirus SPV2.

4. *In planta* production and purification of virus-like particles of two sweet potato potyviruses, SPFMV and SPV2, and one ipomovirus, SPMMV.

5. Structural characterization of VLPs corresponding to SPFMV and SPMMV by cryo-electron microscopy.

MATERIALS & METHODS

3. Materials & Methods

3.1 Biological material

3.1.1 Virus

Four different plant viruses have been used for the experiments included in the present work (Table M1). Taxonomically they are two potyviruses, one ipomovirus and one crinivirus.

The potyvirus isolates SPFMV-AMMB2 and SPV2-AMMB2 were identified by previous laboratory members (Mingot et al. 2016) after performing RNA-seq analysis using samples of commercially acquired sweet potato (*Ipomoea batatas*) plants. The original virus source was acquired back in 2013, and the viruses were maintained by vegetative propagation in CRAG greenhouse facilities since then.

Two different isolates of the ipomovirus SPMMV, denominated 0900 (DSMZ virus collection, Germany) and 130 (kindly provided by Prof. Jari Valkonen, University of Helsinki, Finland), have been maintained as desiccated leaves and propagated occasionally to plants of *N. tabacum* cv. xhanthi by mechanical inoculation, giving them periodical passages in CRAG greenhouse facilities.

The crinivirus SPCSV-Can181-9 isolate was kindly provided by Dr. Jesús Navas (IHSM La Mayora, Málaga, Spain) in an infected *Ipomea setosa* plant. It was transmitted by *Bemisia tabaci* whiteflies to *Ipomea batatas* plants and maintained through vegetative propagation.

Table M1. Sweet potato-infecting viruses used during the present thesis.

Virus	Genus	Family	Genome
Sweet potato feathery mottle virus (SPFMV)	*Potyvirus*	*Potyviridae*	(+)ssRNA-monopartite
Sweet potato virus 2 (SPV2)	*Potyvirus*	*Potyviridae*	(+)ssRNA-monopartite
Sweet potato mild mottle virus (SPMMV)	*Ipomovirus*	*Potyviridae*	(+)ssRNA-monopartite
Sweet potato chlorotic stunt virus (SPCSV)	*Crinivirus*	*Closteroviridae*	(+)ssRNA-bipartite

3.1.2 Plants

Virus infected (with SPFMV, SPV2 or SPCSV) and non-infected plants of *Ipomoea batatas* were maintained by vegetative propagation and kept at greenhouse growing conditions (28/24°C, 16/8 light/darkness).

Virus-free seeds of *Ipomoea nil* and *Ipomoea setosa* were kindly provided by Dr. Jesús Navas, (IHSM La Mayora, Málaga, Spain) and maintained for at 4°C for long-term storage. The seed germination was performed *in vitro* under controlled conditions (28 °C, 16/8 h light/darkness) using a scarification procedure with a razor blade to facilitate hydration. After emergence of cotyledons, they were transplanted into individual pots and placed in growing chambers at 24-26 °C, 16/8 h light/darkness and 60% of relative humidity.

Plants of *Nicotiana benthamiana* were maintained at temperatures ranging from 22-28 °C, 16/8 h light/darkness and 50-65% of relative humidity. Plants of *Nicotiana tabacum* cv. xanthi and *Solanum melongena* were used for rearing virus-free colonies of the green peach aphid *Myzus persicae* and the whitefly *Bemisia tabaci*, respectively. They were grown

from seeds (provided by CRAG greenhouse service) and maintained under the same growing conditions as *N. benthamiana* plants.

Eleven different plants species, belonging to four botanical families were used for SPCSV host susceptibility assays. Details of the used plant species and their growth conditions are given in the table M2.

Table M2. Plant species used to explore susceptibility towards SPCSV infection.

Plant species	**Family**	**Growth conditions**
Ipomoea batatas	*Convolvulaceae*	28/24°C, 16/8 light/darkness
Ipomoea nil	*Convolvulaceae*	28/24°C, 16/8 light/darkness
Ipomoea setosa	*Convolvulaceae*	28/24°C, 16/8 light/darkness
Nicotiana benthamiana	*Solanaceae*	28/22°C, 16/8 light/darkness
Nicotiana tabacum cv. xhanthi	*Solanaceae*	28/22°C, 16/8 light/darkness
Solanum melongena L.	*Solanaceae*	28/22°C, 16/8 light/darkness
Solanum lycoprsicum	*Solanaceae*	28/22°C, 16/8 light/darkness
Cucumis melo	*Cucurbitaceae*	28/24°C, 16/8 light/darkness
Cucurbita pepo	*Cucurbitaceae*	28/24°C, 16/8 light/darkness
Cucurbita maxima	*Cucurbitaceae*	28/24°C, 16/8 light/darkness
Arabidopsis thaliana	*Brassicaceae*	24/20°C, 16/8 light/darkness

3.1.3 Natural virus vectors

3.1.3.1 Aphids

The green peach aphid (*Myzus persicae*-MP89) colony used for transmission assays was provided by Dr. A. Fereres (ICA/CSIC, Madrid,

Spain). Aphid colonies have been reared on *N. tabacum* plants cv. xhanthi and maintained in chambers with controlled environmental conditions (23/20°C, 16/8 hours light/darkness).

3.1.3.2 Whiteflies

The MEAM1 and MED biotypes, previously designated as B and Q (Polston et al. 2014), of *Bemisia tabaci* (Gennadius) have been used as vectors during transmission experiments of the phloem-limited crinivirus SPCSV and in attempts to transmit the ipomovirus SPMMV. MEAM1 and MED individuals were provided respectively by Dr. R. Gabarra (IRTA, Cabrils, Spain) and by personnel of Semillas Fitó company (collected in melon plants grown in Almería, Spain). In the laboratory the two biotypes were reared separately on *Solanum melongena* plants and maintained in chambers with constant environmental conditions (25°C, 16/8 hours light/darkness).

3.1.4 Bacterial strains

3.1.4.1 *Escherichia coli*

TOP10 strain of *E. coli* was used routinely for transformation, multiplication, and purification of plasmids constructs. Also, the DH5a strain was occasionally tested when TOP10 transformation resulted in low efficiency. Both strains were grown at 37°C in LB medium (10 g/L triptone, 5 g/L yeast extract and 10 g/L NaCl; Agar 15 g/L was complemented for preparation of solid medium) supplemented with appropriate antibiotics depending on the resistance genes for each specific plasmid. *E. coli* clones were grown in culture and kept at -80°C for long-term storage in 25% glycerol preparations.

3.1.4.2 *Agrobacterium tumefaciens*

Several strains of *A. tumefaciens* were used for different purposes. EHA 105 strain was used for the Gateway™ destination plasmids. For expression of the chimeric PVX-SPV2 constructs, GV3101 carrying the helper plasmid pJIC_Sa_Rep was employed, and LBA4404 strain was

used for transient expression of the pEff-generated constructs. All *Agrobacterium* cultures were grown at 28°C during 48 hours in YEB medium (5 g/L beef extract, 1 g/L yeast extract, 5 g/L peptone, 5 g/L sucrose, 0.48 g/L $MgCl_2$) containing the appropriate antibiotics for selection of plasmids, with 15 g/L agar added for preparation of solid medium. Transformed *A. tumefaciens* were kept at -80°C for long-term storage in 25% glycerol preparations.

3.1.5 Plasmids and cloning vectors

A set of viral and/or binary vectors have been employed for cloning and expression of constructs (Table M3). The pGEM T Easy vector system (Promega, United States) served for directional cloning of RT-PCR amplified products, primarily for the generation of templates used for *in-vitro* transcription. Gateway technology (Invitrogen, United States) was used to generate plasmids starting with pENTRY/D-TOPO and different pDEST constructs for recombination (Tanaka et al. 2011). An engineered PVX-based viral vector (Valli et al. 2008), denominated pGWC-PVX, was kindly provided by Dr. Adrian Valli (CNB, Madrid, Spain). The PVX-based self-replicating pEff vector (Mardanova et al. 2017; Thuenemann et al. 2021) was used for transient expression of the coat proteins (CPs) of different viruses to assembly VLPs.

Table M3. Generated expression constructs for experimental purposes of the present thesis dissertation.

Generated construct	Vector	Cistron	Virus origin
pENTR-P1-SPV2	pENTR/D-TOPO	P1	SPV2
pENTR-P1ONLY-SPV2	pENTR/D-TOPO	P1ONLY	SPV2
pENTR-P1N_PISPO-SPV2	pENTR/D-TOPO	P1N-PISPO	SPV2

pENTR-HCPro-SPV2	pENTR/D-TOPO	HCPro	SPV2
pENTR-P1HCPro-SPV2	pENTR/D-TOPO	P1HCPro (*cis*)	SPV2
pGWB702Ω-P1-SPV2	pGWB702Ω	P1	SPV2
pGWB702Ω-P1ONLY-SPV2	pGWB702Ω	P1ONLY	SPV2
pGWB702Ω-P1N_PISPOY-SPV2	pGWB702Ω	P1N-PISPO	SPV2
pGWB702Ω-HCPro-SPV2	pGWB702Ω	HCPro	SPV2
pGWB702Ω-P1HCPro-SPV2	pGWB702Ω	P1HCPro	SPV2
pGWB718-P1-SPV2	pGWB718	P1	SPV2
pGWB718-P1ONLY-SPV2	pGWB718	P1ONLY	SPV2
pGWB718-P1N_PISPOY-SPV2	pGWB718	P1N-PISPO	SPV2
pGWB718-HCPro-SPV2	pGWB718	HCPro	SPV2
pGWB718-P1HCPro-SPV2	pGWB718	P1HCPro (*cis*)	SPV2
PXV-P1-SPV2	pGWC-PVX	P1	SPV2
PXV-P1ONLY-SPV2	pGWC-PVX	P1ONLY	SPV2

PXV-P1N_PISPO-SPV2	pGWC-PVX	P1N-PISPO	SPV2
PXV-HCPro-SPV2	pGWC-PVX	HCPro	SPV2
PXV-HCPro-WMV	pGWC-PVX	HCPro	WMV
pGEM-P1-SPMMV130	pGEM T Easy	P1	SPMMV 130
pGEM-P1-SPMMV0900	pGEM T Easy	P1	SPMMV 0900
pGEM-CP-SPMMV0900	pGEM T Easy	CP	SPMMV 0900
pGEM-Poly1-RNA1-SPCSV	pGEM T Easy	Polyprotein1	SPCSV
pGEM-HSP70-RNA2-SPCSV	pGEM T Easy	HSP70	SPCSV
pGEM-GFP	pGEM T Easy	GFP	-
pEff-CP-SPFMV	PVX-based pEff	CP	SPFMV
pEff-CP-SPV2	PVX-based pEff	CP	SPV2
pEff-CP-SPMMV	PVX-based pEff	CP	SPMMV 130

3.2 Virus and vector manipulation

3.2.1 Mechanical inoculation

SPV2 and SPMMV (isolates 130 and 0900) were periodically inoculated to *N. benthamiana* and *N. tabacum* plants, respectively. Mechanical inoculation involved several steps. Briefly, abrasive carborundum was powdered on leaves of plants (about 2 weeks old) to wound the epidermal cells and therefore facilitate the virus entrance when an extract of infected sap was smoothly rubbed on the leaf surface. The inoculation sap was prepared by grinding 1 part of a previously infected plant (such as leaves exhibiting viral symptoms) with 2 parts of phosphate buffer (0.02M, pH 7.2) using a cooled mortar to enable the homogenization. Active carbon was also added to the homogenate to facilitate infection. After inoculation, plants were covered with wet tissues and let to recover overnight before moving to the greenhouse or growth chambers under controlled conditions (28/22°C, 16/8 light/darkness) until they presented characteristic viral symptoms, usually 10-12 days after inoculation for SPV2, and 5-7 days for SPMMV.

3.2.2 Transmission mediated by insect vectors

3.2.2.1 Aphid mediated non-persistent transmission

Green peach aphids (*Myzus persicae*) were used for transmission of potyviruses, in particular SPV2 (Figure M1). Insects were starved for 2 hours in a glass vial before allowing to feed for 10 minutes on virus infected leaves for virus acquisition, and gently moved with a paintbrush to test plants for virus inoculation, allowing them to feed for at least 30 minutes. After the inoculation period, aphids were eliminated by insecticide spraying with a freshly prepared solution of Confidor (active substance: imidacloprid, following the recommendation of the provider). Plants were observed for symptoms and tested for virus infection after 12 days post inoculation (dpi) by RT-PCR using specific primers to confirm infections.

Figure M1. Aphid-mediated transmission process of SPV2 from infected *I. batatas* to *N. benthamiana* plants.

3.2.2.2 Whitefly mediated semi-persistent transmission

Whitefly *B. tabaci*, MED biotype, was used to explore transmissibility of the phloem limited SPCSV to susceptible hosts. Insects reared on virus-free plants were collected in 20 ml tubes using a vacuum suction device and moved to SPCSV-infected *I. batatas* for virus acquisition for 48 hours. After this acquisition period, viruliferous whiteflies were collected and released on plants of different species, allowing them to feed during another 48 hours for virus inoculation. Then the insects were eliminated by insecticide treatment with Confidor (Imidacloprid), as described for aphids. Plants were observed and tested for virus infection by RT-PCR after 15 days dpi using specific primers.

3.2.2.3 Generation of mixed infections

To produce double infections of SPMMV (isolates 130 or 0900) and SPCSV in plants of *N. tabacum* or *I. nil,* first SPMMV was inoculated mechanically on healthy plants as described above, and then SPCSV viruliferous whiteflies were released on those plants and allowed to feed during 48 hours inside insect-proof cages for virus transmission. By the end of the transmission period, the plants were sprayed with insecticide Confidor (Imidacloprid). Characteristic symptoms of SPMMV were observed at around 7 dpi, and then the plants were tested for SPCSV presence by RT-PCR at 12 dpi, using specific primers to confirm mixed infections.

3.2.3 Insect-choice bioassays in Y-tube olfactometer

To evaluate whether volatiles cues emitted by plants affect the choice of insect vectors, an olfactometer (Figure M2) was used, consisting in a Y-shaped tube (stem: 28 cm long, arms: 28 cm long) connected with two separated glass chambers (height: 40cm, diameter: 20cm) via silicon tubes (Analytical Research Systems, Gainesville, USA). One test plant (non-, single-, or mixed-infected) was placed inside each chamber, creating a purified airflow through connections between an air delivery system and the two separated chambers. The choice experiments were performed with a total number of 40 non-viruliferous adult whiteflies (males and females) that were collected using a handmade-vacuum apparatus and starved for one hour before the tests. Every individual whitefly was immobilized by placing in ice for 15 seconds and subsequently released on the intersection of the Y-tube, while an input flow (0.3 liters/minute) was being delivered from the glass chambers to the Y-tube, enabling the volatiles of each test plant to reach the intersection, and thus allowing the whitefly to move inside one of the arms, making a choice based on odor stimuli. A choice was determined only when the whitefly surpassed a longitude of 6 cm or higher into one of the arms and remaining there for at least 3 minutes. In case a whitefly did not have a specific preference after 15 minutes on the intersection zone, it was eliminated from the assay and replaced with another. To avoid any possible visual stimuli interfering with the assay, the glass chambers were covered externally with white bench paper. Also, to ensure that the observed choices were not attributed to any preferred spatial orientation, the plants were systematically switched (every 3 hours) among the two chambers. The environmental conditions during the experiments were maintained consistent with light intensity at 250 μmol·s−1m−2, temperature at 28-30 °C and relative humidity at 70%.

a) b)

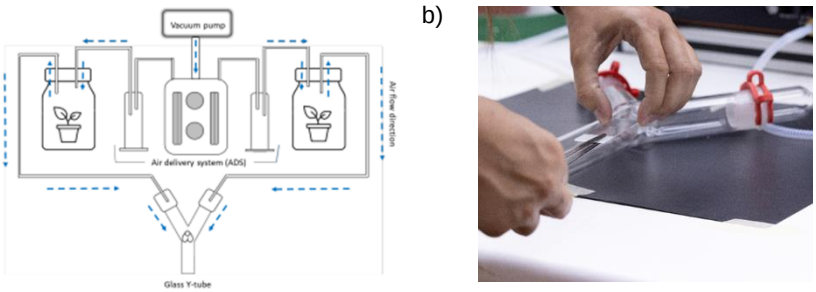

Figure M2. a) Schematic drawing of the olfactometer used for evaluation of insect choices in response to plant emitted volatile cues. Air flow directions are indicated by blue arrows. (Illustration created by Irene Ontiveros). b) Olfactometer Y-section tube, showing the position where each whitefly is deposited before choosing the right or left direction.

3.3 Nucleic acid manipulation

3.3.1 Plant RNA extraction

RNA extraction of plant samples was done using TRizol reagent (Invitrogen, United States), following the manufacturer's instructions. Briefly, 100 mg of leaf tissue was frozen in liquid N_2 and ground in a Tissue Lyser machine (QIAGEN, Germany), before adding 1 ml of Trizol for vortex homogenization with additional 200 µl of chloroform, centrifugation, and collection of the aqueous upper phase. The nucleic acids were precipitated by adding isopropanol and centrifugating. Following the precipitation, the pellet was washed with 70% EtOH, and a second precipitation step was performed to obtain a higher grade for RNA purity, by adding 1/10 sodium acetate (AcNa 3M), 2 volumes of 100% EtOH and 1-hour incubation at -80°C. After centrifugation, the pellet was rinsed with 70% EtOH, dried at room temperature and resuspended in 20 µl of autoclaved RNase-free H_2O. Quality and quantity of the resulted RNA was estimated in a NanoDrop® spectrophotometer (ND-8000, Thermo Fisher Scientific, United States) and by 1% agarose gel electrophoresis of 0.5 µg of the derived RNA.

Maxwell® RSC plant RNA kit (Promega Corporation, United States) was also used for total RNA isolation, particularly for infiltrated *N. benthamiana* tissues. This method provided pure RNA free of DNA contaminants since the reaction included a DNase I treatment that facilitated the use of the RNA as template in qRT-PCR measurements.

The RNA content of the purified VLPs was extracted using the RNeasy Plant Mini Kit (QIAGEN, Germany) following the manufacturer´s instructions.

3.3.2 Reverse transcription

Either the High-Capacity cDNA Reverse Transcription kit (Applied Biosystems, United States) or SuperScript II Reverse Transcriptase (Invitrogen, United States) were used to reverse transcribe samples corresponding to 1 µg of total RNA, using a mix of random or gene specific primers, in accordance with the manufacturer's instructions.

3.3.3 PCR amplification

3.3.3.1 Ex-Taq polymerase amplification

For virus detection, commercial TaKaRa Ex Taq kit (Takara Bio Inc., Japan) was used for the amplification of targeted products using viral specific-primers and about 0.05 µg of RT-derived cDNA as template. Purified plasmid DNA was used as positive control for amplification. Temperatures for primer hybridization and elongation times were optimized on each reaction, according to the amplicons' size and the melting temperature of each pair of specific primers used. The specific primers used for molecular detection of SPFMV, SPV2, SPMMV and SPCSV are listed on Table M4.

Table M4. List of primers used for the specific detection of SPFMV, SPV2, SPMMV and SPCSV.

Virus	Primer name	Sequence (5´- 3´)	Amplicon size
SPFMV	PISPOMiSeq-FW	GCACCACAAGATGGTGCGTAA	300 bp
	PISPOMiSeq-RV	GTCATTTCCAGACTCGCCGATG	
SPV2	HCPro-mid-FW	CGAGAATATTAAGAAAGGATCCCTAGT	459 bp
	HCPro-mid-RV	GGATCACCTGAGTTTCCAATAACCAGA	
SPMMV	P1-Nterm-FW1	ATTGTGAGGATTGCGGTTCG	95 bp
	P1-Nterm-FW1	TTCAGTCCACCCACCAAGAG	
SPCSV	RNase3-FW	ATGATTCCGATCTATTCTGATGTTTCTGAAGAAAGT	678 bp
	RNase3-RV	TCAATTCAAATTCAGAGCTTGGACAG	

3.3.3.2 Phusion polymerase amplification

For the amplification of viral gene products destined for cloning into different expression vectors, the proofreading High Fidelity Phusion Polymerase (Thermo Fisher Scientific, United States) and appropriate primers were used, following the manufacturer's protocol. As in the previous section, for each reaction the specific number of cycles, alignment temperature and elongation time were selected depending on

the melting temperature of primers and on the size of the generated amplicon.

3.3.4 Nucleic acid gel electrophoresis

Size separation of DNA or RNA fragments was done by electrophoresis in EtBr-stained agarose gels (0.8%-2% agarose content, depending on fragment size) and visualization using a BIO-PRINT UV gel documentation imaging equipment (Vilber, France). Gels were prepared with the appropriate amount of agarose in 1x TAE buffer (0.4 M Tris-acetate, 0.001 M EDTA, pH 7.8) and samples were loaded on wells after addition of loading buffer. The electrophoretic separation was done at 100 V for 30 minutes, using a commercially available molecular weight marker (GeneRuler 1 kb Plus DNA Ladder, Thermo Fisher Scientific, United States) to estimate fragment sizes.

3.3.5 Nucleic acid hybridization

3.3.5.1 Generation of (-) sense RNA probes

Different negative-sense RNA probes were generated using DIG-Northern Starter kit (Roche, Switzerland), according to manufacturer's instructions, using 1 µg of purified plasmid DNA template with the sequence of interest, under the control of either the T7 or SP6 promoters. Briefly, a specific region was amplified by RT-PCR, purified, and cloned to an appropriate vector with the flanking promoters, such as pGEM T Easy plasmid (Promega, Unites States). Once the orientation of the insert was determined by Sanger sequencing, the plasmid was linearized using a single site enzyme (one selected to leave preferably 5' overhangs). Then the commercial T7 or SP6 transcriptase (depending on the directional orientation of the insert) was used for in-vitro transcription to generate a negative sense RNA transcript probe incorporating Digoxigenin (DIG), which would be subsequently used for detection of the complementary chain (such as the viral genome or the mRNA corresponding to expressed genes) by molecular hybridization with the positive sense virus mRNA using alkaline phosphatase-conjugated anti-DIG antibody and the

adequate substrate for chemiluminescence detection. RNA probes were generated for the following viruses, with the indicated targeted gene products SPFMV (CP), SPV2 (P1), SPMMV 130 (P1), SPMMV 0900 (CP), SPCSV RNA 1 (Polyprotein 1), SPCSV RNA 2 (HSP70) and PVX (RdRp). Moreover, a negative sense GFP RNA probe was also produced and served for quantification of GFP mRNAs.

3.3.5.2 Molecular hybridization by tissue printing

To test whether virus-inoculated plants were indeed infected, cross sections of fresh tissues (leaves or petioles) were printed on a positively charged nylon membrane (Roche, Germany), and nucleic acids were fixed by crosslinking at 1.200 J for 1 minute, using a UVC500 cross-linker (Amersham Biosciences, United Kingdom). Membrane hybridization steps were performed essentially following previously described protocols (Más and Pallás 1995). Printed RNA was hybridized with Digoxigenin-labelled probes, specific to the sequence of interest and detection was performed using alkaline phosphatase-conjugated anti-DIG antibody. The emitted signal was captured by a ChemiDoc™ imaging system (BioRad Laboratories, United States) after incubation with CDP-Star reagent (Roche, Switzerland).

3.3.5.3 Northern blotting

Northern blot analysis was performed for the detection and quantification of GFP mRNA levels in leaf tissue of *N. benthamiana* plants co-infiltrated with constructs for expression of different proteins and GFP. Samples were usually collected at three different time points after agroinfiltration, and total RNA was isolated from infiltrated tissue using TRIzol (Invitrogen, United States). Then about 1 µg of RNA for each sample was separated on a 1.5% denaturing formaldehyde agarose gel for 5h at 60V. After electrophoresis, RNAs were transferred overnight to positively charged nitrocellulose membrane (Roche, Switzerland) by upward capillary transfer in 10x SSC buffer. Membranes were stained with methylene blue for total RNA visualization and after brief washes with DEPC-H2O, subjected to overnight hybridization at 65 °C using a GFP specific

Digoxigenin-labelled RNA probe. Detection was performed using alkaline phosphatase-conjugated anti-DIG antibody and emitted signal was captured using a ChemiDoc™ imaging system (BioRad Laboratories, United States) after application of CDP-Star reagent (Roche, Switzerland). Total RNA extracted from the purified VLPS was also analyzed by Northern blot, following the same procedure.

3.3.6 Viral load quantification

3.3.6.1 Standard curve for SPMMV

For absolute quantification of SPMMV viral titers a 430 bp positive-sense transcript corresponding to the N-terminal region of the P1 cistron was produced through *in vitro* transcription using T7 promoter (MEGAscript T7 Transcription kit, Ambion Inc, Unites States). The template plasmid with cloned P1 of SPMMV under the control of T7 promoter was prepared by former laboratory members (A. Giner, PhD dissertation 2011, *Caracterización de las proteínas P1 y HCPro del ipomovirus del moteado de batata en supresión de silenciamiento génico*, University of Barcelona). Transcript serial dilutions ranging from 50 ng up to 1/5*10^(-8) were used as template in a qRT-PCR reaction to generate a standard curve for an accurate calculation of SPMMV absolute viral load in single and mixed infected plants. The following software https://www.genscript.com/ssl-bin/app/primer served for the design of two different pairs of primers (Table M5) and two different concentrations (200 and 400 nM) were tested to select the one that resulted in the highest linear regression R^2 (R^2 should be >0.98). Each pair of primers targeted a specific region on the transcript and therefore on the viral RNA, amplifying a 95- and 84-bp PCR product respectively.

Table M5. Primers pairs used for the generation of standard curves for absolute quantification of SPMMV 130 and 0900 viral titers.

Primer name	Sequence (5´- 3´)	Amplicon size
P1N-term-SPMMV-FW1	ATTGTGAGGATTGCGGTTCG	95 bp
P1N-term-SPMMV-RV1	TTCAGTCCACCCACCAAGAG	
P1N-term-SPMMV-FW2	GCCACTTCTGTCCTGATTGC	84 bp
P1N-term-SPMMV-RV2	GCTTGTTGAATTGCGAACCG	

3.3.6.2 Absolute quantification of viral titers

Total RNA from single and mixed infected plants was isolated from samples (about 100 mg) of plant tissue (*N. tabacum* or *I. nil*) collected at 13, 20 and 27-dpi using Maxwell® RSC simply RNA Tissue Kit (Promega Corporation, United States) including a DNase I treatment. 1 µg of total RNA was reverse transcribed using the High-Capacity cDNA Reverse Transcription kit (Applied Biosystems, United States) with random primers, according to provider´s protocol. 50 ng of the generated cDNA was used as template in a 20 µl qPCRs reaction, performed in a Light Cycler 480 (Roche, Switzerland) equipment, using 96 or 384-well plates. Master SYBR green I was employed for the detection of the produced amplicon through fluorescence emission.

3.3.7 Genome sequencing of SPMMV 0900 isolate

A partial sequence of SPMMV 0900 has been obtained previously by members of the Laboratory. The available sequence covered from the P1 cistron up to the beginning of the CI cistron. To determine the rest of the coding sequence (from CI to CP) along with the 5´and 3´ untranslated regions (UTRs), a genome walking approach was adopted (Fitzgerald and McQualter 2014) amplifying virus segments with High Fidelity Phusion Polymerase (Thermo Fisher Scientific, United States), gel purified (NucleoSpin Gel and PCR clean-up kit, Macherey-Nagel, United States)

and sequenced through Sanger Capillary sequencing at CRAG facilities. To obtain the SPMMV 0900 consensus sequence, at least 3 reads of each segment were analyzed independently, and regions with sequences showing inadequate chromatographical curves were filtered out. Licensed SnapGene software (from Insightful Science; available at snapgene.com) was utilized to assemble the complete sequence by overlapping the individual segments, and full sequence annotation was done identifying the polyprotein cleavage sites as described in previous studies (Adams et al. 2005). Nucleotide and amino acids sequence alignment between SPMMV 130, 0900 and the reference sequence (NCBI accession number: NC_003797) was conducted using MEGA- X software (Kumar et al. 2018).

3.4 Transient expression of heterologous proteins in plants

3.4.1 RNA silencing suppressor activity trials

3.4.1.1 Construction of binary plasmids

SPV2-generated constructs were based on the sequence of the AM-MB2 isolate (GenBank accession no. KU511270). The complete cistrons of P1, HCPro and P1HCPro (in cis) were amplified by RT-PCR employing total nucleic acids extracted from infected sweet potato (*I. batatas*) plants, using High Fidelity Phusion Polymerase (ThermoFisher Scientific, United States) and appropriate primers (Table M6). The transframe gene product P1N-PISPO was generated by a recombinant PCR amplification to mutagenize the conserved G2A6 motif by inserting and extra A, and thus resulting in a switch of the reading frame for its production. Similarly, a P1 variant denominated P1-ONLY, was amplified by a recombinant PCR to introduce point mutations to the conserved G2A6 motif in the viral RNA, resulting in the insertion of an out-of frame stop codon to hamper any expression of P1N-PISPO, even after polymerase slippage potentially occurring in the G2A6 motif.

Table M6. List of primers used for amplification of SPV2 proteins, tested for their capacity to block innate plant RNA silencing

Primer name	Sequence (5´- 3´)	Amplicon size
P1_SPV2_FW	CACCATGGCGTGCGTCACGAACG	1855 bp
P1_SPV2_RV	TCAAAATTGCTCCATGTATGGCAGTATTGAGC	
P1-ONLY_SPV2_FW	GATAAGGAGGAGAAGATTTGGAGTGCGTGGG	1855 bp
P1-ONLY_SPV2_RV	CCCACGCACTCCAAATCTTCTCCTCCTTATC	
P1N-PISPO_SPV2_FW	GAGGAAAAAAATTTGGAGTGCGTGGGAACAC	1856 bp
P1N-PISPO_SPV2_RV	GTGTTCCCACGCACTCCAAATTTTTTTCCTCC	
HCPro_SPV2_FW	CACCATGTCACAAACAGGTGATAGATTCTGGAATGG	1374 bp
HCPro_SPV2_RV	TCATCCAACAAGATAGTGTTTCATTTCTGAATCCAATG	
P1HCPro_SPV2_FW	CACCATGGCGTGCGTCACGAACG	3228 bp
P1HCPro_SPV2_RV	TCATCCAACAAGATAGTGTTTCATTTCTGAATCCAATG	

All PCR-derived products were gel purified using the NucleoSpin Gel and PCR Clean-up kit (Macherey-Nagel, United States) and cloned directionally into pENTR D-TOPO (Invitrogen) GATEWAY expression system, using the E. coli strain TOP10. Clones containing the correct inserts were selected by restriction enzyme screening and the point mutations introduced were confirmed by Sanger sequencing. For the silencing suppressor assay, the pENTR-constructs were subsequently mobilized by LR reaction (Invitrogen) into the pDEST plasmids (Tanaka et

al. 2011) pGWB702Ω and pGWB718 (N-4xMyc), both containing the 35S promoter and the NOS-Terminator for transcriptional termination. Plasmids harboring the correct sequence of each cloned cistron, were introduced by heat shock transformation into A. tumefaciens EHA105 strain.

3.4.1.2 Co-infiltration of RSS candidate proteins with GFP

A standard co-agroexpression experiment was adopted to identify potential RSS proteins. Briefly, a binary vector carrying the GFP reported gene was used in co-agroinfiltration experiments to test the capacity of viral-derived gene products to suppress RNA silencing: If a protein confers RNA silencing suppressor activity, the GFP expression will be maintained at high levels and results detectable under UV light. Agroinfiltration of the generated binary plasmids was essentially carried out as previously described (Voinnet et al. 2000; Valli et al. 2006; Helm et al. 2011). Wild type or 16c *N. benthamiana* plants with fully expanded leaves (3-weeks old) were infiltrated with EHA105 *A. tumefaciens* liquid cultures in buffer containing acetosyringone, harboring the individual viral gene products. All tested constructs were co-agroinfiltrated with a GFP-expressing construct (pBIN61S, 35S:GFP) (Silhavy 2002; Valli et al. 2006) at equal volumes. Positive and negative controls were included, being the first a construct of WMV-HCPro, a well characterized RSS (Domingo-Calap et al. 2021)and the negative control corresponding to the reverse complement form of WMV-HCPro, cloned in inverted orientation to avoid any expression, and denominated orPCH, (Figure M3). Bacterial cultures were grown overnight at 28ºC, and the growth was monitored by optical density assessment at 600nm (OD_{600}). All cultures encompassing the different constructs were adjusted to OD_{600}= 0.5 and induced for 3 hours in acetosyringone-supplemented induction buffer (10 mM MES/NaOH, pH 5.6, 10 mM $MgCl_2$, 150 µM acetosyringone), before infiltration with a needless syringe. At least 3 independent *Agrobacterium* cultures were used per each construct, and the assays were repeated several times.

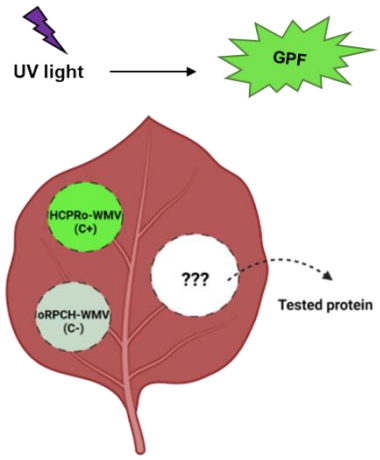

Figure M3. Representative illustration of the co-agroinfiltration experimental design. *N. benthamiana* leaf patches co-infiltrated with GFP and the positive (top) or negative (bottom) control are depicted on the left half leaf, while the agroinfiltrated patch with the tested protein is shown on the right half leaf.

3.4.1.3 GFP imaging and quantification by qRT-PCR

GFP fluorescence was visually inspected under long-wavelength UV light (Black Ray model B 100 AP) at 3, 5 and 7-days post agroinfiltration, and photographs were captured with a Nikon D7000 digital camera. For analysis of GFP expression levels, total RNA was isolated from 100 mg infiltrated *N. benthamiana* leaf samples (4 biological replicates/tested construct) using Maxwell RSC simply RNA Tissue Kit (Promega Corporation, United States) with DNase I treatment. RNA quality and concentration was estimated by NanoDrop spectrophotometer (ND-8000) and 1 µg of total RNA was reverse transcribed using the High-Capacity cDNA Reverse Transcription kit (Applied Biosystems, United States), following the manufacturer's instructions. Gene-specific primers were used to perform the RT-PCRs in a 10 µl reaction mixture, using 50 ng of the single stranded cDNA template. Primers targeting a 102-bp GFP fragment, previously described by Leckie and Steward (Leckie and Neal Stewart 2011) were employed for the relative quantification of the GFP-mRNAs and Ubiquitin was selected as a reference gene, with primers targeting a 88-bp fragment as described by Lacomme and colleagues (Lacomme et al. 2003) (Table M7). Master SYBR green I was used for

the detection of the generated amplicons at a Light Cycler 480 (Roche, Switzerland). ΔC_T values were generated by normalizing the average cycle threshold (C_T) values of the PCR triplicates (of each construct) to the average C_T value of Ubiquitin.

Table M7. Primers used in relative quantification of GFP mRNA levels, targeting GFP (pair 1) and ubiquitin of *N. benthamiana* (pair 2)

Primer name	Sequence (5´- 3´)	Amplicon size
GFP_qPCR-FW	CAACTTCAAGACCCGCCACA	102 bp
GFP_qPCR_RV	TCTGGTAAAAGGACAGGGCCA	
UBI_qPCR_FW	TCCAGGACAAGGAGGGTATCC	88 bp
UBI_qPCR_RV	TAGTCAGCCAAGGTCCTTCCAT	

3.4.1.4 Statistical analysis

Data derived by GFP-mRNA relative quantification are represented by the average +/- SEM for each variable. When data normality was confirmed by Shapiro-Wilk test, a parametric one-way ANOVA was applied for significance assessment in a 95% confidence level (a=0.05). When significance was detected, post-hoc tests with Bonferroni´s correction were conducted to detect among which groups there was a significant difference. In the case that data normality was not fulfilled, the non-parametric Kruskal-Wallis test was chosen instead of ANOVA, followed by Dunn's post-hoc tests.

3.4.1.5 Northern blotting

Apart from relative qRT-PCR quantification, GFP mRNA levels were also assessed by Northern blotting (as explained in section **3.3.5.3**).

3.4.2 Construction of PVX-chimeric plasmids and plant delivery

The genome sequences corresponding to SPV2- P1, P1-ONLY, P1N-PISPO and HCPro were cloned by LR reaction (Invitrogen) to an engineered PVX-derived vector (pGWC-PVX) kindly provided by Dr. Adrian Valli (CNB, Madrid, Spain). Additionally, HCPro of WMV was cloned to generate the PVX-HCPro-WMV plasmid, serving as a positive control along with PVX-P1b-CVYV, since both proteins have been described as strong RNA silencing suppressor by previous studies (Valli et al. 2008; Domingo-Calap et al. 2021). GFP-expressing PVX (pGR106, originally constructed at the laboratory of Dr. David Baulcombe, Sainsbury Laboratory, UK) and PVX full-length infectious clone were employed as additional controls to monitor the symptom severity of PVX infection. Chimeric PVX-derived plasmids were transformed to *A. tumefaciens* by electroporation. *Agrobacterium* strain GV3101, harboring the pJIC_SA_Rep helper plasmid, was the host bacterium for subsequent plant delivery into 2-weeks old *N. benthamiana* plants, following previously described infiltration techniques (Alamillo et al. 2006). To monitor symptom divergence and severity, chimeric PVX-infected plants were photographed at 8- and 15-days post inoculation (dpi) using a Nikon D7000 digital camera

3.4.2.1 Western blotting

Fresh patches of agroinfiltrated *N. benthamiana* plant tissue were homogenized in extraction buffer containing 150 mM Tris-HCl (pH 7.5), 6 M urea, 2% sodium dodecyl sulfate (SDS), and 5% β-mercaptoethanol (100 mg of tissue in 200 µl of extraction buffer). Derived homogenates were boiled for 5 min at 95°C and centrifuged at 10.000 g for 15 min to remove cell debris. 10 µl of supernatants were loaded on a 12% SDS-PAGE and separated by electrophoresis for 1 hour at 200V. Electrophoresed proteins were transferred to a nitrocellulose membrane (Amersham protan 0.45 NC, GE Healthcare, United States) for immunoblotting detection. Commercially available anti-Myc Tag monoclonal antibody (clone 4A6, Millipore, Unites States) was used for

binding to the tested Myc-tagged SPV2 proteins, followed by incubation with secondary goat anti-mouse immunoglobulin G (conjugated to horseradish peroxidase). For the detection of PVX-coat protein produced during the PVX-chimeric constructs infiltration, polyclonal anti-PVX capsid protein (PVAS643; American Type Culture Collection) was used, also followed by incubation with secondary goat anti-rabbit immunoglobulin G (HRP-conjugated). Immunostained proteins were visualized by chemiluminescence (Super Signal West Femto, Thermo Fisher Scientific, United States) according to manufacturer's instructions using a ChemiDoc apparatus (BioRad Laboratories, United States). Total protein content of the samples was assessed by Ponceau-red staining.

3.4.3 *In planta* VLPs production

3.4.3.1 Generation of pEff-constructs

SPFMV-infected *I. batatas*, SPV2-infected *N. benthamiana* and SPMMV-infected *N. tabacum* leaves were used for the isolation of total RNA by TRIzol reagent (Invitrogen, Unites States) following manufacturer´s protocol. RNA templates were transcribed into cDNA using MultiScribe™ reverse transcriptase (Invitrogen, United States) and specific primers (listed in Table M8) were employed for the amplification of SPFMV-CP (GeneBank: KU511268), SPV2-CP (GeneBank: KU511270) and SPMMV-CP (GeneBank: GQ353374). A start codon (ATG) and an Asc I restriction site were inserted upstream of each sequence while a stop codon (TGA) and a Xma I restriction site were included downstream, to facilitate cloning into the pEff-GFP expression vector (Mardanova et al. 2017) after restriction enzyme digestion, purification and incubation with T4 DNA ligase (Thermo Fisher Scientific, United States). The derived pEff-SPFMV-CP, pEff-SPV2-CP and pEff-SPMMV-CP plasmids were transformed by heat-shock to *E. coli* (Top10 strain) and grown in selective LB medium overnight at 37°C. Liquid cultures were grown for plasmid propagation and isolation, using GeneJET Plasmid Miniprep Kit (Thermo Fisher Scientific, United States). Plasmids with expected restriction digestion patterns for the insertions were selected, and the integrity of CPs´ coding regions were confirmed by Sanger capillary sequencing.

Table M8. List of primers for amplification of the coat proteins of SPFMV, SPV2 and SPMMV and cloning into PVX-based pEff vector

Primer name	Sequence (5´- 3´)	Amplicon size
pEff-CP-SPFMV-FW	TACTTCCATCAGGCGCGCCATGTCTAGTGAGAGCACTGA	988 bp
pEff-CP-SPFMV-RV	ATTACTTGTACACCCGGGTCATTGCACACCCCTCATTC	
pEff-CP-SPV2-FW	CTTCCATCAGGCGCGCCATGTCAGGCACTGAAGAAAT	946 bp
pEff-CP-SPV2-RV	TTACTTGTACACCCGGGTCACTGCACACCTCTCATTC	
pEff-CP-SPMMV-FW	ACTTCCATCAGGCGCGCCATGTCGACATCCAAGACAAT	1036 bp
pEff-CP-SPMMV-RV	GATTACTTGTACACCCGGGTCAGTCGAGTTGAGCTCCTC	

3.4.3.2 *In planta* expression, protein extraction and western blot analysis

Confirmed plasmids were transformed to *A. tumefaciens* (LBA4404 strain) by electroporation and grown in selective YEB medium for two days at 28°C. Bacteria cultures with plasmids were grown to 0.5 units of optical density at 600nm (OD_{600}) and induced by acetosyringone for at least 2 hours, before infiltration to leaves of *N. benthamiana* plants (3-weeks old, grown under constant 16/8h light/darkness, 20-23°C) using a needless

syringe, as previously described (Thuenemann and Lomonossoff 2018). Infiltrated leaves were harvested at 3, 5 and 7-days post agroinfiltration and the expression of viral CPs was confirmed by Western blot analysis. For total protein extraction, 2 leaf discs (around 60 mm diameter) of infiltrated tissue were collected in a 2 ml eppendorf tube (Eppendorf Ag, Germany) and pulverized with 2 glass beads (4 mm, Merck KGaA, Germany) in a TissueLyser II disruptor (QIAGEN, Germany). Ground samples were homogenized in 200µl extraction buffer (20 mM Tris-HCl, pH 7.5, 30 mM NaCl, 1 mM Ethylenediaminetetracetic acid, 0.5%NP-40, 2% β-mercaptoethanol) and centrifuged at 8.000 x g for 10 min at 4°C to remove cell debris. Aliquots (20µl) of supernatant were boiled for 5 min at 95°C with 5µl of Laemmli loading buffer 4x (250 mM Tris-HCl, pH 7.5, 40% glycerol, 8% SDS, and 20% β-mercaptoethanol) and 10µl was loaded on a 12% polyacrylamide gel for electrophoresis during 1 hour at 200 V using 1x running buffer (10x Tris-Glycine buffer: Glycine:1.92M; Tris: 0.25M; SDS 1%). InstantBlue (Abcam, United Kingdom) was used for gel staining and total protein quantification. For specific CP detection by western-blotting, total proteins were transferred to a nitrocellulose membrane (Amersham, GE Healthcare, United Kingdom) through a standard wet transfer technique. Primary polyclonal anti-SPFMV-CP, anti-SPV2-CP and anti-SPMMV-CP (DMSZ, Germany) were added at 1:1.000 dilution, and membranes were incubated overnight by shaking at 4°C. After rinses, goat anti-rabbit horseradish peroxide conjugated (HRP) secondary antibody (Cat. 31460, Invitrogen**,** United States) was used at 1:10.000 dilution, and revealed using chemiluminescence substrate (SuperSignal™ West Femto, Thermo Fischer Scientific, United States) in a ChemiDoc™ imaging system (BioRad Laboratories, USA).

3.4.3.3 Virus-like particles assembly *in planta*

Fresh and frozen (in liquid N_2) pEff-SPFMV-CP infiltrated tissue was homogenized in 100 mM Sodium Borate pH 7.95 and subjected to low-speed centrifugation (8.000 x g) for 15 minutes at 4°C. The supernatant was analyzed under Transmission Electron Microscopy (TEM) imaging to visualize the assembled virus-like particles. Similarly, fresh and frozen (in liquid N_2) pEff-SPV2-CP and pEff-SPMMV-CP infiltrated tissue was

ground in Phosphate buffered Saline (PBS) pH 7.2 and VLPs were detected in the supernatant after low-speed centrifugation (12.000 x g) for 15 minutes at 4°C.

3.5 Purification of VLPs and virions

3.5.1 SPFMV-VLPs purification

SPFMV-VLPs purification was based on the protocol established by Nakashima and colleagues for virion purification (Nakashima et al. 1993), with several modifications. *N. benthamiana* infiltrated tissue was harvested at 7 days post agroinfiltration, frozen and homogenized in a laboratory waring blender (Waring Lab, Torrington, USA) with 3 volumes of extraction buffer #1 (50 mM Hepes buffer, 500 mM Urea, 50 mM EDTA, 0.5% Na2SO3, pH 8), containing Mini Complete™ EDTA-free Protease Inhibitor Cocktail (Merck KGaA, Darmstadt, Germany), trying to minimize degradation by protease activity. The homogenate was filtered through 2 layers of Miracloth (Merck KGaA, Darmstadt, Germany) and clarified at low-speed centrifugation (8.000 x g) for 10 minutes at 4°C, and the supernatant was stirred for 1 hour with 2% Triton X-100 (Merck KGaA, Darmstadt, Germany) at 4°C. After a second clarification through low-speed centrifugation (8.000 x g, 10 minutes, 4°C) the supernatant was deposited on the top of a 20% (w/v) sucrose cushion in extraction buffer #2 (20 mM Hepes buffer, 250 mM Urea, 10 mM EDTA, pH 7.2) and centrifuged at 130.000 x g for 2.5 hours at 4°C in a swinging bucket SureSpin 630 Rotor (Thermo Scientific, Waltham, USA). Pellets were resuspended overnight in extraction buffer #3 (10 mM Hepes buffer, 50 mM Urea, 1 mM EDTA, pH 7.2). After clarification at 2.000 x g for 10 minutes at 4°C the supernatant was loaded on a sucrose gradient 10%-40% w/v in extraction buffer #3 and subjected to ultracentrifugation at 90.000 x g for 2 hours at 4°C, in a swinging bucket AH-650 Rotor (Thermo Scientific, Waltham, USA). Fractions of 500ul were collected and their contents were analyzed in a 12% SDS-PAGE gel, stained with InstantBlue (Abcam, Cambridge, UK) and observed under TEM imaging. For cryoEM studies, fractions with higher concentration of VLPs were pooled and the excess of salt removed using PD-10 desalting columns (GE Healthcare,

Chalfont St Giles, UK) equilibrated with extraction buffer #3 and further concentrated by spinning at 103.000 x g for 1 hour at 4°C in AH-650 Rotor. The pellet was resuspended in extraction buffer #3, clarified at 8.000 x g for 5 minutes and the resulted supernatant was used for all subsequent analysis including cryoEM.

3.5.2 SPV2 VLPs purification

SPV2-VLPs purification was adapted from previously published protocols describing the purification process of SPV2 virions (Ateka et al. 2004). In essence, frozen *N. benthamiana* infiltrated tissue harvested at 5 days post agroinfiltration was homogenized in 3 volumes of 50 mM Sodium Phosphate buffer (+5 mM EDTA, +0.1% β-mercaptoethanol, pH 7.5) supplemented with Mini Complete™ EDTA-free Protease Inhibitor Cocktail (Merck KGaA, Germany) again to protect from proteases. Homogenate was filtered through 2 layers of Miracloth (Merck KGaA, Germany) and clarified at low-speed centrifugation (8.000 x g) for 15 minutes at 4°C. The supernatant was stirred for 1 hour with 2% Triton X-100 (Merck KGaA, Germany) at 4°C and again clarified at low-speed centrifugation (8.000 x g, 15 minutes, 4°C). A 20% (w/v) sucrose cushion was used for the first ultra-centrifugation of the supernatant at 130.00 x g for 3 hours at 4°C, using either the 50.2 Ti fixed-angled rotor (Beckman Coulter, United States) or the TH-641 swinging bucket rotor (Thermo Fisher Scientific, United States). The pellet was resuspended in 1ml of extraction buffer by pipetting up and down and clarified at 3.000 x g for 10 minutes before being loaded on a sucrose gradient 10%-40% w/v and subjected to ultra-centrifugation at 85.000 x g for 2 hours at 4°C, using swinging bucket AH650 rotor (Thermo Fisher Scientific, United States). Tubes were punctured at the bottom using a syringe needle and 500 µl fractions were collected. Different fractions were analyzed on a 12% SDS-PAGE gel, stained with InstantBlue (Abcam, United Kingdom) and samples were analyzed under electron microscopy.

3.5.3 SPMMV VLPs and virions purification

SPMMV virus-like particles purification was based on previously described protocols (Hollings et al. 1976) with a few adaptations. Briefly, frozen *N. benthamiana* infiltrated tissue harvested at 5 days post agroinfiltration, was homogenized in 3 volumes of 50 mM Sodium Phosphate buffer (pH 7, +0.1% β-mercaptoethanol) using a laboratory waring blender (Waring Lab, Torrington, USA). The homogenate was filtered through 2 layers of Miracloth (Merck KGaA, Germany) and clarified at low-speed centrifugation (8.000 x g) for 15 minutes at 4°C. Clarified supernatant was subjected to ultra-centrifugation at 100.000 x g for 90 minutes at 4°C, using swinging bucket SureSpin 630 Rotor (Thermo Fisher Scientific, United States). The pellet was resuspended overnight, in 50 mM Sodium Phosphate buffer pH 7, by gentle agitation at 4°C. The resuspended pellet was clarified at 2.000 x g for 10 minutes at 4°C and supernatant was loaded on a sucrose gradient 10%-40% w/v (sucrose was dissolved in 50 mM of extraction buffer without β-mercaptoethanol) and then subjected to ultra-centrifugation at 100.000 x g for 3 hours at 4°C, using swinging bucket AH650 Rotor (Thermo Scientific, Waltham, USA). Fractions of 500ul were obtained through the bottom using a syringe needle, and the fractions´ VLPs content was visualized on a 12% SDS-PAGE gel, stained with InstantBlue (Abcam, Cambridge, UK) and under TEM imaging. For cryo-EM studies, fractions with the higher VLPs-content were pooled and buffer exchanged using PD-10 desalting column (GE Healthcare, Chalfont St Giles, UK) equilibrated with 50 mM Sodium Phosphate buffer pH 7. The same purification protocol was also employed for SPMMV virions purification, starting with *N. benthamiana* or *N. tabacum* infected tissue. In that case the only difference was the speed of the second ultra-centrifugation that was reduced at 60.000 x g instead of 100.000 x g used for the VLPs.

3.6 Negative staining and TEM imaging

For electron microscopy visualization and morphology determination of purified virions and assembled VLPs, 8 µl of sample (clarified crude extracts or fractions of purified virions/VLPs) was applied on carbon-

coated copper grids (EM Resolutions, Sheffield, UK) and allowed to be adsorbed for 1 minute before being washed with 8 µl of mili-Q H2O while sample excess was removed using bench absorbent paper. Subsequently, grids were stained with 2% (w/v) of uranyl acetate (8 µl) and incubated for 1 more minute, before allowed to dry at room temperature (RT). Images were taken using a Talos F200C transmission electron microscopy (Thermo Fischer Scientific, Waltham, USA) fitted with Gatan OneView camera. For routine testing of purifications performed at CRAG laboratory, a Jeol electron microscope JEM-1400 (operated at 120 kV) was also used.

3.7 Thermal shift assay

A differential scanning fluorimetry assay (Pantoliano et al. 2001) was used to compare the thermal stability of purified VLP preparations. Briefly, Sypro Orange was added as an extrinsic fluorophore (Velazquez-Campoy et al. 2016; Gao et al. 2020) to the preparation of VLPs and readings were determined along a gradient of temperatures in a real time qPCR Mx3005p (Agilent). To assure data reproducibility, duplicates for each sample were used in both assays. The melting temperatures (Tm) were calculated after data normalization using the first derivative of a native fraction for each sample, to determine the maximum slopes in the different sections of the curves.

CHAPTER I

4. Chapter I - Results

Natural variability of SPMMV: comparison of two isolates

4.1 Exploring the viral dynamics of SPMMV isolates 130 and 0900 in different hosts

SPMMV readily infects different susceptible plants, such as *N. tabacum* and *I. nil* plants, in which the virus infection causes characteristic symptoms including swelling and distortion of leaves, usually starting after 6 dpi. Previous laboratory members have worked mostly with SPMMV isolate 130 infecting *N. tabacum* plants as an experimental host (Giner et al. 2010). This African isolate originated in Tanzania (GenBank: GQ353374.1) and it was provided by Prof. J. Valkonen from his collection at the University of Helsinki. However, we observed that infection of the same host species by a different isolate of the virus, denominated 0900 in the DSMZ collection, and originally from Kenya, (https://www.dsmz.de/collection/catalogue/details/culture/PC-0900), consistently resulted in different symptoms.

Comparison of viral loads for these two isolates of the same virus has not been measured, therefore we decided to test how these two different isolates behave in two experimental hosts. To determine SPMMV titers for each isolate on single infected plants, we performed absolute qRT-PCR and calculated the amount of virus detected. A standard curve was generated from serial dilutions of positive sense viral transcripts corresponding to a part of the P1 coding sequence, located in the 5' region of the SPMMV genome. Two different set of primers at two concentrations were assayed to select the best reaction efficiency, finding that the higher value of R-squared (R^2) corresponded to the primers denominated "pair1" at 200 nM concentration, and they were chosen for subsequent testing (Figure R1). The comparison of viral loads was done in samples from the younger tissues where both isolates appeared to be always detectable,

sampling discs with 100 mg of tissue from the last 2-3 fully expanded leaves.

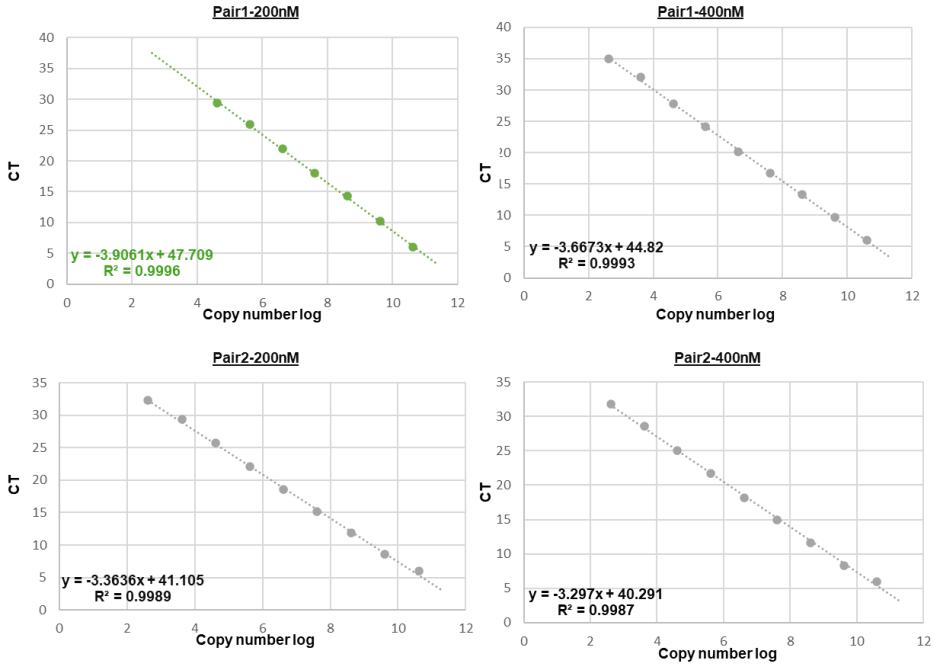

Figure R1. Standard curves derived by two different pair of primers targeting P1 genomic region of SPMMV, used at two different concentrations (200 nM and 400 nM) as indicated on the top of each graph. Absolute quantification of SPMMV titers was based on the standard curve with the highest R2 score, depicted in green.

4.1.1 SPMMV 130 and 0900 dynamics in single infections of *N. tabacum*

To assess the viral titers and symptom expression of SPMMV isolates, five individual *N. tabacum* plants were mechanically inoculated with either the isolate 130 or the isolate 0900. Characteristic symptoms of SPMMV infection appeared in both cases after 6-8 dpi, and the infection progress was monitored over time at 13, 20 and 27 dpi. At 13 dpi, inoculated plants already presented distinctive symptomatology, with SPMMV 130-infected

plants resulting taller compared to the ones infected with 0900. The same differences in height were observed at 20 dpi (Figure R2) and at 27 dpi.

Figure R2. Symptoms caused by SPMMV 0900 and 130. Representative *N. tabacum* plants infected with SPMMV 0900 or 130 at 20 dpi compared with a non-infected control. More severe symptoms of stunting were consistently observed for SPMMV-0900.

To conduct the absolute quantification of SPMMV isolates, the infected material was sampled at the indicated time-points and total RNA was extracted and analyzed by RT-PCR. Five individual plants (biological replicates) were sampled for each isolate at each time-point. The analysis revealed that plants infected with SPMMV 130 consistently accumulated more viral RNA in the upper leaves compared to the plants infected with SPMMV 0900, and these differences were observed at all three time points (Figure R3). Also, the viral titers of each isolate did not change significantly over time, although slight reductions of accumulation (not significative) were observed at 27 dpi for both virus isolates. Our results revealed a negative correlation between the viral loads (measured as SPMMV RNA copy numbers) in the younger tissues and their phenotypic manifestation in terms of stunting severity of the infected tobacco plants.

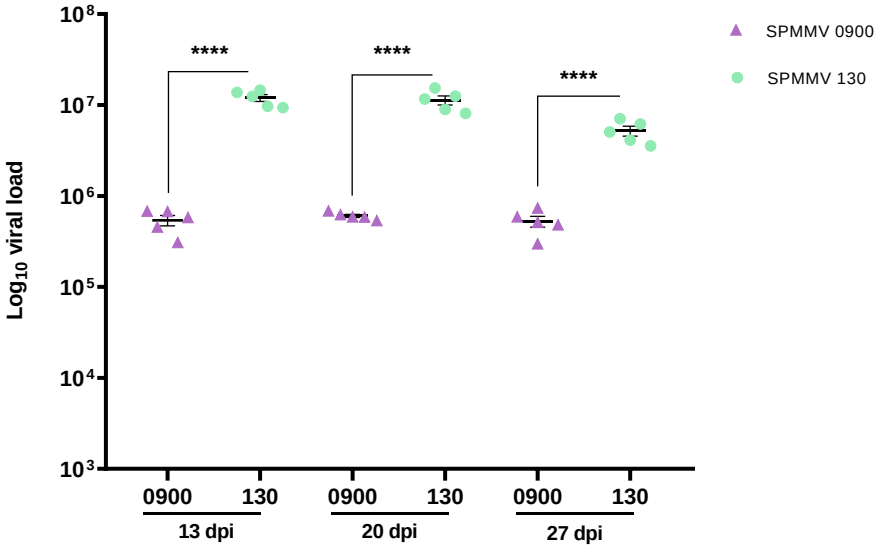

Figure R3. Severity of symptoms negatively correlates with viral load of SPMMV isolates in tobacco. Scatter plot representation of viral loads for SPMMV 0900 and 130 infected *N. tabacum* plants analyzed at three time points (13, 20 and 27 days post inoculation). Black lines represent mean values of viral load +/- standard error (SE) for individual plants as biological replicates (n=5), depicted as lila triangles for SPMMV 0900-infected plants or aqua-green dots for SPMMV 130-infected plants. Statistically significant differences are indicated by asterisks after applying Student´s *t*-test at 0.05 significance level. (****P<0.0001).

4.1.2 SPMMV 130 and 0900 dynamics in single infections of *I. nil*

Following the *N. tabacum* infection monitoring, we investigated the infection of the two SPMMV isolates in *I. nil* plants, a close relative of *I. batatas*. Similarly, 5 individual plants of the selected host were inoculated with each SPMMV isolate and the evolution of the infection was tracked at 13, 20 and 27-dpi, as it was done before. The first viral symptoms appeared after 7 dpi, including conspicuous leaf curling and developmental stunting of the plants compared to the healthy controls. Coinciding with the previous results in tobacco, SPMMV 0900 infected *I. nil* showed more exacerbated symptom manifestation compared to the plants infected with 130 isolate. Again, the same tendency continued at

20 (Figure R4) and at 27-dpi, with 0900 inoculated plants always being shorter and with a reduced foliage area.

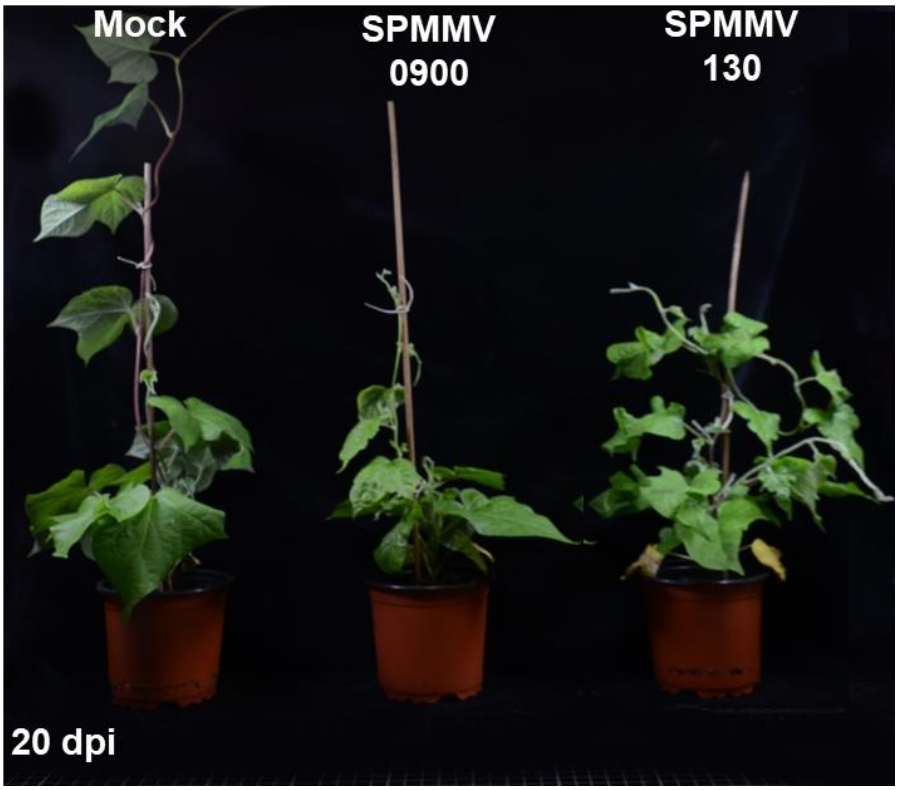

Figure R4. Symptoms caused by SPMMV 0900 and 130 in *I. nil* plants. Representative plants infected with SPMMV 0900 or 130 at 20 dpi compared with a non-infected control. Plants infected with SPMMV-0900 present more severe symptomatology.

The abundance of genomic RNA copies was quantified in young tissues of those plants, as we did in tobacco. Data showed that at 13 dpi the tissue infected with SPMMV 130 contained significantly larger amounts of virus compared to the ones infected with SPMMV 0900, resembling the quantification results obtained in *N. tabacum*. At 20 dpi, titers of 130 remained higher in average than those of 0900 but with a larger dispersion, however without reaching statistical significance. Interestingly, at 27 dpi the tendency for dispersion continued, and at this time point the

average viral titers of 0900-infected plants even slightly surpassed those of the 130-infected ones, again without presenting statistically significant differences (Figure R5). When comparing each isolate separately, we noted that virus levels of 0900 remained almost steady over time, with a minor increment in averages at 20- and 27 dpi. The titers of 130 decreased slightly between the two first time-points and dropped drastically at 27 dpi.

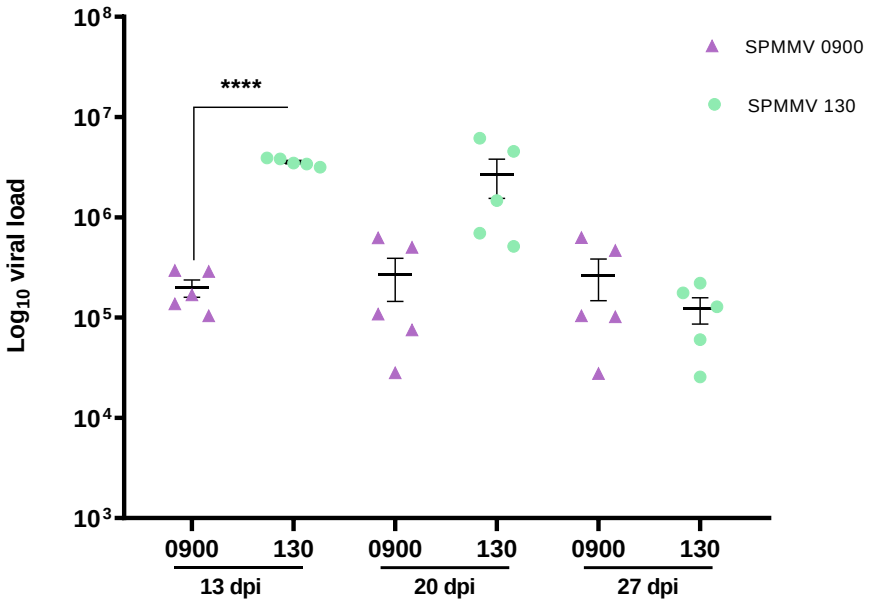

Figure R5. *I. nil* symptomatology of SPMMV 0900 or 130 infection is negatively associated to the virus titers. Scatter plot representation for the viral load of SPMMV 0900 and 130 in *I. nil* plants over time. Viral load was measured at three different time-points (13, 20 and 27-days post inoculation), using five infected plants per condition. Mean values of the viral load +/- the standard error (SE) are depicted by black dashes. Each biological replicate is represented by lila triangles for SPMMV 0900-infected plants or by aqua-green dots for SPMMV 130-infected plants. Asterisks indicate statistical significance in a=0.05, calculated by Student´s *t*-test. (****P<0.0001).

4.2 Distribution of SPMMV 130 and 0900 in *N. tabacum*

Given the discrepancies we observed in symptom expression and viral accumulation between the two isolates in both host plants, we decided to determine their distribution in *N. tabacum* plants where the symptomatology was more pronounced. For this purpose, two non-radioactive DIG-labelled RNA probes were designed to specifically detect the two isolates by tissue print. The probes for 0900 and 130 were generated to hybridize with virus sequence within the CP and P1 genomic regions, respectively. Selected sections from the foliage of *N. tabacum* plants infected with either 0900 or 130 isolates were printed on a positively charged nylon membrane and the virus distribution was detected with the corresponding DIG-labelled probes (Figure R6). After hybridization, we observed specificity of the probes, always with stronger signals in the homologous isolate-probe combinations, while weaker signals of cross-reactions appeared in the heterologous combinations, as expected. Homologies between the sequences for the two isolates were 95% for the CP region probe, and 89% for the P1 region probe.

Interestingly, the isolate 0900 was easily detected in most petioles and leaf sections in both older and younger tissues, with only a slightly less accumulation in the leaves located in the central part of the plant, while the isolate 130 was much more unevenly distributed, showing stronger signals in the oldest petioles and in the petiole-proximal areas of youngest leaf laminas. Considering that the less severe isolate 130 was mainly detected only in younger leaves, the strong symptoms of 0900 might derive from a longer persistence of virus presence in all leaves (both old and young), as revealed by hybridization. This result suggests that the macroscopical differences might be a consequence of acute versus persistent infection.

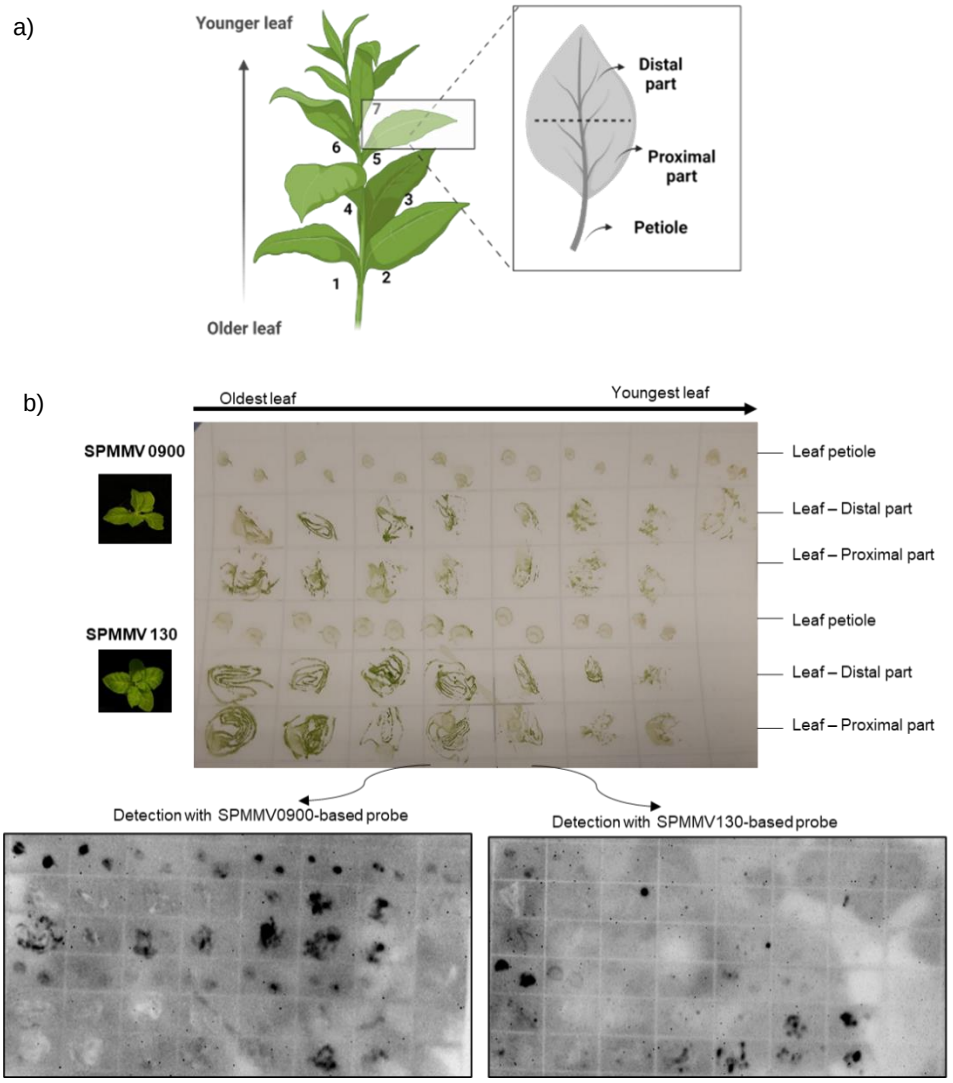

Figure R6. Follow-up of SPMMV distribution in infected plants using non-radioactive molecular hybridization specific probes. a) Cartoon representation of a tobacco plant indicating the numbering of leaves used for the tissue print, from oldest to youngest (left panel). Each leaf was used for printing section of three different areas (leaf petiole, proximal part and distal part) for the assessment of virus distribution (right panel). b) A total number of 7 or 8 leaves derived from plants infected with SPMMV 0900 or 130 respectively, were used for tissue print on positively charged nylon membranes (design as shown in the upper membrane) and subsequent detection of viral RNA using two different DIG-labelled RNA probes, the first targeting the SPMMV 0900-CP genomic region (lower part-left membrane) and the second targeting the P1 genomic region of SPMMV 130 (lower part-right membrane).

4.3 Comparison of SPMMV 130 and 0900 genomic sequences

To further investigate these pronounced differences between SPMMV 130 and 0900 in symptomatology and their distribution in specific plant tissues, we wanted to assess possible differences in their genome sequences that could account for the observed discrepancies. A partial sequence of SPMMV 130 was deposited to GeneBank (accession number: GQ353374.1), and the full sequence was later completed in our laboratory including the 5´ and 3´ untranslated regions (UTRs), (unpublished data). For the isolate 0900, only a partial sequence was available from the P1 to the beginning of CI cistron (unpublished data), with the rest of the sequence awaiting to be determined, including the 5' and 3' UTRs. To perform genomic comparisons between the two virus isolates, we decided to complete the full genome sequencing of isolate 0900.

4.3.1 Complete genome sequencing of SPMMV 0900 isolate

The partial SPMMV 0900 genomic sequence corresponding to the unknown region of the polyprotein was amplified through RT-PCR in two overlapping fragments, covering the regions from the CI up to the NIb (3474 bp) and from the NIb up to the CP (2162 bp) cistrons respectively. The PCR fragments were purified and submitted to Sanger capillary sequencing, using primers originally designed on the reference sequence. Internal primers were designed based on the reads corresponding to the sequenced fragments, following a genome walking approach (Figure R7). The assembly of the sequenced fragments into a consensus was done using at least 3 verified reads for each section, and the sequence annotation was performed considering the conserved *Potyviridae* cleavage sites, as reviewed by Adams and colleagues (Adams et al. 2005). SPMMV 0900 cleavage sites were coincidental with the ones of 130 isolate, except for one difference in 6K2/VPg region, where a lysine instead of an arginine residue was found downstream of the cleavage

motif (position +3) EYIEQH/GRK, being most likely irrelevant for the processing of the polyprotein.

To obtain the sequences of the 5´and 3´ viral UTRs, we performed RACE (rapid amplification cDNA ends) procedures (Price et al. 2003), starting with total RNA extracted from an infected plant as template to generate cDNA and PCR fragments using gene specific primers (GSP). Both dA- and dC-tailing was performed. After the analysis, regions of 138 and 328 nucleotides were determined as the virus 5´and 3´ UTR, respectively. The total length of the viral genome consisted in 10.885 bp, where 10.419 bp corresponded to the polyprotein open reading frame (ORF).

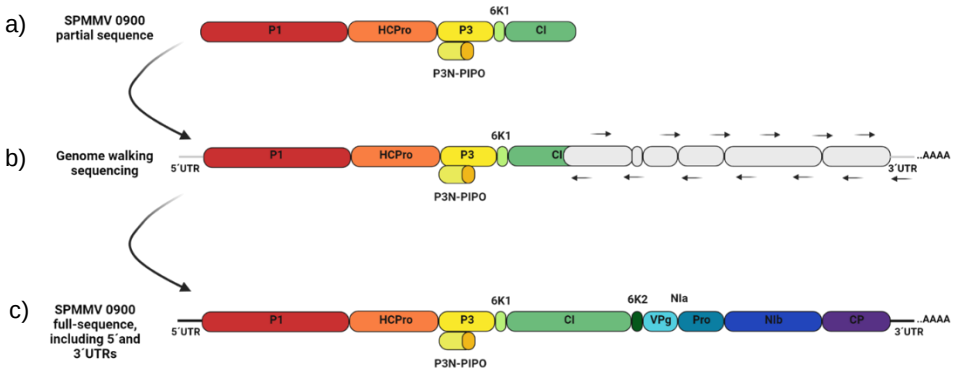

Figure R7. Genome walking strategy followed to obtain the full-length sequence of SPMMV 0900 isolate, including the 5´and 3´ untranslated regions (UTRs) derived by rapid amplification of cDNA ends (5´and 3´RACE, respectively). a) Partial SPMMV 0900 sequence obtained by previous lab members. b) Entire SPMMV 0900, where the missing sequence is depicted in grey and the arrows represent the primers used for the sequencing. c) Complete genomic sequence of SPMMV 0900 isolate.

4.3.2 Comparative genomic analysis of the two isolates, with special attention to the P1 coding region

MEGA-X software (Kumar et al. 2018) was used for the nucleotide and amino acid sequence alignments for the two viral isolates, including comparisons for the complete coding sequence of the polyprotein, and for each gene product individually. Analysis of the complete coding

sequences revealed a 93% of nucleotide identity, resulting in 96% of amino acid identity. Separate analysis of each individual 0900-encoded cistron revealed different identity percentages with isolate 130 or SPMMV reference sequence, summarized in table R1.

Table R1. Amino acids identity percentage of SPMMV 0900 gene products compared to SPMMV 130 or SPMMV reference sequence.

	Identity percentage (%)	
SPMMV 0900 proteins	**SPMMV 130**	**SPMMV NC003797**
P1	89.31	84.04
HCPro	98.01	90.07
P3	97.28	95.92
P3N-PIPO	89.9	90.82
6K1	100	96.2
CI	98.44	96.72
6K2	100	96.2
VPg	94	96.2
NIa	98.3	98.72
NIb	97.02	94.82
CP	95.02	96.37

As shown on the table, the P1 coding region appeared to be the most divergent one among the different viral proteins, thus we explored the discrepancies, considering the possible role in host-specificity attributed to P1 (Salvador et al. 2008; Shan et al. 2015). Alignments of nucleotides and amino acids for the P1 region were performed with SPMMV 0900, 130 and the reference sequence. Interestingly, we observed that our sequences of 0900 as well as 130 contained 45 extra nucleotides (position 1087 to 1130) corresponding to 15 extra amino acids (positions 363 to 378), compared to the reference P1 sequence (Figure R8). It is worth mentioning that these extra amino acids were also detected in other SPMMV isolates originating from Africa (Tugume et al. 2010).

a)

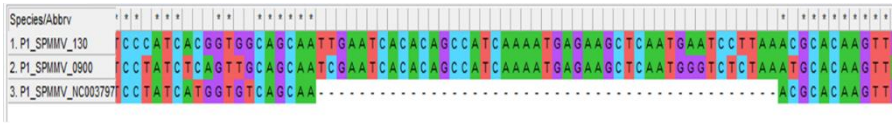

b)

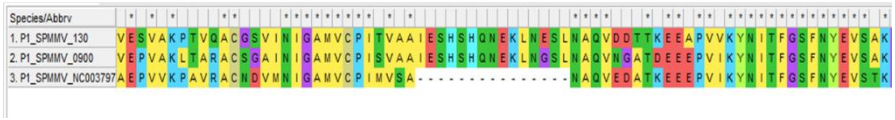

Figure R8. MEGA-X-mediated alignment of SPMMV P1 cistron between isolates 130, 0900 and NC003797 a) DNA alignment showing 45 missing nucleotides in reference NC003797 P1 genome b) Protein alignment of the same region, exhibiting the lack of 15 corresponding amino acids.

4.4 Finding common hosts for SPMMV and SPCSV

To facilitate our studies on mixed infections between SPMMV and SPCSV we explored susceptible experimental hosts for both viruses. Their natural host, *I. batatas,* presents several drawbacks for experimentation, due to its vegetative propagation and the frequent presence of several viral pathogens in the available plant material. Therefore, and to ensure adequate experimental conditions, we preferred to test virus-free plant material originating from seeds (certified in case of species with commercial regulation, or uninfected stocks maintained in seed collections). Considering that our studies on SPMMV single infections were conducted using *N. tabacum* plants, we decided to test whether this host was also susceptible to SPCSV. To inoculate the virus, transmission assays were performed using the natural *vector B. tabaci*. Our results showed that SPCSV could be efficiently transmitted in a semi-persistent manner to *N. tabacum* plants. Although other *Nicotiana spp.* species have been reported to be susceptible to infection with isolates of SPCSV in the literature (Cohen et al. 1992), to our knowledge this result is the first identification of tobacco as a new host for this virus.

4.4.1 SPCSV infectivity assays: Further expansion of the known host range

Since we observed that SPCSV was successfully transmitted by *B. tabaci* to *N. tabacum* plants, a previously unknown host, and considering the rather narrow host range of SPCSV described to date (Cohen et al. 2001), we decided to perform transmission assays to assess whether SPCSV also could successfully infect other hosts. Eleven different plant species belonging to four different botanical families, including already known hosts as controls, (listed on Table M2 of Materials & Methods) were tested for SPCSV infection using the natural vector *B. tabaci* biotype MED for transmission. Inoculations were carried out with at least 25 whiteflies per plant, considered viruliferous after feeding on infected sweet potato plants for 48 hours (acquisition period), and subsequently released to allow feeding on healthy plants during another 48 hours (inoculation period). Regardless of the appearance of symptoms, the presence of SPCSV in all the whitefly-inoculated test plants was assayed at 15 dpi by a specific RT-PCR targeting a sequence of 678 bp in the RNaseIII genomic region of the viral RNA 1.

As expected, previously described hosts such as *I. batatas, I. nil, I. setosa* or *N. benthamiana* were successfully infected by SPCSV, although presenting either no symptoms, or exhibiting only weak vein clearing on leaves and minor distortions (Figure R9a). Regarding the newly identified host *N. tabacum*, again the infected plants did not present almost any conspicuous symptoms on leaves, however at a later time point around 30 dpi the infected plants exhibited a weak stunting phenotype compared to non-infected ones (Figure R9b). Interestingly, SPCSV was detected on tomato plants (*Solanum lycopersicum* cv. Moneymaker) after the transmission assay (3/12 positive by RT-PCR) however the plants did not show any symptomatology along the entire period of observation (not shown).

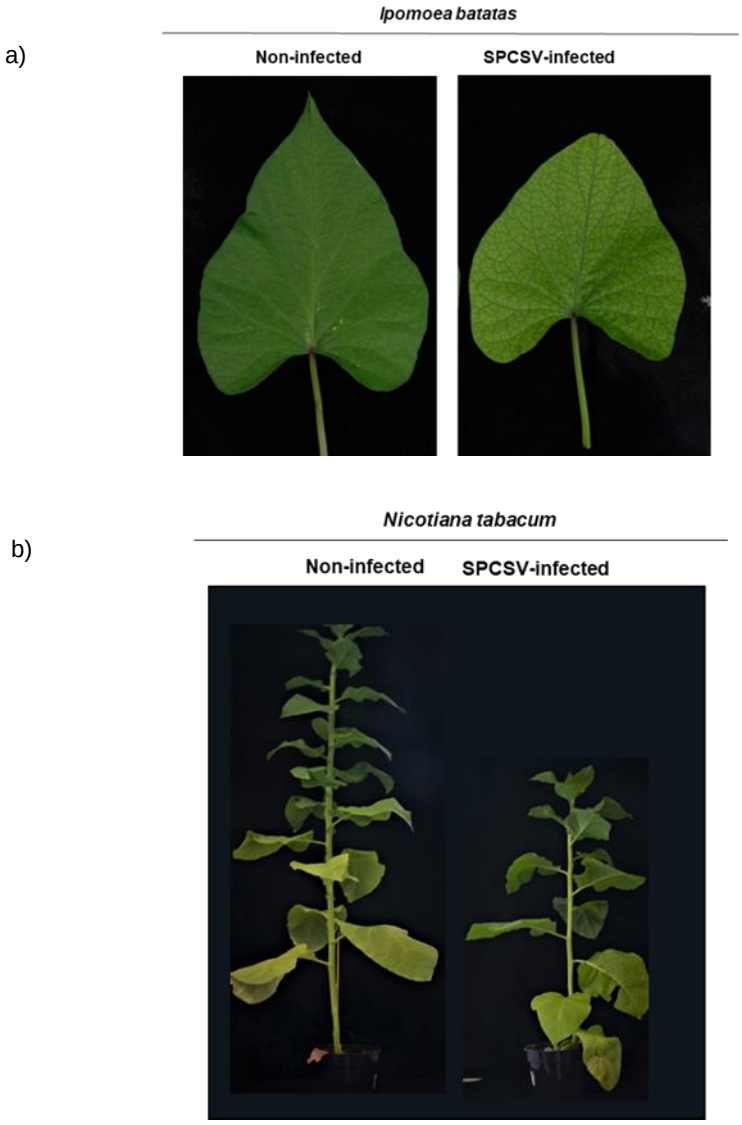

Figure R9. Symptoms associated with SPCSV infection in different hosts. a) Detail of leaves corresponding to a SPCSV-infected sweet potato (right panel) with mild interveinal chlorosis at 15 days post inoculation (dpi), and an uninfected control plant (left panel). b) Healthy *N. tabacum* plant (left panel) compared to a SPCSV-infected plant (right panel) at 30 dpi, showing a stunting phenotype.

Regarding other species, in our experiment the virus apparently failed to infect eggplants (*Solanum melongena L*.), despite belonging to the same botanical family of tomato and tobacco. Similarly, when we tested different *Cucurbitaceae* species such as melon (*C. melo*), squash (*C. pepo*) or pumpkin (*C. maxima*), we were again unable to detect viral infections by RT-PCR in any of the plants.

Lastly, we also tested whether *A. thaliana* plants (Columbia 0 ecotype) could be a permissive host for SPCSV infection, finding that indeed the crinivirus was transmitted with 70% transmission efficiency, the highest rate among all the tested plant species including the natural hosts of *Ipomoea* genus (Figure R10). Despite this high transmissibility rate, there was no detectable symptoms on *A. thaliana* except for a slight stunting phenotype compared to the negative control.

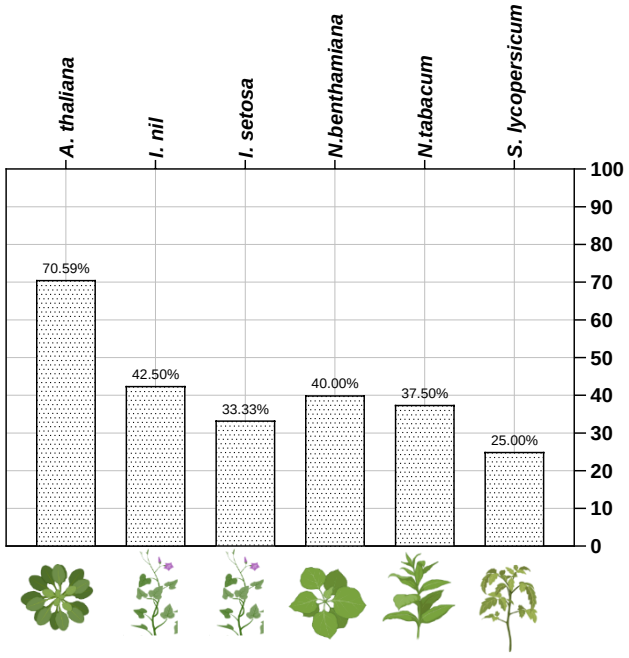

Figure R10. Graphical representation of SPCSV transmissibility efficiency to different susceptible hosts. Transmission percentage of SPCSV to each individual host plant is depicted above the corresponding bars.

Overall, our results indicated that the host range of SPCSV is broader than previously reported. To assess the capacity of these novel hosts to act as reservoirs for the virus, we tested virus transmission from infected tobacco plants back to sweet potato. The assay was designed using SPCSV infected *N. tabacum* plants as inoculum source allowing non-viruliferous whiteflies to feed during 2 days for acquisition, and later the insects were transferred to virus-free sweet potatoes plants for virus inoculation during another 48 hours (Figure R11). Three independent experiments were carried out, using 20 *I. batatas* each time as test plants, finding no infection in any of them by RT-PCR or dot-blot hybridization with a specific RNA probe corresponding to a fragment of the HSP70 genomic region in the viral RNA 2. This negative outcome suggests that the SPCSV susceptible tobacco plants may behave as a dead-end host, at least in our experimental conditions. However, it is important to highlight that this assay cannot be considered conclusive, and further experimentation with the different hosts and in different conditions would be necessary to evaluate the putative importance of these additional hosts for the virus epidemiology.

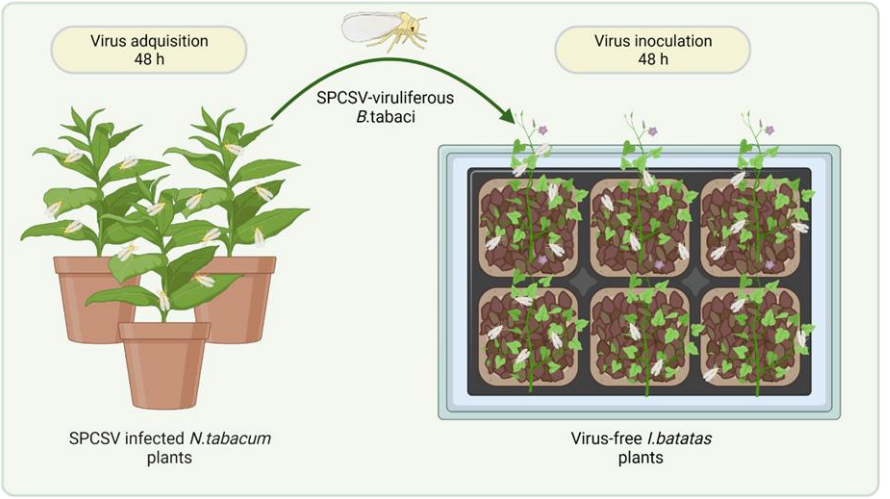

Figure R11. Cartoon illustration of the whitefly mediated SPCSV inoculation assay.

4.5 Effects of SPMMV and SPCSV co-infection in different experimental hosts

Previous studies in *I. batatas* reported strong synergistic outcomes when SPMMV and SPCSV co-infected the same plant (Mukasa et al. 2006). Mixed infected plants with SPMMV+SPCSV were described to present more exacerbated symptoms, including narrowing and distortion of leaves, vein chlorosis, rugosity of the leaf lamina, and extended stunting of the plants (Untiveros et al. 2007). Moreover, SPMMV titers seemed to increase significantly in double infections. To date, SPMMV and SPCSV interactions have not been studied in other hosts apart from sweet potato, therefore we decided to explore how the two viral partners behave when co-infecting different experimental hosts such as *N. tabacum* or *I. nil*.

4.5.1 Mixed infections of SPMMV and SPCSV elicit phenotypic disease synergism in *N. tabacum*

Both isolates of SPMMV were used to reproduce double infections with SPCSV. Essentially, *N. tabacum* plants were first inoculated mechanically with SPMMV isolates 130 or 0900, followed by vector transmission of the crinivirus with SPCSV-viruliferous whiteflies. Single inoculations with each one of the two isolates were also performed as controls. Next, single or double infected plants were analyzed and confirmed the presence of the different viruses at 12 dpi by RT-PCR. The progress of infection was monitored at 13, 20 and 27-dpi with photographs and sampling for total RNA extraction and SPMMV titer measurements by qRT-PCR. At 13 dpi, both single and mixed infected plants developed typical SPMMV symptoms with rugosities and dark green islands in leaves. However, double infected plants already presented a more severe disease phenotype, with more pronounced stunting (Figure R12, top). These symptoms became even more evident at 20 or 27 dpi, where the differences on plant stunting between single or mixed infected plants were notably manifested (Figure R12, middle, bottom), revealing that SPMMV and SPCSV co-infection resulted as expected in more exacerbated symptoms, compared to SPMMV individual infections.

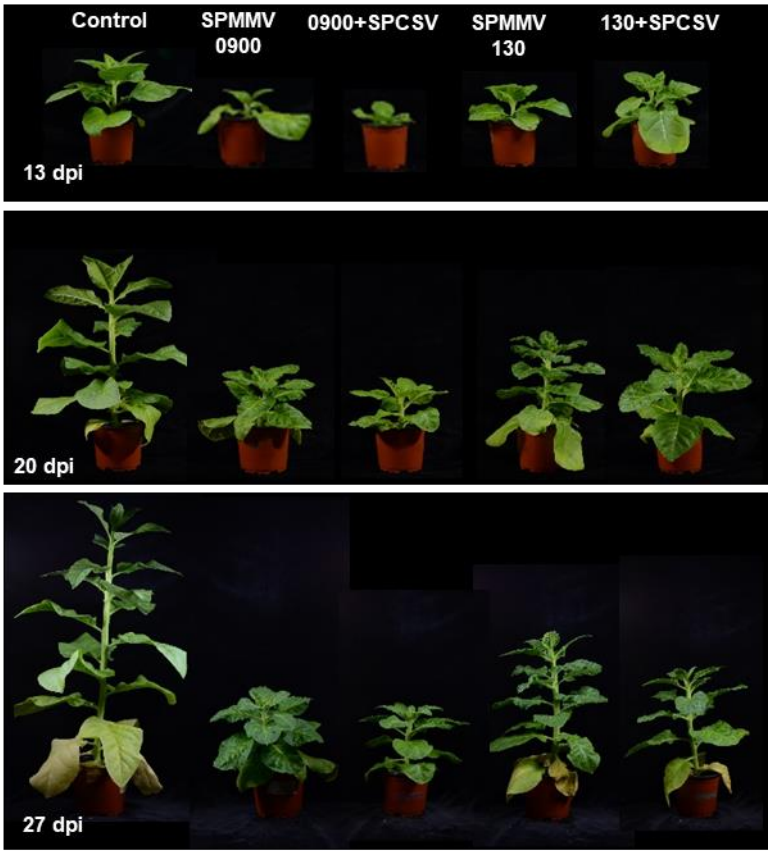

Figure R12. Monitoring infection progress in single- and double- infected plants of *N. tabacum* over time. The plant type according to the infection status (control, single infected or mixed infected) is indicated above. Photographs were captured at the time-points indicated on bottom of each image (13, 20 and 27-days' post inoculation).

Next, we examined the effect of this interaction on SPMMV accumulation using absolute qRT-PCR to measure viral RNA copies. Our results showed that the titers of both SPMMV isolates did not exhibit significant differences between single or double infected plants neither at 13 nor at 20-dpi and only at 27-dpi it was observed a significantly higher number of RNA copies on plants co-infected with SPMMV 130 and SPCSV compared with SPMMV-130 alone, but not in the ones co-infected with 0900 and SPCSV (Figure R13). Interestingly and in accordance with our previous qRT-PCR data of single infections in *N. tabacum*, SPMMV 130 viral levels were higher in both single and double-infected plants

compared to 0900, despite the opposite symptomatology outcome in severity.

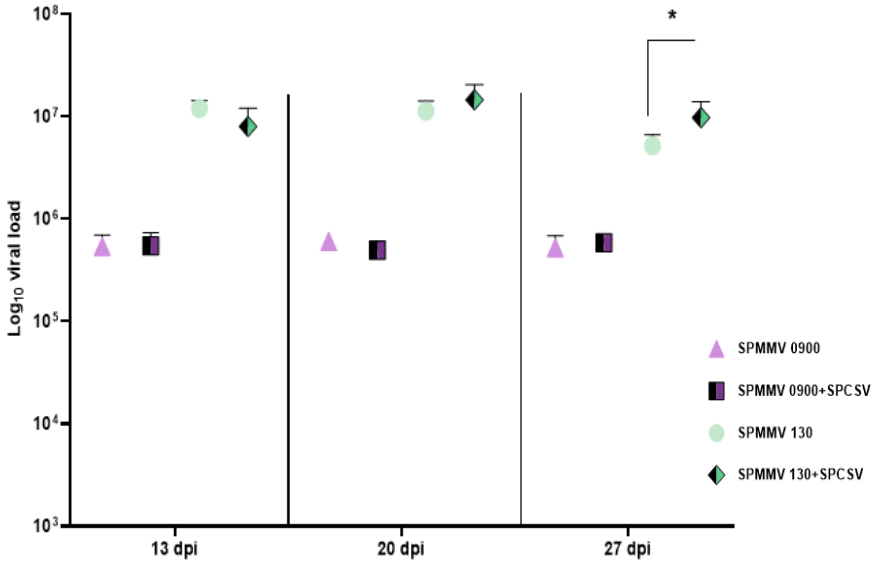

Figure R13. Dynamics of SPMMV viral titers in single- or double-infected plants with SPCSV in *N. tabacum* over time. Absolute quantification of genomic RNA copies of SPMMV 0900 and 130 at 13, 20 and 27-days post inoculation (dpi) in single and mixed infected plants. Geometric symbols indicate the average value of log10 viral genomic RNA copies in 50 ng of total RNA with standard error (SE), derived by five biological replicates (n=5) for each infection state (single infection with SPMMV 0900 or 130 and mixed infections of SPMMV 0900+SPCSV or SPMMV 130+SPCSV). Asterisks indicate significant differences among single or mixed infections at *a*=0.05, calculated by one-way ANOVA and subsequent Tukey's posthoc tests. *P < 0.05, ** P < 0.005, ***P < 0.0005, ****P<0.0001. Triangle: single SPMMV 0900 infection; Square: mixed 0900+SPCSV infection; Circle: single SPMMV 130 infection; Rhomb: mixed 130+SPCSV infection.

4.5.1.1 Vector relationships in the pathosystem SPMMV-tobacco in single and mix-infections with SPCSV

To assess the effect of volatiles emitted from virus infected plants and whether they impact *B. tabaci´*s host preference behavior, we performed Y-tube olfactometer bioassays, comparing 3 different conditions including mock-, single- (SPMMV 130) or mixed-inoculated (SPMMV 130+SPCSV) *N. tabacum* plants at 13 and 20 dpi. The isolate SPMMV130 was chosen since it displayed significantly higher titers in infected plants at the two selected time-points (Figure 13).

Paired comparisons were organized as follows: 1. mock vs. single-inoculated plants; 2. mock vs. mixed-inoculated plants; 3. single vs. mixed-inoculated plants. During the assays, the hypothetical olfactory cues from either type of tested plants were conducted at a fixed flow through the arms of the Y-tube (0.3 liters/minute). Forty individual non-viruliferous adult whiteflies (considered biological replicates) were used per comparison. The insects were released on the base of Y-tube stem, after being briefly immobilized through chilling them for 15 second on ice. Each whitefly was allowed to select either arm of the Y-tube for a period up to 15 minutes. A successful choice was counted only when the individual progressed a distance at least 6 cm or higher inside one of the intersections and hovered there during at least 3 minutes. Whiteflies that did not fulfill those criteria were discarded and considered as non-choice individuals. Visual stimuli interference with the whitefly choice was circumvented by covering the two glass chambers with white bench paper.

The results of the experiment showed no significant differences for any of the three different comparisons at 13 dpi (Figure R14a), and the same outcome was also observed at 20 dpi (Figure R14b). These results indicated that whiteflies did not prefer any type of host plants through perception of volatile stimuli emitted, regardless of their infection status (mock-, single- or mixed-infected).

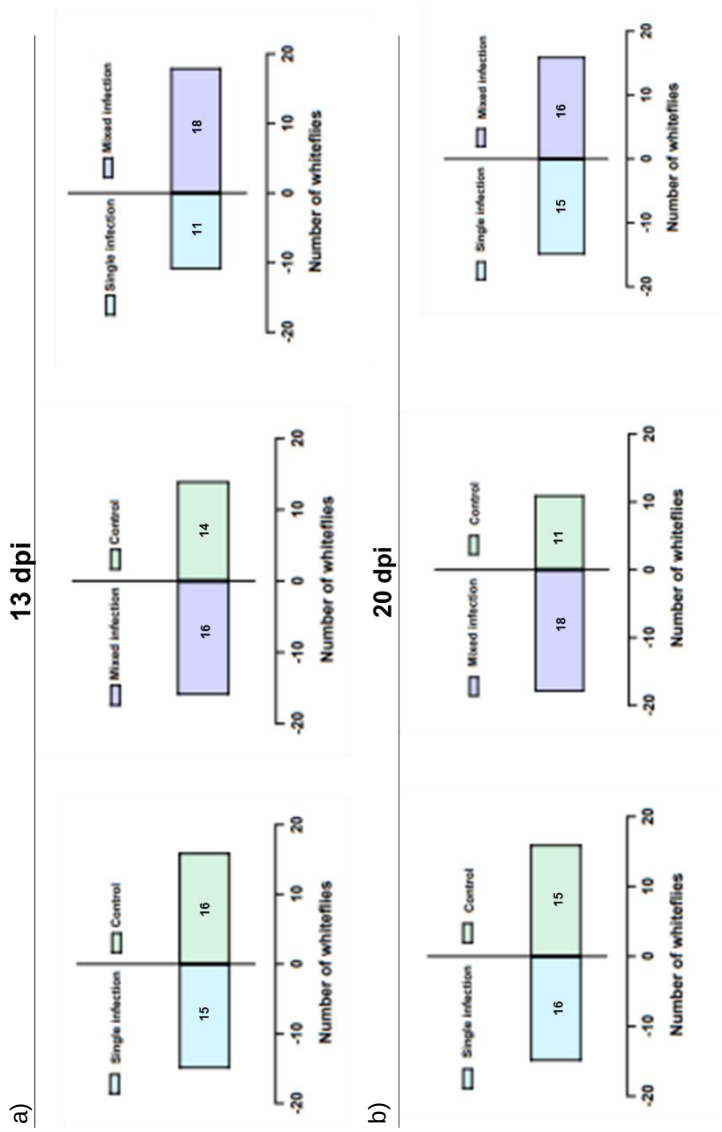

Figure R14. Host selection responses of *B. tabaci*, based on olfactory stimuli. a) Graphical representation of whitefly number responding to volatiles deriving from a SPMMV-infected or mock-inoculated *N. tabacum plant* (left), a SPMMV+SPCSV double-infected or a mock-inoculated *N. tabacum* plant (middle) or a SPMMV-infected versus a SPMMV+SPCSV double-infected *N. tabacum* plant, at 13 days post inoculation and b) at 20 days post inoculation. Each comparison was conducted using a total number of 40 adult whiteflies (replicates), released individually inside the principal arm of the Y-tube and allowed to complete their choice in up to 15 minutes' intervals. When a whitefly remained for more than 3 min across the border line of one of the lateral tube, it was considered as a positive choice, while the whiteflies that did not choose neither of the two directions were discarded and considered as no-choice replicates.

4.5.2 SPMMV and SPCSV co-infection results in detrimental disease phenotype in *I. nil*

In line with our previous comparisons, we investigated the effect of SPMMV and SPCSV mixed infections in *I. nil* plants. We followed the same experimental approach as in the case of *N. tabacum*; therefore, infection evolution of single and double infected plants was monitored at three time points and subsequently virus accumulation was measured by absolute qRT-PCR. At 13 dpi, single or mixed infected plants displayed characteristic viral symptoms, among others leaf curling and vein chlorosis. At that point, double infected plants presented a slightly more intense disease phenotype compared to single infections, with a reduced total foliage area (Figure R15, top).

Remarkably, at 20 or 27-dpi, the mixed infected plants developed exacerbated leaf narrowing, yellowing and severe stunting compared to the ones infected with the individual SPMMV isolates (Figure R15, middle-bottom), indicating that co-infection of the ipomovirus with SPCSV elicit a significant disease synergism, even more pronounced than in *N. tabacum* plants.

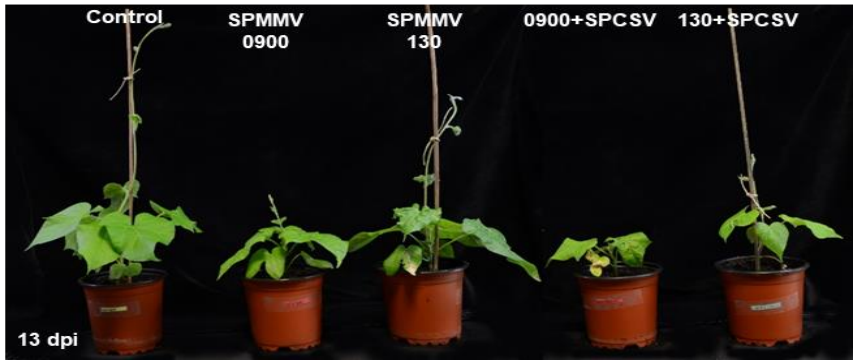

Figure R15. Follow-up of infection evolution in single- and double- infected plants of *I. nil* over time. Infection status of each plant (control, single infected or mixed infected is showed above each picture. Images were taken at three different time-points; 13, 20 and 27-dpi, as indicated on bottom of each image.

We next assessed if this synergism in symptoms was also reflected in the accumulation of SPMMV RNA, measuring virus titers by absolute quantification. We only observed significant differences at 13 dpi for the SPMMV 130 RNA levels, being higher in the case of single- rather than mixed- infected plants (Figure R16). At 20 dpi and 27 dpi, there were no detectable differences in virus accumulation between single or double infections for neither isolate (Figure R16).

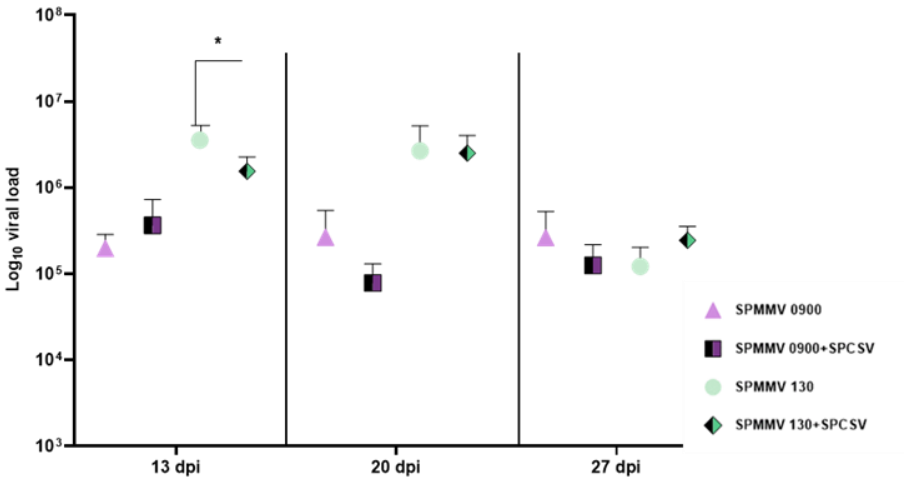

Figure R16. Graphical representation of SPMMV 0900 and 130 RNA copies accumulation at 13, 20 and 27-days dpi, in single or mixed infected *I. nil* plants. Geometric symbols indicate the average value of log10 viral genomic RNA copies in 50 ng of total RNA with standard error (SE), derived by five biological replicates (n=5) for each infection state (single infection with SPMMV 0900 or 130 and mixed infections of SPMMV 0900+SPCSV or SPMMV 130+SPCSV). Asterisks indicate significant differences among single or mixed infections at *a*=0.05, calculated by one-way ANOVA and subsequent Tukey's posthoc tests. *P < 0.05, ** P < 0.005, ***P < 0.0005, ****P<0.0001. Triangle: single SPMMV 0900 infection; Square: mixed 0900+SPCSV infection; Circle: single SPMMV 130 infection; Rhomb: mixed 130+SPCSV infection.

Chapter I - Discussion

Sweet potato is an important crop for food security, being widely used to provide nutrition for the human population in many areas, in particular developing countries. However, its production is threatened by many viral agents that are commonly found in the crop and can elicit a variety of responses, ranging from asymptomatic to rather severe disease outcomes, especially in mixed infections. Certain mixed viral infections of sweet potato can cause very detrimental yield losses, to the point that could endanger food security. The risk of sweet potato epidemics and pandemics is becoming even more alarming given the exponential increase of human population, in combination with other threats like those derived from global warming, rendering the development of efficient and durable control strategies fundamentally urgent. Co-infections between unrelated viruses have been extensively studied by a growing body of literature due to their frequent occurrence in natural and agricultural systems (Alcaide et al. 2020; Moreno and López-Moya 2020). In most cases, these infections can lead to synergistic outcomes with enhanced disease phenotypes, although sometimes they can result in neutralism, causing no effect on the disease compared to individual viruses, while less frequently they can provoke antagonistic interactions, mostly observed in mixed infections of different strains of the same virus rather than between unrelated viruses (Syller 2012; Zhang et al. 2018). One of the most striking examples of a synergistic co-infection between unrelated viruses, is the well characterized SPVD, occurring between the potyvirus SPFMV and the crinivirus SPCSV (Clark et al. 2012). During this interaction, the titers of SPFMV increase up to 600-fold, inducing a pronounced disease phenotype in sweet potato while the titers of the crinivirus remain stable or decrease slightly and the virus remains confined at the phloem (Karyeija et al. 2000). A similar pattern was also observed in mixed infection of SPCSV with other members of the family *Potyviridae*, like the ipomovirus SPMMV, resulting in the denominated sweet potato severe mosaic disease (SPSMD), with an increase on the ipomovirus RNA copies (1000-fold) and yield reductions of 80% (Mukasa et al. 2006). Although well-characterized in sweet potato, these interactions and their putative

repercussions are poorly studied on other alternative hosts that may have a significant impact on virus epidemiology (Tugume et al. 2016). Generally, the outcome of mixed infection is hard to be foreseen due to the natural variability of the viruses involved and the infection timing, and also to diverse ecological factors like the availability of susceptible host species, or the effect of vector organisms, that may modulate the existent interactions (Alcaide et al. 2020).

For all these reasons, in the present chapter we focused on the exploration of mixed infections of the ipomovirus SPMMV and the crinivirus SPCSV. Among the many possible combinations of viruses able to infect sweet potato plants, this particular pathosystem was chosen by several reasons: we have two isolates of SPMMV, the 130 and 0900, that have a differentiated effect (natural variability) on susceptible plants; also, the ipomovirus can be experimentally inoculated to alternative hosts, *N. tabacum* and *I. nil*; and finally, ipomoviruses and criniviruses share the same vector, whiteflies.

First, SPMMV isolates were mechanically inoculated in the two hosts and viral titers were estimated by absolute qRT-PCR, following the infection progress at three different time points. *N. tabacum* plants infected with the isolate 0900, consistently presented a more severe phenotype, including pronounced leaf distortion and general stunting compared to the plants inoculated with the isolate 130 that exhibited a less aggressive disease phenotype. On the other hand, our results showed that at all time points the viral RNA copies of 130 isolate in upper symptomatic leaves were significantly higher than that of 0900, suggesting a negative correlation between the virus accumulation and symptomatology. When testing the other host, *I. nil*, again we observed similar results, with 0900 infected plants presented a more severe disease phenotype compared to the 130 isolate, whilst the titers of the latter were consistently higher at 13 and 20 dpi, with only a slight reduction at 27 dpi. Severity of symptom induction is frequently attributed to high accumulation of viruses, resulting in developmental and morphological alterations, often associated with host transcriptome reprogramming (Bengyella et al. 2015). In fact, the symptom severity caused by certain viruses like the crinivirus CYSDV, has

been directly linked to higher viral loads (Marco et al. 2003; Eid et al. 2006; Domingo-Calap et al. 2020). Puzzled by the fact that we observed more enhanced symptomatology in plants with less virus accumulation and considering that in both hosts the qRT-PCR sampling material derived by the youngest symptomatic leaves, we analyzed the distribution of SPMMV isolates in *N. tabacum* plants, by tissue print. Intriguingly, we observed that the isolate 130 was merely detected in younger leaves, while the isolate 0900 was present in all leaves (both young and old), indicating a longer persistence of the latter. Indeed, plant viruses can have different lifestyles ranging from acute to chronic or persistent, and some of them can switch from one lifestyle to another (Roossinck 2010). The difference we are observing between the two isolates could be partially explained if we assume that isolate 130 is causing an acute infection since it accumulates greatly in the acute phase (young/recently infected tissues) while at later time points the symptoms are reduced and the plant recovers partially. On the contrary, the infection by isolate 0900 could be interpreted as persistent, given its low accumulation in the acute phase but its ubiquitous presence on the entire plant, leading to higher developmental damage.

Virulence is a genetically controlled trait, therefore the genome comparison between the two isolates would be relevant to obtain insights that could account for the distinct phenotypical effects we are observing on the two experimental hosts. To address this, we completed the full genome sequence of SPMMV 0900 and performed comparisons of the coding sequence of each specific gene product between the two isolates, hypothesizing that differences in amino acids sequences could account for changes in their virulence. Our results revealed that P1 protease is the most divergent product between the two isolates (89% identity), coinciding with previously published reports on the high variability of P1 genomic region in members within the family *Potyviridae* (Dombrovsky et al. 2014; Cui and Wang 2019). Both sequences included 15 additional amino acids compared to the SPMMV reference sequence, but this insertion is probably not relevant for the observed phenotype differences since they are present in both isolates (Nigam et al. 2019). Interestingly, several studies have highlighted the importance of P1 protein in the suppression

of host RNA silencing pathway by different ipomoviruses (Valli et al. 2006; Giner et al. 2010; Kenesi et al. 2017; Kenesi et al. 2021). Given the pivotal importance of RNAi in plant defense against viral pathogens, we could speculate that the differences observed in P1 protein of the two isolates could modulate its function during the arms race with the host defenses and thus could affect differently the host fitness. This notion can be further supported by the fact that RNAi plays a pivotal role in plant recovery or tolerance to viral infections and our results show that SPMMV 130 infected plants present a mild recovery at later timepoints while the same does not apply for SPMMV 0900 infected plants (Paudel and Sanfaçon 2018; Sanfaçon 2020). Of course, we should be particularly cautious when raising conclusions related to sequence-specific differences as more studies are required to identify whether the observed discrepancies between the two isolates could account for the host phenotypical outcome.

While looking for an adequate experimental system for mixed infection between the two isolates of SPMMV with SPCSV, we performed preliminary transmission assays of SPCSV using the whitefly *B. tabaci*, to *N. tabacum* plants, a well-established experimental host for SPMMV. Notably, we observed that indeed the crinivirus was successfully transmitted to tobacco plants, a novel host previously uncharacterized, leading us to the exploration of additional susceptible hosts (Cohen et al. 1992; Tugume et al. 2016). Eleven different plant species were tested, and our results confirmed systemic susceptibility for SPCSV in several previously unknown hosts like *S. lycopersicum* or *A. thaliana*, further expanding the host repertoire of the virus. The relevance of new hosts could be particularly high in virus epidemiology, given the possibility of acting as virus reservoirs, especially when grown nearby sweet potato fields. As a first attempt to evaluate the risk of this scenario, we tested whether SPCSV infected *N. tabacum* could act as virus reservoir and our data showed that the crinivirus failed repeatedly to be transmitted back to sweet potato plants through viruliferous *B. tabaci* (biotype MED). This outcome could indicate that *N. tabacum* is a dead-end host, however we should consider that this negative result is not conclusive, and the absence of transmission may be attributed to a lower efficiency, or to

technical issues since all our transmission assays were performed under laboratory conditions and using only a single whitefly species, while under natural environmental conditions or with different vectors the outcome may be different. Of course, the rest of the newly identified hosts should be also tested, and the conditions of the experimental assay should be further optimized before drawing conclusions. Furthermore, the range of susceptible plants to be tested should be expanded, in particular to weeds and other plants likely to be found nearby sweet potato orchards.

The results about the natural variability of the two isolates of SPMMV in two different hosts suggested that the observed differences might reflect the relative weight of acute versus persistent infections. It is too early to establish which one of the two possibilities is the norm in most of the natural isolates but considering the frequent occurrence of multiple infections in sweet potato, our next goal was the exploration of its co-infections with SPCSV in those hosts. With this purpose in mind, mixed infections were established between the two viruses, including the combinations of isolates SPMMV 0900+SPCSV and SPMMV 130+SPCSV, and the progress of infection was monitored over time, focusing on symptom manifestation and absolute quantification of SPMMV 0900 and 130 titers. For practical reasons, vector inoculation with SPCSV required at least a period of 48 h, creating a slight but inevitable time lag between the early mechanical inoculation with SPMMV and the later arrival of the crinivirus. Unfortunately, with this procedure we cannot guarantee the occurrence of co-infections (meaning simultaneous arrival of the two viruses). On the other hand, analyzing super-infections would have required waiting > 10-12 days to verify the establishment of SPMMV infection before the whitefly inoculation with SPCSV. This time lag could be managed experimentally in *Ipomoea* species through propagation of SPMMV-infected cuttings, but certainly not in the herbaceous host tobacco, where the growth period is limited. Therefore, we decided to use the described experimental conditions, although they might indeed differ drastically of the usual dynamics of viral infections in natural conditions. Consequently, our results need to be interpreted as only a first attempt to consider the full complexity of the virus-virus interactions under different

conditions, and it is important to realize these limitations in our experiments.

In both hosts, double infected plants presented more exacerbated symptomatology as compared to SPMMV single infected plants, suggesting that a synergistic interaction might be taking place between the two viral partners, and thus coinciding with previously reported cases when combining these viral players (Moreno and López-Moya 2020). Notably, *I. nil* plants were significantly more affected compared to *N. tabacum,* exhibiting detrimental stunting and developmental arrestment, a phenomenon probably correlated with the close taxonomical relationship to the natural host *I. batatas*. A simplistic and superficial analysis of this pronounced synergism of SPMMV and SPCSV in terms of symptomatology could lead to the assumption that this species displays more vulnerable defense layers than *N. tabacum*, allowing the viral pathogens to cause more evident developmental disruptions, that can eventually turn against the viral fitness (Sanfaçon 2020). Nonetheless, the phenotypic synergism between the two viruses was not reflected on the accumulation on the viral RNA copies as expected from available data in sweet potato. Overall, our results contrasted with the previously reported synergism between SPMMV and SPCSV in sweet potato, although it should be contemplated that our experimental approach includes two experimental hosts with distinct genetic background that could influence the virus-virus-host interactions. In our case, the titers of both isolates do not differ significantly in single of mixed infection of *N. tabacum* at 13 or 20 dpi, although curiously at 27 dpi, and only for the isolate 130, mixed infections with SPCSV resulted in significantly higher viral copies compared to single infections. Similarly, both single and mixed infected plants of *I. nil* did not exhibit important differences in SPMMV accumulation at all the three time points analyzed, despite their severely affected phenotype when both viruses were present. Paradoxically, at 13 dpi SPMMV 130 presented significantly higher titers in single infected plants rather than in mixed infected plants. As recently reviewed, the virus-virus interactions might be quite variable depending on viral strains, hosts, and many other conditions

To continue with this study, we also wanted to test whether volatile cues emitted by single (SPMMV) or mixed (SPMMV+SPCSV) infected plants of *N. tabacum* could influence the vector choice towards a specific host. We opted to start analyzing the possible effect of volatiles in the first choice of vectors. Indeed, accumulative experimental data is highlighting the importance of volatiles stimuli emitted by virus infected plants to attract natural vectors and facilitate their horizontal propagation (Mauck et al. 2014; Fereres et al. 2016; Darshanee et al. 2017; Chang et al. 2021). Nonetheless, our results showed that the first choice of *B. tabaci* towards a specific host was not driven by odor cues, since it was independent to the infection state of the tested plants (mock, single or mixed infected) when using these specific viral pathogens under our experimental conditions. With this data, future works should be designed to evaluate other possible cues, and also to address the vector behavior in the different plants using monitoring systems like EPG (electrical penetration graphs), a powerful tool frequently used with aphids (Fereres and Moreno 2009) but much less applied to whiteflies (Rodríguez-López et al. 2011).

To summarize, we can conclude that it is not straightforward to explain the differences between the virus accumulation and the symptom manifestation between single and mixed infected plants in the case of SPMMV and SPCSV, as diverse factors can be implicated. Although future works are necessary to shed more light into the complex mechanisms of mixed infections in sweet potato and the epidemiology of sweet potato viruses, we believe that our results might be useful for a better knowledge of their interactions, providing novel data that might assist the establishment of future management measures to reduce the negative impact of viral infections in sweet potatoes.

CHAPTER II

Results presented in this chapter are included within a manuscript currently in preparation.

Authors

Ornela Chase[1], Giannina Bambaren[1], Adrián A. Valli[2] and Juan José López-Moya[1]

Affiliation

[1]Centre for Research in Agricultural Genomics, CRAG, CSIC-IRTA-UAB-UB, Campus UAB, Cerdanyola del Valles, Barcelona, Spain.
[2]National Centre for Biotechnology, CNB-CSIC, Campus UAM, Madrid, Spain

5. Chapter II - Results

Unravelling the SPV2-encoded proteins with RNA silencing suppressor activity

5.1 Identification of RSS activity in gene products of SPV2

5.1.1 Gene products of SPV2 conferring local RSS activity

The genome of SPV2 encodes the usual gene products of members of the *Potyvirus* genus, plus the predicted P1N-PISPO, which only can be found in some sweet potato potyviruses (Figure R17a). Since the gene products encoded at the 5' ends of potyviral genomes frequently exhibit RNA silencing suppression capacity, five constructs expressing SPV2-encoded proteins in this region were tested by using standard *Agrobacterium tumefaciens* co-infiltration approaches (Voinnet et al. 2000; Valli et al. 2006). These proteins were P1, HCPro, P1HCPro in tandem, P1N-PISPO, and a P1 variant (denominated P1-ONLY) expressed from a cistron that harbors modifications aiming to abolish the expression of P1N-PISPO. The viral-derived cistrons were first cloned in suitable binary vectors, which were further mobilized into *A. tumefaciens* (Figure R17b) for subsequent co-infiltration with a second *A. tumefaciens* strain that harbors a GFP-expressing construct in *N. benthamiana* leaves.

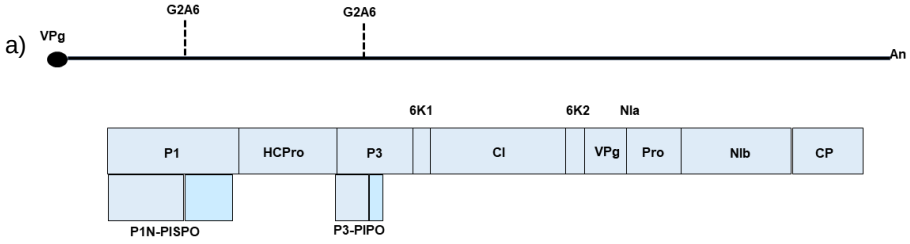

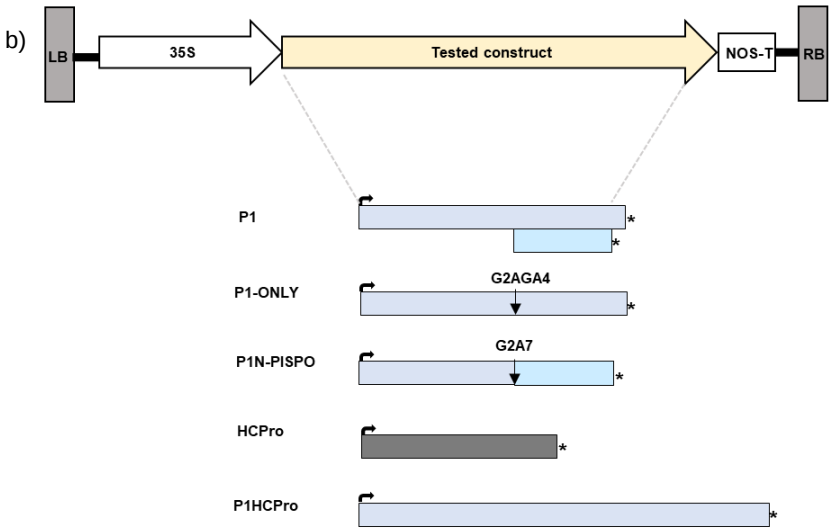

Figure R17. a) Genome map of SPV2 where the genomic +ssRNA is represented as a black solid line. The VPg protein is covalently linked to the virus 5´-end and is depicted as a black circle while the polyA tail at the 3´-end is shown as An. The viral open reading frame (ORF) is proteolytically cleaved into ten mature gene products (represented as boxes), while two additional cistrons denominated P1N-PISPO and P3N-PIPO, are produced by a polymerase slippage event in conserved G2A6 motifs of P1 and P3 genomic regions respectively. b) 5´prime SPV2-encoded gene products tested for RNA silencing suppressor activity. Black arrows on the beginning of each cistron indicate the methionine start codon (AUG) and the asterisks at the end represent each stop codon. P1N-ONLY and P1N-PISPO proteins contain site-directed mutagenesis on the G2A6 genomic region, to avoid or ensure the polymerase slippage in each case. All proteins were cloned to adequate binary vectors for subsequent *in planta* expression under the 35S promoter.

As controls, a well-characterized RSS (WMV HCPro) and a negative control (an untranslatable HCPro of WMV in inverted orientation, designated orPCH) were included side-by-side with the different tested constructs, and the GFP-derived fluorescence in each leaf was monitored at 3, 5 and 7 dpa under UV light. At 3 dpa, patches infiltrated with the negative control consistently showed very low intensity of GFP fluorescence, with a further reduction at 5 and 7 dpa as result of plant RNAi induction (Figure R18). In contrast, patches expressing the positive control, as well as those expressing P1N-PISPO, HCPro and P1HCPro

showed evident fluorescence signal at 3 dpa, supporting the idea that these proteins can locally suppress plant RNA silencing (Figure R18a, 3 dpa). The positive control (HCPro-WMV), HCPro and P1HCPro presented the most intense fluorescence, with comparatively less fluorescence in the case of P1N-PISPO. Remarkably, GFP signals slightly higher than that in the negative control was also observed in patches expressing P1 and its variant P1-ONLY (Figure R18a, 3 dpa). Consistent with these observations, and with a genuine effect of these viral proteins over RNA silencing, qRT-PCR showed significant difference when comparing the accumulation of GFP mRNA at 3 dpa in patches expressing the positive control, P1N-PISPO, HCPro and P1HCPro with that of patches from the negative control (Figure R18b, 3 dpa). At later time points, however, significance was maintained only for the case of patches expressing the positive control (Figure R18b, 5 and 7 dpa). These results were further confirmed by Northern blotting, using a specific RNA-probe detecting GFP mRNA levels in the infiltrated patches (Figure R18c). The differences of GFP fluorescence and mRNA expression between P1N-PISPO and HCPro with the positive control suggests that the antisilencing capacity of SPV2 RSSs is weak.

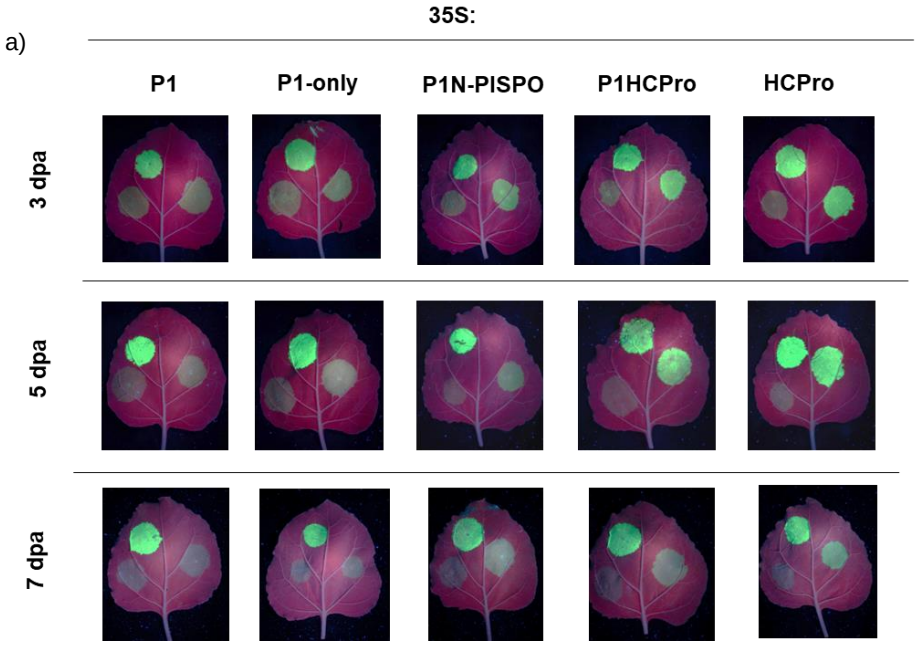

b)

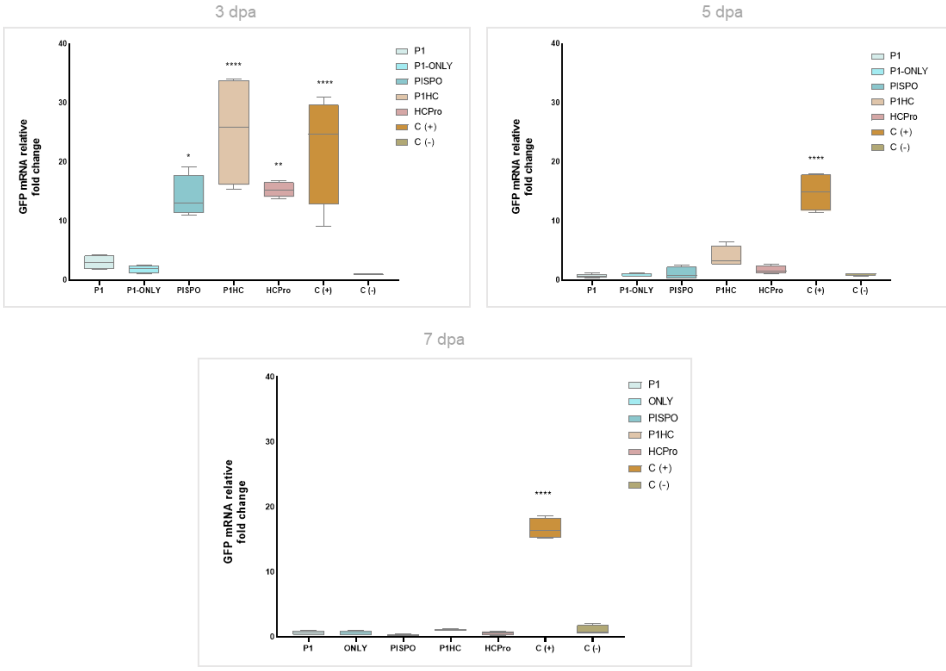
3 dpa
5 dpa
7 dpa
GFP mRNA relative fold change
P1
P1-ONLY
PISPO
P1HC
HCPro
C (+)
C (-)
ONLY
****
**
*

c)

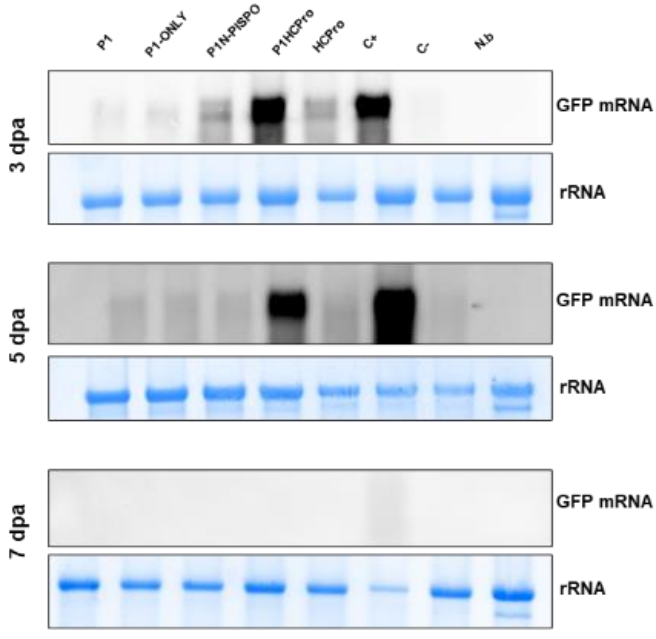
P1
P1-ONLY
P1N-PISPO
P1HCPro
HCPro
C+
C-
N.b
3 dpa
5 dpa
7 dpa
GFP mRNA
rRNA

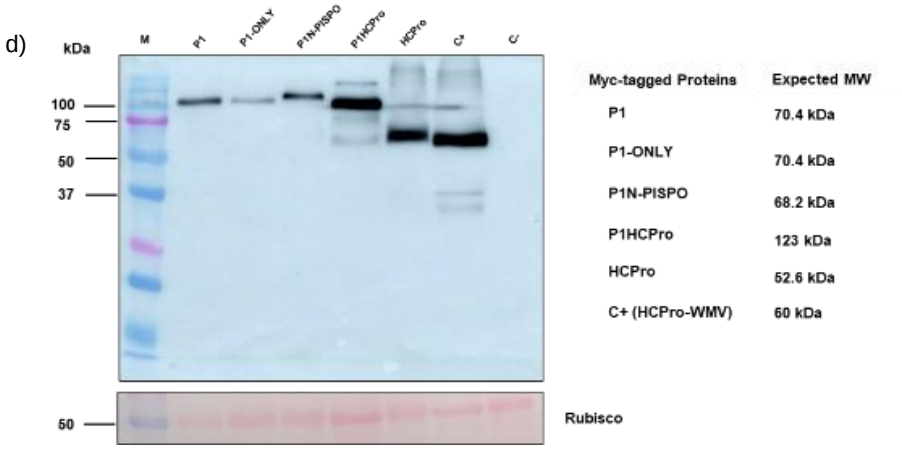

Figure R18. SPV2 proteins exhibiting RNA silencing suppressor activity in *N. benthamiana* plants. a) Representative images of the agroinfiltrated leaves with the different tested constructs (P1; P1N-ONLY; P1N-PISPO; P1HCPro; HCPro;) under UV light at 3 (top), 5 (middle) or 7-days post infiltration (bottom). A positive (HCPro-WMM) and negative control (inverted form HCPro-WMV, hampering its expression), were also included on the left leaf side (top and bottom, respectively). b) Relative quantification of GFP mRNAs level, assessed by qRT-PCR and normalized against the negative control mean value at three different time-points (3, 5 and 7-dpa). Asterisks indicate statistically significant differences compared to the negative control in a=0.05, derived by one-way ANOVA test and subsequent Bonferroni´s multiple comparisons tests. c) Assessment of GFP mRNAs level by Northern blotting, using a specific DIG-labelled GFP RNA probe at three different time-points (3, 5 and 7-dpa). RNA derived by WMV-HCPro infiltrated plants served as positive control while RNA derived by WMV-orPCH- or mock-infiltrated *N. benthamiana* was used as negative control. Methylene blue staining of rRNAs was employed as loading control. d) Western blot analysis of the N-terminus MYC-tagged SPV2-tested proteins (corresponding molecular weights are shown on the right table) at dpa. Specific anti-MYC primary antibody and the corresponding anti-mouse secondary Ab were used to reveal the blot. Total protein extract derived by a non-agroinfiltrated *N. benthamiana,* was used a negative control (C-). M lane represents the migration of the molecular weight marker in kDa. Ponceau red staining was used for visualization of Rubisco's large subunit (53 kDa), serving as loading control.

To ensure the proper expression of all viral proteins, N-terminal MYC-tagged versions were generated from the same pENTR intermediate constructs, to be then agroinfiltrated in *N. benthamiana* leaves for further analyses of total protein extracts, from samples collected at different time

points, by SDS-PAGE and Western blot. All viral gene products were detected properly at early stages (Figure R18d); however, after 3-4 dpa their accumulation was notably reduced (Figure R19), and at later times (7 dpa) they were mostly undetectable (data not shown).

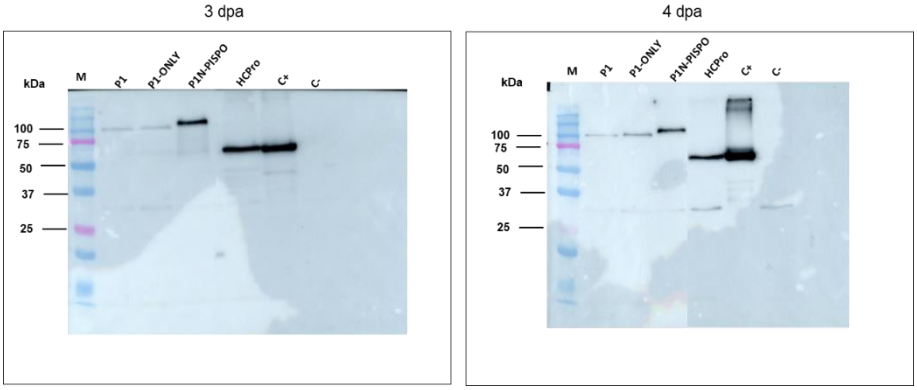

Figure R19. Western blot analysis of the N-terminus MYC-tagged SPV2-tested proteins at 3 (left panel) and 4 dpa (right panel) showing their gradual degradation at early stages of expression. Blot detection was done using a specific anti-MYC serum and extract derived by a non-agroinfiltrated *N. benthamiana,* was used as negative control (C-). Molecular weight marker migration is shown in M lane (kDa).

5.1.2 *Cis* or *trans* expression of P1 does not affect the local RSS capacity of HCPro, neither does the co-expression of P1N-PISPO

In early studies, potyviral P1 was suggested to strengthen the RNA silencing suppression capacity of HCPro when they were expressed together (Kasschau and Carrington 1998; Anandalakshmi et al. 1998; Valli et al. 2006), although later works showed that P1 plays a major function in PPV infection independent of RNA silencing (Pasin et al. 2014; Shan et al. 2015). Since P1 and HCPro are expressed in *cis* naturally as part of the viral-encoded polyprotein, we wanted to examine whether P1 of SPV2 enhances the suppressor activity of HCPro. To do so, we co-expressed the GFP reporter independently with P1HCPro (in *cis*) and P1+HCPro (in *trans*), as well as with positive and negative controls. The expression of GFP was inspected over time, showing that leaf patches expressing

P1HCPro produced similar GFP fluorescence than patches expressing P1+HCPro (Figure R20a). ImageJ quantification of GFP fluorescence intensity at 3 dpa showed non-significant differences when comparing patches expressing either P1HCPro or P1+HCPro, while significant differences were observed on patches expressing P1HCPro, P1+HCPro or the positive control compared with those corresponding to the negative control, as revealed by one-way ANOVA test, followed by Bonferroni's multiple comparisons test (Figure R20b). These results indicate that P1 of SPV2 does not have a stimulatory effect on the RSS activity of HCPro when co-expressed in *cis* as in the viral genome.

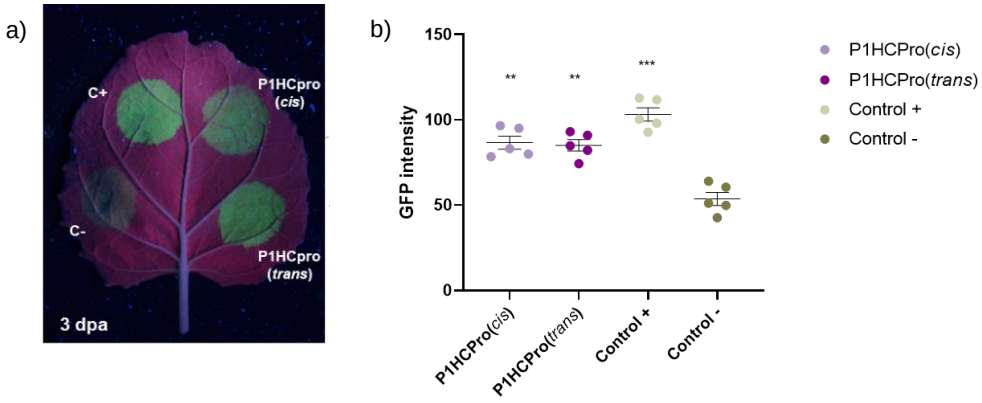

Figure R20. The RNA silencing activity of P1HCPro construct is independent of P1 expression in *cis* or *trans.* a) Image of a *N. benthamiana* leaves co-infiltrated with the different combination of constructs, captured under UV light at 3 dpa, depicting leaf patches with P1HCPro in *cis* (top-right patch) or *trans* (bottom-right patch). A positive (top-left) and negative control (bottom-left) were included as well. b) Scatterplot representation of GFP intensity exhibited on the four different agroinfiltrated patches, assessed by ImageJ quantification at 3 dpa. Each dot represents a biological replicate (5 replicates) and the average value +/- standard error of the mean (SEM) is depicted in black dashes. Asterisks indicate significant differences compared to the negative control derived by one-way ANOVA, and subsequent Bonferroni´s multiple comparisons tests a=0.05.

We also aimed to know whether the frameshift protein P1N-PISPO affects the silencing suppression capacity of P1HCPro when they are co-expressed. Considering that P1N-PISPO derives through polymerase slippage and its presence under native viral infection is expected to be

significantly lower compared to the rest of viral proteins derived from the viral polyprotein, we set out to co-express P1HCPro with different serial dilutions of P1N-PISPO (1/5 and 1/10), trying to approximate the ratio occurring during the native viral infections. The GFP reporter was co-expressed with P1HCPro, and the GFP expression estimated by the emitted fluorescence was compared to that of leaf patches co-expressing P1HCPro+P1N-PISPO (1/5 dilution) and P1HCPro+P1N-PISPO (1/10 dilution) plus GFP. Two controls were also used, including the orPCH construct and P1N-PISPO (1/10 dilution). As in previous experiments, GFP was monitored at 3, 5, and 7 dpa, and visual florescence did not differ among the patches infiltrated with merely P1HCPro or P1HCPro+P1N-PISPO, suggesting that P1N-PISPO does not exert any significant alteration of the activity of P1HCPro (Figure R21).

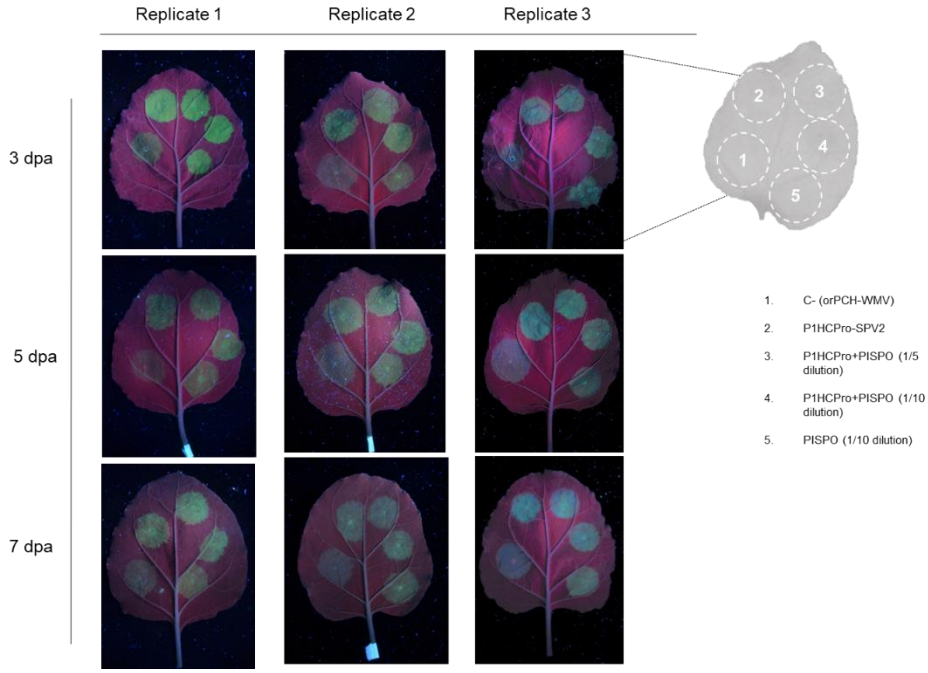

Figure R21. P1N-PISPO does not affect the RNA silencing activity of P1HCPro. Images of *N. benthamiana* (3 biological replicates) captured under UV light at 3, 5 and 7 dpa, co-agroinfiltrated with a combination of different constructs as illustrated on the right panel, where each patch number refers to the corresponding individual constructs or to the co-expression at the indicated dilutions.

5.1.3 SPV2-encoded RSS proteins do not hamper systemic spread of RNA silencing

To assess whether SPV2-encoded RSSs interfere with the spread of RNA silencing signals from basal leaves to distal tissues, we used a well-characterized GFP-transgenic *N. benthamiana* plant (line 16c). In this experiment, we co-expressed the GFP reporter along with P1, P1-ONLY, P1N-PISPO or HCPro in basal leaves, and followed the spread of silencing signals over a period of 28 days by monitoring the fluorescence produced through the whole plants due to the expression of the integrated GFP transgene. At 7 dpa, leaves expressing P1N-PISPO and HCPro, the two confirmed RSSs, exhibited a faint red halo around the infiltrated area as an indication of transgene silencing via cell-to-cell movement of RNA silencing signals (Figure R22a). At 28 dpa, GFP fluorescence completely disappeared in all plants co-expressing the two constructs (Figure R22b), suggesting that none of the viral gene products is able to efficiently block the systemic movement of RNA silencing signals from infiltrated leaves to distal parts of the plants.

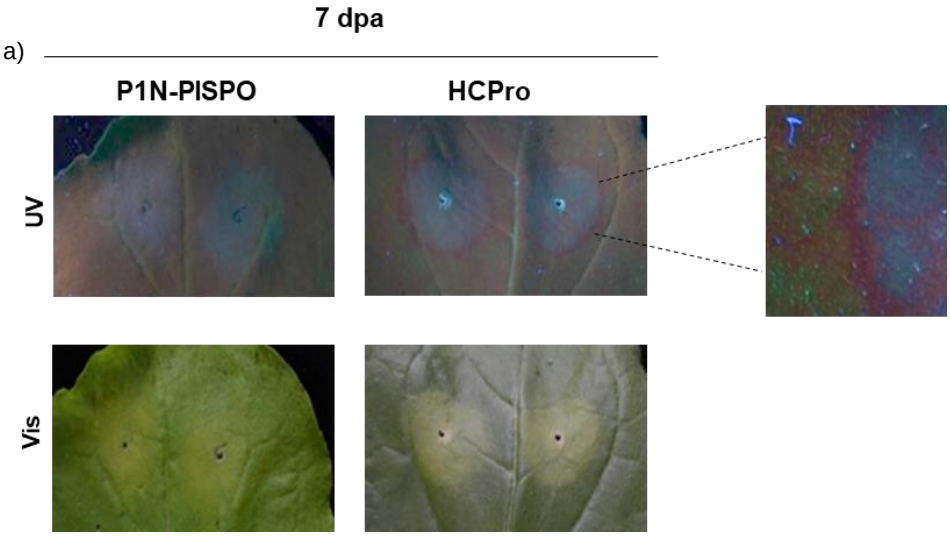

b)

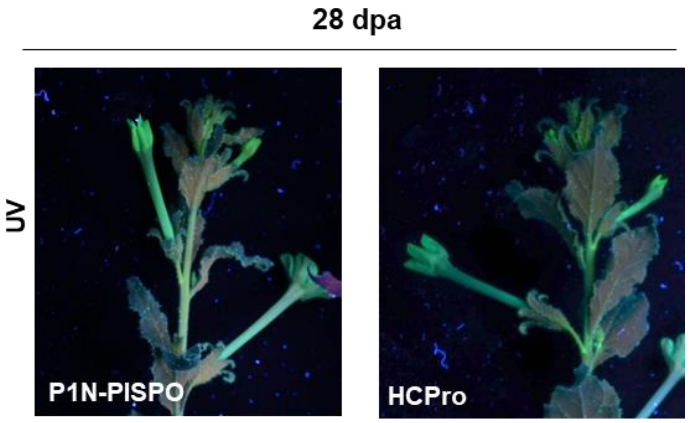

Figure R22. SPV2 proteins with RSS activity do not hamper the systemic movement of the silencing signal. a) Detail of *N. benthamiana* 16c leaves under UV (top) or normal light (bottom) at 7 dpa, co-infiltrated with P1N-PISPO and HCPro. Red halos around agroinfiltrated patches indicate that neither P1N-PISPO nor HCPro suppress the movement of RNA silencing. b) Images of the same plants captured at 28 dpa under UV light, where GFP expression has been silenced systemically.

5.2 PVX pathogenicity is reinforced by different SPV2-encoded proteins

To test the relevance of SPV2 encoded proteins in the context of a viral infection, we took advantage of a PVX-based vector (Valli et al. 2008). P1, P1-ONLY, P1N-PISPO and HCPro of SPV2 were cloned into the PVX-derived vector, generating the chimeric-PVX constructs depicted in Figure R23a. HCPro of WMV and P1b of CVYV were cloned as well, serving as positive controls, since they are strong and well-characterized RSSs (Valli et al. 2006; Domingo-Calap et al. 2021). Juvenile *N. benthamiana* plants approximately at the stage of five true leaves were independently agro-inoculated with several controls: PVX, PVX-GFP, PVX-HCPro-WMV, PVX-P1b-CVYV, as well as PVX-SPV2 chimeric viruses, and viral symptoms were observed at 8 dpa. Symptoms in upper non-inoculated leaves of plants infected with PVX or PVX-GFP resulted in mild mosaic and slight vein clearing, whereas more exacerbated symptoms appeared in equivalent leaves of those plants inoculated with the PVX-SPV2

chimerical viruses, PVX-HCPro-WMV, and PVX-P1b-CVYV (data not shown). After 15 dpa, a generalized necrosis was observed in plants infected with PVX-P1N-PISPO, similarly to that detected in plants infected with the two positive controls (Figure R23b), leading to complete wilt after 20 dpa (data not shown). Interestingly, plants infected with PVX-HCPro, likewise plants infected with PVX or PVX-GFP, presented a milder phenotype and did not suffer severe symptoms, suggesting a mild recovery. To our surprise, PVX-P1 and PVX-P1-ONLY induced more severe symptoms than PVX, PVX-GFP and even PVX-HCPro, but milder than those produced by PVX-P1N-PISPO and the two positive controls (Figure R23b). When we measured the total foliage weight of plants, we observed that all individuals inoculated with the PVX-SPV2 chimerical viruses developed a significantly lower amount of leaf tissue compared to those plants inoculated with PVX or PVX-GFP, suggesting that PVX infection can result in more detrimental disease outcomes when combined with different SPV2 proteins (Figure R23c). Although we were not able to quantify PVX titers due to extended necrotic phenotype in most plants, the coat protein levels of PVX were assessed by Western blotting and showed a higher accumulation in upper non-inoculated leaves of plants infected with P1N-PISPO and the two positive controls compared with those in equivalent tissues of plants infected with PVX-GFP and PVX-HCPro (Figure R23d). Altogether, these results indicate that different SPV2 encoded proteins enhance PVX pathogenicity like other previously described RSS proteins (Pruss et al. 1997; Valli et al. 2008; Feng et al. 2018), and suggest that this effect is likely related to the capacity of these proteins to interfere with the RNA silencing machinery of the plant.

a)

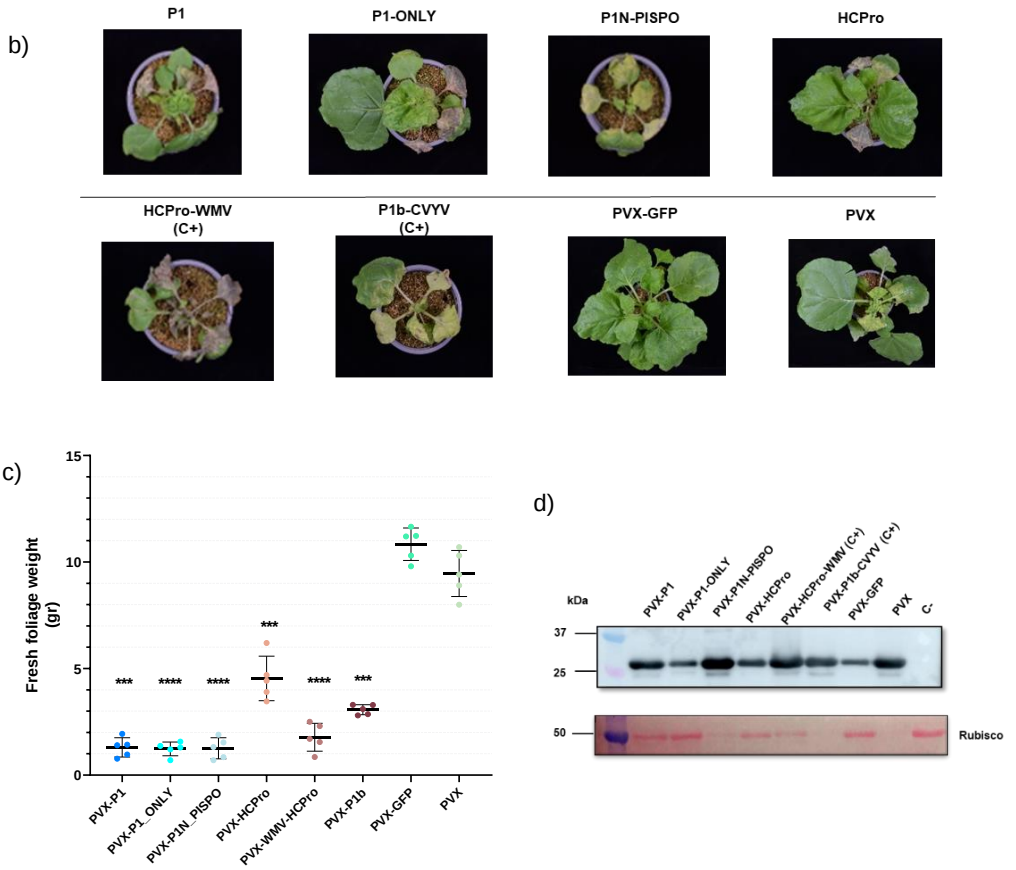

Figure R23. PVX pathogenicity is enhanced by SPV2-encoded proteins. a) Schematic illustration of pGWC-PVX, a Gateway-adapted binary vector where the RSS protein coding sequence is inserted adjacent to attB1 and attB2 cloning sites. b) Infection symptomatology of *N. benthamiana* plants inoculated with PVX expressing P1, P1-ONLY, P1N-PISPO, HCPro, WMV-HCPro (C+), P1b-CVYV (C+), GFP or wild-type PVX. Photographs were captured at 15 dpi. c) Scatterplot representation of the fresh foliage weight of *N. benthamiana* plants infected with the different PXV constructs at 15 dpi. 5 biological replicates were inoculated with each specific PXV-chimeric construct and the fresh tissue weight (gr) of each individual plant was estimated and illustrated by the mean value +/- SD. Asterisks indicate statistical significance of each value compared to the average value of PXV bare infection (a=0.05), calculated by one-way ANOVA and subsequent Dunnett's multiple comparisons test. d) Western blot analysis of total protein extracts derived by *N. benthamiana* leaves infected with different SPV2-PVX chimeric constructs or PVX-GFP and PVX alone, using anti-PVX CP primary antibody at 15 dpi. Extracts derived by infiltrated tissue with PVX-HCPro-WMV or PVX-P1b-CVYV were used as positive control. Healthy *N. benthamiana* leaves were also analyzed as negative control. A Ponceau red-stained blot depicting the large subunit of Rubisco (53 kDa) is shown at the bottom and served as a loading control.

Chapter II - Discussion

RNA silencing constitutes a vital antiviral defense mechanism in plants (Baulcombe 2022). To circumvent this defense barrier and facilitate infection, plant viruses encode proteins that interfere with one or multiple steps of the silencing pathway (Burgyán and Havelda 2011). Virtually all plant viruses have evolved at least one gene product with RNA silencing capacity and many times these proteins are multifunctional, being essentially involved in different steps of the viral infection cycle (Csorba et al. 2015; Li and Wang 2019). In this work we have explored the complexity of RSS function in one particular potyvirus infecting sweet potato plants, the SPV2. Sweet potato represents an attractive case of study for pathologists, being susceptible to an extensive group of different viruses, as revealed by numerous studies (Clark et al. 2012; Moreno and López-Moya 2020). The description of the different viruses capable to infect sweet potato plants has required additional efforts due to the peculiarities of the pathosystem, characterized by frequent emergence of multiple infections that only resulted in noticeable diseases for certain combinations of viral agents, particularly those involving potyvirids plus the crinivirus SPCSV (Mukasa et al. 2006; Aritua et al. 2007; Untiveros et al. 2007). Contrarily to most mixed infections in plants where the potyvirus partner usually contributes to synergistically enhance the severity of the unrelated viruses, sweet potato appears to be the other way around, with the potyvirids experimenting great accumulation boosts when they coincide with the crinivirus SPCSV. It was tempting to attribute this outcome to peculiarities of the partner virus´s RNA silencing suppressor functions, however the complexities of the interactions have difficulted the task. On one hand, the RNA silencing suppressor function in SPCSV has attracted logically a major attention (Kreuze et al. 2005; Cuellar et al. 2009; Weinheimer et al. 2014; Weinheimer et al. 2015), that also lead even to propose high throughput screenings to find inhibitors targeting the RNase III enzyme (Wang et al. 2021); but on the other hand, valid explanations for the puzzling behavior of sweet potato potyviruses remained elusive until recently. Even after revealing the existence of P1N-PISPO and its contribution to RSS activity in SPFMV, gleaning further

information regarding the perplexity of sweet potato viruses and their intricate RSS system continues to be a need (Mingot et al. 2016; Rodamilans et al. 2018).

Following our exploration of the sweet potato pathosystem with particular attention to potyvirids, we have started to consider the evolutionary perspective laying behind these viruses. Indeed, sweet potato potyviruses constitute a taxonomically different cluster within the large potyvirus genus (Inoue-Nagata et al. 2022). Particularly intriguing is the case of SPLV where no P1N-PISPO is present: we are starting to explore in a separate piece of work as a side project this rather peculiar virus that could represent a relict ancestor of other sweet potato potyviruses before acquiring the longer P1s with P1N-PISPO, although we cannot exclude the alternative hypothesis of having lost precisely that element (Chase, Ros and Lopez-Moya, unpublished results).

As a starting point in our study that clearly differs from the SPFMV case, we have found that SPV2 HCPro locally confer RSS activity. Thus, we envisage that its mode of action might be similar to previously characterized homologous HCPro proteins of other potyviruses, since many of the proposed antisilencing domains (like the FRNK motif) appeared to be conserved in SPV2 HCPro. Based on this good conservation, we can speculate that SPV2 HCPro might interact with and sequester siRNAs and/or disrupt the silencing machinery at a different step (Ivanov et al. 2016; del Toro et al. 2017). Interestingly, SPV2 HCPro did not enhance PVX pathogenicity at the same level of other gene products, however it caused a significantly lower production of foliage on the infected plants compared to the PVX sole infection (see Figure R23). The behavior of SPV2 HCPro in the PVX assay resembles earlier results about the synergism between PVX and TEV (Shi et al. 1997). Furthermore, also the HCPro of SPFMV failed to provide clear RSS activity in a transient assay in *N. benthamiana*, but it functioned in the context of a PPV-based chimeric viral construct to rescue infection (Mingot et al. 2016; Rodamilans et al. 2018). These apparent discrepancies stress the importance of testing the RSS capacity of any given protein with more than one experimental system to grasp all their

singularities. For instance, while SPV2 HCPro did not enhance greatly PVX pathogenicity compared to the other gene products, in the case of P1N-PISPO we observed both strong local activity (Figure R18), and fully functional enhancement in the course of a PVX infection (Figure R23).

Regarding the possible mode of action of the identified RSS, we noticed the presence of WG/GW motifs that are considered important for interactions with AGO proteins (Azevedo et al. 2010; Pérez-Cañamás and Hernández 2015). In the case of the P1N-PISPO of SPV2, the first (out of 4) WG/GW motif appeared to be precisely aligned to equivalent positions as in the P1N-PISPO of SPFMV. Mutagenesis in SPFMV P1N-PISPO demonstrated that disruption of this first motif, but not the others, abolished its RNA silencing suppressor capacity (Mingot et al. 2016; Untiveros et al. 2016). Therefore, it is tempting to speculate that SPV2 P1N-PISPO might interact with AGO and deploy similar molecular mechanisms as it does the P1 of SPMMV in which the presence of conserved WG/GW motifs were key elements for the silencing capacity of the protein (Giner et al. 2010; Kenesi et al. 2017). Interestingly, it was recently shown that GW motifs in HCPro facilitate AGO1 recruitment for proviral functions, and the association of VARICOSE to a multiprotein complex, with involvement in the production of stable potyviral particles (Pollari et al. 2020; De et al. 2020).

The role of P1 appears to be also relevant for the RSS function in SPV2, but not associated to the *cis*-acting enhancement of HCPro (Kasschau and Carrington 1998; Anandalakshmi et al. 1998; Valli et al. 2006). An increase in translation efficiency of HCPro by P1 was considered to explain this enhancement, although the exact mechanisms are still controversial, and it cannot be excluded some specificity for each combination of host and virus (Tena Fernández et al. 2013). For instance, our data with SPV2 coincides with previous observations in PPV where P1 exhibited positive roles for infection that were independent of RNA silencing (Pasin et al. 2014). In our hands SPV2 P1 acted apparently as RSS in the context of a PVX infection, since it enhances PVX symptom severity, although did not appear to present significant local silencing activity. Again, the evolutionary perspective could serve to provide a frame

for this apparent contradiction: the P1 of SPFMV has been proposed to result from a recombination event between a potyvirus and an ipomovirus, and the P1s of ipomoviruses are known to act as RSSs, although P1 of potyviruses normally does not (Valli et al. 2007; Untiveros et al. 2010). Interestingly, SPV2 and SPFMV P1 present high homology in the N- and C-terminal regions, while sequence variation occurs mainly in the central hypervariable region (Li et al. 2012). The role of potyvirid P1s have been largely linked to host range specificity, and indeed in some cases P1 relies on a still unknown host factor for its activation however its possible direct role in RNA silencing still awaits to be elucidated in most viruses within the genus *Potyvirus* (Salvador et al. 2008; Maliogka et al. 2012; Shan et al. 2015; Cui and Wang 2019).

In early studies with the potyvirus TEV, P1 was proved to be dispensable for virus viability and authors claimed that P1 might function in trans to stimulate genome amplification (Verchot and Carrington 1995b). They also proposed that P1 exerted a negative effect on HCPro when the 2 proteins are not separated proteolytically, showing that the cleavage of P1-HCPro was critical for TEV infectivity. In a similar way, we can speculate that the polymerase slippage mechanism could serve to regulate the sequential and ordered production of P1 and HCPro instead of the alternative P1N-PISPO, according to the changes needed along the infection process. Then, the slippage mechanism would be a way of fine-tunning RSS activity. In this scenario, the arrival of a synergistic partner might require further adjustments, and indeed we have observed that the frequency of slippage changed when comparing the infection of a potyvirus alone with the mixed infection of potyvirus+crinivirus (Mingot et al. 2016). A remarkably similar situation was also observed in a different pathosystem, in which a potyvirus and a crinivirus also appeared to cross-modulate their RSS functions (Domingo-Calap et al. 2021). The case of the sweet potato viruses could represent a further complexity in the same trend, with the equilibrium of the host and the well adapted potyvirids being dramatically unbalanced by the arrival of the crinivirus. Further experimentation will be required to elucidate the roles of all the players involved, and to eventually derive a model capable to explain, and hopefully interfere with the extreme pathogenicity of SPVD. In addition, a

better understanding of the pathosystem could be instrumental for future biotechnological uses.

CHAPTER III

Results presented in this chapter are included within a manuscript submitted for publication.

Authors

Ornela Chase[1], Abid Javed[2], Matthew J. Byrne[2,4], Eva C. Thuenemann[3], George P. Lomonossoff[3], Neil A. Ranson[2] and Juan José López-Moya[1]

Affiliation

[1]Centre for Research in Agricultural Genomics (CRAG, CSIC-IRTA-UAB-UB), 08193 Cerdanyola del Vallès, Barcelona, Spain

[2]Astbury Centre for Structural Molecular Biology, School of Molecular and Cellular Biology, Faculty of Biological Sciences, University of Leeds, Leeds, UK

[3] Department of Biochemistry and Metabolism, John Innes Centre, Norwich Research Park, Norwich NR4 7UH, UK

[4] Electron Bio-Imaging Centre, Diamond Light Source, Harwell Science and Innovation Campus, Fermi Ave, Didcot, Oxfordshire OX11 0DE, UK

6. Chapter III - Results

Biotechnological tools to explore potyvirid infections in sweet potato

6.1 *In planta* production of SPFMV, SPV2 and SPMMV virus-like particles (VLPs) using the self-replicating pEff vector

The previously described potexvirus-based pEff vector was used for the transient production of VLPs in *N. benthamiana* plants (Mardanova et al. 2017). The system had already served to successfully generate VLPs of filamentous viruses belonging to different genera within the family *Potyviridae*, in particular potyviruses and ipomoviruses (Thuenemann et al. 2021). The use of a replicating viral vector was considered essential, attending to the functional link between replication and virion assembly described for potyviruses (Gallo et al. 2018). After cloning the corresponding CP genes of the three viruses, namely SPFMV, SPV2 and SPMMV, to create the pEff-SPFMV-CP, pEff-SPV2-CP and pEff-SPMMV-CP constructs (Figure R24a), we tested the transient expression of their CPs in *N. benthamiana* plants. Regarding the appearance of the infiltrated leaves, in the case of pEff-SPV2-CP and pEff-SPMMV-CP they remained apparently healthy after agroinfiltration, while for pEff-SPFMV-CP the leaves exhibited extended necrotic patches corresponding to the infiltrated areas at 7 dpa (data not shown). To evaluate the production of CPs *in planta,* samples of agroinfiltrated leaf tissues were collected at 3, 5, and 7 dpa and CP accumulation was determined in total protein extracts by SDS-PAGE and Western blot analysis, using commercially available polyclonal antibodies. All the CPs were detected as bands with the expected sizes (Figure R24b), showing an increase in accumulation for SPFMV-CP at late times, while the amount of SPV2 or SPMMV CP was roughly similar for the three time points.

To investigate whether the generated CP units were assembled into VLPs, we examined under transmission electron microscopy clarified

crude extracts of leaf tissue agroinfiltrated with the three different pEff-constructs, finding the presence of VLPs in all samples (Figure R24, c-e).

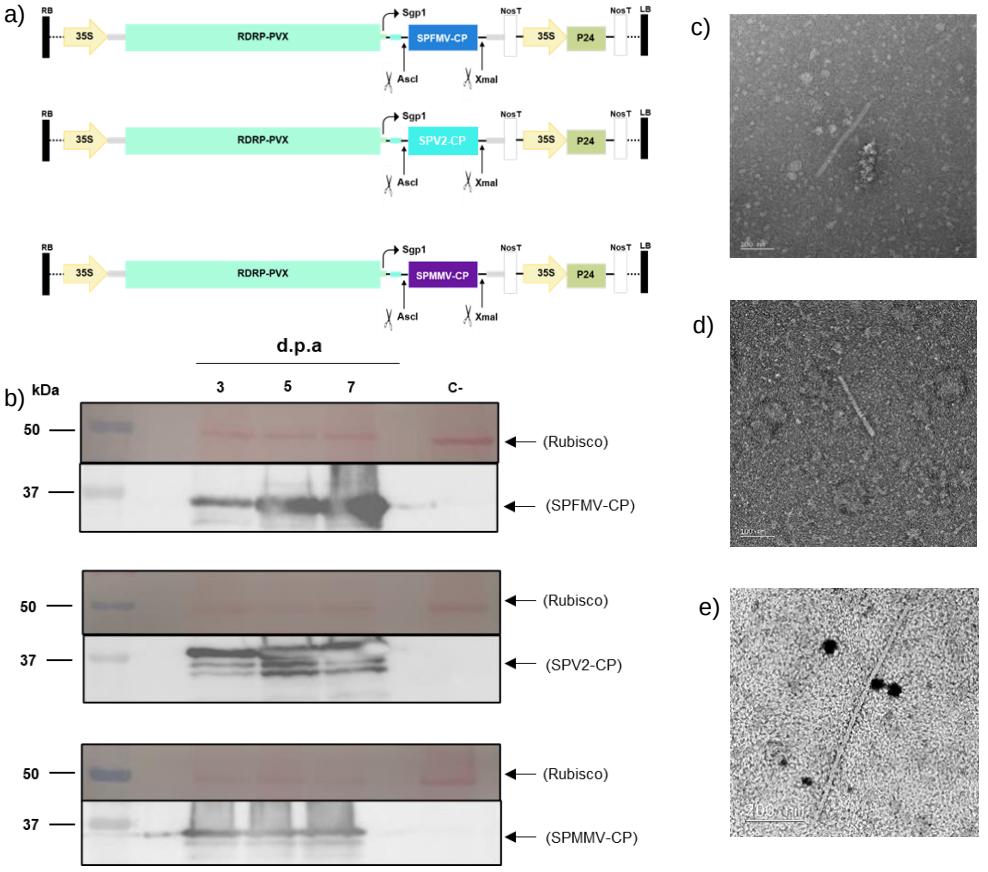

Figure R24. Transient expression and formation of virus-like particles (VLPs) of the potyvirus *Sweet potato feathery mottle virus* (SPFMV), *Sweet potato virus 2* (SPV2) the ipomovirus *Sweet potato mild mottle virus* (SPMMV). a) Representative illustration of the constructs used to express the coat protein of each virus using the self-replicating pEff vector. CP expression results through a subgenomic mRNA from a subgenomic promoter (Sgp1) on the PVX replicon, under the 35S promoter. b) Western blot analysis detecting the expression of the coat protein (CP) at 3, 5 and 7-days post agroinfiltration for the three viruses. The corresponding size of SPFMV, SPV2 and SPMMV-CP is 35, 37 and 34 kDa, respectively. Specific polyclonal antibodies against SPFMV-CP, SPV2-CP and SPMMV-CP were employed and a sample infiltrated with the pEff empty vector was used as a negative control (C-). The large subunit of Rubisco protein (53kDa) stained with Ponceau S is presented as loading control. c) Transmission electron microscopy (TEM) image of an assembled particle derived from clarified crude extract infiltrated with pEff-SPFMV-CP, d) pEff-SPV2-CP and e) pEff-SPMMV-CP. Talos F200C and JEM-1400 TEM fitted with a Gatan OneView camera were used to capture the images c, d and e, respectively.

Interestingly, we also observed that our polyclonal antibodies against SPFMV and SPMMV allowed cross-detection of the two CPs, suggesting that some epitopes might be common for the two viruses, a case not infrequent for the CPs of viruses belonging to related taxons with a moderate amino acid identity (29% according to BLAST alignment), including stretches of local similarity that can be identified in the alignment of the two sequences (Figure R25).Our results further confirmed that the pEff vector can serve as an efficient platform for production of filamentous VLPs corresponding to potyviruses and ipomoviruses.

a)

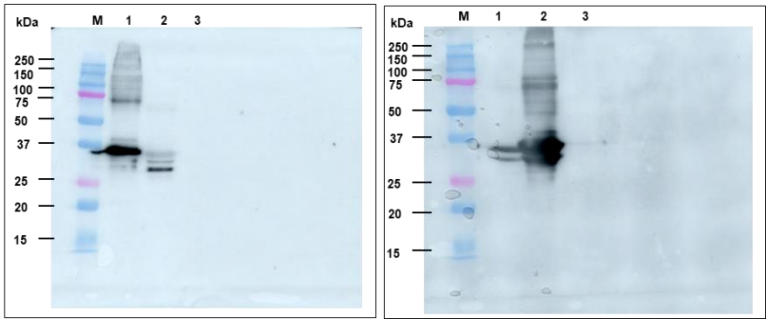

b)

```
SPFMV   SSESTEFKNAGADPPAPKPKNIPPPPTTEITDPE---DPKQAALKAADAKQPAVIPESYGRDTSKERES 67
SPMMV   ----------------------ASTSKTIEELQQEMEDLDADTTITVVQETQKARIRSQIET--L-RAQQ 46

        IVGASSKGVKDKDWNV-----------GTVGTFVVPRVKMNANKKRQPMVNGRAIINFQHLSTYSEEQFE 126
        MVRP-SEAQLQPLVTPTQIVTFEPPRVTGFGALWIPRQQRNY----------MTTAYIEKIKAVVEHSNL 105

        VANTRSTQEQFQAVYEGVKGDYGV-DDTGVGILVNGLMVWCHENGTSPNING--VW-----TMVDGDEQV 188
        IESGLASEAQLTSWIENTCRDYQVSMDVFVTTVIPAWIVNCHINGTSQERTNEHTWRAVIMANVEDQEVL 175

        TYPIKELLDHAVETPRGIVTHESDVAEA-YIEMRNRTKAYMPRYGLQRNLTDMSLARYAPDDYELHSTTP 257
        YYPIKEIIVNAQPTPRGVVRHEGEQAVAQVMNSLQAGKPFTVKGAVTAGYANVQDAWLGIDGLRDTMQLT 245

        ARAKEAHLQMKAAALKNARNRLFGLDGNVSTQEDTERHTTTDVTRNIHNLGMRGVQ 315
        TKQMEVKHQIIAANVTRRKIRVFALAAPGDGDLDTERHVVDDVARGRHSIRGAQLD- 302
```

Figure R25. SPFMV-CP antibody cross reacts with SPMMV-CP and vice versa a) Western blot analysis of SPFMV-VLPs (1), SPMMV-VLPs (2) and empty vector (3) using a commercial polyclonal antibody against SFPMV-CP (left panel) or using a commercial polyclonal antibody against SPMMV-CP (right panel). c) Clustal Omega aminoacid alignment among SPFMV-CP and SPMMV-CP, showing 29% identity (59/206).

6.1.1 Purification of potyvirids-VLPs and comparison of procedures

To examine the structural characteristics of the three potyvirids VLPs and compare features related with the particles' architecture we proceed to their purification. As a first difference, the purification of SPMMV VLPs was straightforward following standard procedures for virion purification based on a previously described method whereas the purification of SPFMV or SPV2 VLPs required adoption of several modifications and additional steps (Hollings et al. 1976; Cohen 1988). More specifically, previously published protocols for purification of SPFMV virions proved inadequate or consistently resulted in low yields (mg per g of fresh weight tissue) when applied to VLPs (not shown). Despite extensive modifications aiming to improve the methods, yields remained around 0.04 mg/g. Nevertheless, we opted to use a modified procedure (based on Nakashima et al. 1993) starting with more plant material to compensate for the low yield. After separation of the sample in sucrose density gradients and analysis by SDS-PAGE, several fractions showed a major protein of around 35 kDa as the expected size for CP (Figure R6a-left). TEM analysis of these fractions showed the presence of flexuous VLP filaments with a diameter of 12-15 nm, but with lengths shorter than that expected for native virions (around 850 nm) in the range of 60-700 nm (average 262 nm), with the most abundant sizes in categories around 200-250 nm and an additional secondary peak about 400 nm (Figure R26a-right). Similarly, SPV2 VLPs were purified following a modified protocol published by by Ateka and co-workers, with adaptations described in the Materials and Methods (section 3.5.2). After their purification, sucrose fractions containing a single band coinciding with SPV2-CP (around 37 kDa) were examined under TEM, showing again the presence of elongated particles with varying lengths from 50 nm up to 1 μm and diameter approximately 12-15 nm (Figure R26b). The purification of SPMMV VLPs was achieved with less difficulties following a published procedure for virion purification in phosphate buffer (based on Hollings et al. 1976), reaching yields around 0.35 mg/g of fresh weight tissue. In the SDS-PAGE analysis after fractionation in sucrose gradients, two products

around 34kDa and 30kDa were observed, both recognized by CP antibodies (not shown), likely corresponding to the full-length CP and a partially degraded product (Figure R26c-left). In TEM, VLPs with a structure similar to the virions were observed as flexuous filaments of 12-15 nm in diameter, and lengths ranging from 60 to 550 nm (average 250 nm), with the most abundant sizes again in categories around 200-250 nm and 400-450 nm (Figure R26c-right).

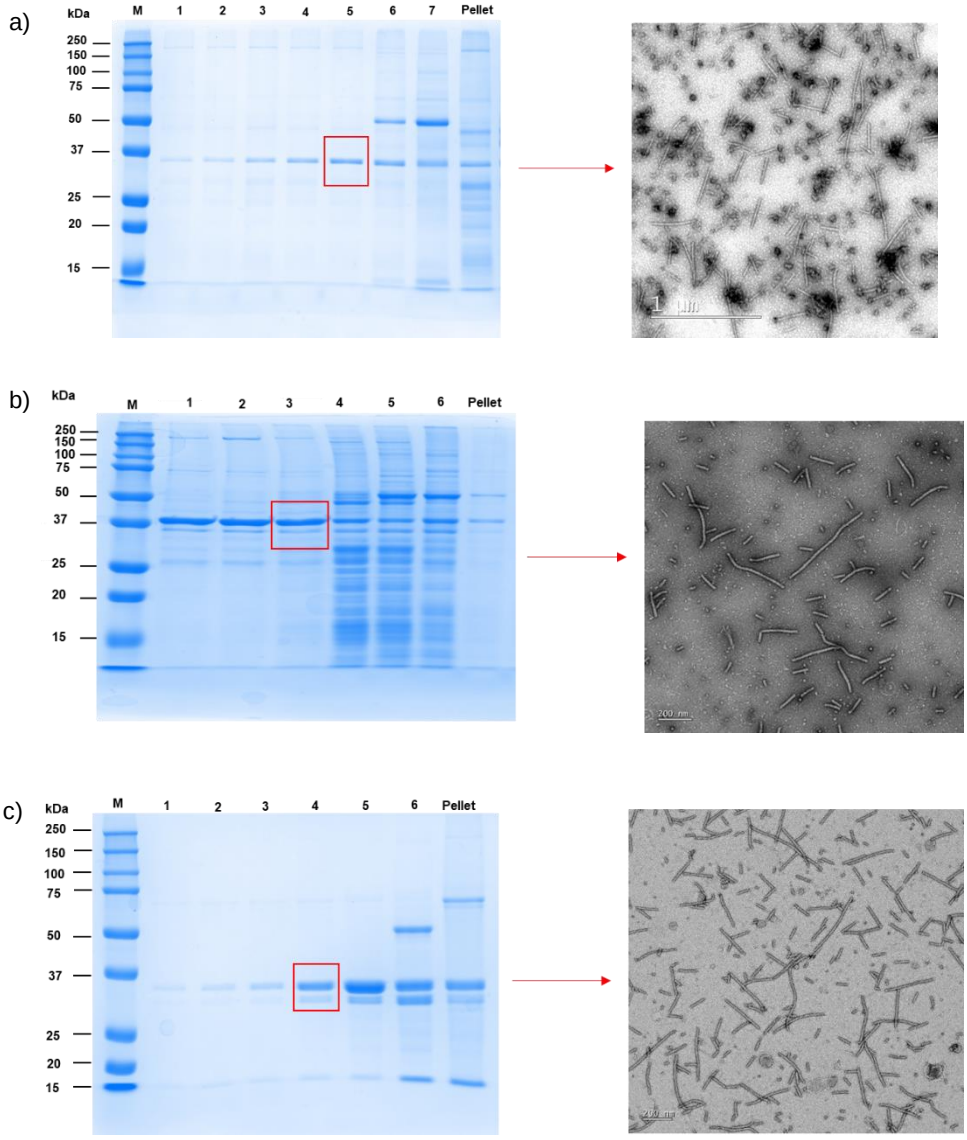

Figure R26. Purification of SPFMV, SPV2 and SPMMV VLPs. a) InstantBlue stained SDS-PAGE loaded with sucrose gradient fractions (40-10%, starting from 1-7) of purified SPFMV-VLPs (left panel). A single band of approximately 35 kDa is detected in all fractions, coinciding with the expected size of SPFMV-CP. In fractions 6 and 7, an additional band of approximately 50 kDa is shown, most probably representing the large subunit of Rubisco. TEM analysis of fraction #5 reveals flexuous filaments, resembling the native virions (right panel). b) Similarly, InstantBlue stained SDS-PAGE loaded with sucrose gradient fractions (40-10%, starting from 1-6) of purified SPV2-VLPs (left panel) shows a prominent band that coincides with SPV2-CP size (37 kDa). From fraction 1-6, a smaller band around 35 kDa is present, presumably being a truncated CP form. An additional band of approximately 50 kDa is appearing in fractions 4-6, most probably representing the large subunit of Rubisco. TEM analysis of fraction #3 reveals filamentous particles, similar to the wildtype virus (right panel). c) InstantBlue stained SDS-PAGE loaded with sucrose gradient fractions (40-10%, starting from 1-6) of purified SPMMV-VLPs (left panel) depicts a dominant band that coincides with SPMMV-CP size (34kDa). A meager band around 30kDa is present, presumably representing a truncated form of the CP. In fraction 6, an additional band of approximately 50 kDa is appearing, most probably representing the large subunit of Rubisco. TEM analysis of fraction #4 shows rod-shaped filaments, resembling the wildtype virus (right panel).

Apart from the TEM analysis of the fractions that displayed single bands corresponding to the CP sizes of the three viruses, we also verified the identity of those bands by Western blotting using specific polyclonal antibodies against each CP (Figure R27).

Moreover, side-by-side attempts for purification of all types of VLPs were performed using the individual protocols established for SPFMV-VLPs and for the SPMMV-VLPs, to better compare the procedures for VLPs extractions. We observed that the VLPs of the potyvirus SPFMV and SPV2 could not be purified with the established protocol for SPMMV-VLPs purification. On the contrary, the ipomovirus-VLPs were successfully purified using both protocols. Overall, the comparison of the properties of the three VLPs types was consistently indicative of a higher stability in the case of SPMMV-VLPs, and this was corroborated also with later observations showing that the VLPs remained stable for at least 3 months at 4 °C, when checked under transmission electron microscopy (data not shown).

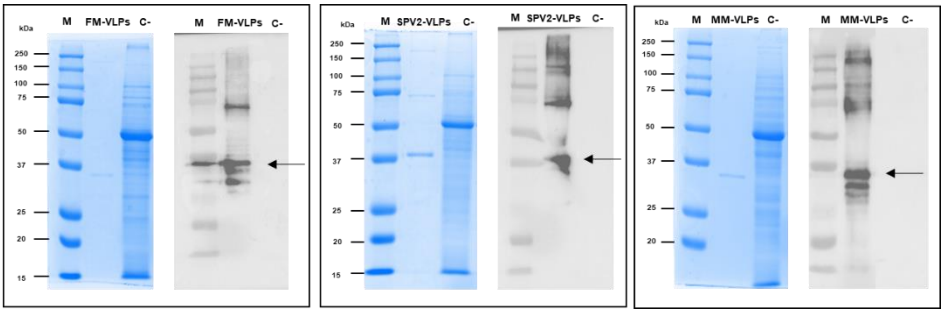

Figure R27. Western blot analysis of three different types of purified VLPs. Instant-blue stained SDS page gel (left panel of each box) and western blotting (right panel of each box) for SPFMV-VLPS (left box), SPV2-VLPs (middle box) and SPMMV-VLPs (right box) using specific antibodies for each coat protein (CP) respectively. Black arrows indicate location of bands corresponding to each CP (SPFMV-CP: 35 kDa; SPV2-CP: 37 kDa; SPMMV-CP: 34 kDa). Crude protein extract derived by a mock-agroinfiltrated *N. benthamiana* was used as a negative control (C-).

6.1.2 Side by side purifications of SPMMV virions and VLPs: yield comparative analysis

Similarly, a side-by-side purification of the native SPMMV virions from infected *N. tabacum* or *N. benthamiana* plants and its VLPs, revealed that the wildtype virions were also particularly stable at 4 °C, retaining their shape under TEM and a high infectivity when inoculated to susceptible plants during at least 2 months (not shown). Unsurprisingly, the concentration of purified SPMMV-VLPs was significantly higher as shown under TEM analysis (Figure R28, a-b), being approximately 10-fold higher (as measure by protein content assessed on an InstantBlue-stained SDS-PAGE) compared to the native virions, when the same amount (10gr) of infiltrated or infected plant tissue was used (Figure R28c), further confirming the robustness of the pEff vector-based system. On the other hand, virion purification of SPFMV was rather difficult, starting with the limitations posed by its narrow host range (only few experimental hosts available), its low accumulation in the single infected sweet potato plants, and the instability of preparations that rapidly lost infectivity and appeared degraded (not shown).

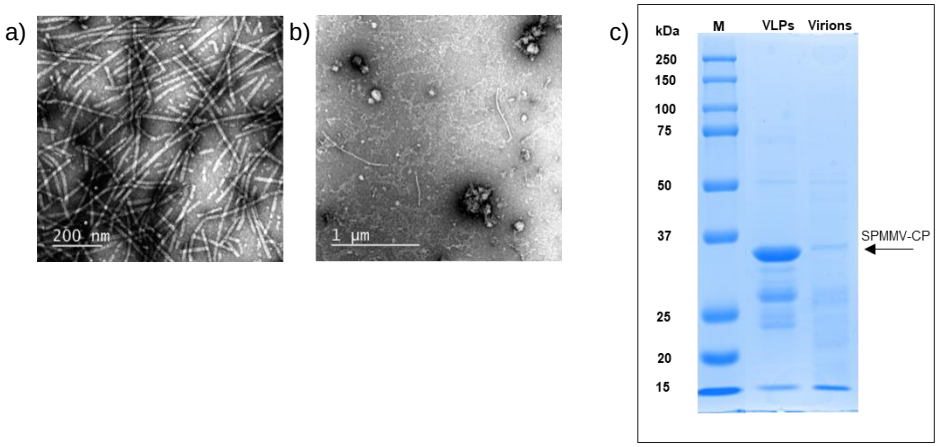

Figure R28. *In planta* amount of pEff-produced VLPs is significantly higher compared to virion yields produced during the native infection. a) Electron microscopy image depicting purified VLPs and b) virions derived by 10gr of initial leaf tissue infiltrated with pEff-SPMMV-CP and 10 gr of infected tissue with SPMMV wildtype virus, respectively. c) Analysis of the CP content in purified preparations of VLPs and native virions by InstantBlue- stained SDS-PAGE.

6.1.3 Thermal stability of SPFMV and SPMMV VLPs

Differential scanning fluorimetry was employed to assess the thermal stability of the VLPs, using Sypro Orange as an extrinsic fluorophore that interacts with exposed hydrophobic residues (Velazquez-Campoy et al. 2016; Gao et al. 2020). Two shifting temperatures were determined for each type of VLPs (Figure R29a, b), consistent with two transitions corresponding the first to the dissociation of the VLP into its constituent CP monomers (T_{m1}), and the second to the unfolding of the CP subunits (T_{m2}). The fluorescence signal obtained for SPFMV-VLPs was significantly lower than for SPMMV-VLPs, indicating different interactions between the fluorophore and the VLP/CP for each system. The transition temperatures were calculated after data normalization using the first derivative of a native fraction for each sample (Figure R29c), and the results showed that SPFMV-VLPs dissociated at 55°C (T_{m1}), while the CP units unfolded at 66°C (T_{m2}), whilst SPMMV-VLPs dissociated at 60°C (T_{m1}), with unfolding of CP units at 69°C (T_{m2}). Altogether these values further proved that the

ipomovirus VLPs exhibited a measurable higher stability compared to the potyvirus VLPs.

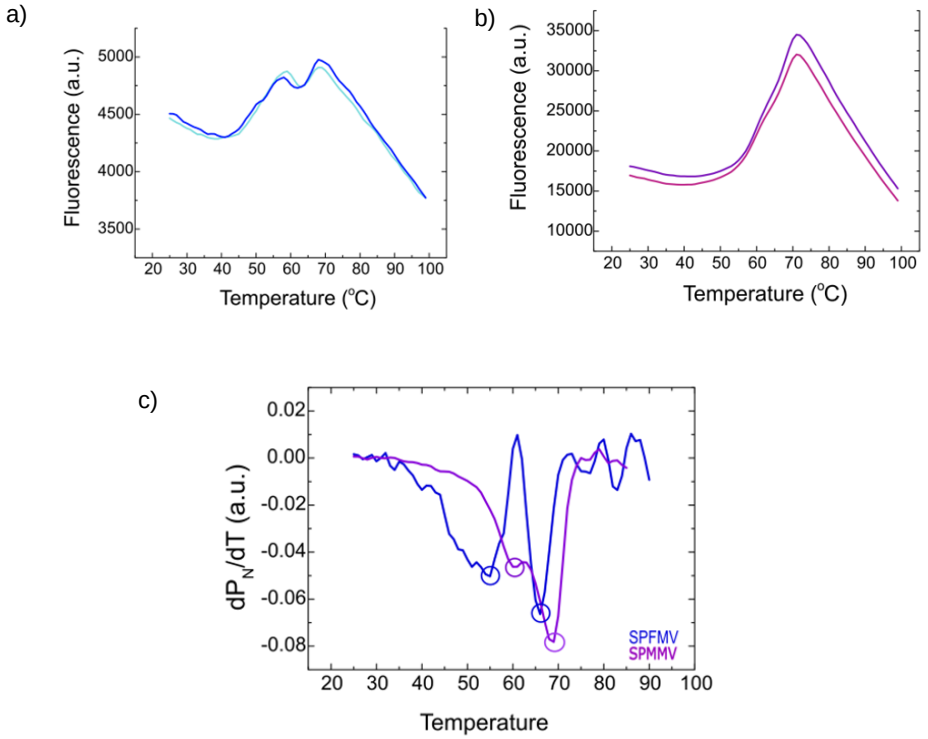

Figure R29. Thermal stability assay of purified VLPs of SPFMV and SPMMV. Differential scanning fluorimetry analysis revealing 2 shifting temperatures for a) SPFMV-VLPs and b) SPMMV-VLPs. The first shifting temperature (Tm1) accounts for the particle's oligomeric dissociation, while the second (Tm2) represents most probably the CPs unfolding. c) First derivative graphical representation of the melting temperatures for the two types of VLPs, after data normalization.

6.1.4 Detection of RNAs present in VLPs

Previous work suggested that pEff-generated potexvirus and virgavirus VLPs contain RNAs derived from the replication of the vector, reinforcing the idea that an RNA scaffold was important for filamentous particles formation (Thuenemann et al. 2021; Saunders et al. 2022). To assess whether this also applies for pEff-produced potyvirid VLPs, we analyzed the RNA content of both types of purified SPFMV and SPMMV VLPs. RNA was extracted from VLP preparations, electrophoresed, transferred to membranes, and hybridized with specific probes (Goto et al. 2003). To confirm specificity, probes were also tested in heterologous combinations, finding that each probe hybridized only with RNAs present in the corresponding homologous VLPs, while no hybridization signals were observed in control lanes corresponding to RNA derived by tissue infiltrated with the empty pEff vector or a mock *N. benthamiana* plant where methylene blue-staining revealed RNA bands corresponding to the expected plant-derived ribosomal RNAs (Figure R30).

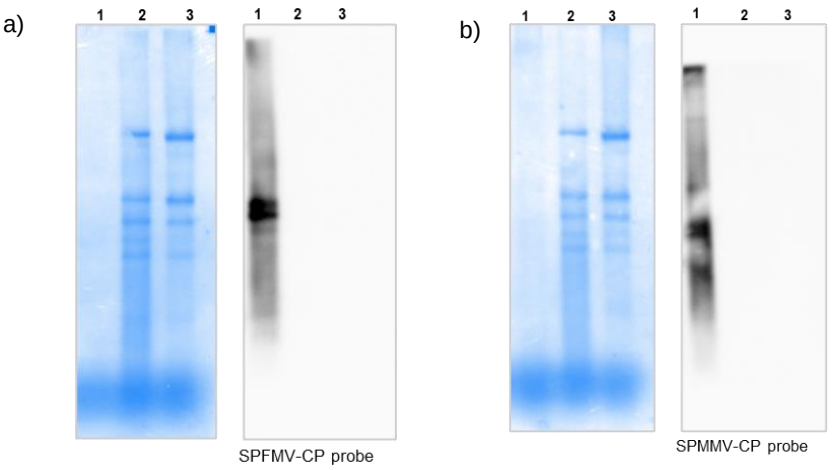

Figure R30. RNA content of SPFMV and SPMMV VLPs. a) Methylene blue staining (left) and Northern blot analysis (right) of RNA samples extracted from purified SPFMV-VLPs (lane 1), *N. benthamiana* plant tissue agroinfiltrated with the corresponding pEff vector (lane2), and tissue from a mock plant (lane 3). The Northern blot was incubated with a SPFMV-CP specific probe. b) Methylene blue staining (left) and Northern blot analysis (right) of RNA samples extracted from purified SPMMV-VLPs (lane 1), plant tissue agroinfiltrated with the corresponding pEff vector (lane2), and tissue from a mock plant (lane 3). The Northern blot was incubated with a SPMMV-CP specific probe.

The estimated size of the majority RNA components in samples of both SPFMV and SPMMV VLPs was above 1000 nucleotides, likely corresponding to the sub-genomic promoter driven sgRNA for expression of CP genes particles. To evaluate whether the observed RNAs were originated from the replicating vectors, a probe against the PVX replicase gene was also tested to specifically detect pEff-derived mRNA. This confirmed that the pEff-derived potyvirid VLPs contain RNA that originates from the replicated pEff vector (Figure R31).

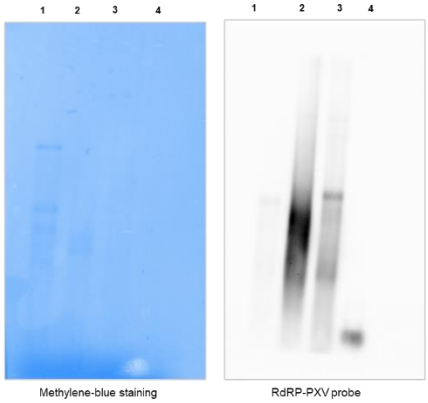

Figure R31. Potyvirus and Ipomovirus VLPs encapsidate pEff-derived RNA. Methylene blue (left) and Northern blot (right) analysis of samples (1µg of RNA) extracted from (1) infiltrated tissue with pEff vector, (2) purified SPFMV-VLPs and (3) purified SPMMV-VLPs, using an anti-RdRP probe for PVX, revealing the presence of vector-derived RNA in both types of VLPs. A PCR product (DNA) of PVX RdRP encompassing the probe binding site was used as a positive control (4).

Regarding the sizes of encapsidated RNAs, the most abundant RNAs were expected to correspond to the subgenomic components expressing CPs, calculated to be >1100 nucleotides for both SPFMV-CP and SPMMV-CP, while the complete pEff-derived mRNAs were > 5600 nucleotides. Considering the proportional sizes compared to virions, the expected sizes of VLPs would be around 100 nm for the sgRNAs and 470 nm for the full-size replicating mRNAs. These two sizes were compatible with our measurements of VLPs (data not shown), although the distribution did not fit exactly a bimodal curve, indicating that different

RNAs might be encapsidated, or that VLPs might suffer a partial breakdown by shearing forces during purification.

6.2 Determination of the near-atomic structure of SPFMV and SPMMV VLPs

Up to date, only 3 potyviruses out of almost 200 members have been structurally determined to near atomic resolution by cryo-EM studies (Zamora et al. 2017; Kežar et al. 2019; Cuesta et al. 2019) , while there are still no cryo-EM data for any member belonging to the genus Ipomovirus. For this reason, in the current dissertation we resolved the near-atomic conformation of two different potyvirids; the potyvirus SPFMV and the ipomovirus SPMMV, using cryoEM analysis and leveraging the great potential of their corresponding VLPs. In both cases, *N. benthamiana* tissue infiltrated with the two different pEff constructs was harvested and homogenized for subsequent purification of each VLPs type, with final isolation of the particles in sucrose gradients. The purified samples were visualized under TEM to assess whether their concentration and distribution was adequate for subsequent CryoEM studies. Both preparations showed a sufficient concentration and proper homogeneity, with few contaminants, allowing their further process by cryo-EM.

6.2.1 Architecture of SPFMV and SPMMV

The structures of SPFMV and SPMMV were determined using single particle cryoEM with helical symmetry, at resolutions of 2.7 Å (SPFMV) and 2.9 Å (SPMMV) (Figure R32). The overall architecture of both SPFMV and SPMMV VLPs was similar to those determined for other plant flexuous filamentous viruses (Zamora et al. 2017; Kežar et al. 2019; Cuesta et al. 2019). Both structures form a left-handed helical arrangement, made up of around 8.8 subunits per turn with a diameter of 130 Å. Each subunit is separated by helical rises of 3.97 Å and 3.98 Å and helical twists of 41.2° and 40.83°, respectively for SPFMV and SPMMV. Comparing the two structures overall, the helical organization is relatively

similar. Small variations within the three domains of the individual coat proteins are apparent.

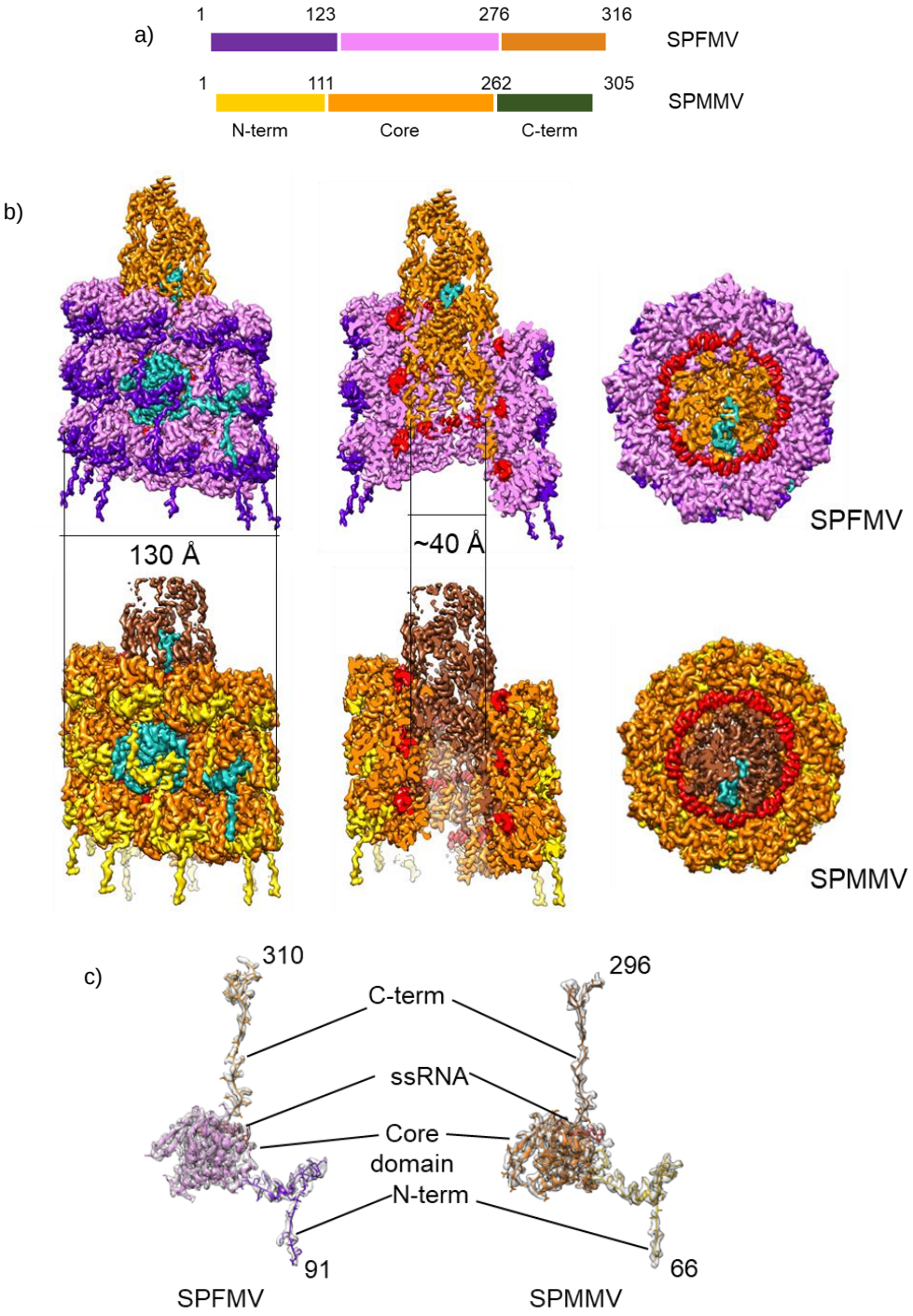

Figure 32. CryoEM structures of *Potyviridae*-VLPs a) A schematic for the sequence organization of SPFMV and SPMMV VLPs, color coded according to the three domains and number of residues indicated. b) Top panel shows the cryoEM map for SPFMV and bottom panel showing the cryoEM map for SPMMV. The maps are colored according to the three domains in the single coat protein with one of the coat proteins in both structures colored in cyan. Both panels show the cryoEM maps in side-view (left), cut-away view (middle) and top view (right). ssRNA is colored in red and the outer and inner diameters are labelled. c) CryoEM map fitted structural models for individual coat proteins from SPFMV (left) and SPMMV (right) are shown, labelled with coat protein regions.

The cryoEM maps of sweet potato viruses allow an atomic model to be built for most of the coat protein sequence. Owing to the flexible nature of the N- and C-termini, parts of these segments lacked sufficient residue to model the precise sequence but were modelled as polyalanine wherever the polypeptide backbone could be traced. Coat proteins from both structures contain three domains; an N-terminal domain made up of 1-123 (SPFMV), 1-111 (SPMMV) residues, a core domain with residues 124-276 (SPFMV), 112-262 (SPMMV) and a C-terminal tail comprising 277-316 (SPFMV), 263-305 (SPMMV) residues. The cryoEM density allowed residues 91-310 (SPFMV) and residues 66-296 (SPMMV) to be modelled, identifying the major components of the three domains in each CP structure. The core domain consists of nine α-helices (SPFMV) and two β-strands, a feature which appears to be conserved amongst other viruses in the *Potyviridae* family. An RNA binding pocket is situated at a crevice formed by the core domain and the C-terminal tail. The C-terminus in the filament forms a spiral arrangement, resulting in the formation of an inner tube of density, formed by the extreme C-terminus of the CPs.

6.2.2 Inter-subunit interactions

In both structures, the subunits are connected to form a helical screw shape that forms the capsid. The N-terminal portion from each CP connects to the adjacent subunit around the helical screw, as well as to subunits in the next layer ‘down’ (Figure R33).

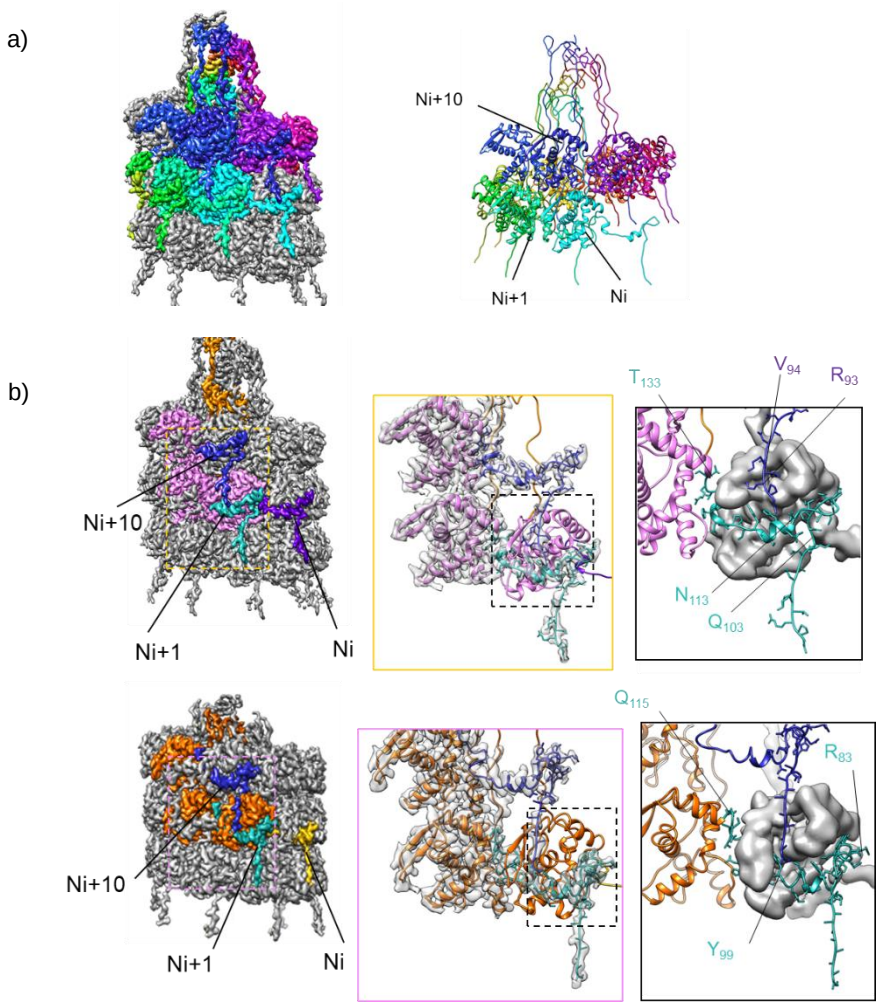

Figure R33. Subunit arrangement in the sweet potato VLPs. a) Left panel shows the SPFMV cryoEM map colored according to the subunit elevation along a helical turn (starting subunit in cyan and 10th subunit in dark blue). Right panel shows the corresponding structural model of one complete segment with first, second and 10th subunits labelled. b) CryoEM map of SPFMV (top panel) colored according to N-termini of first CP (in purple), N+1 (in cyan) and N+10 CP (in dark blue) along the helical segment. The three CPs are colored in pink with the C-terminus in orange. Bottom panel shows cryoEM map of SPMMV, colored according to N-termini of first CP (in gold), N+1 (in cyan) and N+10 (in dark blue). Middle panels show a close-up view of the N-terminus organization between Nth, N+1 and N+10 CP in both SPFMV and SPMMV structures. Right panels show the outlined, zoomed-in area for N-terminal interaction with Nth CP via N+1 (cyan) and N+10 (dark blue) N-terminus in SPFMV (top right) and SPMMV (bottom right) respectively. Key residues are labelled with the Nth CP shown as gaussian filtered map to illustrate binding pockets, N+1 model in pink (SPFMV) and in orange (SPMMV), with their N-terminal segments in cyan and the N+10 N-terminal segments are shown in dark blue.

Similar to the other *Potyviridae* structures, the N-terminus takes a 90° turn after connecting to the adjacent subunit in order to hold the subunit facing downwards by a series of interactions. This arrangement is strikingly different to *Alphaflexiviridae* structures where each CP N-terminus only connects the adjacent subunit (Agirrezabala et al. 2015; Grinzato et al. 2020). A series of hydrogen bonds and salt bridges in both structures hold the subunits together tightly (Figure R33).

The architecture of the N-terminal arm as well as the mode of interaction is conserved between the two structures, with local variations observed based on the sequences. For instance, α-helix 1, which slots in the crevice of the adjacent subunit is tilted downwards in SPMMV, compared with SPFMV and PVY N-terminal regions (Figure R34, with a root-mean square deviation (RMSD) of 4.7 Å). Overall, the high degree of similarity between the coat proteins of the two viruses suggests a common mode of interaction between CPs during capsid assembly.

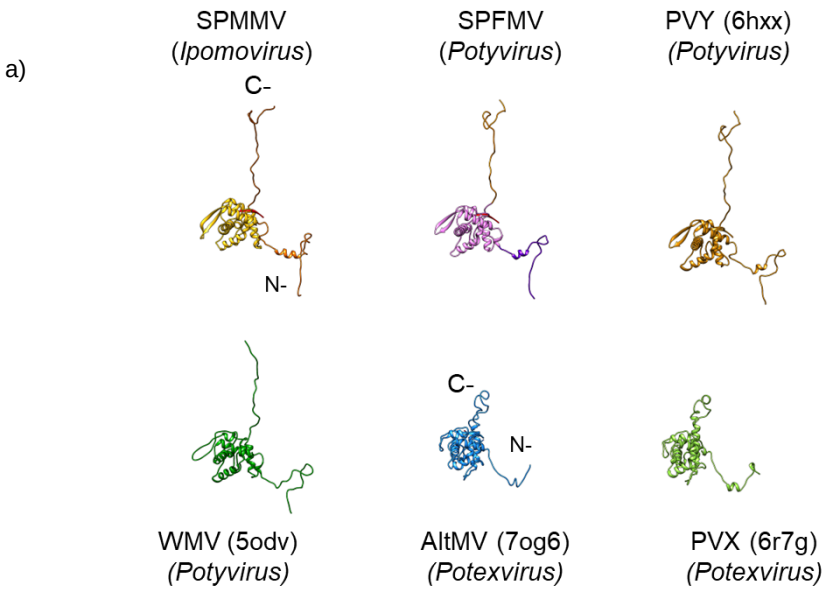

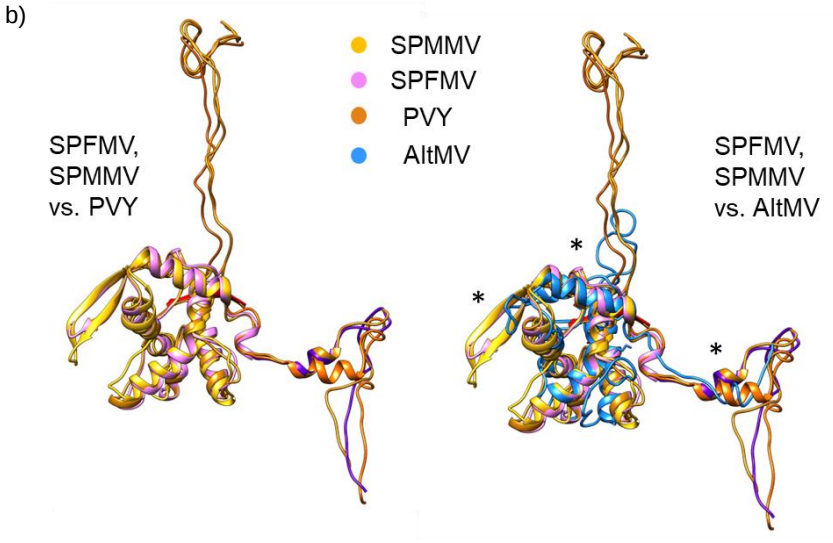

Figure R34. A comparison of *Potyviridae* and *Alphaflexiviridae* coat protein structures. a) Panel showing reported structures of the coat proteins from the *Potyviridae* and *Alphaflexiviridae* families of helical viruses. b) Left panel shows aligned structures of the three *Potyviridae* coat proteins and the right panel showing aligned structures of the two sweet potato *Potyviridae* coat proteins with AltMV coat protein from *Alphaflexiviridae* family. Key structural differences between the two families are indicated by an asterisk.

6.2.3 CP-ssRNA interactions

In the high-resolution structures for SPFMV and SPFMV, five nucleotides of the ssRNA genome are observed in the inner binding pockets of individual coat proteins. The high resolution of the maps was sufficient to build the five nucleotides RNA chain *de novo* with uridine nucleotides. The exact RNA sequence is difficult to discern as the densities for the RNA observed are a result of the averaged segments from the different parts of the virus filament. Both structures show the RNA spanning a length of 23Å, corresponding to a major part of the inner core domain of the coat proteins as well as a similar conformation with an RMSD of 0.7 Å.

The RNA segments are bound to an inner RNA binding pocket, forming by residues from the core domain and the C-terminal segment of the coat protein (Figure R35). Properties of this binding pocket show a largely charged pocket formed by arginines and lysines that bind and interact with the negatively charged RNA backbone, as well as making a series of hydrogen bonds (data not shown). Similar to other *Potyviridae* structures, two to three residues (Arg, Ser, Asp) are found to be conserved at this binding pocket which are believed to be important in correct packaging of the RNA during viral assembly as shown also in the case of the potexvirus PepMV (Agirrezabala et al. 2015; Zamora et al. 2017). In the sweet potato virus structures, these correspond to Arg 235, Ser 172, Asp 248 (SPFMV) and Arg 262, Ser 152, Asp 236 (SPMMV) respectively (Figure 35). Another conserved feature observed in the two sweet potato structures is the fourth nucleotide of the RNA having its nucleotide base facing inwards towards the pocket. This appears to be a common feature observed in other *Potyviridae* and *Alphaflexiviridae* structures, suggesting the importance of this interaction within the RNA binding pocket amongst the plant viruses. Together, the cumulative effect of the interactions at the RNA binding pocket from the core domain of the coat protein shields the RNA from damage.

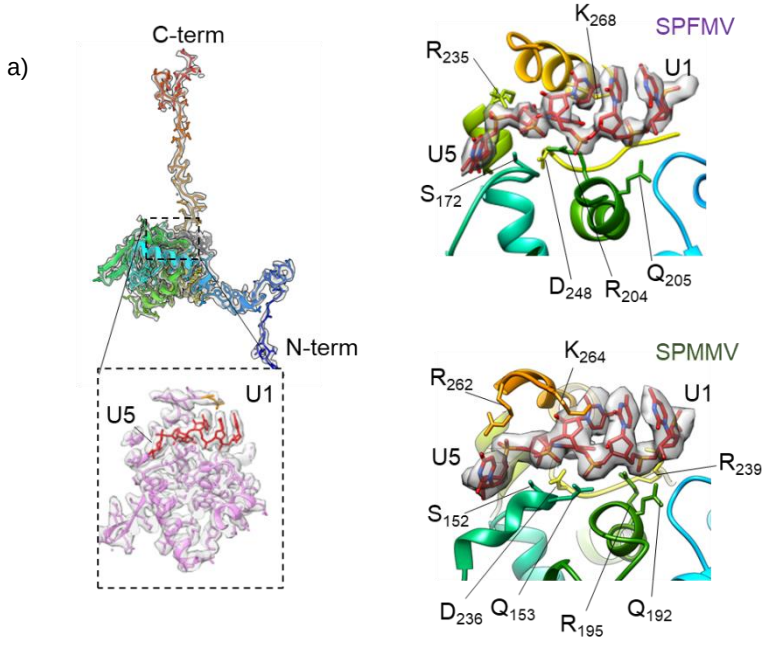

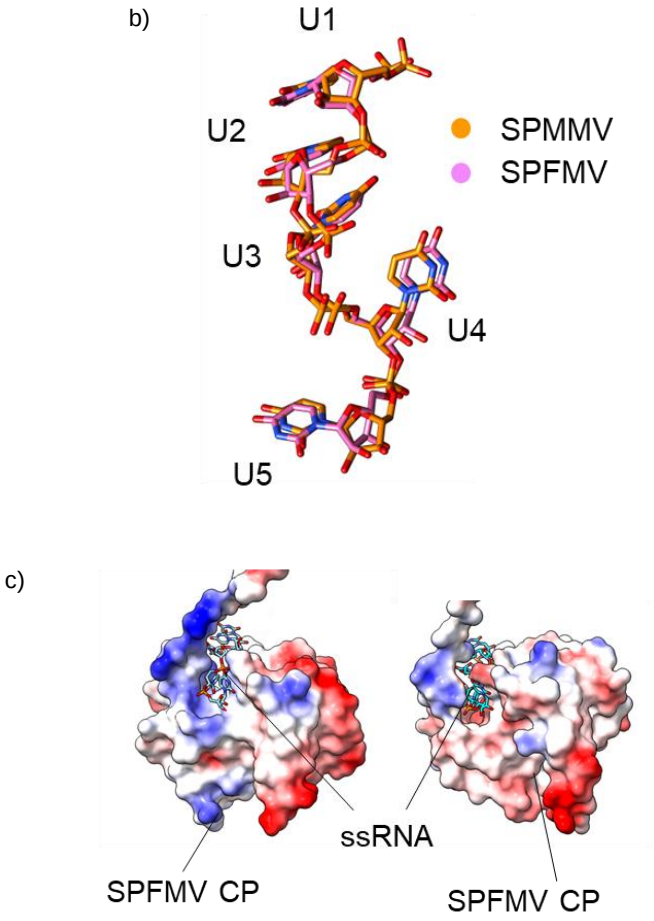

Figure R35. CP-ssRNA interactions in SPFMV and SPMMV cryoEM structures a) Left panel shows fitted atomic model of SPFMV CP, colored from N- (blue) to C-termini (red) with cryoEM densities shown in grey. A zoomed-in panel shows the RNA binding cavity located within the core domain; SPFMV model shown in pink with RNA nucleotides U1 to U5 in red. Top right and bottom right panels show the RNA binding site in SPFMV and SPMMV respectively, with fitted atomic coordinates for ssRNA (in red) inside cryoEM map (shown in grey). Key interacting residues are labelled. b) Aligned structures of ssRNA from SPFMV (in pink) and SPMMV (in gold) with labelled nucleotides. c) Computed surface electrostatic potential maps for CPs, viewed along the RNA binding pockets, with the ssRNA shown as an atomic model in cyan. The coloring ranges between positively charged (blue), neutral (white) and negatively charged (red) spots.

Chapter III - Discussion

The economic impact of crop diseases caused by potyvirids prompts research aiming to develop efficient control strategies. Among others, the molecular mechanisms of virus-host-vector interactions are highly relevant for this purpose since any possible interference might result in reduction of virus dispersal (Chase et al. 2021).

The present study enabled the determination of the structural composition of two different *Potyviridae* members at near-atomic resolution, taking advantage of the high yields of RNA-containing VLPs of helical viruses produced by a replicating PVX-based viral vector to overcome limiting factors such the scarcity of virions found in natural host infections (Thuenemann et al. 2021). This recently developed and robust technology allowed us to explore the structures of the potyvirus SPFMV and the ipomovirus SPMMV.

Derived atomic models confirmed the assembly of helical filaments, structurally resembling other previously published potyvirus virions (Zamora et al. 2017; Kežar et al. 2019; Cuesta et al. 2019). As expected, both types of produced VLPs proved to contain vector-derived RNA, in accordance with previously published works that stressed the importance of an RNA scaffold for assembly and stability of helical virions or VLPs (Gallo et al. 2018; Thuenemann et al. 2021). Under certain conditions, previously published investigations showed that the CPs of some potyvirids were able to self-assemble apparently in absence of RNA (McDonald et al. 1976; Jagadish et al. 1991), and indeed different RNA-devoid potyvirus and potexvirus VLPs have been produced (Tyulkina et al. 2011; González-Gamboa et al. 2017; Donchenko et al. 2017; Kežar et al. 2019). Nonetheless, in some cases such as PVY, the absence of RNA compromised the precise helical symmetry, resulting instead in the assembly of stacked-ring filaments, revealing again the crucial role of RNA during proper virion assembly (Kežar et al. 2019). Similarly, TuMV VLPs lacking RNA were less stable and highly heterogeneous compared to wildtype virions, precluding an accurate atomic model and providing poor structural details (Cuesta et al. 2019). Moreover, comparing the yield

of empty TuMV VLPs (around 10 µg/g) reported in the literature (González-Gamboa et al. 2017), our pEff-mediated constructs generated higher yields of VLPs, ranging from 4 to >30 times respectively for SPFMV and SPMMV, suggesting that production of VLPs was indeed facilitated by the system that provided the replicating RNA. Our observations on the size of VLPs showed a distribution of lengths that does not fit exactly with the expected sizes calculated considering the most abundant RNAs derived from the replicative pEff-vector based constructs. In other cases the predicted equivalences were more evident, as it happened with the tobamovirus TMV and with the potexvirus AltMV, suggesting that for the sweet potato potyvirids the encapsidation of RNAs into VLPs was less strictly regulated (Thuenemann et al. 2021; Saunders et al. 2022). Alternatively, we cannot exclude that the conditions required for our purifications might be more aggressive resulting in more abundance of broken VLPs.

Although belonging to the same family and sharing a similar structural organization, SPFMV and SPMMV particles presented a clear divergence in terms of stability, as reflected by their properties during the purification processes. Whereas SPMMV VLPs were readily purified and maintained integrity during long-storage at low temperatures (4 °C), this was not the case for SPFMV VLPs, where particles were apparently easily disassembled and/or degraded, likely contributing to the much poorer purification yields. We cannot exclude that differences in aggregation properties might also result in losses during early stages of purification. When submitted to differential scanning fluorimetry to analyze thermal stability, the two types of VLPs exhibited measurable differences, with SPFMV VLPs being less stable than SPMMV since they were disassociated at lower temperatures. Further on this, differences were also observed in the second thermal shifts interpreted as corresponding to denaturation of monomeric CPs. Recent investigations are revealing the importance of structural characteristics, such as stability and dynamics of virions, in relation to biologically relevant functions of different viruses (Chakravarty et al. 2020). Comparing the two cryoEM structures, the two virions appear similar in terms of particle stability.

Regarding the integrity of CPs, it is known that endogenous plant peptidases could be responsible for the susceptibility of the N-terminal region of many potyviral CPs to proteolytic cleavage (Laín et al. 1988). We confirmed the occasional presence of CP-related products with faster mobilities in SDS-PAGE than the expected for intact CPs, especially for SPFMV. To minimize the damage, a Protease Inhibitor Cocktail was incorporated to our purification protocols. However, despite reducing the CP proteolytic degradation, this treatment did not modify the yields of VLPs, which for SPFMV always remained below those of SPMMV, probably reflecting other structural differences. Again, intrinsic solubility with less aggregation might help to explain the consistently higher yields obtained for SPMMV VLPs.

Taken together, the accumulated evidence supports the idea that SPFMV particles are more fragile compared to SPMMV particles, and it is tempting to consider that these divergences in the stability of virions might account for other subtle differences in important biological functions, such as the use of different vectors organisms for plant-to-plant transmission. Indeed, potyviruses rely on aphids for their natural dissemination, whereas ipomoviruses are transmitted by whiteflies, and in both cases the CP should play a major role (Dombrovsky et al. 2014; Gadhave et al. 2020)

Computational analysis has classified potyviral CP as one of the most intrinsically disordered proteins among the virus-encoded gene products (Charon et al. 2016), a feature probably linked to its functional versatility, enabling multiple interactions with other virus, host or vector factors (Martínez-Turiño and García 2020). Our cryoEM data revealed a high resemblance between SPFMV and SPMMV atomic structures, adopting a similar architecture compared with other poty- and potexviruses (DiMaio et al. 2015; Agirrezabala et al. 2015; Zamora et al. 2017; Kežar et al. 2019; Cuesta et al. 2019). Nonetheless, in virtually all available structures, the first N-terminal residues could not be traced (in this study, 90 aa for SPFMV and 65 aa for SPMMV). The N-terminus comprises the most variable region within potyviral CPs, where there is a conserved DAG motif related to aphid-mediated virus transmission, with the assistance of HCPro (Atreya et al. 1991; Lopez-Moya et al. 1995; Blanc et al. 1997). On

the other hand, no specific motifs nor vector receptors have been identified to date accounting for *B. tabaci* transmission of ipomoviruses, although recent investigations on CP mutational analysis using a CVYV clone showed a clear implication of the protein N-terminus in whitefly transmissibility (Lindenau et al. 2021). Considering the difficulties in experimentally reproducing the transmissibility of SPMMV by *B. tabaci* , it would be particularly interesting to further explore the implication of CP during this process and our SPMMV high-resolution data could facilitate future studies (Hollings et al. 1976; Tairo et al. 2005)

In contrast to the highly variable N-terminal region, the central core region of the coat protein is well conserved (Dolja et al. 1991), showing a common pattern among many other filamentous viruses, some even belonging to distantly related families infecting animals (Agirrezabala et al. 2015). The complete structural resolution of the CP core for both viruses, allowed us to determine common features with other potyviruses, including the position of three key residues (Ser 172/152, Arg 235/262 and Asp 248/236 in SPFMV/SPMMV) apparently responsible for the RNA binding in the predicted pocket spanning five RNA nucleotides in our structures (see Figure R35) and conserved in other potyviral CPs (Zamora et al. 2017; Kežar et al. 2019; Cuesta et al. 2019). Notably, these three amino acids are present in equivalent positions in both CPs of the potyvirus and the ipomovirus, suggesting that the RNA binding pocket is not limited to potyviruses, but it is a shared feature among potyvirids. These conserved residues might play key roles also during the assembly process of TEV VLPs (Malpica et al. 2004). In summary, the interaction of RNA and CP in potyvirids seems to be quite conserved, what makes it an attractive target for designing hypothetical specific antiviral drugs with broader specificity that could disrupt virion formation.

The density maps of both sweet potato VLPs allowed mapping of nearly the complete CP C-terminus, only missing the last 6 and 9 aa for SPFMV and SPMMV, respectively. In both particles the C-terminus appeared inside the viral lumen, an observation contrasting with earlier models based on immunogenicity and proteolytic treatments with trypsin that proposed that both N- and C-terminal regions of the potyviral CPs were

surface exposed (Shukla et al. 1988). However, all recent structural data have showed that the folding of potyviral CPs results in the C-terminal region being located at the inner surface as a tube with a 4 nm diameter where molecules of certain sizes could have access (Kežar et al. 2019). Our results fully agree with these data. The involvement of the CP distal arms (N- and C-) in the virion structure have been addressed for empty TuMV VLPs, demonstrating that deletions affecting either the N-terminal protrusions or the C-terminal distal regions do not interfere with CP accumulation or VLPs assembly. This suggests that these parts might be dispensable during particle formation (Yuste-Calvo et al. 2020). The same study proposed a direct role of the C-terminal domain in particle length determination; however, the same did not apply in case of PVY VLPs, reflecting possible differences between potyvirus species in that concrete region (Kežar et al. 2019). Overall, in both SPFMV and SPMMV structures, CP polymerization appears to be facilitated by side-to-side and axial connections of the N-terminal part of each CP subunit, a feature that seems universal to *Potyviridae* members (Zamora et al. 2017; Kežar et al. 2019; Cuesta et al. 2019). Nonetheless, the same does not apply in *Potexvirus* members, where only adjacent CPs seem to interact, likely suggesting a less compact and stable structure for *Alphaflexiviridae* species (Agirrezabala et al. 2015; Grinzato et al. 2020).

The contribution of our study is the generation of novel structures of two sweet potato potyvirids belonging to the aphid-transmitted genus *Potyvirus* and to the whitefly-transmitted genus *Ipomovirus*. The structures allow a direct comparison of the coat protein organization and the bound RNA, structural features that are key to virus infectivity and mobility. Besides providing a basis for further investigations of viral infection processes in this important crop, our work also allows comparisons of virions that are transmitted naturally by two different insect vectors. This could assist in the development of effective measures for preventing the spread of sweet potato viral diseases. Moreover, the production of two different types of flexuous VLPs might be potentially useful as novel nanobiotechnological tools, further expanding the list of plant virus-derived systems with potential for agricultural, biomedical, or industrial applications (Steele et al. 2017; Balke and Zeltins 2020).

CONCLUSIONS

7. Conclusions

1. In our experiments SPMMV isolates 130 and 0900 behaved differently during single infections of *N. tabacum* and *I. nil* plants, presenting a divergence in symptom severity and viral accumulation: SPMMV 130 accumulates more but caused less pronounced symptomatology compared to SPMMV 0900.

2. SPMMV 130 distribution in *N. tabacum* was uneven and mainly detected in younger tissues, while SPMMV 0900 was present in both old and young tissues, suggesting a more persistent mode of infection.

3. The complete genome sequence of SPMMV 0900 was obtained, and comparison with SPMMV 130 revealed identities of 93% and 96% for nucleotides and amino acids, respectively. P1 protein was the most divergent gene product, presenting 89% of aa sequence identity.

4. Novel hosts were identified for the crinivirus SPCSV, further expanding its known host range.

5. Mixed infections of SPMMV 130 or 0900 with SPCSV resulted in phenotypical synergism in *N. tabacum* and *I. nil*, with mixed infected plants presenting more exacerbated symptomatology compared to single infected plants. However, the viral loads for isolates 130 or 0900 did not differ significantly between single or mixed infected plants in both experimental hosts.

6. P1N-PISPO and HCPro of SPV2 exhibited local RNA silencing suppressor activity in transient expression experiments in *N. benthamiana* leaves, and the suppressor capacity of HCPro appeared to be independent from the *cis* or *trans* expression of the preceding P1. No interference with the systemic movement of the silencing signal was observed in the 16c transgenic line of *N. benthamiana*.

7. PXV pathogenicity was enhanced by SPV2 proteins conferring RNA silencing suppressor capacity, including the P1 that did not exhibit local RNA silencing capacity in transient assays in *N. benthamiana.*

8. VLPs of SPFMV, SPV2 and SPMMV were produced *in planta* using a replicating PVX-based vector. Produced VLPs were purified and proved to contain vector-derived RNA.

9. The near-atomic resolution of VLPs corresponding to the potyvirus SPFMV and the ipomovirus SPMMV were determined using cryoEM at 2.7 Å and 2.9 Å respectively. Derived models showed a left-handed helix composed by 8.8 CP units per turn, resembling previously published structures for other potyviruses.

10. Density maps of both viruses allowed the reconstructions of an atomic model for both potyvirus and ipomovirus CPs. The two structures are composed by CP subunits that support side-to-side and axial polymerization. Each CP binds and interacts with 5 nucleotides of the ssRNA through a conserved pocket of three amino acids (Arg-Ser-Asp), universally conserved in other families of flexuous helical viruses.

BIBLIOGRAPHY

8. Bibliography

Abrescia NGA, Bamford DH, Grimes JM, Stuart DI (2012) Structure unifies the viral universe. Annu Rev Biochem 81:795–822. https://doi.org/10.1146/annurev-biochem-060910-095130

Adams MJ, Antoniv JF, Beaudoin F (2005) Overview and analysis of the polyprotein cleavage sites in the family Potyviridae. Mol Plant Pathol 6:471–487. https://doi.org/10.1111/j.1364-3703.2005.00296.x

Agirrezabala X, Méndez-López E, Lasso G, Sánchez-Pina MA, Aranda M, Valle M (2015) The near-atomic cryoEM structure of a flexible filamentous plant virus shows homology of its coat protein with nucleoproteins of animal viruses. Elife 4:e11795. https://doi.org/10.7554/eLife.11795

Agranovsky AA (2016) Closteroviruses: Molecular biology, evolution and interactions with cells. In: Plant Viruses: Evolution and Management. Springer Singapore, Singapore, pp 231–252. https://doi.org/10.1007/978-981-10-1406-2_14

Agranovsky AA, Lesemann DE, Maiss E, Hull R, Atabekov JG (1995) “Rattlesnake” structure of a filamentous plant RNA virus built of two capsid proteins. Proc Natl Acad Sci 92:2470–2473. https://doi.org/10.1073/pnas.92.7.2470

Alamillo JM, Monger W, Sola I, García B, Perrin Y, Bestagno M, Burrone OR, Sabella P, Plana-Durán J, Enjuanes L, Lomonossoff GP, García JA (2006) Use of virus vectors for the expression in plants of active full-length and single chain anti-coronavirus antibodies. Biotechnol J 1:1103–1111. https://doi.org/10.1002/biot.200600143

Alcaide C, Rabadán MP, Moreno-Pérez MG, Gómez P (2020) Implications of mixed viral infections on plant disease ecology and evolution. In: Advances in Virus Research. pp 145–169. https://doi.org/10.1016/bs.aivir.2020.02.001

Alconero R (1975) Meristem tip culture and virus indexing of sweet potatoes. Phytopathology 65:769. https://doi.org/10.1094/Phyto-65-769

Amoanimaa-Dede H, Su C, Yeboah A, Chen C, Yang S, Zhu H, Chen M (2020) Flesh color diversity of sweet potato: An overview of the composition, functions, biosynthesis, and gene regulation of the major pigments. Phyton (B Aires) 89:805–833. https://doi.org/10.32604/phyton.2020.011979

Anandalakshmi R, Pruss GJ, Ge X, Marathe R, Mallory AC, Smith TH, Vance VB (1998) A viral suppressor of gene silencing in plants. Proc Natl Acad Sci 95:13079–13084. https://doi.org/10.1073/pnas.95.22.13079

Anderson PK, Cunningham AA, Patel NG, Morales FJ, Epstein PR, Daszak P (2004) Emerging infectious diseases of plants: pathogen pollution, climate change and

agrotechnology drivers. Trends Ecol Evol 19:535–544. https://doi.org/10.1016/j.tree.2004.07.021

Anindya R, Savithri HS (2004) Potyviral NIa proteinase, a proteinase with novel deoxyribonuclease activity. J Biol Chem 279:32159–32169. https://doi.org/10.1074/jbc.M404135200

Aritua V, Bua B, Barg E, Vetten HJ, Adipala E, Gibson RW (2007) Incidence of five viruses infecting sweet potatoes in Uganda; the first evidence of Sweet potato caulimo-like virus in Africa. Plant Pathol 56:324–331. https://doi.org/10.1111/j.1365-3059.2006.01560.x

Ateka EM, Barg E, Njeru RW, Lesemann DE, Vetten HJ (2004) Further characterization of "sweet potato virus 2": A distinct species of the genus Potyvirus. Arch Virol 149:225–239. https://doi.org/10.1007/s00705-003-0233-3

Ateka EM, Barg E, Njeru RW, Thompson G, Vetten HJ (2007) Biological and molecular variability among geographically diverse isolates of sweet potato virus 2. Arch Virol 152:479–488. https://doi.org/10.1007/s00705-006-0879-8

Atreya PL, Atreya CD, Pirone TP (1991) Amino acid substitutions in the coat protein result in loss of insect transmissibility of a plant virus. Proc Natl Acad Sci USA 88:7887–7891. https://doi.org/10.1073/pnas.88.17.7887

Atreya PL, Lopez-Moya JJ, Chu M, Atreya CD, Pirone TP (1995) Mutational analysis of the coat protein N-terminal amino acids involved in potyvirus transmission by aphids. J Gen Virol 76:265–270. https://doi.org/10.1099/0022-1317-76-2-265

Azevedo J, Garcia D, Pontier D, Ohnesorge S, Yu A, Garcia S, Braun L, Bergdoll M, Hakimi MA, Lagrange T, Voinnet O (2010) Argonaute quenching and global changes in Dicer homeostasis caused by a pathogen-encoded GW repeat protein. Genes Dev 24:904–915. https://doi.org/10.1101/gad.1908710

Bagyalakshmi K, Viswanathan R (2020) Identification of the RNA silencing suppressor activity of Sugarcane streak mosaic virus P1 gene. Virus Disease 31:333–340. https://doi.org/10.1007/s13337-020-00618-7

Balke I, Zeltins A (2020) Recent advances in the use of plant virus-like particles as vaccines. Viruses 12:270. https://doi.org/10.3390/v12030270

Baltimore D (1971) Expression of animal virus genomes. Bacteriol Rev 35:235–241. https://doi.org/10.1128/br.35.3.235-241.1971

Bass BL (2000) Double-stranded RNA as a template for gene silencing. Cell 101:235–238. https://doi.org/10.1016/S0092-8674(02)71133-1

Baulcombe D (2004) RNA silencing in plants. Nature 431:356–363. https://doi.org/10.1038/nature02874

Baulcombe DC (2022) The role of viruses in identifying and analyzing RNA silencing. Annu Rev Virol 9:10.1–10.21. https://doi.org/10.1146/annurev-virology-091919-064218

Baumann P (2005) Biology of bacteriocyte-associated endosymbionts of plant sap-sucking insects. Annu Rev Microbiol 59:155–189. https://doi.org/10.1146/annurev.micro.59.030804.121041

Beauchemin C, Boutet N, Laliberté J-F (2007) Visualization of the interaction between the precursors of VPg, the viral protein linked to the genome of Turnip mosaic virus, and the translation eukaryotic initiation factor iso 4E In planta. J Virol 81:775–782. https://doi.org/10.1128/jvi.01277-06

Bednarek R, David M, Fuentes S, Kreuze J, Fei Z (2021) Transcriptome analysis provides insights into the responses of sweet potato to sweet potato virus disease (SPVD). Virus Res 295:198293. https://doi.org/10.1016/j.virusres.2020.198293

Bengyella L, Waikhom SD, Allie F, Rey C (2015) Virus tolerance and recovery from viral induced symptoms in plants are associated with transcriptome reprograming. Plant Mol Biol 89:243–252. https://doi.org/10.1007/s11103-015-0362-6

Bhattacharyya D, Chakraborty S (2018) Chloroplast: the Trojan horse in plant–virus interaction. Mol Plant Pathol 19:504–518. https://doi.org/10.1111/mpp.12533

Blanc S, López-Moya J-J, Wang R, García-Lampasona S, Thornbury DW, Pirone TP (1997) A specific interaction between coat protein and helper component correlates with aphid transmission of a potyvirus. Virology 231:141–147. https://doi.org/10.1006/viro.1997.8521

Blanc S, Michalakis Y (2016) Manipulation of hosts and vectors by plant viruses and impact of the environment. Curr Opin Insect Sci 16:36–43. https://doi.org/10.1016/j.cois.2016.05.007

Boller T, He SY (2009) Innate immunity in plants: An arms race between pattern recognition receptors in plants and effectors in microbial pathogens. Science 324:742–744. https://doi.org/10.1126/science.1171647

Bragard C, Caciagli P, Lemaire O, Lopez-Moya JJ, MacFarlane S, Peters D, Susi P, Torrance L (2013) Status and prospects of plant virus control through interference with vector transmission. Annu Rev Phytopathol 51:177–201. https://doi.org/10.1146/annurev-phyto-082712-102346

Brown JK, Frohlich DR, Rosell RC (1995) The sweet potato or silverleaf whiteflies: Biotypes of Bemisia tabaci or a species complex? Annu Rev Entomol 40:511–534. https://doi.org/10.1146/annurev.en.40.010195.002455

Burgyán J, Havelda Z (2011) Viral suppressors of RNA silencing. Trends Plant Sci 16:265–272. https://doi.org/10.1016/j.tplants.2011.02.010

Butler PJG (1999) Self–assembly of Tobacco mosaic virus: the role of an intermediate aggregate in generating both specificity and speed. Philos Trans R Soc London Ser B Biol Sci 354:537–550. https://doi.org/10.1098/rstb.1999.0405

Byers JA (2008) Aphids as crop pests. Crop Sci 48:1219. https://doi.org/10.2135/cropsci2008.02.0001br

Cao M, Du P, Wang X, Yu Y-Q, Qiu Y-H, Li W, Gal-On A, Zhou C, Li Y, Ding S-W (2014) Virus infection triggers widespread silencing of host genes by a distinct class of endogenous siRNAs in Arabidopsis. Proc Natl Acad Sci 111:14613–14618. https://doi.org/10.1073/pnas.1407131111

Carbonell A, Carrington JC (2015) Antiviral roles of plant ARGONAUTES. Curr Opin Plant Biol 27:111–117. https://doi.org/10.1016/j.pbi.2015.06.013

Carmo-Sousa M, Moreno A, Garzo E, Fereres A (2014) A non-persistently transmitted-virus induces a pull–push strategy in its aphid vector to optimize transmission and spread. Virus Res 186:38–46. https://doi.org/10.1016/j.virusres.2013.12.012

Carrington JC, Cary SM, Parks TD, Dougherty WG (1989) A second proteinase encoded by a plant potyvirus genome. EMBO J 8:365–370. https://doi.org/10.1002/j.1460-2075.1989.tb03386.x

Caspar DLD, Klug A (1962) Physical principles in the construction of regular viruses. Cold Spring Harb Symp Quant Biol 27:1–24. https://doi.org/10.1101/SQB.1962.027.001.005

Castón JR (2013) Conventional electron microscopy, cryo-electron microscopy and cryo-electron tomography of viruses. In: Subcellular Biochemistry. Springer New York, pp 79–115. https://doi.org/10.1007/978-94-007-6552-8_3

Chai M, Wu X, Liu J, Fang Y, Luan Y, Cui X, Zhou X, Wang A, Cheng X (2020) P3N-PIPO interacts with P3 via the shared N-Terminal domain to recruit viral replication vesicles for cell-to-cell movement. J Virol 94:e01898-19. https://doi.org/10.1128/JVI.01898-19

Chakravarty A, Reddy VS, Rao ALN (2020) Unravelling the stability and capsid dynamics of the three virions of Brome mosaic virus assembled autonomously In Vivo. J Virol 94:e01794-19. https://doi.org/10.1128/JVI.01794-19

Chang X, Wang F, Fang Q, Chen F, Yao H, Gatehouse AMR, Ye G (2021) Virus-induced plant volatiles mediate the olfactory behaviour of its insect vectors. Plant Cell Environ 44:2700–2715. https://doi.org/10.1111/pce.14069

Charon J, Theil S, Nicaise V, Michon T (2016) Protein intrinsic disorder within the Potyvirus genus: from proteome-wide analysis to functional annotation. Mol Biosyst 12:634–652. https://doi.org/10.1039/C5MB00677E

Chase O, Ferriol I, López-Moya JJ (2021) Control of plant pathogenic viruses through interference with insect transmission. In: Plant Virus-Host Interaction. Elsevier, pp 359–381. https://doi.org/10.1016/b978-0-12-821629-3.00019-1

Cheng X, Wang A (2017) The potyvirus silencing suppressor protein VPg mediates degradation of SGS3 via ubiquitination and autophagy pathways. J Virol 91:e01478-16. https://doi.org/10.1128/JVI.01478-16

Chiu MH, Chen IH, Baulcombe DC, Tsai CH (2010) The silencing suppressor P25 of Potato virus X interacts with Argonaute1 and mediates its degradation through the proteasome pathway. Mol Plant Pathol. https://doi.org/10.1111/j.1364-3703.2010.00634.x

Chung BYW, Miller WA, Atkins JF, Firth AE (2008) An overlapping essential gene in the Potyviridae. Proc Natl Acad Sci 105:5897–5902. https://doi.org/10.1073/pnas.0800468105

Clark C., Ferrin D., Smith T., Holmes G. (2013) Compendium of Sweetpotato Diseases, Pests, and Disorders, Second Edition, Second Edi. The American Phytopathological Society. https://doi.org/10.1094/9780890544952

Clark CA, Davis JA, Abad JA, Cuellar WJ, Fuentes S, Kreuze JF, Gibson RW, Mukasa SB, Tugume AK, Tairo FD, Valkonen JPT (2012) Sweetpotato viruses: 15 years of progress on understanding and managing complex diseases. Plant Dis 96:168–185. https://doi.org/10.1094/PDIS-07-11-0550

Clark CA, Hoy MW (2006) Effects of common viruses on yield and quality of Beauregard sweetpotato in Louisiana. Plant Dis 90:83–88. https://doi.org/10.1094/PD-90-0083

Claverie S, Bernardo P, Kraberger S, Hartnady P, Lefeuvre P, Lett J-M, Galzi S, Filloux D, Harkins GW, Varsani A, Martin DP, Roumagnac P (2018) From spatial metagenomics to molecular characterization of plant viruses: A geminivirus case study. In: Advances in Virus Research. pp 55–83. https://doi.org/10.1016/bs.aivir.2018.02.003

Cohen J (1988) An improved method for purification of Sweet potato feathery mottle virus directly from sweet potato. Phytopathology 78:809. https://doi.org/10.1094/Phyto-78-809

Cohen J, Franck A, Vetten HJ, Lesemann DE, Loebenstein G (1992) Purification and properties of closterovirus-like particles associated with a whitefly-transmitted disease of sweet potato. Ann Appl Biol 121:257–268. https://doi.org/10.1111/j.1744-7348.1992.tb03438.x

Cohen J, Lapidot M, Loebenstein G, Gera A (2001) First report of Sweet potato sunken vein virus occurring in Lisianthus. Plant Dis 85:679–679. https://doi.org/10.1094/PDIS.2001.85.6.679A

Colinet D, Kummert J, Lepoivre P (1998) The nucleotide sequence and genome organization of the whitefly transmitted Sweet potato mild mottle virus: a close relationship with members of the family Potyviridae. Virus Res 53:187–196. https://doi.org/10.1016/S0168-1702(97)00148-2

Csorba T, Kontra L, Burgyán J (2015) viral silencing suppressors: Tools forged to fine-tune host-pathogen coexistence. Virology 479–480:85–103. https://doi.org/10.1016/j.virol.2015.02.028

Cuellar WJ, Kreuze JF, Rajamäki M-L, Cruzado KR, Untiveros M, Valkonen JPT (2009) Elimination of antiviral defense by viral RNase III. Proc Natl Acad Sci 106:10354–10358. https://doi.org/10.1073/pnas.0806042106

Cuellar WJ, Tairo F, Kreuze JF, Valkonen JPT (2008) Analysis of gene content in Sweet potato chlorotic stunt virus RNA1 reveals the presence of the p22 RNA silencing suppressor in only a few isolates: implications for viral evolution and synergism. J Gen Virol 89:573–582. https://doi.org/10.1099/vir.0.83471-0

Cuesta R, Yuste-Calvo C, Gil-Cartón D, Sánchez F, Ponz F, Valle M (2019) Structure of Turnip mosaic virus and its viral-like particles. Sci Rep 9:15396. https://doi.org/10.1038/s41598-019-51823-4

Cui H, Wang A (2019) The biological impact of the hypervariable N-terminal region of potyviral genomes. Annu Rev Virol 6:255–274. https://doi.org/10.1146/annurev-virology-092818-015843

Cui H, Wang A (2016) Plum pox virus 6K1 protein is required for viral replication and targets the viral replication complex at the early stage of infection. J Virol 90:5119–5131. https://doi.org/10.1128/JVI.00024-16

Dai Z, He R, Bernards MA, Wang A (2020) The cis-expression of the coat protein of Turnip mosaic virus is essential for viral intercellular movement in plants. Mol Plant Pathol 21:1194–1211. https://doi.org/10.1111/mpp.12973

Darshanee HLC, Ren H, Ahmed N, Zhang Z-F, Liu Y-H, Liu T-X (2017) Volatile-mediated attraction of greenhouse whitefly Trialeurodes vaporariorum to tomato and eggplant. Front Plant Sci 8:1285. https://doi.org/10.3389/fpls.2017.01285

De Barro PJ (2012) The Bemisia tabaci species complex: Questions to guide future research. J Integr Agric 11:187–196. https://doi.org/10.1016/S2095-3119(12)60003-3

De S, Pollari M, Varjosalo M, Mäkinen K (2020) Association of host protein VARICOSE with HCPro within a multiprotein complex is crucial for RNA silencing suppression, translation, encapsidation and systemic spread of Potato virus A infection. PLOS Pathog 16:e1008956. https://doi.org/10.1371/journal.ppat.1008956

del Toro FJ, Donaire L, Aguilar E, Chung B-N, Tenllado F, Canto T (2017) Potato virus Y HCPro suppression of antiviral silencing in Nicotiana benthamiana plants correlates with its ability to bind in vivo to 21- and 22-nucleotide small RNAs of viral sequence. J Virol 91:e00367-17. https://doi.org/10.1128/JVI.00367-17

Deleris A, Gallego-Bartolome J, Bao J, Kasschau KD, Carrington JC, Voinnet O (2006) Hierarchical action and inhibition of plant Dicer-like proteins in antiviral defense. Science 313:68–71. https://doi.org/10.1126/science.1128214

Denis J, Majeau N, Acosta-Ramirez E, Savard C, Bedard M-C, Simard S, Lecours K, Bolduc M, Pare C, Willems B, Shoukry N, Tessier P, Lacasse P, Lamarre A, Lapointe R, Lopez

Macias C, Leclerc D (2007) Immunogenicity of Papaya mosaic virus-like particles fused to a Hepatitis C virus epitope: Evidence for the critical function of multimerization. Virology 363:59–68. https://doi.org/10.1016/j.virol.2007.01.011

DiMaio F, Chen C-C, Yu X, Frenz B, Hsu Y-H, Lin N-S, Egelman EH (2015) The molecular basis for flexibility in the flexible filamentous plant viruses. Nat Struct Mol Biol 22:642–644. https://doi.org/10.1038/nsmb.3054

Ding X, Liu D, Booth G, Gao W, Lu Y (2018) Virus-like particle engineering: From rational design to versatile applications. Biotechnol J 13:1700324. https://doi.org/10.1002/biot.201700324

Dinsdale A, Cook L, Riginos C, Buckley YM, Barro P De (2010) Refined global analysis of Bemisia tabaci (Hemiptera: Sternorrhyncha: Aleyrodoidea: Aleyrodidae) mitochondrial cytochrome oxidase 1 to identify species level genetic boundaries. Ann Entomol Soc Am 103:196–208. https://doi.org/10.1603/AN09061

Dolja V V., Boyko VP, Agranovsky AA, Koonin E V. (1991) Phylogeny of capsid proteins of rod-shaped and filamentous RNA plant viruses: Two families with distinct patterns of sequence and probably structure conservation. Virology 184:79–86. https://doi.org/10.1016/0042-6822(91)90823-T

Dolja V V., Haldeman-Cahill R, Montgomery AE, Vandenbosch KA, Carrington JC (1995) Capsid protein determinants involved in cell-to-cell and long-distance movement of Tobacco etch potyvirus. Virology 206:1007–1016. https://doi.org/10.1006/viro.1995.1023

Dolja V V., Koonin E V. (2011) Common origins and host-dependent diversity of plant and animal viromes. Curr Opin Virol 1:322–331. https://doi.org/10.1016/j.coviro.2011.09.007

Dolja V V., Kreuze JF, Valkonen JPT (2006) Comparative and functional genomics of closteroviruses. Virus Res 117:38–51. https://doi.org/10.1016/j.virusres.2006.02.002

Dolja V V., Krupovic M, Koonin E V. (2020) Deep roots and splendid boughs of the global plant virome. Annu Rev Phytopathol 58:23–53. https://doi.org/10.1146/annurev-phyto-030320-041346

Dolja VV, Haldeman R, Robertson NL, Dougherty WG, Carrington JC (1994) Distinct functions of capsid protein in assembly and movement of Tobacco etch potyvirus in plants. EMBO J 13:1482–1491. https://doi.org/10.1002/j.1460-2075.1994.tb06403.x

Dombrovsky A, Reingold V, Antignus Y (2014) Ipomovirus - an atypical genus in the family Potyviridae transmitted by whiteflies. Pest Manag Sci 70:1553–1567. https://doi.org/10.1002/ps.3735

Domingo-Calap ML, Chase O, Estapé M, Moreno AB, López-Moya JJ (2021) The P1 protein of Watermelon mosaic virus compromises the activity as RNA silencing suppressor of the P25 protein of Cucurbit yellow stunting disorder virus. Front Microbiol 12:645530. https://doi.org/10.3389/fmicb.2021.645530

Domingo-Calap ML, Moreno AB, Díaz Pendón JA, Moreno A, Fereres A, López-Moya JJ (2020) Assessing the impact on virus transmission and insect vector behavior of a viral mixed infection in melon. Phytopathology 110:174–186. https://doi.org/10.1094/PHYTO-04-19-0126-FI

Donaire L, Wang Y, Gonzalez-Ibeas D, Mayer KF, Aranda MA, Llave C (2009) Deep-sequencing of plant viral small RNAs reveals effective and widespread targeting of viral genomes. Virology 392:203–214. https://doi.org/10.1016/j.virol.2009.07.005

Donchenko EK, Pechnikova E V., Mishyna MY, Manukhova TI, Sokolova OS, Nikitin NA, Atabekov JG, Karpova O V. (2017) Structure and properties of virions and virus-like particles derived from the coat protein of Alternanthera mosaic virus. PLoS One 12:e0183824. https://doi.org/10.1371/journal.pone.0183824

Dougherty WG, Dawn Parks T (1991) Post-translational processing of the tobacco etch virus 49-kDa small nuclear inclusion polyprotein: Identification of an internal cleavage site and delimitation of VPg and proteinase domains. Virology 183:449–456. https://doi.org/10.1016/0042-6822(91)90974-G

Dubochet J (2012) Cryo-EM-the first thirty years. J Microsc 245:221–224. https://doi.org/10.1111/j.1365-2818.2011.03569.x

Dubochet J, Chang J-J, Freeman R, Lepault J, McDowall AW (1982) Frozen aqueous suspensions. Ultramicroscopy 10:55–61. https://doi.org/10.1016/0304-3991(82)90187-5

Eagles RM, Balmori-Melian E, Beck DL, Gardner RC, Forster RLS (1994) Characterization of NTPase, RNA-binding and RNA-helicase activities of the cytoplasmic inclusion protein of Tamarillo mosaic potyvirus. Eur J Biochem 224:677-684. https://doi.org/10.1111/j.1432-1033.1994.t01-1-00677.x

Edgar RC, Taylor J, Lin V, Altman T, Barbera P, Meleshko D, Lohr D, Novakovsky G, Buchfink B, Al-Shayeb B, Banfield JF, de la Peña M, Korobeynikov A, Chikhi R, Babaian A (2022) Petabase-scale sequence alignment catalyses viral discovery. Nature 602:142–147. https://doi.org/10.1038/s41586-021-04332-2

Eid S, Abou-Jawdah Y, El-Mohtar C, Sobh H, Havey M (2006) Tolerance in cucumber to Cucurbit yellow stunting disorder virus. Plant Dis 90:645–649. https://doi.org/10.1094/PD-90-0645

Elena SF, Agudelo-Romero P, Lalic J (2009) The evolution of viruses in multi-host fitness landscapes. Open Virol J 3:1–6. https://doi.org/10.2174/1874357900903010001

Eskelin K, Hafrén A, Rantalainen KI, Mäkinen K (2011) Potyviral VPg enhances viral RNA translation and inhibits reporter mRNA translation in planta. J Virol 85:9210–9221. https://doi.org/10.1128/jvi.00052-11

Evtushenko EA, Ryabchevskaya EM, Nikitin NA, Atabekov JG, Karpova O V. (2020) Plant virus particles with various shapes as potential adjuvants. Sci Rep 10:10365. https://doi.org/10.1038/s41598-020-67023-4

Fauquet CM (2008) Taxonomy, classification and nomenclature of viruses. In: Encyclopedia of Virology. Elsevier, pp 9–23. https://doi.org/10.1016/B978-012374410-4.00509-4

Feng M, Zuo D, Jiang X, Li S, Chen J, Jiang L, Zhou X, Jiang T (2018) Identification of Strawberry vein banding virus encoded P6 as an RNA silencing suppressor. Virology 520:103–110. https://doi.org/10.1016/j.virol.2018.05.003

Fereres A, Moreno A (2009) Behavioural aspects influencing plant virus transmission by homopteran insects. Virus Res 141:158–168. https://doi.org/10.1016/j.virusres.2008.10.020

Fereres A, Peñaflor M, Favaro C, Azevedo K, Landi C, Maluta N, Bento J, Lopes J (2016) Tomato infection by whitefly-transmitted circulative and non-circulative viruses induce contrasting changes in plant volatiles and vector behaviour. Viruses 8:225. https://doi.org/10.3390/v8080225

Fiallo-Olivé E, Pan L-L, Liu S-S, Navas-Castillo J (2020) Transmission of begomoviruses and other whitefly-borne viruses: Dependence on the vector species. Phytopathology 110:10–17. https://doi.org/10.1094/PHYTO-07-19-0273-FI

Fire A, Xu S, Montgomery MK, Kostas SA, Driver SE, Mello CC (1998) Potent and specific genetic interference by double-stranded RNA in Caenorhabditis elegans. Nature 391:806–811. https://doi.org/10.1038/35888

Fitzgerald TL, McQualter RB (2014) The quantitative real-time polymerase chain reaction for the analysis of plant gene expression. In: Methods in Molecular Biology. Humana Press Inc., pp 97–115. https://doi.org/10.1007/978-1-62703-715-0_9

Fraenkel-Conrat H, Williams RC (1955) Reconstitution of active Tobacco mosaic virus from its inactive protein and nucleic acid components. Proc Natl Acad Sci 41:690–698. https://doi.org/10.1073/pnas.41.10.690

Fuchs M, Bar-Joseph M, Candresse T, Maree HJ, Martelli GP, Melzer MJ, Menzel W, Minafra A, Sabanadzovic S (2020) ICTV virus taxonomy profile: Closteroviridae. J Gen Virol 101:364–365. https://doi.org/10.1099/jgv.0.001397

Gabrenaite-Verkhovskaya R, Andreev IA, Kalinina NO, Torrance L, Taliansky ME, Mäkinen K (2008) Cylindrical inclusion protein of Potato virus A is associated with a subpopulation of particles isolated from infected plants. J Gen Virol 89:829–838. https://doi.org/10.1099/vir.0.83406-0

Gadhave KR, Gautam S, Rasmussen DA, Srinivasan R (2020) Aphid transmission of Potyvirus: The largest plant-infecting RNA virus genus. Viruses 12:773. https://doi.org/10.3390/v12070773

Gallet R, Michalakis Y, Blanc S (2018) Vector-transmission of plant viruses and constraints imposed by virus–vector interactions. Curr Opin Virol 33:144–150. https://doi.org/10.1016/j.coviro.2018.08.005

Gallie DR (2001) Cap-independent translation conferred by the 5′ leader of Tobacco etch virus is eukaryotic initiation factor 4G dependent. J Virol 75:12141–12152. https://doi.org/10.1128/JVI.75.24.12141-12152.2001

Gallo A, Valli A, Calvo M, García JA (2018) A functional link between RNA replication and virion assembly in the potyvirus Plum pox virus. J Virol 92:e02179-17. https://doi.org/10.1128/JVI.02179-17

Gao K, Oerlemans R, Groves MR (2020) Theory and applications of differential scanning fluorimetry in early-stage drug discovery. Biophys Rev 12:85–104. https://doi.org/10.1007/s12551-020-00619-2

Ghosh S, Kanakala S, Lebedev G, Kontsedalov S, Silverman D, Alon T, Mor N, Sela N, Luria N, Dombrovsky A, Mawassi M, Haviv S, Czosnek H, Ghanim M (2019) Transmission of a new polerovirus infecting pepper by the whitefly Bemisia tabaci. J Virol 93:e00488-19. https://doi.org/10.1128/JVI.00488-19

Gibbs AJ, Ohshima K, Phillips MJ, Gibbs MJ (2008) The prehistory of potyviruses: Their initial radiation was during the dawn of agriculture. PLoS One 3:e2523. https://doi.org/10.1371/journal.pone.0002523

Gibson RW, Kreuze JF (2015) Degeneration in sweetpotato due to viruses, virus-cleaned planting material and reversion: A review. Plant Pathol 64:1–15. https://doi.org/10.1111/ppa.12273

Gibson RW, Mpembe I, Alicai T, Carey EE, Mwanga ROM, Seal SE, Vetten HJ (1998) Symptoms, aetiology and serological analysis of sweet potato virus disease in Uganda. Plant Pathol 47:95–102. https://doi.org/10.1046/j.1365-3059.1998.00196.x

Giner A, Lakatos L, García-Chapa M, López-Moya JJ, Burgyán J (2010) Viral protein inhibits RISC activity by argonaute binding through conserved WG/GW motifs. PLoS Pathog 6:e1000996. https://doi.org/10.1371/journal.ppat.1000996

González-Gamboa I, Manrique P, Sánchez F, Ponz F (2017) Plant-made potyvirus-like particles used for log-increasing antibody sensing capacity. J Biotechnol 254:17–24. https://doi.org/10.1016/j.jbiotec.2017.06.014

Goto K, Kanazawa A, Kusaba M, Masuta C (2003) A simple and rapid method to detect plant siRNAs using nonradioactive probes. Plant Mol Biol Report 21:51–58. https://doi.org/10.1007/BF02773396

Grangeon R, Jiang J, Wan J, Agbeci M, Zheng H, Laliberté J-F (2013) 6K2-induced vesicles can move cell to cell during Turnip mosaic virus infection. Front Microbiol 4:351. https://doi.org/10.3389/fmicb.2013.00351

Gray S, Cilia M, Ghanim M (2014) Circulative, “nonpropagative” virus transmission. In: Advances in Virus Research. Academic Press Inc., pp 141–199. https://doi.org/10.1016/B978-0-12-800172-1.00004-5

Grinzato A, Kandiah E, Lico C, Betti C, Baschieri S, Zanotti G (2020) Atomic structure of potato virus X, the prototype of the Alphaflexiviridae family. Nat Chem Biol 16:564–569. https://doi.org/10.1038/s41589-020-0502-4

Guo Q, Liu Q, A. Smith N, Liang G, Wang M-B (2016) RNA silencing in plants: Mechanisms, technologies and applications in horticultural crops. Curr Genomics 17:476–489. https://doi.org/10.2174/1389202917666160520103117

Guo Z, Li Y, Ding S-W (2019) Small RNA-based antimicrobial immunity. Nat Rev Immunol 19:31–44. https://doi.org/10.1038/s41577-018-0071-x

Gutiérrez S, Michalakis Y, Munster M, Blanc S (2013) Plant feeding by insect vectors can affect life cycle, population genetics and evolution of plant viruses. Funct Ecol 27:610–622. https://doi.org/10.1111/1365-2435.12070

Hammond-Kosack KE, Jones JDG (1997) Plant disease resistance genes. Annu Rev Plant Physiol Plant Mol Biol 48:575–607. https://doi.org/10.1146/annurev.arplant.48.1.575

Hannon GJ (2002) RNA interference. Nature 418:244–251. https://doi.org/10.1038/418244a

He H, Li J, Zhang Z, Tang X, Song D, Yan F (2021) Impacts of Cucurbit chlorotic yellows virus (CCYV) on biological characteristics of its vector Bemisia tabaci (Hemiptera: Aleyrodidae) MED species. J Insect Sci 21:18. https://doi.org/10.1093/jisesa/ieab084

Helm JM, Dadami E, Kalantidis K (2011) Local RNA silencing mediated by agroinfiltration. Methods Mol Biol 744:97–108. https://doi.org/10.1007/978-1-61779-123-9_7

Hervás M, Navajas R, Chagoyen M, García JA, Martínez-Turiño S (2020) Phosphorylation-related crosstalk between distant regions of the core region of the coat protein contributes to virion assembly of Plum pox virus. Mol Plant-Microbe Interact. https://doi.org/10.1094/MPMI-10-19-0305-R

Hogenhout SA, Ammar E-D, Whitfield AE, Redinbaugh MG (2008) Insect vector interactions with persistently transmitted viruses. Annu Rev Phytopathol 46:327–359. https://doi.org/10.1146/annurev.phyto.022508.092135

Hollings M, Stone OM, Bock KR (1976) Purification and properties of Sweet potato mild mottle, a whitefly borne virus from sweet potato (Ipomoea batatas) in East Africa. Ann Appl Biol 82:511–528. https://doi.org/10.1111/j.1744-7348.1976.tb00588.x

Hong Y, Hunt AG (1996) RNA polymerase activity catalyzed by a potyvirus-encoded RNA-dependent RNA polymerase. Virology 226:146–151. https://doi.org/10.1006/viro.1996.0639

Hu J, Nakatani M, Garcia Lalusin A, Kuranouchi T, Fujimura T (2003) Genetic analysis of sweetpotato and wild relatives using inter-simple sequence repeats (ISSRs). Breed Sci 53:297–304. https://doi.org/10.1270/jsbbs.53.297

Huang X, Yu R, Li W, Geng L, Jing X, Zhu C, Liu H (2019) Identification and characterization of a glycine-rich RNA-binding protein as an endogenous suppressor of RNA silencing from Nicotiana glutinosa. Planta 249:1811–1822. https://doi.org/10.1007/s00425-019-03122-5

Hull R (2021) An introduction to plant viruses. In: Encyclopedia of Virology. Elsevier, pp 3–7. https://doi.org/10.1016/B978-0-12-814515-9.00589-0

Hull R (2014) Architecture and assembly of virus particles. In: Plant Virology. Elsevier, pp 69–143. https://doi.org/10.1016/B978-0-12-384871-0.00003-0

Ibrahim A, Odon V, Kormelink R (2019) Plant viruses in plant molecular pharming: Toward the use of enveloped viruses. Front Plant Sci 10:1–18. https://doi.org/10.3389/fpls.2019.00803

Incarbone M, Dunoyer P (2013) RNA silencing and its suppression: novel insights from in planta analyses. Trends Plant Sci 18:382–392. https://doi.org/10.1016/j.tplants.2013.04.001

Inoue-Nagata AK, Jordan R, Kreuze J, Li F, López-Moya JJ, Mäkinen K, Ohshima K, Wylie SJ (2022) ICTV virus taxonomy profile: Potyviridae 2022. J Gen Virol 103(5). https://doi.org/10.1099/jgv.0.001738

Ivanov KI, Eskelin K, Bašić M, De S, Lõhmus A, Varjosalo M, Mäkinen K (2016) Molecular insights into the function of the viral RNA silencing suppressor HCPro. Plant J 85:30–45. https://doi.org/10.1111/tpj.13088

Ivanov KI, Eskelin K, Lõhmus A, Mäkinen K (2014) Molecular and cellular mechanisms underlying potyvirus infection. J Gen Virol 95:1415–1429. https://doi.org/10.1099/vir.0.064220-0

Jagadish MN, Ward CW, Gough KH, Tulloch PA, Whittaker LA, Shukla DD (1991) Expression of potyvirus coat protein in Escherichia coli and yeast and its assembly into virus-like particles. J Gen Virol 72:1543–1550. https://doi.org/10.1099/0022-1317-72-7-1543

Janssen D, Martín G, Velasco L, Gómez P, Segundo E, Ruiz L, Cuadrado IM (2005) Absence of a coding region for the helper component-proteinase in the genome of Cucumber vein yellowing virus, a whitefly-transmitted member of the Potyviridae. Arch Virol 150:1439–1447. https://doi.org/10.1007/s00705-005-0515-z

Jayasinghe WH, Akhter MS, Nakahara K, Maruthi MN (2022) Effect of aphid biology and morphology on plant virus transmission. Pest Manag Sci 78:416–427. https://doi.org/10.1002/ps.6629

Jiang J, Laliberté J-F (2011) The genome-linked protein VPg of plant viruses-a protein with many partners. Curr Opin Virol 1:347–354. https://doi.org/10.1016/j.coviro.2011.09.010

Jiang W, Tang L (2017) Atomic cryo-EM structures of viruses. Curr Opin Struct Biol 46:122–129. https://doi.org/10.1016/j.sbi.2017.07.002

Jo Y, Kim S-M, Choi H, Yang JW, Lee BC, Cho WK (2020) Sweet potato viromes in eight different geographical regions in Korea and two different cultivars. Sci Rep 10:2588. https://doi.org/10.1038/s41598-020-59518-x

Jones RAC (2021) Global plant virus disease pandemics and epidemics. Plants 10:233. https://doi.org/10.3390/plants10020233

Jones RAC, Naidu RA (2019) Global dimensions of plant virus diseases: Current status and future perspectives. Annu Rev Virol 6:387–409. https://doi.org/10.1146/annurev-virology-092818-015606

Karyeija RF, Gibson RW, Valkonen JPT (1998) The significance of Sweet potato feathery mottle virus in subsistence sweet potato production in Africa. Plant Dis 82:4–15. https://doi.org/10.1094/PDIS.1998.82.1.4

Karyeija RF, Kreuze JF, Gibson RW, Valkonen JPT (2000) Synergistic interactions of a potyvirus and a phloem-limited crinivirus in sweet potato plants. Virology 269:26–36. https://doi.org/10.1006/viro.1999.0169

Kassanis B (1939) Intranuclear inclusions in virus infected plants. Ann Appl Biol 26:705–709. https://doi.org/10.1111/j.1744-7348.1939.tb06995.x

Kassanis B, Govier DA (1971) The role of the helper virus in aphid transmission of Potato aucuba mosaic virus and Potato virus C. J Gen Virol 13:221–228. https://doi.org/10.1099/0022-1317-13-2-221

Kasschau KD, Carrington JC (1998) A counterdefensive strategy of plant viruses: Suppression of posttranscriptional gene silencing. Cell 95:461–470. https://doi.org/10.1016/S0092-8674(00)81614-1

Kekarainen T, Savilahti H, Valkonen JPT (2002) Functional genomics on Potato virus A: Virus genome-wide map of sites essential for virus propagation. Genome Res 12:584–59. https://doi.org/10.1101/gr.220702

Kenesi E, Carbonell A, Lózsa R, Vértessy B, Lakatos L (2017) A viral suppressor of RNA silencing inhibits ARGONAUTE 1 function by precluding target RNA binding to pre-assembled RISC. Nucleic Acids Res 45:7736–7750. https://doi.org/10.1093/nar/gkx379

Kenesi E, Lopez-Moya J-J, Orosz L, Burgyán J, Lakatos L (2021) Argonaute 2 controls antiviral activity against Sweet potato mild mottle virus in Nicotiana benthamiana. Plants 10:867. https://doi.org/10.3390/plants10050867

Kennedy GG, Moyer JW (1982) Aphid transmission and separation of two strains of Sweet potato feathery mottle virus from sweet Potato. J Econ Entomol 75:130–133. https://doi.org/10.1093/jee/75.1.130

Kežar A, Kavčič L, Polák M, Nováček J, Gutiérrez-Aguirre I, Žnidarič MT, Coll A, Stare K, Gruden K, Ravnikar M, Pahovnik D, Žagar E, Merzel F, Anderluh G, Podobnik M (2019) Structural basis for the multitasking nature of the Potato virus Y coat protein. Sci Adv 5:eaaw3808. https://doi.org/10.1126/sciadv.aaw3808

Khan MA, Miyoshi H, Gallie DR, Goss DJ (2008) Potyvirus genome-linked protein, VPg, directly affects wheat germ in vitro translation: Interactions with translation initiation factors eIF4F and eIFiso4F. J Biol Chem 283:1340–1349. https://doi.org/10.1074/jbc.M703356200

Kiss ZA, Medina V, Falk BW (2013) Crinivirus replication and host interactions. Front Microbiol 4:99. https://doi.org/10.3389/fmicb.2013.00099

Klein PG, Klein RR, Rodriguez-Cerezo E, Hunt AG, Shaw JG (1994) Mutational analysis of the Tobacco vein mottling virus genome. Virology 204:759–769. https://doi.org/10.1006/viro.1994.1591

Knuhtsen H, Hiebert E, Purcifull DE (1974) Partial purification and some properties of Tobacco etch virus induced intranuclear inclusions. Virology 61:200–209. https://doi.org/10.1016/0042-6822(74)90254-2

Kogoma T (1993) Phage and the origins of molecular biology. Trends Microbiol 1:72. https://doi.org/10.1016/0966-842X(93)90038-S

Kokkinos CD, Clark CA (2006) Real-time PCR assays for detection and quantification of sweetpotato viruses. Plant Dis 90:783–788. https://doi.org/10.1094/PD-90-0783

Koonin E V. (2016) Viruses and mobile elements as drivers of evolutionary transitions. Philos Trans R Soc B Biol Sci 371:20150442. https://doi.org/10.1098/rstb.2015.0442

Koonin E V., Dolja V V., Krupovic M, Varsani A, Wolf YI, Yutin N, Zerbini FM, Kuhn JH (2020) Global organization and proposed megataxonomy of the virus world. Microbiol Mol Biol Rev 84:e00061-19. https://doi.org/10.1128/mmbr.00061-19

Kreuze J, Cuellar WJ, Low JW (2021) Challenge of virus disease threats to ensuring sustained uptake of vitamin-A-rich sweetpotato in Africa. In: Plant Diseases and Food Security in the 21st Century. Springer International Publishing, pp 73–94. https://doi.org/10.1007/978-3-030-57899-2_5

Kreuze JF, Karyeija RF, Gibson RW, Valkonen JPT (2000) Comparisons of coat protein gene sequences show that East African isolates of Sweet potato feathery mottle virus form a genetically distinct group. Arch Virol 145:567–574. https://doi.org/10.1007/s007050050047

Kreuze JF, Savenkov EI, Cuellar W, Li X, Valkonen JPT (2005) Viral class 1 RNase III involved in suppression of RNA silencing viral class 1 RNase III involved in suppression of RNA silencing. J Virol 79:7227–7238. https://doi.org/10.1128/JVI.79.11.7227

Kreuze JF, Savenkov EI, Valkonen JPT (2002) Complete genome sequence and analyses of the subgenomic RNAs of Sweet potato chlorotic stunt virus reveal several new features for

the genus crinivirus. J Virol 76:9260–9270. https://doi.org/10.1128/JVI.76.18.9260-9270.2002

Kumar S, Stecher G, Li M, Knyaz C, Tamura K (2018) MEGA X: Molecular evolutionary genetics analysis across computing platforms. Mol Biol Evol 35:1547–1549. https://doi.org/10.1093/molbev/msy096

Kushnir N, Streatfield SJ, Yusibov V (2012) Virus-like particles as a highly efficient vaccine platform: Diversity of targets and production systems and advances in clinical development. Vaccine 31:58–83. https://doi.org/10.1016/j.vaccine.2012.10.083

Kyndt T, Quispe D, Zhai H, Jarret R, Ghislain M, Liu Q, Gheysen G, Kreuze JF (2015) The genome of cultivated sweet potato contains Agrobacterium T-DNAs with expressed genes: An example of a naturally transgenic food crop. Proc Natl Acad Sci 112:5844–5849. https://doi.org/10.1073/pnas.1419685112

Lacomme C, Hrubikova K, Hein I (2003) Enhancement of virus-induced gene silencing through viral-based production of inverted-repeats. Plant J 34:543–553. https://doi.org/10.1046/j.1365-313X.2003.01733.x

Laín S, Riechmann J, Méndez E, García JA (1988) Nucleotide sequence of the 3' terminal region of Plum pox potyvirus RNA. Virus Res 10:325–341. https://doi.org/10.1016/0168-1702(88)90074-3

Lain S, Riechmann JL, Garciá JA (1990) RNA helicase: a novel activity associated with a protein encoded by a positive strand RNA virus. Nucleic Acids Res 18:7003–7006. https://doi.org/10.1093/nar/18.23.7003

Lakatos L, Csorba T, Pantaleo V, Chapman EJ, Carrington JC, Liu Y-P, Dolja V V., Calvino LF, López-Moya JJ, Burgyán J (2006) Small RNA binding is a common strategy to suppress RNA silencing by several viral suppressors. EMBO J 25:2768–2780. https://doi.org/10.1038/sj.emboj.7601164

Lakatos L, Szittya G, Silhavy D, Burgyán J (2004) Molecular mechanism of RNA silencing suppression mediated by p19 protein of tombusviruses. EMBO J 23:876–884. https://doi.org/10.1038/sj.emboj.7600096

Laurie S, Faber M, Adebola P, Belete A (2015) Biofortification of sweet potato for food and nutrition security in South Africa. Food Res Int 76:962–970. https://doi.org/10.1016/j.foodres.2015.06.001

Leckie BM, Neal Stewart C (2011) Agroinfiltration as a technique for rapid assays for evaluating candidate insect resistance transgenes in plants. Plant Cell Rep 30:325–334. https://doi.org/10.1007/s00299-010-0961-2

Lee D, Lal NK, Lin Z-JD, Ma S, Liu J, Castro B, Toruño T, Dinesh-Kumar SP, Coaker G (2020) Regulation of reactive oxygen species during plant immunity through phosphorylation and

ubiquitination of RBOHD. Nat Commun 11:1838. https://doi.org/10.1038/s41467-020-15601-5

Lefeuvre P, Martin DP, Elena SF, Shepherd DN, Roumagnac P, Varsani A (2019) Evolution and ecology of plant viruses. Nat Rev Microbiol 17:632–644. https://doi.org/10.1038/s41579-019-0232-3

Lefèvre T, Lebarbenchon C, Gauthier-Clerc M, Missé D, Poulin R, Thomas F (2009) The ecological significance of manipulative parasites. Trends Ecol Evol 24:41–48. https://doi.org/10.1016/j.tree.2008.08.007

Li F, Wang A (2019) RNA-targeted antiviral immunity: More than just RNA silencing. Trends Microbiol 27:792–805. https://doi.org/10.1016/j.tim.2019.05.007

Li F, Xu D, Abad J, Li R (2012) Phylogenetic relationships of closely related potyviruses infecting sweet potato determined by genomic characterization of Sweet potato virus G and Sweet potato virus 2. Virus Genes 45:118–125. https://doi.org/10.1007/s11262-012-0749-2

Li S, Wang H, Zhou G (2014) Synergism between Southern rice black-streaked dwarf virus and Rice ragged stunt virus enhances their insect vector acquisition. Phytopathology 104:794–799. https://doi.org/10.1094/PHYTO-11-13-0319-R

Li Y, Cui H, Cui X, Wang A (2016) The altered photosynthetic machinery during compatible virus infection. Curr Opin Virol 17:19–24. https://doi.org/10.1016/j.coviro.2015.11.002

Lindenau S, Winter S, Margaria P (2021) The amino-proximal region of the coat protein of Cucumber vein yellowing virus (family Potyviridae) affects the infection process and whitefly transmission. Plants 10:2771. https://doi.org/10.3390/plants10122771

Ling KS, Jackson DM, Harrison H, Simmons AM, Pesic-VanEsbroeck Z (2010) Field evaluation of yield effects on the U.S.A. heirloom sweetpotato cultivars infected by Sweet potato leaf curl virus. Crop Prot 29:757–765. https://doi.org/10.1016/j.cropro.2010.02.017

Liu Y, Huynh DT, Yeates TO (2019) A 3.8 Å resolution cryo-EM structure of a small protein bound to an imaging scaffold. Nat Commun 10:1864. https://doi.org/10.1038/s41467-019-09836-0

Livieratos IC, Eliasco E, Müller G, Olsthoorn RCL, Salazar LF, Pleij CWA, Coutts RHA (2004) Analysis of the RNA of Potato yellow vein virus: evidence for a tripartite genome and conserved 3′-terminal structures among members of the genus Crinivirus. J Gen Virol 85:2065–2075. https://doi.org/10.1099/vir.0.79910-0

Llave C (2010) Virus-derived small interfering RNAs at the core of plant–virus interactions. Trends Plant Sci 15:701–707. https://doi.org/10.1016/j.tplants.2010.09.001

Loebenstein G (2009) Origin, distribution and economic importance. In: The Sweetpotato. Springer Netherlands, Dordrecht, pp 9–12. https://doi.org/10.1007/978-1-4020-9475-0_2

Loebenstein G (2012) Viruses in sweetpotato. In: Advances in Virus Research. Elsevier, pp 325–343. https://doi.org/10.1016/B978-0-12-394314-9.00009-9

Loebenstein G (2015) Control of sweet potato virus diseases. In: Advances in Virus Research. Elsevier, pp 33–45. https://doi.org/10.1016/bs.aivir.2014.10.005

Loebenstein G, Thottappilly G, Fuentes S, Cohen J (2009) Virus and phytoplasma diseases. In: The Sweetpotato. Springer Netherlands, Dordrecht, pp 105–134. https://doi.org/10.1007/978-1-4020-9475-0_8

Lopez-Moya JJ, Canto T, Diaz-Ruiz JR, Lopez-Abella D (1995) Transmission by aphids of a naturally non-transmissible Plum pox virus isolate with the aid of Potato virus Y helper component. J Gen Virol 76:2293–2297. https://doi.org/10.1099/0022-1317-76-9-2293

López-Moya JJ, Wang RY, Pirone TP (1999) Context of the coat protein DAG motif affects potyvirus transmissibility by aphids. J Gen Virol 80:3281–3288. https://doi.org/10.1099/0022-1317-80-12-3281

Louten J (2016) Virus structure and classification. In: Essential Human Virology. Elsevier, pp 19–29. https://doi.org/10.1016/B978-0-12-800947-5.00002-8

Lozano G, Trenado HP, Valverde RA, Navas-Castillo J (2009) Novel begomovirus species of recombinant nature in sweet potato (Ipomoea batatas) and Ipomoea indica: taxonomic and phylogenetic implications. J Gen Virol 90:2550–2562. https://doi.org/10.1099/vir.0.012542-0

Lozsa R, Csorba T, Lakatos L, Burgyan J (2008) Inhibition of 3' modification of small RNAs in virus-infected plants require spatial and temporal co-expression of small RNAs and viral silencing-suppressor proteins. Nucleic Acids Res 36:4099–4107. https://doi.org/10.1093/nar/gkn365

Lu Y, Tsuda K (2021) Intimate association of PRR- and NLR-mediated signaling in plant immunity. Mol Plant-Microbe Interact 34:3–14. https://doi.org/10.1094/MPMI-08-20-0239-IA

Luan H, Shine MB, Cui X, Chen X, Ma N, Kachroo P, Zhi H, Kachroo A (2016) The potyviral P3 protein targets eukaryotic elongation factor 1A to promote the unfolded protein response and viral pathogenesis. Plant Physiol 172:221–234. https://doi.org/10.1104/pp.16.00505

Luque D, Castón JR (2020) Cryo-electron microscopy for the study of virus assembly. Nat. Chem. Biol. 16:231–239. https://doi.org/10.1038/s41589-020-0477-1

Lustig A, Levine AJ (1992) One hundred years of virology. J Virol 66:4629–4631. https://doi.org/10.1128/jvi.66.8.4629-4631.1992

Mäkinen K, Hafrén A (2014) Intracellular coordination of potyviral RNA functions in infection. Front Plant Sci 5:110. https://doi.org/10.3389/fpls.2014.00110

Maliogka VI, Salvador B, Carbonell A, Sáenz P, León DS, Oliveros JC, Delgadillo MO, García JA, Simón-Mateo C (2012) Virus variants with differences in the P1 protein coexist in a Plum pox virus population and display particular host-dependent pathogenicity features. Mol Plant Pathol 13:877–886. https://doi.org/10.1111/j.1364-3703.2012.00796.x

Maliogka VI, Wintermantel WM, Orfanidou CG, Katis NI (2019) Criniviruses infecting vegetable crops. In: Applied Plant Biotechnology for Improving Resistance to Biotic Stress. Elsevier, pp 251–289. https://doi.org/10.1016/B978-0-12-816030-5.00012-4

Malka O, Feldmesser E, Brunschot S, Santos-Garcia D, Han W, Seal S, Colvin J, Morin S (2021) The molecular mechanisms that determine different degrees of polyphagy in the Bemisia tabaci species complex. Evol Appl 14:807–820. https://doi.org/10.1111/eva.13162

Malpica CA, Aleman-Verdaguer M-E, Stark DM, Fauquet CM, Beachy RN, Voloudakis AE (2004) Structural characterization of Tobacco etch virus coat protein mutants. Arch Virol 149:699–712. https://doi.org/10.1007/s00705-003-0247-x

Marco CF, Aguilar JM, Abad J, Gómez-Guillamón ML, Aranda MA (2003) Melon resistance to Cucurbit yellow stunting disorder virus is characterized by reduced virus accumulation. Phytopathology 93:844–852. https://doi.org/10.1094/PHYTO.2003.93.7.844

Mardanova ES, Blokhina EA, Tsybalova LM, Peyret H, Lomonossoff GP, Ravin N V. (2017) Efficient transient expression of recombinant proteins in plants by the novel pEff vector based on the genome of Potato virus X. Front Plant Sci 8:247. https://doi.org/10.3389/fpls.2017.00247

Martelli GP (2019) A brief historical account of the family Closteroviridae. In: Methods in Molecular Biology. Humana Press Inc., pp 7–13. https://doi.org/10.1007/978-1-4939-9558-5_2

Martelli GP, Abou Ghanem-Sabanadzovic N, Agranovsky AA, Al Rwahnih M, Dolja V V., Dovas CI, Fuchs M, Gugerli P, Hu JS, Jelkmann W, Katis NI, Maliogka VI, Melzer MJ, Menzel W, Minafra A, Rott ME, Rowhani A, Sabanadzovic S, Saldarelli P (2012) Taxonomic revision of the family Closteroviridae with special reference to the Grapevine leafroll-associated members of the genus Ampelovirus and the putative species unassigned to the family. J. Plant Pathol. 94:7–19. http://doi.org/10.4454/jpp.fa.2012.022

Martin JH, Mound LA (2007) An annotated check list of the world's whiteflies (Insecta: Hemiptera: Aleyrodidae). Zootaxa 1492:1–84. https://doi.org/10.11646/zootaxa.1492.1.1

Marťin MT, García JA, Cervera MT, Goldbach RW, van Lent JWM (1992) Intracellular localization of three non-structural Plum pox potyvirus proteins by immunogold labelling. Virus Res 25:201–211. https://doi.org/10.1016/0168-1702(92)90134-U

Martínez-Pérez M, Aparicio F, López-Gresa MP, Bellés JM, Sánchez-Navarro JA, Pallás V (2017) Arabidopsis m6A demethylase activity modulates viral infection of a plant virus and the m6A abundance in its genomic RNAs. Proc Natl Acad Sci 114:10755–10760. https://doi.org/10.1073/pnas.1703139114

Martínez-Turiño S, García JA (2020) Potyviral coat protein and genomic RNA: A striking partnership leading virion assembly and more. In: Advances in Virus Research. Academic Press Inc., pp 165–211. https://doi.org/10.1016/bs.aivir.2020.09.001

Martinez F, Daros J-A (2014) Tobacco etch virus protein P1 traffics to the nucleolus and associates with the host 60S ribosomal subunits during infection. J Virol 88:10725–10737. https://doi.org/10.1128/JVI.00928-14

Más P, Pallás V (1995) Non-isotopic tissue-printing hybridization: a new technique to study long-distance plant virus movement. J Virol Methods 52:317–326. https://doi.org/10.1016/0166-0934(94)00167-F

Mascia T, Cillo F, Fanelli V, Finetti-Sialer MM, De Stradis A, Palukaitis P, Gallitelli D (2010) Characterization of the interactions between Cucumber mosaic virus and Potato virus Y in mixed infections in tomato. Mol Plant-Microbe Interact 23:1514–1524. https://doi.org/10.1094/MPMI-03-10-0064

Mauck KE, De Moraes CM, Mescher MC (2014) Biochemical and physiological mechanisms underlying effects of Cucumber mosaic virus on host-plant traits that mediate transmission by aphid vectors. Plant Cell Environ 37:1427–1439. https://doi.org/10.1111/pce.12249

Mauck KE, De Moraes CM, Mescher MC (2016) Effects of pathogens on sensory-mediated interactions between plants and insect vectors. Curr Opin Plant Biol 32:53–61. https://doi.org/10.1016/j.pbi.2016.06.012

Mayer A. (1886) Concerning the mosaic disease of tobacco. Die Landwirtschaftliche Versuchsstationen 32:451-467. Translation published in English as Phytopathological Classics Number 7 (1942). American Phytopathological Society Press. St. Paul

Mbanzibwa DR, Tian Y, Mukasa SB, Valkonen JPT (2009) Cassava brown streak virus (Potyviridae) encodes a putative Maf/HAM1 pyrophosphatase implicated in reduction of mutations and a P1 proteinase that suppresses RNA silencing but contains no HC-Pro. J Virol 83:6934–6940. https://doi.org/10.1128/JVI.00537-09

McDonald JG, Beveridge TJ, Bancroft JB (1976) Self-assembly of protein from a flexuous virus. Virology 69:327–331. https://doi.org/10.1016/0042-6822(76)90220-8

McGrath PF, Harrison BD (1995) Transmission of Tomato leaf curl geminiviruses by Bemisia tabaci: effects of virus isolate and vector biotype. Ann Appl Biol 126:307–316. https://doi.org/10.1111/j.1744-7348.1995.tb05368.x

McGregor CE, Miano DW, LaBonte DR, Hoy M, Clark CA, Rosa GJM (2009) Differential gene expression of resistant and susceptible sweetpotato plants after infection with the causal agents of sweet potato virus disease. J Am Soc Hortic Sci 134:658–666. https://doi.org/10.21273/JASHS.134.6.658

Melnyk CW, Molnar A, Baulcombe DC (2011) Intercellular and systemic movement of RNA silencing signals. EMBO J 30:3553–3563. https://doi.org/10.1038/emboj.2011.274

Merits A, Rajamäki M-L, Lindholm P, Runeberg-Roos P, Kekarainen T, Puustinen P, Mäkeläinen K, Valkonen JPT, Saarma M (2002) Proteolytic processing of potyviral proteins and polyprotein processing intermediates in insect and plant cells. J Gen Virol 83:1211–1221. https://doi.org/10.1099/0022-1317-83-5-1211

Minato N, Hatori S, Okawa A, Nakagawa K, Hironaka M (2022) Manipulation of insect vectors' host selection behavior by Barley yellow dwarf virus is dependent on the host plant species and viral co-infection. Life 12:644. https://doi.org/10.3390/life12050644

Mingot A, Valli A, Rodamilans B, San León D, Baulcombe DC, García JA, López-Moya JJ (2016) The P1N-PISPO trans-frame gene of Sweet potato feathery mottle potyvirus is produced during virus infection and functions as an RNA silencing suppressor. J Virol 90:3543–3557. https://doi.org/10.1128/JVI.02360-15

Miranda K, Girard-Dias W, Attias M, de Souza W, Ramos I (2015) Three-dimensional reconstruction by electron microscopy in the life sciences: An introduction for cell and tissue biologists. Mol Reprod Dev 82:530–547. https://doi.org/10.1002/mrd.22455

Mohanraj R, Sivasankar S (2014) Sweet potato (Ipomoea batatas [L.] Lam) - a valuable medicinal food: A review. J Med Food 17:733–741. https://doi.org/10.1089/jmf.2013.2818

Moissiard G, Voinnet O (2006) RNA silencing of host transcripts by Cauliflower mosaic virus requires coordinated action of the four Arabidopsis Dicer-like proteins. Proc Natl Acad Sci 103:19593–19598. https://doi.org/10.1073/pnas.0604627103

Monteiro F, Nishimura MT (2018) Structural, functional, and genomic diversity of plant NLR proteins: An evolved resource for rational engineering of plant immunity. Annu Rev Phytopathol 56:243–267. https://doi.org/10.1146/annurev-phyto-080417-045817

Moreno AB, López-Moya JJ (2020) When viruses play team sports: Mixed infections in plants. Phytopathology 110:29–48. https://doi.org/10.1094/PHYTO-07-19-0250-FI

Moritz G, Kumm S, Mound L (2004) Tospovirus transmission depends on thrips ontogeny. Virus Res 100:143–149. https://doi.org/10.1016/j.virusres.2003.12.022

Movahed N, Patarroyo C, Sun J, Vali H, Laliberté J-F, Zheng H (2017) Cylindrical inclusion protein of Turnip mosaic virus serves as a docking point for the intercellular movement of viral replication vesicles. Plant Physiol 175:1732–1744. https://doi.org/10.1104/pp.17.01484

Mukasa SB, Rubaihayo PR, Valkonen JPT (2006) Interactions between a crinivirus, an ipomovirus and a potyvirus in coinfected sweetpotato plants. Plant Pathol 55:458–467. https://doi.org/10.1111/j.1365-3059.2006.01350.x

Mukhopadhyay SK, Chattopadhyay A, Chakraborty I, Bhattacharya I (2011) Crops that feed the world 5. Sweetpotato. Sweetpotatoes for income and food security. Food Secur 3:283–305. https://doi.org/10.1007/s12571-011-0134-3

Mulabisana MJ, Cloete M, Laurie SM, Mphela W, Maserumule MM, Nhlapo TF, Cochrane NM, Oelofse D, Rey MEC (2019) Yield evaluation of multiple and co-infections of begomoviruses and potyviruses on sweet potato varieties under field conditions and confirmation of multiple infection by NGS. Crop Prot 119:102–112. https://doi.org/10.1016/j.cropro.2019.01.009

Mwanga ROM, Swanckaert J, da Silva Pereira G, Andrade MI, Makunde G, Grüneberg WJ, Kreuze J, David M, De Boeck B, Carey E, Ssali RT, Utoblo O, Gemenet D, Anyanga MO, Yada B, Chelangat DM, Oloka B, Mtunda K, Chiona M, Koussao S, Laurie S, Campos H, Yencho GC, Low JW (2021) Breeding progress for vitamin A, iron and zinc biofortification, drought tolerance, and sweetpotato virus disease resistance in sweetpotato. Front Sustain Food Syst 5:616674. https://doi.org/10.3389/fsufs.2021.616674

Nakashima JT, Salazar LF, Wood KR (1993) Sweet potato feathery mottle potyvirus (C1 isolate) virion and RNA purification. J Virol Methods 44:109–116. https://doi.org/10.1016/0166-0934(93)90013-H

Namba K, Pattanayek R, Stubbs G (1989) Visualization of protein-nucleic acid interactions in a virus. Refined structure of intact Tobacco mosaic virus at 2.9 Å resolution by X-ray fiber diffraction. J Mol Biol 208:307–325. https://doi.org/10.1016/0022-2836(89)90391-4

Napoli C, Lemieux C, Jorgensen R (1990) Introduction of a chimeric chalcone synthase gene into petunia results in reversible co-suppression of homologous genes in trans. Plant Cell 2:279. https://doi.org/10.2307/3869076

Narayanan KB, Han SS (2018) Recombinant helical plant virus-based nanoparticles for vaccination and immunotherapy. Virus Genes 54:623–637. https://doi.org/10.1007/s11262-018-1583-y

Navas-Castillo J, Fiallo-Olivé E, Sánchez-Campos S (2011) Emerging virus diseases transmitted by whiteflies. Annu Rev Phytopathol 49:219–248. https://doi.org/10.1146/annurev-phyto-072910-095235

Navas-Castillo J, López-Moya JJ, Aranda MA (2014) Whitefly-transmitted RNA viruses that affect intensive vegetable production. Ann Appl Biol 165:155–171. https://doi.org/10.1111/aab.12147

Ng JCK, Perry KL (2004) Transmission of plant viruses by aphid vectors. Mol Plant Pathol 5:505–511. https://doi.org/10.1111/j.1364-3703.2004.00240.x

Nicaise V (2014) Crop immunity against viruses: outcomes and future challenges. Front Plant Sci 5:660. https://doi.org/10.3389/fpls.2014.00660

Nigam D, LaTourrette K, Souza PFN, Garcia-Ruiz H (2019) Genome-wide variation in potyviruses. Front Plant Sci 10:1439. https://doi.org/10.3389/fpls.2019.01439

Nishad R, Ahmed T, Rahman VJ, Kareem A (2020) Modulation of plant defense system in response to microbial interactions. Front Microbiol 11:1298. https://doi.org/10.3389/fmicb.2020.01298

Opiyo SA, Ateka EM, Owuor PO, Manguro LOA, Miano DW (2010) Development of a multiplex PCR technique for simultaneous detection of Sweet potato feathery mottle virus and Sweet potato chlorotic stunt virus. J Plant Pathol 92:363–366. https://www.jstor.org/stable/41998810

Otulak K, Garbaczewska G (2012) Cytopathological Potato virus Y structures during Solanaceous plants infection. Micron 43:839–850. https://doi.org/10.1016/j.micron.2012.02.015

Pakkianathan BC, Kontsedalov S, Lebedev G, Mahadav A, Zeidan M, Czosnek H, Ghanim M (2015) Replication of Tomato yellow leaf curl virus in its whitefly vector, Bemisia tabaci. J Virol 89:9791–9803. https://doi.org/10.1128/JVI.00779-15

Pantoliano MW, Petrella EC, Kwasnoski JD, Lobanov VS, Myslik J, Graf E, Carver T, Asel E, Springer BA, Lane P, Salemme FR (2001) High-density miniaturized thermal shift assays as a general strategy for drug discovery. J Biomol Screen 6:429–40. https://doi.org/10.1089/108705701753364922

Pasin F, Daròs J-A, Tzanetakis IE (2022) Proteome expansion in the Potyviridae evolutionary radiation. FEMS Microbiol Rev 46:1–22. https://doi.org/10.1093/femsre/fuac011

Pasin F, Simón-Mateo C, García JA (2014) The hypervariable amino-terminus of P1 protease modulates potyviral replication and host defense responses. PLoS Pathog 10:e1003985. https://doi.org/10.1371/journal.ppat.1003985

Patarroyo C, Laliberté J-F, Zheng H (2013) Hijack it, change it: how do plant viruses utilize the host secretory pathway for efficient viral replication and spread? Front Plant Sci 3:308. https://doi.org/10.3389/fpls.2012.00308

Paudel DB, Sanfaçon H (2018) Exploring the diversity of mechanisms associated with plant tolerance to virus infection. Front Plant Sci 9:1575. https://doi.org/10.3389/fpls.2018.01575

Pérez-Cañamás M, Hernández C (2015) Key importance of small RNA binding for the activity of a glycine-tryptophan (GW) motif-containing viral suppressor of RNA silencing. J Biol Chem 290:3106–3120. https://doi.org/10.1074/jbc.M114.593707

Perez-Egusquiza Z, Ward LI, Clover GRG, Fletcher JD (2009) Detection of Sweet potato virus 2 in sweet potato in New Zealand. Plant Dis 93:427–427. https://doi.org/10.1094/PDIS-93-4-0427B

Peyret H, Lomonossoff GP (2013) The pEAQ vector series: the easy and quick way to produce recombinant proteins in plants. Plant Mol Biol 83:51–58. https://doi.org/10.1007/s11103-013-0036-1

Pirone TP, Blanc S (1996) Helper-dependent vector transmission of plant viruses. Annu Rev Phytopathol 34:227–247. https://doi.org/10.1146/annurev.phyto.34.1.227

Pollari M, De S, Wang A, Mäkinen K (2020) The potyviral silencing suppressor HCPro recruits and employs host ARGONAUTE1 in pro-viral functions. PLOS Pathog 16:e1008965. https://doi.org/10.1371/journal.ppat.1008965

Polston JE, De Barro P, Boykin LM (2014) Transmission specificities of plant viruses with the newly identified species of the Bemisia tabaci species complex. Pest Manag Sci 70:1547–1552. https://doi.org/10.1002/ps.3738

Price NJ, Pinheiro C, Soares CM, Ashford DA, Ricardo CP, Jackson PA (2003) A biochemical and molecular characterization of LEP1, an extensin peroxidase from Lupin. J Biol Chem 278:41389–41399. https://doi.org/10.1074/jbc.M304519200

Pruss G, Ge X, Shi XM, Carrington JC, Bowman Vance V (1997) Plant viral synergism: the potyviral genome encodes a broad-range pathogenicity enhancer that transactivates replication of heterologous viruses. Plant Cell 9:859–868. https://doi.org/10.1105/tpc.9.6.859

Pruss GJ, Lawrence CB, Bass T, Li QQ, Bowman LH, Vance V (2004) The potyviral suppressor of RNA silencing confers enhanced resistance to multiple pathogens. Virology 320:107–120. https://doi.org/10.1016/j.virol.2003.11.027

Pumplin N, Voinnet O (2013) RNA silencing suppression by plant pathogens: defence, counter-defence and counter-counter-defence. Nat Rev Microbiol 11:745–760. https://doi.org/10.1038/nrmicro3120

Puustinen P, Mäkinen K (2004) Uridylylation of the potyvirus VPg by viral replicase NIb correlates with the nucleotide binding capacity of VPg. J Biol Chem 279:38103–38110. https://doi.org/10.1074/jbc.M402910200

Qi X, Bao FS, Xie Z (2009) Small RNA deep sequencing reveals role for Arabidopsis thaliana RNA-dependent RNA polymerases in viral siRNA biogenesis. PLoS One 4:e4971. https://doi.org/10.1371/journal.pone.0004971

Qin L, Shen W, Tang Z, Hu W, Shangguan L, Wang Y, Tuo D, Li Z, Miao W, Valli AA, Wang A, Cui H (2020) A newly identified virus in the family Potyviridae encodes two leader cysteine proteases in tandem that evolved contrasting RNA silencing suppression functions. J Virol 95:e01414-20. https://doi.org/10.1128/JVI.01414-20

Quispe-Huamanquispe DG, Gheysen G, Yang J, Jarret R, Rossel G, Kreuze JF (2019) The horizontal gene transfer of Agrobacterium T-DNAs into the series Batatas (Genus Ipomoea) genome is not confined to hexaploid sweetpotato. Sci Rep 9:12584. https://doi.org/10.1038/s41598-019-48691-3

Rajabaskar D, Wu Y, Bosque-Pérez NA, Eigenbrode SD (2013) Dynamics of Myzus persicae arrestment by volatiles from Potato leafroll virus infected potato plants during disease progression. Entomol Exp Appl 148:172–181. https://doi.org/10.1111/eea.12087

Revers F, García JA (2015) Molecular biology of potyviruses. In: Advances in Virus Research. pp 101–199. https://doi.org/10.1016/bs.aivir.2014.11.006

Riechmann JL, Lain S, Garcia JA (1989) The genome-linked protein and 5' end RNA sequence of Plum pox potyvirus. J Gen Virol 70:2785–2789. https://doi.org/10.1099/0022-1317-70-10-2785

Rodamilans B, Valli A, Mingot A, San León D, Baulcombe D, López-Moya JJ, García JA (2015) RNA polymerase slippage as a mechanism for the production of frameshift gene products in plant viruses of the Potyviridae family. J Virol 89:6965–6967. https://doi.org/10.1128/jvi.00337-15

Rodamilans B, Valli A, Mingot A, San León D, López-Moya JJ, García JA (2018) An atypical RNA silencing suppression strategy provides a snapshot of the evolution of sweet potato-infecting potyviruses. Sci Rep 8:15937. https://doi.org/10.1038/s41598-018-34358-y

Rodríguez-Cerezo E, Findlay K, Shaw JG, Lomonossoff GP, Qiu SG, Linstead P, Shanks M, Risco C (1997) The coat and cylindrical inclusion proteins of a potyvirus are associated with connections between plant cells. Virology 236:296–306. https://doi.org/10.1006/viro.1997.8736

Rodríguez-López MJ, Garzo E, Bonani JP, Fereres A, Fernández-Muñoz R, Moriones E (2011) Whitefly resistance traits derived from the wild tomato Solanum pimpinellifolium affect the preference and feeding behavior of Bemisia tabaci and reduce the spread of Tomato yellow leaf curl virus. Phytopathology 101:1191–1201. https://doi.org/10.1094/PHYTO-01-11-0028

Roossinck MJ (2015) Plants, viruses and the environment: Ecology and mutualism. Virology 479–480:271–277. https://doi.org/10.1016/j.virol.2015.03.041

Roossinck MJ (2010) Lifestyles of plant viruses. Philos Trans R Soc B Biol Sci 365:1899–1905. https://doi.org/10.1098/rstb.2010.0057

Rossel H, Thottappilly G (1988) Complex virus diseases of sweet potato. Exploration, maintenance, and utilization of sweet potato genetic resources. In: Report of First Sweet Potato Planning Conference 1987. International Potato Center, Lima, Peru, pp 291–302

Rossmann MG (2013) Structure of viruses: a short history. Q Rev Biophys 46:133–180. https://doi.org/10.1017/S0033583513000012

Roullier C, Duputié A, Wennekes P, Benoit L, Fernández Bringas VM, Rossel G, Tay D, McKey D, Lebot V (2013) Disentangling the origins of cultivated sweet potato (Ipomoea batatas (L.) Lam.). PLoS One 8:e62707. https://doi.org/10.1371/journal.pone.0062707

Rubio L (2013) Genetic variability and evolutionary dynamics of viruses of the family Closteroviridae. Front Microbiol 4:151. https://doi.org/10.3389/fmicb.2013.00151

Ruiz L, Simón A, García C, Velasco L, Janssen D (2018) First natural crossover recombination between two distinct species of the family Closteroviridae leads to the emergence of a new disease. PLoS One 13:e0198228. https://doi.org/10.1371/journal.pone.0198228

Saha S, Mäkinen K (2020) Insights into the functions of eIF4E-binding motif of VPG in Potato virus A infection. Viruses 12:197. https://doi.org/10.3390/v12020197

Saijo Y, Loo EP (2020) Plant immunity in signal integration between biotic and abiotic stress responses. New Phytol 225:87–104. https://doi.org/10.1111/nph.15989

Sainsbury F, Lomonossoff GP (2014) Transient expressions of synthetic biology in plants. Curr Opin Plant Biol 19:1–7. https://doi.org/10.1016/j.pbi.2014.02.003

Sakai J, Mori M, Morishita T, Tanaka M, Hanada K, Usugi T, Nishiguchi M (1997) Complete nucleotide sequence and genome organization of Sweet potato feathery mottle virus (S strain) genomic RNA: the large coding region of the P1 gene. Arch Virol 142:1553–1562. https://doi.org/10.1007/s007050050179

Saldaña J, Elena SF, Solé R V. (2003) Coinfection and superinfection in RNA virus populations: a selection–mutation model. Math Biosci 183:135–160. https://doi.org/10.1016/S0025-5564(03)00038-5

Salem NM, Chen AYS, Tzanetakis IE, Mongkolsiriwattana C, Ng JCK (2009) Further complexity of the genus Crinivirus revealed by the complete genome sequence of Lettuce chlorosis virus (LCV) and the similar temporal accumulation of LCV genomic RNAs 1 and 2. Virology 390:45–55. https://doi.org/10.1016/j.virol.2009.04.025

Salvador B, Saenz P, Yanguez E, Quiot JB, Quiot L, Delgadillo MO, García JA, Simón-Mateo C (2008) Host-specific effect of P1 exchange between two potyviruses. Mol Plant Pathol 9:147–155. https://doi.org/10.1111/j.1364-3703.2007.00450.x

Sánchez-Campos S, Rodríguez-Negrete EA, Cruzado L, Grande-Pérez A, Bejarano ER, Navas-Castillo J, Moriones E (2016) Tomato yellow leaf curl virus: No evidence for replication in the insect vector Bemisia tabaci. Sci Rep 6:30942. https://doi.org/10.1038/srep30942

Sanfaçon H (2020) Modulation of disease severity by plant positive-strand RNA viruses: The complex interplay of multifunctional viral proteins, subviral RNAs and virus-associated RNAs with plant signaling pathways and defense responses. In: Advances in Virus Research. Academic Press Inc., pp 87–131. https://doi.org/10.1016/bs.aivir.2020.04.003

Sastry KS (2013) Introduction. In: Seed-borne Plant Virus Diseases. Springer India, India, pp 1–53. https://doi.org/10.1007/978-81-322-0813-6_1

Saunders K, Thuenemann EC, Shah SN, Peyret H, Kristianingsih R, Lopez SG, Richardson J, Lomonossoff GP (2022) The use of a replicating virus vector for in planta generation of

Tobacco mosaic virus nanorods suitable for metallization. Front Bioeng Biotechnol 10:877361. https://doi.org/10.3389/fbioe.2022.877361

Schaad MC, Jensen PE, Carrington JC (1997) Formation of plant RNA virus replication complexes on membranes: role of an endoplasmic reticulum-targeted viral protein. EMBO J 16:4049–4059. https://doi.org/10.1093/emboj/16.13.4049

Schaefers GA (1976) Insect transmission of sweet potato disease agents in Nigeria. Phytopathology 66:642. https://doi.org/10.1094/Phyto-66-642

Scholthof K-BG (2004) Tobacco mosaic virus: a model system for plant biology. Annu Rev Phytopathol 42:13–34. https://doi.org/10.1146/annurev.phyto.42.040803.140322

Scholthof K-BG, Adkins S, Czoniek H, Palukaitis P, Jacquaot E, Hohn T, Hohn B, SAUNDERS K, Candresse T, Ahlquist P, Hemenway C, Foster GD (2011) Top 10 plant viruses in molecular plant pathology. Mol Plant Pathol 12:938–954. https://doi.org/10.1111/j.1364-3703.2011.00752.x

Schwach F, Vaistij FE, Jones L, Baulcombe DC (2005) An RNA-dependent RNA polymerase prevents meristem invasion by Potato virus X and is required for the activity but not the production of a systemic silencing signal. Plant Physiol 138:1842–1852. https://doi.org/10.1104/pp.105.063537

Scott GJ (2021) A review of root, tuber and banana crops in developing countries: past, present and future. Int J Food Sci Technol 56:1093–1114. https://doi.org/10.1111/ijfs.14778

Shan H, Pasin F, Tzanetakis IE, Simón-Mateo C, García JA, Rodamilans B (2018) Truncation of a P1 leader proteinase facilitates potyvirus replication in a non-permissive host. Mol Plant Pathol 19:1504–1510. https://doi.org/10.1111/mpp.12640

Shan H, Pasin F, Valli A, Castillo C, Rajulu C, Carbonell A, Simón-Mateo C, García JA, Rodamilans B (2015) The Potyviridae P1a leader protease contributes to host range specificity. Virology 476:264–270. https://doi.org/10.1016/j.virol.2014.12.013

Shaw JG, Plaskitt KA, Wilson TMA (1986) Evidence that Tobacco mosaic virus particles disassemble contranslationally in vivo. Virology 148:326–336. https://doi.org/10.1016/0042-6822(86)90329-6

Sheffield F (1957) Virus diseases of sweet potato in East Africa-Identification of the viruses and their insect vector. Phytopathology 47:582–590

Shi XM, Miller H, Verchot J, Carrington JC, Vance VB (1997) Mutations in the region encoding the central domain of helper component-proteinase (HC-Pro) eliminate Potato virus X/potyviral synergism. Virology 231:35–42. https://doi.org/10.1006/viro.1997.8488

Shi Y (2014) A Glimpse of structural biology through X-ray crystallography. Cell 159:995–1014. https://doi.org/10.1016/j.cell.2014.10.051

Shukla DD, Strike PM, Tracy SL, Gough KH, Ward CW (1988) The N and C termini of the coat proteins of potyviruses are surface-located and the N terminus contains the major virus-specific epitopes. J Gen Virol 69:1497–1508. https://doi.org/10.1099/0022-1317-69-7-1497

Silhavy D (2002) A viral protein suppresses RNA silencing and binds silencing-generated, 21- to 25-nucleotide double-stranded RNAs. EMBO J 21:3070–3080. https://doi.org/10.1093/emboj/cdf312

Simmons HE, Munkvold GP (2014) Seed transmission in the Potyviridae. In: Global Perspectives on the Health of Seeds and Plant Propagation Material. Springer Netherlands, Dordrecht, pp 3–15. https://doi.org/10.1007/978-94-017-9389-6_1

Singh S, Awasthi LP, Jangre A (2020) Transmission of plant viruses in fields through various vectors. In: Applied Plant Virology. Elsevier, pp 313–334. https://doi.org/10.1016/B978-0-12-818654-1.00024-4

Sorel M, Garcia JA, German-Retana S (2014) The Potyviridae cylindrical inclusion helicase: A key multipartner and multifunctional protein. Mol Plant-Microbe Interact 27:215–226. https://doi.org/10.1094/MPMI-11-13-0333-CR

Souto ER, Sim J, Chen J, Valverde RA, Clark CA (2003) Properties of strains of Sweet potato feathery mottle virus and two newly recognized potyviruses infecting sweet potato in the United States. Plant Dis 87:1226–1232. https://doi.org/10.1094/PDIS.2003.87.10.1226

Steele JFC, Peyret H, Saunders K, Castells-Graells R, Marsian J, Meshcheriakova Y, Lomonossoff GP (2017) Synthetic plant virology for nanobiotechnology and nanomedicine. WIREs Nanomedicine and Nanobiotechnology 9:e1447. https://doi.org/10.1002/wnan.1447

Susaimuthu J, Tzanetakis IE, Gergerich RC, Martin RR (2008) A member of a new genus in the Potyviridae infects Rubus. Virus Res 131:145–151. https://doi.org/10.1016/j.virusres.2007.09.001

Syller J (2005) The roles and mechanisms of helper component proteins encoded by potyviruses and caulimoviruses. Physiol Mol Plant Pathol 67:119–130. https://doi.org/10.1016/j.pmpp.2005.12.005

Syller J (2014) Biological and molecular events associated with simultaneous transmission of plant viruses by invertebrate and fungal vectors. Mol Plant Pathol 15:417–426. https://doi.org/10.1111/mpp.12101

Syller J (2012) Facilitative and antagonistic interactions between plant viruses in mixed infections. Mol Plant Pathol 13:204–216. https://doi.org/10.1111/j.1364-3703.2011.00734.x

Tairo F, Jones RAC, Valkonen JPT (2006) Potyvirus complexes in sweetpotato: Occurrence in Australia, serological and molecular resolution, and analysis of the Sweet potato virus 2 (SPV2) component. Plant Dis 90:1120–1128. https://doi.org/10.1094/PD-90-1120

Tairo F, Mukasa SB, Jones RAC, Kullaya A, Rubaihayo PR, Valkonen JPT (2005) Unravelling the genetic diversity of the three main viruses involved in Sweet Potato Virus Disease (SPVD), and its practical implications. Mol Plant Pathol 6:199–211. https://doi.org/10.1111/J.1364-3703.2005.00267.X

Tanaka Y, Nakamura S, Kawamukai M, Koizumi N, Nakagawa T (2011) Development of a series of Gateway binary vectors possessing a tunicamycin resistance gene as a marker for the transformation of Arabidopsis thaliana. Biosci Biotechnol Biochem 75:804–807. https://doi.org/10.1271/bbb.110063

Tang D, Wang G, Zhou J-M (2017) Receptor kinases in plant-pathogen interactions: More than pattern recognition. Plant Cell 29:618–637. https://doi.org/10.1105/tpc.16.00891

Tatineni S, Qu F, Li R, Jack Morris T, French R (2012) Triticum mosaic poacevirus enlists P1 rather than HC-Pro to suppress RNA silencing-mediated host defense. Virology 433:104–115. https://doi.org/10.1016/j.virol.2012.07.016

Tavert-Roudet G, Anne A, Barra A, Chovin A, Demaille C, Michon T (2017) The potyvirus particle recruits the plant translation initiation factor eif4e by means of the vpg covalently linked to the viral RNA. Mol Plant-Microbe Interact 30:754–762. https://doi.org/10.1094/MPMI-04-17-0091-R

Taylor KA, Glaeser RM (1974) Electron diffraction of frozen, hydrated protein crystals. Science 186:1036–1037. https://doi.org/10.1126/science.186.4168.1036

Tena Fernández F, González I, Doblas P, Rodríguez C, Sahana N, Kaur H, Tenllado F, Praveen S, Canto T (2013) The influence of cis-acting P1 protein and translational elements on the expression of Potato virus Y helper-component proteinase (HCPro) in heterologous systems and its suppression of silencing activity. Mol Plant Pathol 14:530–541. https://doi.org/10.1111/mpp.12025

Thuenemann EC, Byrne MJ, Peyret H, Saunders K, Castells-Graells R, Ferriol I, Santoni M, Steele JFC, Ranson NA, Avesani L, Lopez-Moya JJ, Lomonossoff GP (2021) A Replicating viral vector greatly enhances accumulation of helical virus-like particles in plants. Viruses 13:885. https://doi.org/10.3390/v13050885

Thuenemann EC, Lomonossoff GP (2018) Delivering cargo: Plant-based production of Bluetongue virus core-like and virus-like particles containing fluorescent proteins. In: Methods in Molecular Biology. pp 319–334. https://doi.org/10.1007/978-1-4939-7808-3_22

Torrance L, Andreev IA, Gabrenaite-Verhovskaya R, Cowan G, Mäkinen K, Taliansky ME (2006) An unusual structure at one end of potato potyvirus particles. J Mol Biol 357:1–8. https://doi.org/10.1016/j.jmb.2005.12.021

Trenado HP, Lozano G, Valverde RA, Navas-Castillo J (2007) First report of Sweet potato virus G and Sweet potato virus 2 infecting sweet potato in Spain. Plant Dis 91:1687–1687. https://doi.org/10.1094/PDIS-91-12-1687C

Tugume AK, Amayo R, Weinheimer I, Mukasa SB, Rubaihayo PR, Valkonen JPT (2013) Genetic variability and evolutionary implications of RNA silencing suppressor genes in RNA1 of Sweet potato chlorotic stunt virus isolates infecting sweetpotato and related wild species. PLoS One 8:e81479. https://doi.org/10.1371/journal.pone.0081479

Tugume AK, Mukasa SB, Kalkkinen N, Valkonen JPT (2010) Recombination and selection pressure in the ipomovirus Sweet potato mild mottle virus (Potyviridae) in wild species and cultivated sweetpotato in the centre of evolution in East Africa. J Gen Virol 91:1092–1108. https://doi.org/10.1099/vir.0.016089-0

Tugume AK, Mukasa SB, Valkonen JPT (2008) Natural wild hosts of Sweet potato feathery mottle virus show spatial differences in virus incidence and virus-like diseases in Uganda. Phytopathology 98:640–652. https://doi.org/10.1094/PHYTO-98-6-0640

Tugume AK, Mukasa SB, Valkonen JPT (2016) Mixed infections of four viruses, the incidence and phylogenetic relationships of sweet potato chlorotic fleck virus (Betaflexiviridae) isolates in wild species and sweetpotatoes in Uganda and evidence of distinct isolates in east Africa. PLoS One 11:e0167769. https://doi.org/10.1371/journal.pone.0167769

Tyulkina LG, Skurat E V, Frolova OY, Komarova T V, Karger EM, Atabekov IG (2011) New viral vector for superproduction of epitopes of vaccine proteins in plants. Acta Naturae 3:73–82. https://doi.org/10.32607/20758251-2011-3-4-73-82

Tzanetakis IE, Martin RR, Wintermantel WM (2013) Epidemiology of criniviruses: an emerging problem in world agriculture. Front Microbiol 4:119. https://doi.org/10.3389/fmicb.2013.00119

Untiveros M, Fuentes S, Kreuze J (2008) Molecular variability of Sweet potato feathery mottle virus and other potyviruses infecting sweet potato in Peru. Arch Virol 153:473–483. https://doi.org/10.1007/s00705-007-0019-0

Untiveros M, Fuentes S, Salazar LF (2007) Synergistic Interaction of Sweet potato chlorotic stunt virus (Crinivirus) with carla-, cucumo-, ipomo-, and potyviruses infecting sweet potato. Plant Dis 91:669–676. https://doi.org/10.1094/PDIS-91-6-0669

Untiveros M, Olspert A, Artola K, Firth AE, Kreuze JF, Valkonen JPT (2016) A novel sweet potato potyvirus open reading frame (ORF) is expressed via polymerase slippage and suppresses RNA silencing. Mol Plant Pathol 17:1111-1123. https://doi.org/10.1111/mpp.12366

Untiveros M, Quispe D, Kreuze J (2010) Analysis of complete genomic sequences of isolates of the Sweet potato feathery mottle virus strains C and EA: Molecular evidence for two distinct potyvirus species and two P1 protein domains. Arch Virol 155:2059–2063. https://doi.org/10.1007/s00705-010-0805-y

Valli A, Dujovny G, García JA (2008) Protease activity, self interaction, and small interfering RNA binding of the silencing suppressor P1b from Cucumber vein yellowing ipomovirus. J Virol 82:974–986. https://doi.org/10.1128/JVI.01664-07

Valli A, Gallo A, Calvo M, Perez J d. J, Garcia JA (2014) A novel role of the potyviral helper component proteinase contributes to enhance the yield of viral particles. J Virol. 88:9808-9818. https://doi.org/10.1128/jvi.01010-14

Valli A, García JA, López-Moya JJ (2021) Potyviruses (Potyviridae). In: Encyclopedia of Virology. Elsevier, pp 631–641. https://doi.org/10.1016/B978-0-12-809633-8.21252-1

Valli A, López-Moya JJ, García JA (2007) Recombination and gene duplication in the evolutionary diversification of P1 proteins in the family Potyviridae. J Gen Virol 88:1016–1028. https://doi.org/10.1099/vir.0.82402-0

Valli A, Martín-Hernández AM, López-Moya JJ, García JA (2006) RNA silencing suppression by a second copy of the P1 serine protease of Cucumber vein yellowing ipomovirus, a member of the family Potyviridae that lacks the cysteine protease HCPro. J Virol 80:10055–10063. https://doi.org/10.1128/JVI.00985-06

Valli AA, Gallo A, Rodamilans B, López-Moya JJ, García JA (2018) The HCPro from the Potyviridae family: an enviable multitasking Helper Component that every virus would like to have. Mol Plant Pathol 19:744–763. https://doi.org/10.1111/mpp.12553

Valli AA, García López R, Ribaya M, Martínez FJ, Gómez DG, García B, Gonzalo I, Gonzalez de Prádena A, Pasin F, Montanuy I, Rodríguez-Gonzalo E, García JA (2022) Maf/ham1-like pyrophosphatases of non-canonical nucleotides are host-specific partners of viral RNA-dependent RNA polymerases. PLOS Pathog 18:e1010332. https://doi.org/10.1371/journal.ppat.1010332

Valverde RA, Sim J, Lotrakul P (2004) Whitefly transmission of sweet potato viruses. Virus Res 100:123–128. https://doi.org/10.1016/j.virusres.2003.12.020

van den Born E, Omelchenko MV, Bekkelund A, Leihne V, Koonin EV, Dolja VV, Falnes PØ (2008) Viral AlkB proteins repair RNA damage by oxidative demethylation. Nucleic Acids Res 36:5451–5461. https://doi.org/10.1093/nar/gkn519

Vance V, Vaucheret H (2001) RNA Silencing in plants-defense and counterdefense. Science 292:2277–2280. https://doi.org/10.1126/science.1061334

Vance VB (1991) Replication of potato virus X RNA is altered in coinfections with Potato virus Y. Virology 182:486–494. https://doi.org/10.1016/0042-6822(91)90589-4

Vance VB, Berger PH, Carrington JC, Hunt AG, Ming Shi X (1995) 5' Proximal potyviral sequences mediate Potato virus X/potyviral synergistic disease in transgenic tobacco. Virology 206:583–590. https://doi.org/10.1016/S0042-6822(95)80075-1

Velazquez-Campoy A, Sancho J, Abian O, Vega S (2016) Biophysical screening for identifying pharmacological chaperones and inhibitors against conformational and infectious

diseases. Curr Drug Targets 17:1492-505. https://doi.org/10.2174/1389450117666160201110449

Verchot J, Carrington JC (1995a) Debilitation of plant potyvirus infectivity by P1 proteinase-inactivating mutations and restoration by second-site modifications. J Virol 69:1582–1590. https://doi.org/10.1128/jvi.69.3.1582-1590.1995

Verchot J, Carrington JC (1995b) Evidence that the potyvirus P1 proteinase functions in trans as an accessory factor for genome amplification. J Virol 69:3668–3674. https://doi.org/10.1128/JVI.69.6.3668-3674.1995

Verchot J, Koonin E V., Carrington JC (1991) The 35-kDa protein from the N-terminus of the potyviral polyprotein functions as a third virus-encoded proteinase. Virology 185:527–535. https://doi.org/10.1016/0042-6822(91)90522-D

Vijayapalani P, Maeshima M, Nagasaki-Takekuchi N, Miller WA (2012) Interaction of the trans-frame potyvirus protein P3N-PIPO with host protein PCaP1 facilitates potyvirus movement. PLoS Pathog 8:e1002639. https://doi.org/10.1371/journal.ppat.1002639

Voinnet O, Lederer C, Baulcombe DC (2000) A Viral movement protein prevents spread of the gene silencing signal in Nicotiana benthamiana. Cell 103:157–167. https://doi.org/10.1016/S0092-8674(00)00095-7

Völkl W, Woodring J, Fischer M, Lorenz MW, Hoffmann KH (1999) Ant-aphid mutualisms: The impact of honeydew production and honeydew sugar composition on ant preferences. Oecologia 118:483–491. https://doi.org/10.1007/s004420050751

Walker PJ, Siddell SG, Lefkowitz EJ, Mushegian AR, Adriaenssens EM, Alfenas-Zerbini P, Davison AJ, Dempsey DM, Dutilh BE, García ML, Harrach B, Harrison RL, Hendrickson RC, Junglen S, Knowles NJ, Krupovic M, Kuhn JH, Lambert AJ, Łobocka M, Nibert ML, Oksanen HM, Orton RJ, Robertson DL, Rubino L, Sabanadzovic S, Simmonds P, Smith DB, Suzuki N, Van Dooerslaer K, Vandamme AM, Varsani A, Zerbini FM (2021) Changes to virus taxonomy and to the international code of virus classification and nomenclature ratified by the international committee on taxonomy of viruses (2021). Arch Virol 166:2633–2648. https://doi.org/10.1007/s00705-021-05156-1

Walkey DGA, Cooper VC (1975) Effect of temperature on virus eradication and growth of infected tissue cultures. Ann Appl Biol 80:185–190. https://doi.org/10.1111/j.1744-7348.1975.tb01620.x

Walsh D, Mohr I (2011) Viral subversion of the host protein synthesis machinery. Nat Rev Microbiol 9:860–875. https://doi.org/10.1038/nrmicro2655

Wan J, Cabanillas DG, Zheng H, Laliberté J-F (2015) Turnip mosaic virus moves systemically through both phloem and xylem as membrane-associated complexes. Plant Physiol 167:1374–1388. https://doi.org/10.1104/pp.15.00097

Wang L, Poque S, Laamanen K, Saarela J, Poso A, Laitinen T, Valkonen JPT (2021) In vitro identification and in vivo confirmation of inhibitors for Sweet potato chlorotic stunt virus RNA silencing suppressor, a viral RNase III. J Virol 95:e00107-21. https://doi.org/10.1128/JVI.00107-21

Wang M, Abad J, Fuentes S, Li R (2013) Complete genome sequence of the original Taiwanese isolate of Sweet potato latent virus and its relationship to other potyviruses infecting sweet potato. Arch Virol 158:2189–2192. https://doi.org/10.1007/s00705-013-1705-8

Wang QC, Panis B, Engelmann F, Lambardi M, Valkonen JPT (2009) Cryotherapy of shoot tips: a technique for pathogen eradication to produce healthy planting materials and prepare healthy plant genetic resources for cryopreservation. Ann Appl Biol 154:351–363. https://doi.org/10.1111/j.1744-7348.2008.00308.x

Wang RY, Pirone TP (1999) Purification and characterization of Turnip mosaic virus helper component protein. Phytopathology 89:564–567. https://doi.org/10.1094/PHYTO.1999.89.7.564

Wanjala BW, Ateka EM, Miano DW, Low JW, Kreuze JF (2020) Storage root yield of sweet potato as influenced by Sweet potato leaf curl virus and its interaction with Sweet potato feathery mottle virus and Sweet potato chlorotic stunt virus in Kenya. Plant Dis 104:1477–1486. https://doi.org/10.1094/PDIS-06-19-1196-RE

Watson JD, Crick FHC (1953) Molecular structure of nucleic acids: A structure for deoxyribose nucleic acid. Nature 171:737–738. https://doi.org/10.1038/171737a0

Wei T, Wang A (2008) Biogenesis of cytoplasmic membranous vesicles for plant potyvirus replication occurs at endoplasmic reticulum exit sites in a COPI- and COPII-dependent manner. J Virol 82:12252–12264. https://doi.org/10.1128/JVI.01329-08

Weinheimer I, Boonrod K, Moser M, Wassenegger M, Krczal G, Butcher SJ, Valkonen JPT (2014) Binding and processing of small dsRNA molecules by the class 1 RNase III protein encoded by Sweet potato chlorotic stunt virus. J Gen Virol 95:486–495. https://doi.org/10.1099/vir.0.058693-0

Weinheimer I, Jiu Y, Rajamäki ML, Matilainen O, Kallijärvi J, Cuellar WJ, Lu R, Saarma M, Holmberg CI, Jäntti J, Valkonen JPT (2015) Suppression of RNAi by dsRNA degrading RNaseIII enzymes of viruses in animals and plants. PLoS Pathog 11:1–25. https://doi.org/10.1371/journal.ppat.1004711

Wen R-H, Hajimorad MR (2010) Mutational analysis of the putative pipo of Soybean mosaic virus suggests disruption of PIPO protein impedes movement. Virology 400:1–7. https://doi.org/10.1016/j.virol.2010.01.022

Whitfield AE, Falk BW, Rotenberg D (2015) Insect vector-mediated transmission of plant viruses. Virology 479–480:278–289. https://doi.org/10.1016/j.virol.2015.03.026

Winey M, Meehl JB, O'Toole ET, Giddings TH (2014) Conventional transmission electron microscopy. Mol Biol Cell 25:319–323. https://doi.org/10.1091/mbc.e12-12-0863

Wintermantel WM (2016) CHAPTER 8: Semipersistent whitefly-transmitted viruses: Criniviruses. In: Vector-Mediated Transmission of Plant Pathogens. The American Phytopathological Society. pp 111–119. https://doi.org/10.1094/9780890545355.008

Wintermantel WM, Cortez AA, Anchieta AG, Gulati-Sakhuja A, Hladky LL (2008) Co-infection by two criniviruses alters accumulation of each virus in a host-specific manner and influences efficiency of virus transmission. Phytopathology 98:1340–1345. https://doi.org/10.1094/PHYTO-98-12-1340

Wisler GC, Duffus JE, Liu H-Y, Li RH (1998) Ecology and epidemiology of whitefly-transmitted Closteroviruses. Plant Dis 82:270–280. https://doi.org/10.1094/PDIS.1998.82.3.270

Wosula EN, Clark CA, Davis JA (2012) Effect of host plant, aphid species, and virus infection status on transmission of Sweet potato feathery mottle virus. Plant Dis 96:1331–1336. https://doi.org/10.1094/PDIS-11-11-0934-RE

Wu S, Lau KH, Cao Q, Hamilton JP, Sun H, Zhou C, Eserman L, Gemenet DC, Olukolu BA, Wang H, Crisovan E, Godden GT, Jiao C, Wang X, Kitavi M, Manrique-Carpintero N, Vaillancourt B, Wiegert-Rininger K, Yang X, Bao K, Schaff J, Kreuze J, Gruneberg W, Khan A, Ghislain M, Ma D, Jiang J, Mwanga ROM, Leebens-Mack J, Coin LJM, Yencho GC, Buell CR, Fei Z (2018) Genome sequences of two diploid wild relatives of cultivated sweetpotato reveal targets for genetic improvement. Nat Commun 9:4580. https://doi.org/10.1038/s41467-018-06983-8

Xu H, He X, Zheng X, Yang Y, Tian J, Lu Z (2014) Southern rice black-streaked dwarf virus (SRBSDV) directly affects the feeding and reproduction behavior of its vector, Sogatella furcifera (Horváth) (Hemiptera: Delphacidae). Virol J 11:55. https://doi.org/10.1186/1743-422X-11-55

Yang J, Moeinzadeh MH, Kuhl H, Helmuth J, Xiao P, Haas S, Liu G, Zheng J, Sun Z, Fan W, Deng G, Wang H, Hu F, Zhao S, Fernie AR, Boerno S, Timmermann B, Zhang P, Vingron M (2017) Haplotype-resolved sweet potato genome traces back its hexaploidization history. Nat Plants 3:696–703. https://doi.org/10.1038/s41477-017-0002-z

Yang S, Wang T, Bohon J, Gagné M-ÈL, Bolduc M, Leclerc D, Li H (2012) Crystal structure of the coat protein of the flexible filamentous Papaya mosaic virus. J Mol Biol 422:263–273. https://doi.org/10.1016/j.jmb.2012.05.032

Yip KM, Fischer N, Paknia E, Chari A, Stark H (2020) Atomic-resolution protein structure determination by cryo-EM. Nature 587:157–161. https://doi.org/10.1038/s41586-020-2833-4

Young BA, Stenger DC, Qu F, Morris TJ, Tatineni S, French R (2012) Tritimovirus P1 functions as a suppressor of RNA silencing and an enhancer of disease symptoms. Virus Res 163:672–677. https://doi.org/10.1016/j.virusres.2011.12.019

Yuste-Calvo C, Ibort P, Sánchez F, Ponz F (2020) Turnip mosaic virus coat protein deletion mutants allow defining dispensable protein domains for 'in planta' eVLP formation. Viruses 12:661. https://doi.org/10.3390/v12060661

Zaitlin M, Palukaitis P (2000) Advances in understanding plant viruses and virus diseases. Annu Rev Phytopathol 38:117–143. https://doi.org/10.1146/annurev.phyto.38.1.117

Zamora M, Méndez-López E, Agirrezabala X, Cuesta R, Lavín JL, Sánchez-Pina MA, Aranda MA, Valle M (2017) Potyvirus virion structure shows conserved protein fold and RNA binding site in ssRNA viruses. Sci Adv 3:eaao2182. https://doi.org/10.1126/sciadv.aao2182

Zamore PD, Tuschl T, Sharp PA, Bartel DP (2000) RNAi: double-stranded RNA directs the ATP-dependent cleavage of mRNA at 21 to 23 nucleotide intervals. Cell 101:25–33. https://doi.org/10.1016/S0092-8674(00)80620-0

Zeenko V, Gallie DR (2005) Cap-independent translation of Tobacco etch virus is conferred by an RNA pseudoknot in the 5′-leader. J Biol Chem 280:26813–26824. https://doi.org/10.1074/jbc.M503576200

Zeng R, Liao Q, Feng J, Li D, Chen J (2007) Synergy between Cucumber mosaic virus and Zucchini yellow mosaic virus on Cucurbitaceae hosts tested by real-time reverse transcription-polymerase chain reaction. Acta Biochim Biophys Sin (Shanghai) 39:431–437. https://doi.org/10.1111/j.1745-7270.2007.00292.x

Zhang X-F, Zhang S, Guo Q, Sun R, Wei T, Qu F (2018) A new mechanistic model for viral cross protection and superinfection exclusion. Front Plant Sci 9:40. https://doi.org/10.3389/fpls.2018.00040

Zvereva A, Pooggin M (2012) Silencing and innate immunity in plant defense against viral and non-viral pathogens. Viruses 4:2578–2597. https://doi.org/10.3390/v4112578